Linear Multifunctional PEG-Alternatives for Bioconjugation and Hydrogel Formation

Dissertation zur Erlangung des naturwissenschaftlichen Doktorgrades

der Julius-Maximilians-Universität Würzburg

vorgelegt von

Willi Smolan

aus Riga

Würzburg 2022

Eingereicht bei der Fakultät für Chemie und Pharmazie am

_____

Gutachter der schriftlichen Arbeit

1. Gutachter: _____

2. Gutachter: _____

Prüfer des öffentlichen Promotionskolloquiums

1. Prüfer: _____

2. Prüfer: _____

3. Prüfer: _____

Datum des öffentlichen Promotionskolloquiums

_____

Doktorurkunde ausgehändigt am

_____

Die vorliegende Arbeit wurde in der Abteilung für Funktionswerkstoffe der Medizin und Zahnheilkunde, Universität Würzburg, im Zeitraum von Dezember 2014 bis Dezember 2018 unter der Leitung von Prof. Groll angefertigt.

List of publications

1. **W. Smolan**[#], C. Gergely[#], J. Teßmar, J. Groll, Taming the Monomer Activated Anionic Polymerization of Glycidols: Allyl-Functionalized High-Molecular Weight Linear Polyglycidols with Narrow Dispersity, *Macromolecular Rapid Communications*, submitted. [#]Equal contribution

2. J.-M. Noy, Y. Li, **W. Smolan** and P. J. Roth, Azide–*para*-Fluoro Substitution on Polymers: Multipurpose Precursors for Efficient Sequential Postpolymerization Modification, *Macromolecules* **2019**, 52, 3083-3091.

3. S. Stichler, T. Böck, N. Paxton, S. Bertlein, R. Levato, V. Schill, **W. Smolan**, J. Malda, J. Teßmar, T. Blunk and J. Groll, Double Printing of Hyaluronic Acid/Poly(Glycidol) Hybrid Hydrogels with Poly(ε-Caprolactone) for MSC Chondrogenesis, *Biofabrication* **2017**, 9, 044108.

4. N. Paxton, **W. Smolan**, T. Böck, F. Melchels, J.Groll and T. Juengst, Proposal to Assess Printability of Bioinks for Extrusion-Based Bioprinting and Evaluation of Rheological Properties Governing Bioprintability, *Biofabrication* **2017**, 9, 044107.

5. T. Jüngst[#], **W. Smolan**[#], K. Schacht, T. Scheibel and J. Groll, Strategies and Molecular Design Criteria for 3D Printable Hydrogels, *Chemical Reviews* **2016**, 116, 1496-1539. [#]Equal contribution

Table of Contents

1 Objective of the thesis 1

2 Theoretical background 5

2.1 Polymers as biomaterials 5

2.2 Synthesis of polymers 7

2.2.1 Living polymerisation 7

2.2.2 Polymerisation of oligo(ethylene glycol) methyl ether (meth)acrylate *via* reversible addition fragmentation chain transfer 8

2.2.3 Anionic ring opening polymerisation of glycicdyl ether based monomers 11

2.2.3.1 Alcoholate initiated polymerisation 11

2.2.3.2 Nucleophilic initiated and metal complex assisted polymerisation 14

2.2.4 Modification of polymers *via* thiol-ene chemistry 16

2.3 Bioconjugation 18

2.3.1 Definition and techniques 18

2.3.2 Native chemical ligation 19

2.4 Hydrogels 23

2.4.1 Definition and characteristics 23

2.4.2 Crosslinking methods 24

2.4.2.1 Electrostatic interactions 25

2.4.2.2 π-π Stacking interactions 26

3 Results and discussion 29

3.1 Polymers with peptide binding units 29

3.1.1 Polymer synthesis via RAFT polymerisation 29

3.1.2 Thioester-linker synthesis and modification of P(OEGMEA-co-HEA) 35

3.1.3 RAFT Z-group cleavage and native chemical ligation 41

3.1.4 Polymer synthesis *via* free radical polymerisation 45

3.1.5 Modification of P(OEGMEA-*co*-HEA) with thioester-linker 50

3.1.6 Determination of the monomer ratios 54

3.1.7 Reaction of copolymers with CGGGF 60

3.1.8 Hydrolysis stability tests 64

3.2 Low molecular weight polyglycidols 69

3.2.1 Monomer and polymer synthesis 69

3.2.2 Electrolyte functionalisation 79

3.2.2.1 Positively charged polymers 79

3.2.2.2 Negatively charged polymers 85

3.2.2.3 Gel tests 95

3.2.3 π-π Functionalisation 96

3.2.3.1 Electron rich compound 99

3.2.3.2 Electron poor compound 104

3.2.3.3 Gel tests 114

3.3 High molecular weight polyglycidols 115

3.3.1 Polymer synthesis 115

3.3.2 Electrolyte functionalisation 126

3.3.3 Gel tests 133

4 Summary/Zusammenfassung 135

4.1 Summary 135

4.2 Zusammenfassung 137

5 Experimental section 139

5.1 Materials and methods 139

5.1.1 Materials 139

5.1.2 Methods 140

5.1.2.1 NMR spectroscopy 140

5.1.2.2 GPC 141

5.1.2.3 FT-IR spectroscopy 141

5.1.2.4 RAMAN spectroscopy 141

5.1.2.5 ASAP-MS 141

5.1.2.6 UV-Vis spectroscopy 141

5.1.2.7 Dialysis tubes 142

5.1.2.8 Lyophilisation 142

5.1.2.9 UV-light 142

5.1.2.10 Karl-Fischer titration 142

5.2 Acrylate based copolymers with peptide binding units 143

5.2.1 RAFT-copolymerisation 143

5.2.1.1 Poly(oligo(ethylene glycol) methyl ether acrylate-*co*-2-hydroxyethyl acrylate) (P(OEGMEA-*co*-HEA)) 143

5.2.1.2 Poly(oligo(ethylene glycol) methyl ether acrylate-*co*-thiolactone acrylamide) (P(OEGMEA-*co*-TLA)) 144

5.2.1.3 Poly(oligo(ethylene glycol) methyl ether acrylate-*co*-vinyl azlactone) (P(OEGMEA-*co*-VAL)) 145

5.2.1.4 Ethyl 3-mercaptopropionate-succinic acid (EMP-SA) 146

5.2.1.5 Reaction of P(OEGMEA-co-HEA) with EMP-SA (P(OEGMEA-co-EMP-SA)) 147

5.2.1.6 RAFT Z-group cleavage 148

5.2.1.7 Reaction of P(OEGMEA-*co*-EMP-SA) with CGGGF 149

5.2.1.8 Reaction of P(OEGMEA-*co*-TLA) with CGGGF 150

5.2.1.9 Reaction of P(OEGMEA-*co*-VAL) with CGGGF 151

5.2.2 Free radical copolymerisation 152

5.2.2.1 Poly(oligo(ethylene glycol) methyl ether acrylate-*co*-2-hydroxyethyl acrylate) (P(OEGMEA-*co*-HEA)) 152

5.2.2.2 Poly(oligo(ethylene glycol) methyl ether acrylate-*co*-thiolactone acrylamide) (P(OEGMEA-*co*-TLA)) 153

5.2.2.3 Poly(oligo(ethylene glycol) methyl ether acrylate-*co*-vinyl azlactone) (P(OEGMEA-*co*-VAL)) 154

5.2.2.4 Reaction of P(OEGMEA-co-HEA) with EMP-SA (P(OEGMEA-co-EMP-SA)) 155

5.2.2.5 Reaction of P(OEGMEA-*co*-TLA) with benzylamine 156

5.2.2.6 Reaction of P(OEGMEA-*co*-VAL) with benzylamine 157

5.2.2.7 Reaction of P(OEGMEA-*co*-EMP-SA) with CGGGF 158

5.2.2.8 Reaction of P(OEGMEA-*co*-TLA) with CGGGF 159

5.2.2.9 Reaction of P(OEGMEA-*co*-VAL) with CGGGF 159

5.2.2.10 Stability tests of P(OEGMEA-*co*-EMP-SA), P(OEGMEA-*co*-TLA) and P(OEGMEA-*co*-VAL) 161

5.3 Low molecular weight polyglycidols 163
5.3.1 Ethoxyethyl glycidyl ether (EEGE) 163
5.3.2 Poly(ethoxyethyl glycidyl ether-*co*-allyl glycidyl ether) (P(EEGE-*co*-AGE)) 164
5.3.3 Poly(glycidol-*co*-allyl glycidyl ether) (P(G-*co*-AGE)) 165
5.3.4 Thiol modification of P(G-*co*-AGE) (P(G-*co*-SH)) 167

5.4 Electrolyte functionalised polyglycidols 168
5.4.1 1-Methyl-3-(3-propanethiol)-imidazolium chloride 168
5.4.2 Chloride modification of P(G-*co*-AGE) (P(G-*co*-Cl)) 169
5.4.3 Imidazolium modification of P(G-*co*-Cl) P(G-*co*-Im) 170
5.4.4 Bis(diethylphosphonamide)disulfide 172
5.4.5 Diethylphosphonamide modification of P(G-*co*-AGE) (P(G-*co*-POEt)) 173
5.4.6 Phosphonamide modification of P(G-*co*-POEt) (P(G-*co*-POH)) 175
5.4.7 Gel tests 176

5.5 π-π Functionalised polyglycidols 177
5.5.1 Bis(1-pyrenebutyric)cystamide 177
5.5.2 Carboxylic acid modification of P(G-*co*-AGE) (P(G-*co*-COOH)) 178
5.5.3 Pyrene modification of P(G-*co*-COOH) (P(G-*co*-Pyr)) 179
5.5.4 *n*-Propyl naphthalene monoimide (*n*Pr-NMI) 181
5.5.5 Bis(*n*-propyl naphthalene)cystdiimide (*n*Pr-CA-NDI) 182
5.5.6 *n*-Propyl allyl naphthalene diimide (*n*Pr-Allyl-NDI) 183
5.5.7 Reaction of P(G-*co*-SH) with *n*Pr-Allyl-NDI (P(G-*co*-*n*Pr-NDI)) 184
5.5.8 Reaction of P(G-*co*-AGE) with cysteamine hydrochloride (P(G-*co*-NH_2)) 185
5.5.9 Reaction of P(G-*co*-NH_2) with *n*Pr-NMI (P(G-*co*-*n*Pr-NDI)) 186
5.5.10 Gel tests 187

5.6 High molecular weight polyglycidols 187
5.6.1 Poly(ethoxyethyl glycidyl ether) (PEEGE) 187
5.6.2 Polyglycidol (PG) 189
5.6.3 Poly(allyl glycidyl ether) (PAGE) 190
5.6.4 Poly(ethoxyethyl glycidyl ether-*co*-allyl glycidyl ether) (P(EEGE-*co*-AGE)) 192
5.6.5 Poly(glycidol-*co*-allyl glycidyl ether) (P(G-*co*-AGE)) 194

5.7 Electrolyte functionalised high molecular weight polyglycidols 196
5.7.1 Poly(ethoxyethyl glycidyl ether-*co*-allyl glycidyl ether) (P(EEGE-*co*-AGE)) 196
5.7.2 Poly(glycidol-*co*-allyl glycidyl ether) (P(G-*co*-AGE)) 197
5.7.3 Chloride modification of P(G-*co*-AGE) (P(G-*co*-Cl)) 198
5.7.4 Imidazolium modification of P(G-*co*-Cl) (P(G-*co*-Im)) 199
5.7.5 Diethylphosphonamide modification of P(G-*co*-AGE) (P(G-*co*-POEt)) 200
5.7.6 Phosphonamide modification of P(G-*co*-POEt) (P(G-*co*-POH)) 201
5.7.7 Gel tests 202
5.7.7.1 P(G-*co*-Im) with P(G-*co*-POH) 202
5.7.7.2 P(G-*co*-POH) with $CaCl_2$ 202
5.7.7.3 High molecular weight P(G-*co*-POH) with low molecular weight P(G-*co*-Im) 202

6 References 203

Abbreviations and symbols

Abbreviations

Å	Ångstrom (10^{-10} m)
AIBN	2,2'-Azobis(2-methylpropionitrile)
AGE	Allyl glycidyl ether
$Al^{i}Bu_3$	Triisobutylaluminium
ASAP-MS	Atmospheric Solids Analysis Probe Mass Spectrometry
ATR	Attenuated total reflection
a.u.	Arbitrary unit
br	Broad
Br	Bromide
C	Carbon
Cl	Chloride
$CaCl_2$	Calcium chloride
CaH_2	Calcium hydride
CA·2 HCl	Cystamine dihydrochloride
CeA·HCl	Cysteamine hydrochloride
$CDCl_3$	Deuterated chloroform
CGGGF	Peptide sequence containing L-derivatives of cysteine (C), glycine (G) and phenylalanine (F)
CPDB	2-Cyano-2-propyl benzodithioate
Cu	Copper
co	*Co* (together)
COOH	Carboxylic acid
cm	Centimetre
d	Doublet or deuterated
Da	Dalton
DCC	*N*,*N*'-Dicyclohexylcarbodiimide
DCM	Dichloromethane
DMF	*N*,*N*'-Dimethylformamide
DMAP	4-(Dimethylamino)pyridine
DMPA	2,2'-Dimethoxy-2-phenylacetophenon
DMSO	Diemthyl sulfoxide
DMSO-d_6	Deuterated dimethyl sulfoxide
DNA	Deoxyribonucleic acid

DP	Degree of polymerisation
EEGE	Ethoxyethyl glycidyl ether
EDC·HCl	*N*-Ethyl-*N'*-(3-dimethylaminopropyl)carbodiimide hydrochloride
EMP-SA	Ethyl 3-mercaptopropionate-succinic acid
et al.	*Et alii* (and others)
etc.	*Et cetera* (and so on)
e.g.	*Exempli gratia* (for example)
EtOH	Ethanol
Et_2O	Diethyl ether
EtOAc	Ethyl acetate
eq	Equivalent
FT-IR	Fourier-transform infrared
g	Gram
G	Glycidol
GPC	Gel permeation chromatography
h	Hour
H	Hydrogen
H_3PO_4	Ortho-phosphoric acid
HCl	Hydrochloric acid
HEA	2-Hydroxyethyl acrylate
HOAc	Acetic acid
^{i}PrOH	Isopropanol
Im	Imidazole
I 2959	Irgacure 2-Hydroxy-1-(4-hydroxyethoxy)-phenyl)-2-methyl-1-propanone
kDa	Kilo Dalton
kg	Kilogram
KOH	Potassium hydroxide
KO^{t}Bu	Potassium *tert*-butoxide
LED	Light emitting diode
LiBr	Lithium bromide
M	Molarity
mbar	Millibar
MeOH	Methanol
MeCN	Acetonitrile
mg	Milligram
$MgSO_4$	Magnesium sulfate

MeCN	Acetonitrile
MHz	Megahertz
min	Minute
mL	Millilitre
mmol	Millimole
nm	Nanometre
m	Multiplet or mass
m	*Meta* (1,3-positions)
M_n	Number averaged molecular weight
M_w	Weight averaged molecular weight
MΩ	Megaohm
m/z	Mass-to-charge ratio
MWCO	Molecular weight cut off
N	Nitrogen
n	Amount of substance
NaCl	Sodium chloride
$NaHCO_3$	Sodium bicarbonate
NaOH	Sodium hydroxide
$NaNO_3$	Sodium nitrate
NaN_3	Sodium azide
Na_2SO_4	Sodium sulfate
NH_2	Primary amine
NMR	Nuclear magnetic resonance
NMI	Naphthalene monoimide
NDI	Naphthalene diimide
$NOct_4Br$	Tetraoctylammonium bromide
NTCA	1,4,5,8-Naphthalenetetracarboxylic dianhydride
OEGME(M)A	Oligo(ethylene glycol) methyl ether (meth)acrylate
o	*Ortho* (1,2-positions)
O	Oxygen
p	Para (1,4-positions)
P	Phosphorus
PBS	Phosphate buffered saline
PEG	Poly(ethylene glycol)
PG	Polyglycidol
POEt	Ethyl phosphonate

POH	Phosphonic acid
pH	Pondus hydrogenii, negative logarithmic value of the hydrogen ion concentration
$P_m^{\cdot}$	New polymer chain carrying a radical
$P_n^{\cdot}$	Growing polymer chain carrying a radical
ppm	Part per million
p-TsOH·H_2O	*para*-Toluene sulfonic acid monohydrate
Pyr	Pyrene
q	Quartet
quin	Quintet
R	Rest or R-group from the RAFT-agent for re-initiation
RAFT	Reversible Addition Fragmentation Chain Transfer
RI	Refractive index
RT	Room temperature
s	Singlet
S	Sulphur
SH	Thiol
SiO_2	Silica gel
sext	Sextet
TCEP·HCl	Tris(2-carboxyethyl) phosphine hydrochloride
t	Triplet
T	Temperature
TLA	Thiolactone acrylamide
TEA	Triethylamine
THF	Tetrahydrofuran
TMS	Tetramethylsilane
TMSBr	Bromotrimethylsilane
UV-vis	Ultraviolet and visible
V	Volume
VAL	Vinylazlactone
W	Watt
Z	Z-group from the RAFT-agent for stabilisation

Symbols

.	Radical
°C	Degree Celsius
%	Per cent
δ	Chemical shift
Đ	Dispersity
hν	Light
π	Molecular orbital called pi
μ	Micro
wt-%	Weight percent

1 Objective of the thesis

Polymers accompany our everyday life and can be found in areas like packaging, textiles, and medicine. [1] Especially the medical field gained an increasing interest in polymers as they can be modified for specific applications, like wound dressings, implants or therapeutic agents. [2] Such modifications can be changes in the molecular weight, in the macromolecular architecture and in the functional groups of the polymer. The most important property of the used material is its acceptance by the body without causing any side effects, like allergies or toxicity. [3, 4]

One prominent currently often used polymer for various medical applications is the water soluble polyethylene glycol (PEG). But its disadvantage is that it can only be functionalised at the chain ends. Additionally its stealth effect has decreased and has therefore developed immune responses. [5, 6] Chemists have developed several polymerisation techniques in order to synthesise alternative reproducible linear PEG based polymers with defined macromolecular structures, like comb polymers. In order to get this, short mono-(meth)acrylate functionalised polyethylene glycol is used as a macro-monomer for the polymerisation. This monomer is called oligo(ethylene glycol) methyl ether (meth)acrylate (OEGME(M)A). By polymerising this with other functional monomers, the polymer's properties can be modified with the aim to overcome the problems which occurred by the solely use of the linear polyethylene glycol. [7] The hydrophilic character of the PEG-side chain leads to a water soluble comb polymer and the ester bonds between the PEG-side chains and the (meth)acrylate units allow additional partial degradation of the material.

Additional functionalisation of polymers are particularly necessary as biomaterials not only consist of one type of polymer and are connected to other compounds, like peptides, proteins or DNA, in order to control the biomaterial's physical, chemical and biological properties. This linkage with biomolecules is called bioconjugation. [8] Native chemical ligation is one example of a technique which has gained importance in peptide and polymer chemistry due to its specificity, high efficiency rates, mild reaction conditions, and performance at physiological conditions. [9] Its drawback however is the release of a toxic thiol compound demanding an additional purification step of the biomaterial before usage. Cyclic compounds like thiolactone and azlactone were found to be promising substitute candidates for this method [10, 11] but have not yet been compared by researches to it in terms of conjugation efficiencies in oligo(ethylene glycol) methyl ether (meth)acrylate based copolymer systems.

Besides that, polyethylene glycol is used for medical applications as hydrogels, a three-dimensional network possessing a high water binding capacity. [12] They can still be improved by the use of polyglycidols, a second linear alternative to polyethylene glycol, containing side chain groups for a higher degree of functionalisation of the polymer beyond the chain ends. [13] Chemical crosslinking is a method for stabilising these three-dimensional polymer networks, e.g. with UV light or in a wet-chemical way. They lead to mechanically stable networks but the irradiation and crosslinking agents may be harmful for cells being inside of the polymer matrix. [14] In contrast to this, physical crosslinking methods are alternatives which stabilise the hydrogel by non-covalent interactions and show a good compatibility with biological systems. Additionally, they give the hydrogel rheological flexibility e.g. for direct injections or 3D printing techniques. The physically stabilised polymer network can be adjusted by the kind and amount of functional groups for physical interactions. [14]

Therefore, **the objective of this thesis** was the synthesis and characterisation of hydrophilic poly(oligo(ethylene glycol) methyl ether acrylate) based copolymers containing peptide binding units and hydrophilic polyglycidol based copolymers containing physical crosslinking units for hydrogel formation.

Chapter 2 gives the reader an overview of the theoretical background of the thesis. First, an introduction into polymers as biomaterials is given (**section 2.1**). After that, in **section 2.2** different methods for the synthesis of polymers will be explained. In **section 2.2.1** the term living polymerisation will be explained. The Reversible Addition Fragmentation Chain Transfer Polymerisation (**section 2.2.2**) will be highlighted with focus on its mechanism and the versatility of the monomer oligo(ethylene glycol) methyl ether (meth)acrylate. After that, an introduction into the anionic ring opening polymerisation of glycidyl ether based monomers is given (**section 2.2.3**) by using either alcoholates as initiators or nucleophiles as initiators assisted with an additional metal complexation. The next sections highlight different methods for the modification of polymers: In **section 2.2.4**, the modification of polymers *via* thiol-ene chemistry will be explained. **Section 2.3** gives an overview of bioconjugation with its definition and techniques (**section 2.3.1**) by explaining the method of native chemical ligation in detail. At the end, an introduction into hydrogels (**section 2.4**) will be given starting with **section 2.4.1** about the definition and characteristics. Crosslinking methods will be explained in **section 2.4.2** with a focus on electrostatic interactions and π-π stacking interactions.

Chapter 3 presents the discussed results divided into three parts:

Section 3.1 is about the synthesis, modification, and characterisation of acrylate based copolymers for the specific bioconjugation technique native chemical ligation. The synthesis of acrylate based copolymers containing oligo(ethylene glycol) methyl ether acrylate with either linear thioester functional 2-hydroxyethyl acrylate, thiolactone acrylamide, or vinyl azlactone *via* the living radical polymerisation technique Reversible Addition Fragmentation Chain Transfer is described in the **sections 3.1.1-3.1.3**. For comparison, additional polymers were synthesised *via* free-radical polymerisation (**section 3.1.4-3.1.6**) with tests in terms of binding of the short model peptide sequence CGGGF (**section 3.1.7**) and the proof of its binding. Additionally, the hydrolytic stability (**section 3.1.8**) of these peptide binding units was investigated.

Section 3.2 describes the synthesis, modification, and characterisation of short linear polyglycidols carrying allyl side groups up to 20 % (targeting of 60 repeating units in total, M_n ~ 4.5 kDa) *via* anionic ring opening polymerisation initiated by the alcoholate potassium *tert*-butoxide. First, the monomer and polymer synthesis are described in **section 3.2.1.** After that, the modification of the allyl functionalities *via* thiol-ene chemistry is presented to obtain positively charged functionalities *via* imidazolium moieties and negatively charged functionalities *via* phosphonamide moieties for hydrogels which should be stabilised *via* electrostatic interactions (**section 3.2.2**). The introduction of electron rich and electron poor compounds on the allyl group for the stabilisation of the hydrogels *via* π–π stacking interactions is described in **section 3.2.3**. Basically, the short polymers were used for finding optimum reaction conditions for the modification of the polymers which should then be transferred to long polymers.

Section 3.3 shows a newly established synthesis, modification, and characterisation of long linear polyglycidols with and without allyl side groups (targeting up to 684 repeating units, M_n ~ 50 kDa) *via* anionic ring opening polymerisation initiated by the salt tetraoctylammonium bromide assisted by the complexation of triisobutylaluminium. After that the polymers were modified with additional charges: Allyl side groups were used for thiol-ene chemistry to obtain positively charged functionalities *via* imidazolium moieties and negatively charged functionalities *via* phosphonamide moieties for hydrogels which should be stabilised by electrostatic interactions. Additionally, the long polyglycidols carrying phosphonamide groups were used either with calcium chloride or with short polyglycidols with imidazolium groups for hydrogel formation tests.

Chapter 4 summarises the results of the thesis in English and in German.

Chapter 5 gives an overview of the experimental section containing the used materials, methods, and the performed synthesis with the corresponding analysis.

2 Theoretical background

2.1 Polymers as biomaterials

"Biomaterials are materials intended to interface with biological systems to evaluate, treat, augment, or replace any tissue, organ, or function of the body. Biocompatibility is the ability of a material to perform with an appropriate host response in a specific application."

(L.S. Nair, C.T. Laurencin, 2005)

In order to fulfil these expectations, biomaterials have to be customised to make sure they are being tolerated by the body without causing any side effects, like allergies or toxicity. [4] From the synthetic material point of view, they can be divided into three categories: Metals, polymers and ceramics (Figure 2.1):

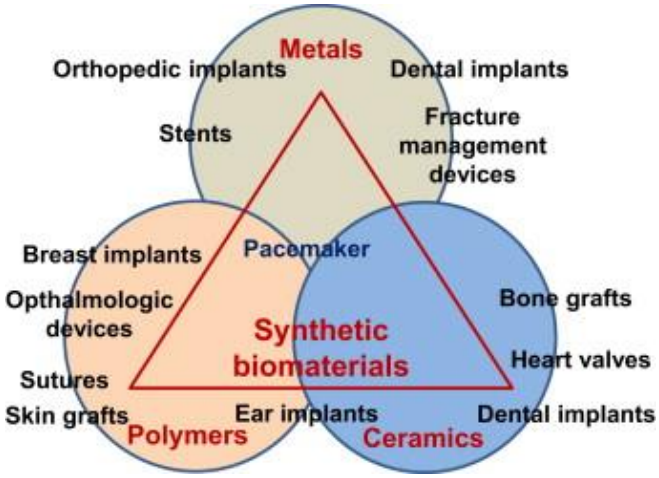

Figure 2.1: Overview of synthetic biomaterials. Reprinted with permission from reference [15]. Copyright 2017 Springer Nature Switzerland AG.

For example, metals can be used as orthopaedic implants, ceramics as dental ones and polymers as skin grafts. Also composite materials are possible like ear implants which consist of polymers and ceramics. Pacemakers are even built from all three material classes. Polymers are promising candidates for many applications, also where ceramics and metals are being used, because they can be modified for its end purpose by having specific physical, chemical and biological properties especially to promote desired cellular interactions. [16] They are molecules of high relative molecular mass consisting of multiple repetitive molecules of low relative molecular mass. [17] The polymer's properties can be tuned e.g. by functional monomers, the polymer chain length and its macromolecular architecture making them versatile as biomaterials. [18] Polymers can either derive from nature or be artificially obtained by chemical synthesis having various biomedical application opportunities (Table

2.1). [19-21] In this work, the focus will be on alternatives to polyethylene glycol based materials which can be used e.g. as hydrogels for waveguides. The aim is to overcome polyethylene glycol's disadvantage like the limited functionalisation at the chain ends and its decreased stealth effect with developed immune response. [5, 6]

Table 2.1: Applications of natural and synthetic polymers. [19-21]

Applications of natural polymers	
Alginate	Wound dressings
DNA	Waveguides
Silk	Optical fibres
Chitosan/cellulose/agarose	Biosensors
Applications of synthetic polymers	
Polyethylene	Epidural catheters
Polypropylene	Mechanical heart valves
Polytetrafluorethylene	Foley catheters
Polyethylene terephthalate	Hip implants
Polymethyl methacrylate	Dental implants
Polyether ether ketone	Orthopaedic implants
Polyamide	Central venous access devices
Polyimide	Cognitive prostheses
Polyurethane	Fetal micro-pacemakers
Polydimethylsiloxane	Implants for nose construction
Polyethylene glycol	Waveguides

2.2 Synthesis of polymers

2.2.1 Living polymerisation

Living polymerisation will be used in this work because it allows the synthesis of polymers with a defined monomer composition and a defined molecular weight. The term "living polymer" was introduced by Michael Szwarc *et al.* in 1956. [22] There he described the polymerisation of styrene *via* electron transfer, which was initiated by sodium naphthalenide. He found anionic species that do not terminate and assumed that the chain propagation continued until all the monomer has been consumed. In order to prove his assumption, he added further styrene and observed that the polymerisation restarted again until full conversion of the monomer. He established the successful synthesis and set a milestone in polymer science with this term "living polymer". In 1991, Owen W. Webster highlighted further properties of the living polymerisation. [23] The degree of polymerisation DP can be controlled by the amount of monomer and initiator (Equation 1) whereas the initiation step has to be at least as fast as the propagation without occurring chain transfers or termination to obtain almost equal chain growth and a control of the molecular weight. This equation applies for a full consumption of monomers:

$$DP = \frac{[\text{Monomer}]}{[\text{Initiator}]} \quad (1)$$

A living polymerisation differs from a free radical or free condensation polymerisation in the polymerisation kinetics. The molecular weight is directly proportional to the conversion of the monomer. [23] Additionally, the polymer's parallel chains growth leads to a very narrow molecular weight distribution according to Poisson resulting in very low dispersities Đ (Equation 2):

$$Đ = \frac{M_w}{M_n} = 1 + \frac{1}{DP} \quad (2)$$

The number average molecular weight M_n and the weight average molecular weight M_w can be determined e.g. by gel permeation chromatography. Given the fact that all polymer chain ends stay active until "killed", different macromolecular architectures can be achieved by living polymerisation techniques: Mono/multiple functional ended, AB/ABA block, graft, comb, star, ladder, cyclic and network polymers. Finally in 1996, the term "living polymerization" was incorporated by the International Union of Pure and Applied Chemistry into their Glossary of Basic Terms in Polymer Science based on the previously mentioned observations during the polymerisation process. There it is described as a chain

polymerisation without a chain transfer and termination. The rate of chain initiation is comparably fast to the rate of the chain propagation leading to a constant number of kinetic-chain carriers throughout the whole polymerisation. [17]

2.2.2 Polymerisation of oligo(ethylene glycol) methyl ether (meth)acrylate *via* reversible addition fragmentation chain transfer

In this work, the polymerisation of oligo(ethylene glycol) methyl ether acrylate will be used by the living free-radical polymerisation technique Reversible Addition Fragmentation Chain Transfer (RAFT) which was introduced by John Chiefari *et al.* [24] in 1998. The polymerisation is controlled *via* a chain transfer agent, also called RAFT agent, which is an organic compound consisting of a dithioester group for the radical transfer, a Z-group for the radical stabilisation, and an R-group for the chain propagation (Figure 2.1.2).

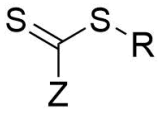

Figure 2.1.2: General structure of a RAFT-Agent. Modified with permission from reference [24]. Copyright 1998 American Chemical Society.

The authors investigated various combinations of Z-groups (e.g. phenyl, methyl) and R-groups (e.g. benzyl, cumyl, cyanopropyl) for the polymerisation e.g. of methyl methacrylate, *n*-butyl (meth)acrylat, styrene, and acrylic acid. The polymerisations showed a linear evolution of M_n depending on the monomer conversion and the obtained polymers possessed low dispersities. Additionally, the RAFT agent's Z- and R-groups could be found at the chain ends which is characteristic for these living polymers. The monomer oligo(ethylene glycol) methyl ether (meth)acrylate (OEGME(M)A) was widely copolymerised with other functional comonomers by various polymerisation techniques, e.g. also RAFT to obtain water soluble polymers, abbreviated as POEGME(M)A. [7] This inspired the use of this monomer with the polymerisation technique for the bioconjugation in this work. OEGME(M)A consists of a polymerisable (meth)acrylate unit combined *via* an ester group with a linear water soluble methyl ether terminated oligo(ethylene glycol) (Figure 2.1.2.2). [7]

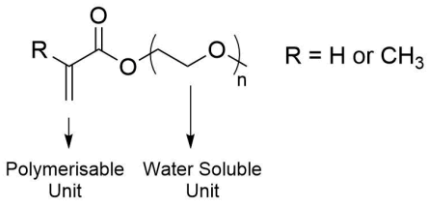

Figure 2.1.2.2: Structure of oligo(ethylene glycol) methyl ether (meth)acrylate. Modified with permission from reference [7]. Copyright 2008 Wiley Periodicals, Incorporated.

The polymerisation process is divided into five steps and is shown in Scheme 2.1.2.1. In this work, the RAFT agent 2-cyano-2-propyl benzodithioate (CPDB) and the initiator 2,2'-azobis(2-methylpropionitrile) (AIBN) were used.

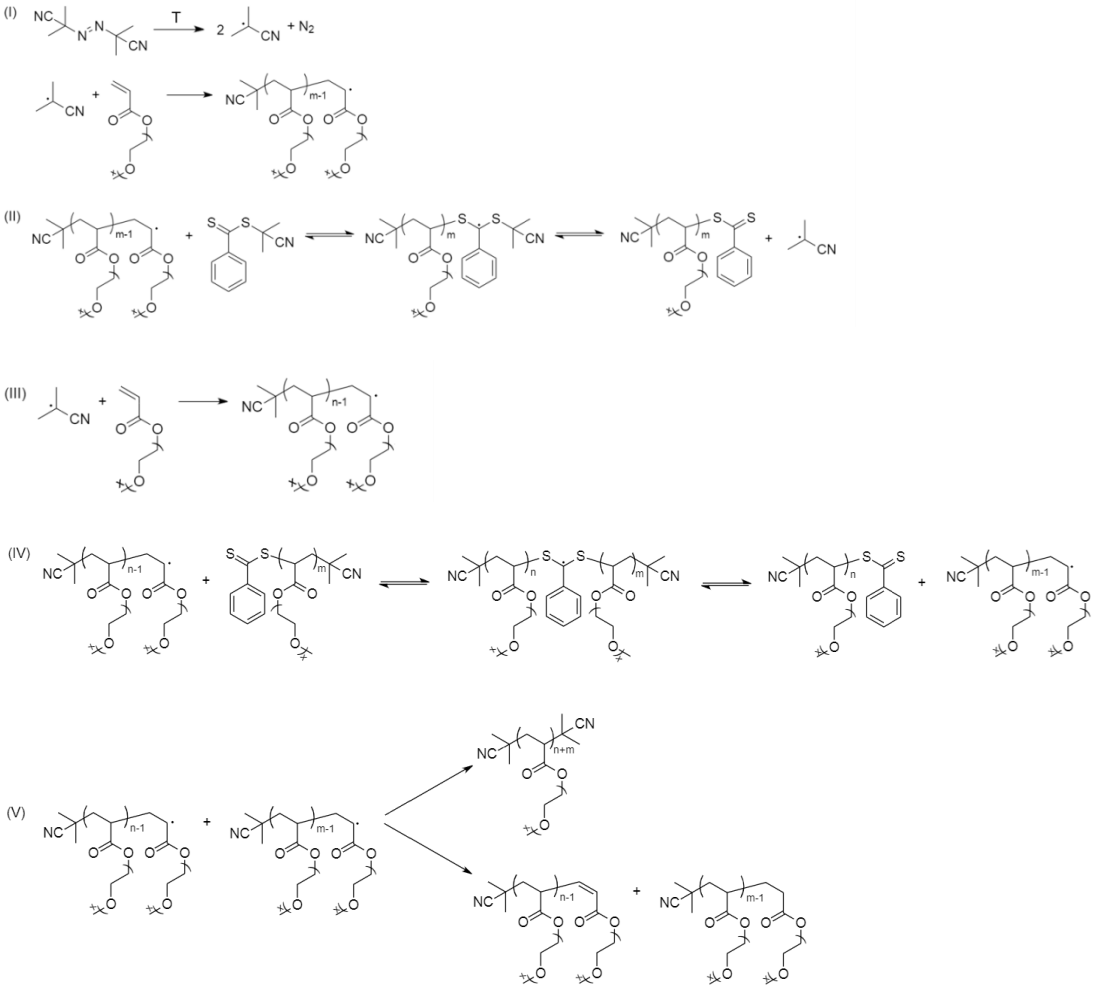

Scheme 2.1.2.1: Mechanism of the RAFT process [25] exemplary with OEGMEA, CPDB and AIBN.

In step (I), the initiation takes place and the formed radical reacts with monomers. The growing polymer chain or residual radicals quickly add to the RAFT agent's reactive C=S group in step (II) and form a radical intermediate which leads to a fragmentation by releasing the R-group (pre-equilibrium). In step (III), the R-group re-initiates the polymerisation and monomers are added until all RAFT agents from step (II) are consumed. Afterwards, the growing polymer chain enters step (IV) where a fast exchange between active and dormant

polymer chain takes place *via* a radical intermediate (main-equilibrium). This ensures the growth of all polymer chains with an equal probability until full consumption of the available monomers or early quenching of the polymerisation. By this, functional monomers can be copolymerised and polymers with similar chain lengths will be obtained by this polymerisation technique. Additionally, the chain length can be controlled and short polymers are targeted in this work due to analytical reasons. The side reaction step (V), termination *via* combination or disproportionation, takes place at a minimum because the majority of the polymer chains are growing with the RAFT agent ([CPDB] >> [AIBN]). [24, 25]

The oligo(ethylene glycol) methyl ether side chain can be varied and has an influence on the polymer's water solubility respectively its lower critical solution temperature in the range of 26-90 °C depending on the amount of repeating units (two until nine ethylene glycol units). Therefore in this work the commercially available OEGMEA with eight repeating units will be chosen to ensure a very good water solubility of the polymer for bioconjugation techniques at room temperatures. OEGME(M)A was copolymerised with various functional monomers by RAFT for bioconjugation by several research groups. The synthesis, modification and characterisation of these polymers are simple and make it therefore easy to transfer it on the polymerisation with other functional monomers for this work. For example, Khairil Karim *et al.* [26] synthesised a statistical copolymer based on OEGMEMA and 3-(trimethylsilyl) prop-2-ynyl methacrylate. Afterwards, the trimethylsilyl protecting groups were removed and the obtained free propargyl groups were used for Cu catalysed azide-alkyne Huisgen cycloadditions with Boc-protected azide modified amino ligands. Subsequent deprotection of the amino groups allowed the conjugation of a modified anticancer drug cisplatin with over 80 %. Furthermore, the authors also showed a successful binding of this macromolecular anticancer drug to DNA. The same research group also modified nanodiamonds by the grafting-to technique for drug delivery [27]: A statistical copolymer based on OEGMEA and an acid labile hydroxyethyl acrylate modified gemcitabine were synthesised by using a dibenzocyclooctyne modified RAFT agent. Afterwards, the obtained polymers were bound on nanodiamonds carrying azide functionalities by the strain-promoted alkyne-azide cycloaddition. The obtained coated nanodiamonds were successfully taken up by cells proven by fluorescence microscopy and showed a pH dependent drug release. Hien Dong *et al.* [28] synthesised also block-copolymers based on OEGMEA, a vinyl benzene modified methanethiosulfonate and pentafluorophenyl acrylate. The copolymers self-assembled into micelles and were crosslinked with a diamine by the reaction with the pentafluorophenyl activated ester. Afterwards, a thiol-modified fluorescein was bound by thiol-exchange

reaction with the methanethiosulfonate group so that the encapsulation of the micelles into cells could be tracked.

2.2.3 Anionic ring opening polymerisation of glycicdyl ether based monomers

An alternative for POEGMEA are polyglycidols, which are PEG chains with additional side functionalities. Polyglycidols will be used in this work for hydrogel formation by using physical crosslinking methods. Glycidol is an ethylene oxide (1) derivative carrying a methylene alcohol group (2) and glycidyl ether based monomers (3) contain this alcohol group protected in form of an ether (Figure 2.1.3). [29]

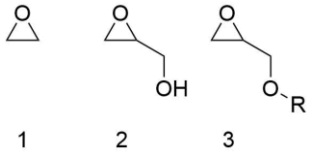

Figure 2.1.3: Ethylene oxide (1), glycidol (2) and glycidyl ether based monomer (3). Modified with permission from reference [29]. Copyright 2009 Wiley Periodical, Incorporated.

For the polymerisation of glycidols, there exist two anionic ring opening polymerisation techniques: (1) The initiation by alcoholates and (2) the initiation by nucleophiles with assisted complexation.

2.2.3.1 Alcoholate initiated polymerisation

In 1966, Stanley R. Sandler and Florence R. Berg polymerised for the first time in history glycidol and used several basic initiators e.g. sodium hydroxide or trimethylamine. A hyperbranched product was obtained. [30] This inspired Edwin J. Vandenberg to introduce the protection groups trimethylsilyl and *tert*-butyl to obtain linear polyglycidols by using potassium hydroxide as initiator in 1968. [31] The polymerisation process of glycidyl ether based monomers is divided into three steps and is shown in Scheme 2.1.3.1-1: In step (I), the initiation takes place where the nucleophilic alcoholate (e.g. KO^{t}Bu) attacks the lower substituted position of the monomer. The epoxide opens and the formed alcoholate is stabilised *via* the metal cation from the initiator. In case of glycidols, an H-transfer can take place (H). This new alcoholate continues in step (II) the propagation and performs further nucleophilic attacks on remaining monomers. Protected glycidols lead to a linear and unprotected ones lead to a hyperbranched polymer. In step (III), the termination can be performed by the addition of electrophiles or H-donors (e.g. alcohols). The subsequent

removal of the protection groups (e.g. acetale with strong acid) leads to a linear and water soluble polyglycidol (D). [13, 32, 33]

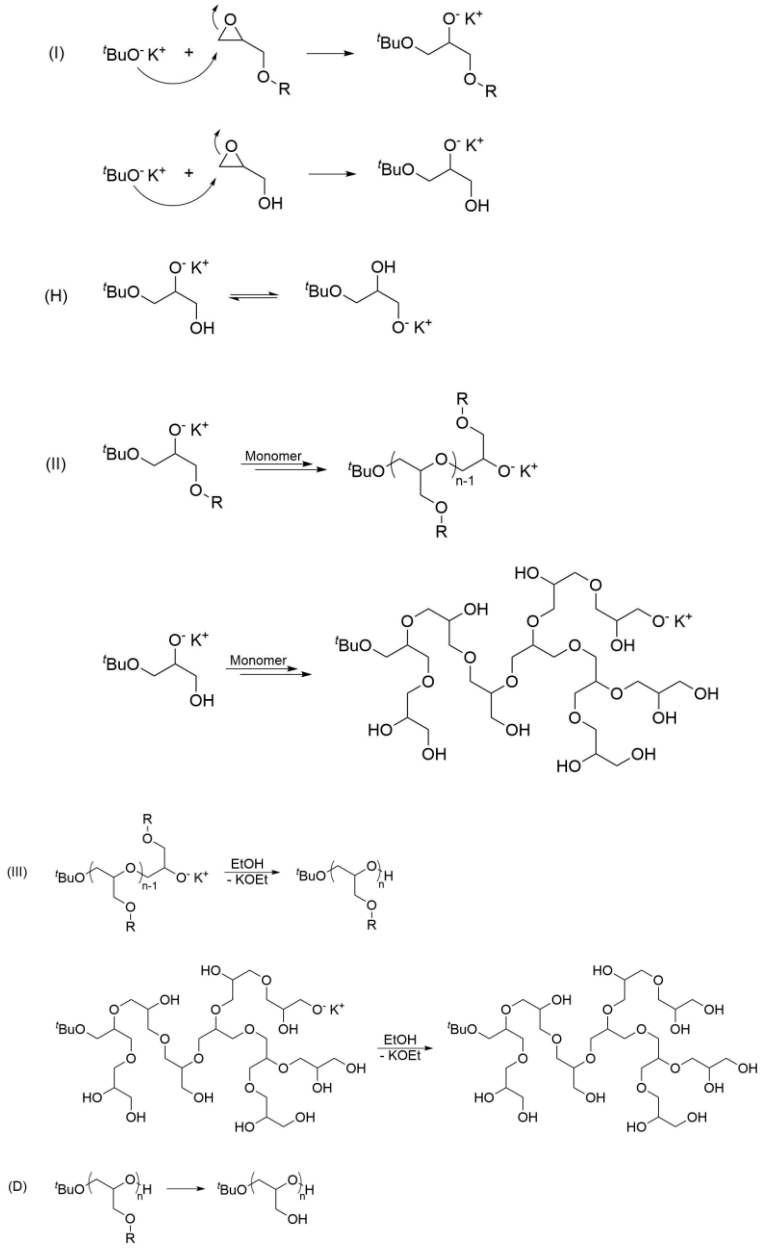

Scheme 2.1.3.1-1: Initiation (I), H-transfer (H), propagation (II), termination (III) and deprotection (D). Modified with permission from reference [33]. Copyright 2016 by the authors; licensee MDPI, Basel, Switzerland.

With this polymerisation technique, various research groups synthesised linear and hyperbranched polyglycidols: Michael Erberich *et al.* [34] described the preparation of linear polyglycidols containing two orthogonal protecting groups (e.g. *tert*-butyl, allyl, ethyl vinyl ether) which could be selectively removed *via* acidic hydrolysis or hydrogenation. ABA block copolymers were synthesised by Silvia Halacheva *et al*. [35] In there, the research group used polypropylene oxide as a macroinitiator to polymerise protected glycidol in order to obtain a Pluronic mimic after deprotection. These ABA block copolymers form micelles in aqueous

solution. The authors have shown that the temperature and the chain length of the polyglycidols lead to different critical micelle concentrations. Marc Hans *et al.* [36] synthesised linear and star-shaped polyglycidols, which were later used as macroinitiators for the polymerisation of ε-caprolactone. The combination of the biocompatible polyglycidol and the biodegradable poly(ε-caprolactone) shows potential use for biomedical applications such as drug carriers. Hyperbranched polyglycidols were synthesised by Dirk Steinhilber *et al.* [37] which were crosslinked in order to obtain particles. The size of these could be controlled *via* the templating method, either 32 nm *via* miniemulsion or 140-220 nm *via* microfluidic emulsification. Daniel Wilms *et al.* [38] gave an overview about modifications and applications of hyperbranched polyglycidols. In there, macromolecular architectures like block copolymers, multiarm stars, and hyperbranched nanocapsules are presented. Drug delivery and protein resistance surfaces are potential biomedical applications for these polymers.

Due to the strong basic character of the alcoholate, H-abstraction on the methylene side group of the monomers is occurring as a side reaction. This leads to a rearrangement of the monomer generating a new alcoholate species which performs as an initiator at later time points and causes an unequal polymer chain growth. [13] Additionally, a chain transfer and therefore an early termination avoids the synthesis of long polymer chains. These scenarios lead to an increased dispersity of the polymer in the end and are prominent drawbacks of this polymerisation method. [29] The occurring side reactions are shown in Scheme 2.1.3.1-2. Slow monomer addition is one method to overcome this problem by avoiding an excess of free monomers in presence of the initiator and to supress the described side reaction. [39]

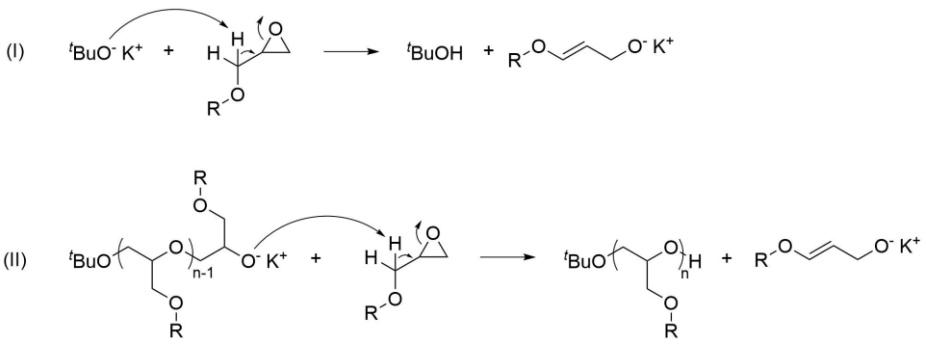

Scheme 2.1.3.1-2: Reaction between monomer and initiator (I) and growing chain end (II). Modified with permission from reference [29]. Copyright 2009 Wiley Periodical, Incorporated.

2.2.3.2 Nucleophilic initiated and metal complex assisted polymerisation

This polymerisation method will be used in this work because it is a method to synthesise high molecular weight polyglycidols. The initiation by nucleophiles with metal assisted complexation does not lead to chain transfer reactions and polymers with low dispersities can be obtained. [6] The polymerisation process consists of five steps and is shown in Scheme 2.1.3.2 which was introduced by Alain Deffieux [40]. Step (I) – (III) are favoured at low temperatures in the range -30 – 0 °C depending on the targeted polymer chain length. In step (I), the monomer is activated by the coordination of the oxygen of the monomer with the aluminium of the catalyst (e.g. triisobutylaluminium). Afterwards, the catalyst reacts with the initiator salt (e.g. tetraoctylammonium bromide) by forming an "ate" complex in step (II). This is followed by the initiation process in step (III) by the nucleophilic attack of the anionic part of the "ate" complex on the lower substituted side of the monomer. The resulting alcoholate after the ring opening remains and is coordinated to the aluminium catalyst which is stabilised by the cation of the initiator salt. In step (IV), the propagation takes place by the coordination (C) between the oxygens of the monomer and the aluminium catalyst ensuring the proper chain growth of the polymer which can be run at various temperatures depending on the monomer, the targeted molecular weight, the catalyst-initiator-ratio and the monomer concentration. Termination proceeds in the end in step (V) by the addition of electrophiles or H-donors (e.g. alcohols). [6, 41]

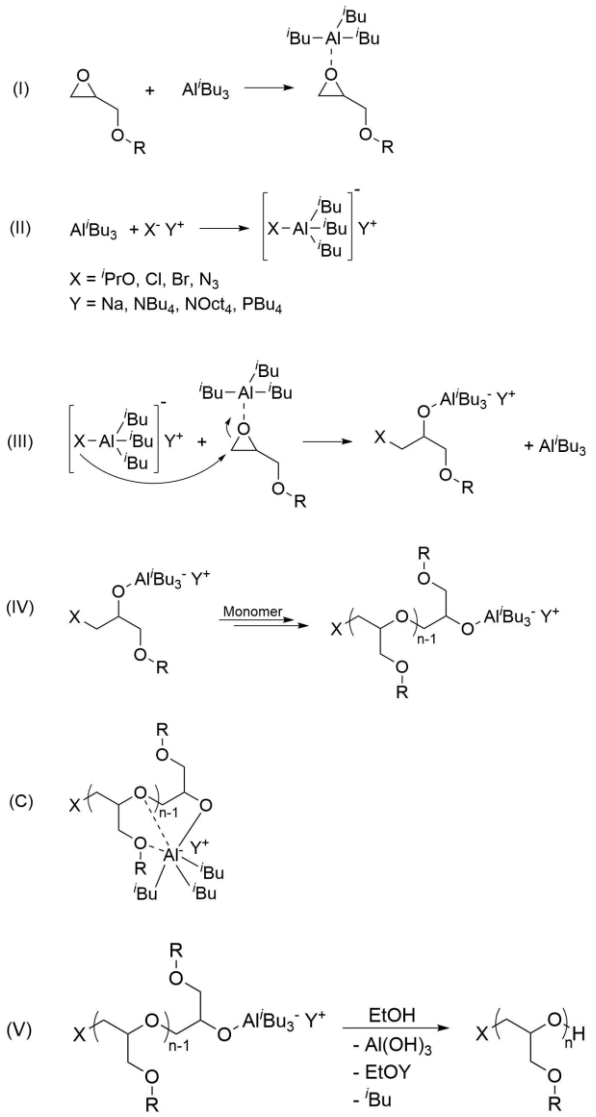

Scheme 2.1.3.2: Epoxide activation (I), "ate" complex formation (II), initiation (III), propagation (IV), complexation (C) and termination (V). Modified with permission from reference [6] (I-V) and [41] (C). I-V: Copyright 2015 American Chemical Society. C: Copyright 2010 American Chemical Society.

Various monomers were polymerised by this technique: Stéphane Carlotti *et al.* [40] synthesised polypropylene with molecular weights up to 27 kD using alkali metal *tert*-amyloxides (metal = Li^+, Na^+, K^+)/sodium *iso*-propanolate with triisobutylaluminium as catalyst. The same research group polymerised ethylene oxide, propylene oxide, epichlorohydrin, and ethoxyethyl glycidyl ether with tetrabutylammonium azide as initiator and triisobutylaluminium as catalyst. The catalyst/initiator-ratio and monomer concentration were varied in order to obtain molecular weights in the range 5-30 kDa with dispersities in the range 1.10-1.30. [42] In follow-up experiments, the authors investigated the homopolymerisation of ethoxyethyl glycidyl ether, *tert*-butyl glycidyl ether and the copolymerisation of ethoxyethyl glycidyl ether with propylene oxide and of *tert*-butyl glycidyl ether with butane oxide more in detail by using tetraoctylammonium bromide as initiator and triisobutylaluminium as catalyst. [41] Here the catalyst/initiator-ratio and

monomer concentration were varied as well resulting in molecular weights for poly(ethoxyethyl glycidyl ether) in the range 10-85 kDa with dispersities in the range 1.03-1.30. Poly(*tert*-butyl glycidyl ether) was obtained with molecular weights in the range 14-52 kDa with dispersities in the range 1.02-1.37. The copolymers had molecular weights in the range 12-36 kDa with dispersities in the range 1.14-1.58. Furthermore, the same research group polymerised allyl glycidyl ether with and without epichlorohydrin by using the same initiator and catalyst. [43] By variation of the catalyst/initiator-ratio and monomer concentration, molecular weights in the range 3-70 kDa with dispersities in the range 1.06-1.37 were obtained. Ethoxy ethyl glycidyl ether and allyl glycidyl ether were for the first time copolymerised by Siwei Liu *et al.* [44] and attempted copolymers with molecular weights in the range of 11-21 kDa. The synthesised copolymers contained an AGE-ratio of 13-59 %. But the polymerisations were run constantly at 0 °C which led to dispersities in the range 1.43-1.76. This inspired a detailed investigation of the copolymerisation in this work with attempts of similar and higher molecular weights with narrow dispersities which have not been reported in literature yet. Silke Heinen *et al.* [45] copolymerised methyl glycidyl ether with ethyl glycidyl ether with the same catalyst/initiator and obtained molecular weights in the range 2-25 kDa with dispersities in the range 1.05-1.23 which showed thermoresponsive behaviour. The same authors functionalised these polymers with thiols/disulfides at the chain end and used them as an anchor groups for the attachment on gold surfaces. [46] The grafting density and polymer chain overlap could be tuned *via* the molecular weight of the polymer, the anchor group, and the conditions for the grafting-to procedure. Furthermore, the research group copolymerised the same monomers with a monomer carrying a UV-labile benzophenone group for coatings of polystyrene. [47] After UV-irradiation, a covalent immobilisation of the polymer was obtained and human dermal fibroblasts were seeded on it. Due to the polymers thermoresponsive behaviour, the cells could be removed as a sheet.

2.2.4 Modification of polymers *via* thiol-ene chemistry

Thiol-ene reaction will be used in this work for the modification of polyglycidols as it is a very fast and efficient modification reaction with high yields and a flexible choice of solvents. This reaction describes the hydrothiolation of a C=C bond, which can be performed in presence of e.g. radicals, phosphine/amine/metal catalysts. [48, 49] The mechanism for a radical induced thiol-ene reaction is shown in Scheme 2.1.4 which is initiated by a photoinitiator and light. [48]

The reaction cycle consists of four steps: In step (I), the photoinitiator decomposes under irradiation of light and creates a radical which reacts in step (II) with the thiol group under H-abstraction and forming a thiyl-radical. The generated thiyl-radical reacts in step (III) with the C=C bond at the lower substituted position of the alkene by forming the *anti*-Markovnikov product. The radical is transferred to the initial secondary carbon atom of the alkene. In the last step (IV), this radical abstracts an H-atom of another thiol group generating the final thiol-ene product and a new thiyl-radical which starts the cycle from the beginning. [48]

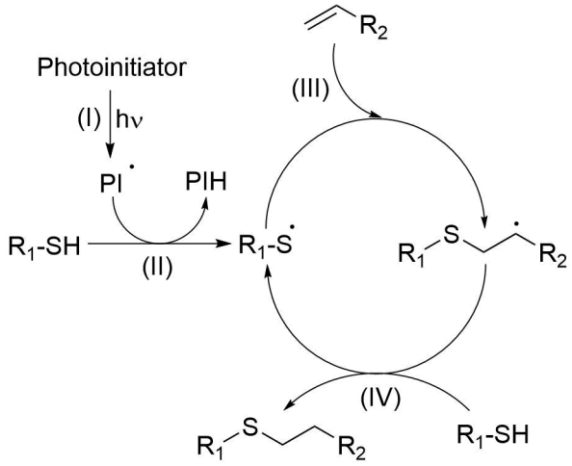

Scheme 2.1.4: Mechanism of the radical induced hydrothiolation of a C=C. Modified with permission from reference [48]. Copyright 2010 The Royal Society of Chemistry.

Charles E. Hoyle, Christopher N. Bowman, [50] and Andrew B. Lowe [48, 51] gave overviews of the kinetics of the thiol-ene reaction with different thiol-compounds (e.g. methanetiol, hexanethiol, three/four-arm PEG-stars with terminal thiol groups) and ene-compounds (e.g. triethyleneglycol divinyl ether, triallyl-functionalised pentaerythritol). The authors showed that different classes of polymers can be modified with this reaction what makes it interesting to transfer it to polyglycidols: Matthias Kuhlmann *et al.* [52] attached a thiol-linker containing a cysteine functionality onto the polymer which was used for binding of peptides *via* native chemical ligation. Simone Stichler *et al.* [53] modified the polymers with ester-containing/ester-free thiols for the production of hydrogels for 3D-printing. There, the amount of polymer and time for the crosslinking were varied which influenced the hydrogels' properties. The same research groups also investigated thioether containing polymers (e.g. with cysteamine hydrochloride, thioacetic acid, 1-dodecane thiol) as coatings for the stabilisation of gold-nanoparticles [54] and ester-containing/ester-free thiol modified polymers for the synthesis of nanogels for labelling and drug delivery. [55, 56]

2.3 Bioconjugation

2.3.1 Definition and techniques

Bioconjugation means the linkage of a biomolecule with one or more other moieties which could also be a biomolecule, a synthetic polymer, or small molecules like drugs, ligands, or fluorescent dyes by the reaction of specific functional groups. By this, a new complex will be formed that have combined properties of its individual compounds. [8] The motivation for this technique derived from various fields like understanding biological interactions, developing biochemical assays, investigating diagnostic methods, enhancing water solubility of hydrophobic proteins, and improving chemical syntheses catalysed *via* enzymes in industry. [57]

Various specific chemical reactions can be used for bioconjugation which have been described comprehensively: Martina Stenzel [58] described methods for thiol-ene chemistry by using thiol functionalised proteins, DNA, and carbohydrates. These could react with halogen compounds, C=C (ene, vinylsulfonone, maleimide) / C≡C (yne) bonds, pyridyl disulfides, thiosulfonates, bisulfones, and thioester groups. The usage of maleimides was highlighted by João M.J.M. Ravasco *et al.* [59] who gave insights into topics like strategies of hydrolytically stable thiosuccinimide conjugates, impact of protein microenvironment in thiosuccinimide hydrolysis/bioconjugate plasma stability, impact of intramolecular acid/base catalysis for hydrolysis, impact of acetal containing maleimide in plasma stability, the role of maleimide alkene substitution in post-conjugation hydrolysis, mono/di-bromomaleimides as reversible scaffolds for reactions with peptides, and therapeutic applications of peptide conjugates. Omar Boutureira and Gonçalo J.L. Bernardes [60] highlighted advanced chemical modification methods of proteins besides the before mentioned ones. This includes for example the reactions of amines with active esters, iso/thio-cyanates, aldehydes, imino compounds, diazonium salts and ketenes. Active esters and iso/thio-cyanade groups are very active, however they are not specific. This motivates the use of specific bioconjugation methods like thiol-ene and native chemical ligation in this work. More bioconjugation techniques on amino acids, peptides, and proteins were performed for diagnosis and therapeutic applications. [61-63] Xianglong Hu *et al.* [64] investigated metal-free Michael additions of carbonyl activated alkynes with amines, thiols, and alcohols. The alkyne compounds carried activation groups like ethyoxyl, phenyl, triphenylamine, or tetraphenylethylene. The nucleophiles derived from a synthetic polymer, carbohydrates, peptide, and protein which could be fluorescently labelled by the binding with

triphenylamine. A more detailed insight into bioconjugation techniques with aromatic compounds was given by Chi Zhang *et al.* [65] Several arylation methods of peptides and nucleic acids were presented, e.g. for biosensing and catalysis: cysteine modification was possible *via* nucleophilic substitution with aryl chlorides, dichlorotetrazine, heteroaryl methylsulfones, perfluoroarenes, and with metal catalysts. Other amino acids like lysine, tyrosine, and tryptophan could also be modified *via* nucleophilic substitution with aryl halogenides and with metal catalysts. Aryl compounds reacted with nucleic acids containing halogenated purine and pyrimidine bases or by modification of primary amines with halogenated benzoic acid with subsequent arylation. Although these reactions were specific and were performed at mild and biomolecule compatible conditions, the functional groups are very hydrophobic and bulky. This could lead to solubility and reactivity problems by using these groups at water soluble polymers, e.g. due to self-assembly and shielding effects for bioconjugation. Therefore the native chemical ligation was chosen for this work which does not have these disadvantages.

2.3.2 Native chemical ligation

Native chemical ligation is a bioconjugation technique which derived from the common peptide synthesis reported by Philip E. Dawson *et al.* [9] in 1994. There, the researchers combined an unprotected peptide carrying a C-terminal thioester group with an unprotected peptide carrying an unprotected N-terminal L-cysteine residue. It has been chosen for this work because it is a very selective technique which selectively conjugates terminal unprotected cysteines that does not require deprotection steps and purification with great effort. The reaction mechanism of the native chemical ligation in peptide chemistry is shown in Scheme 2.2.2-1.

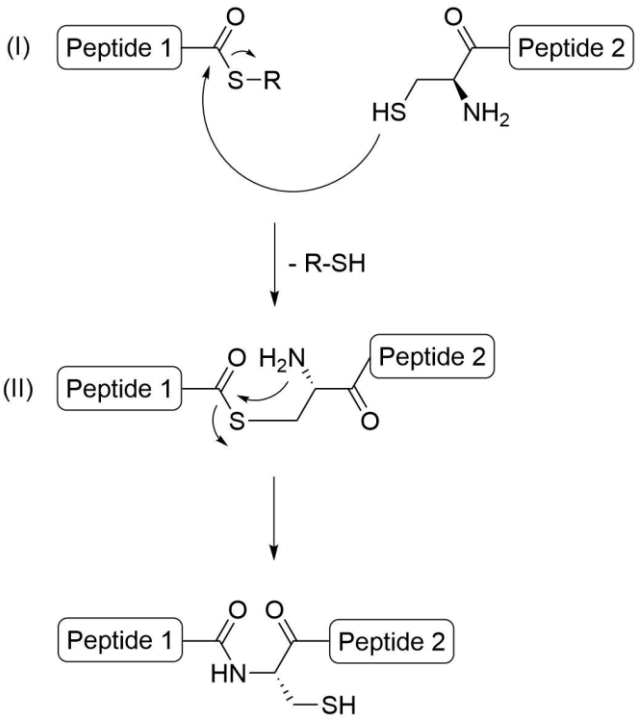

Scheme 2.2.2-1: Mechanism of native chemical ligation transthioesterification (I) and rearrangement (II). Modified with permission from reference [66]. Copyright 2009 Springer Nature Switzerland AG.

The mechanism consists of two steps: In step (I), the thiol functionality of the cysteine at the N-terminal of the peptide reacts with the thioester group at the C-terminal of the peptide by forming a new thioester bond and releasing a thiol RSH (chemoselective transthioesterification). Afterwards, a spontaneous rearrangement takes place in step (II). There, the free amine group of the cysteine reacts with the neighbouring thioester group (S→N acyl shift) forming a new amide bond and releasing the free thiol group of the cysteine. [9] Both peptides are now stably connected *via* an amide linkage.

Philip E. Dawson *et al.* [9] used an alkyl group at the thioester and showed that this reaction was faster by using an electron withdrawing and better leaving group like 5-thio-2-nitrobenzoic acid. The pH-value also had an influence on this reaction: at pH = 7 the reaction finished after 5 min and at pH = 5 only ~ 50 % conversion was observed. This is reasonable because the thiol group is protonated under acidic conditions which lowers the thiol's nucleophilic character. Additionally, a slightly reductive medium was important to prevent oxidation of thiol groups from cysteine. This successful technique was proved by the authors by the preparation of human interleukin 8 which is a peptide consisting of 78 amino acids. With that, a milestone in the history of peptide synthesis was set as before only peptides up 50 amino acids could be synthesised *via* stepwise solid phase peptide synthesis. [67] Furthermore, native chemical ligation did not show any racemisation at the site of the ligation

and addition of denaturing agents (e.g. 6 M guanidine hydrochloride) even allowed this technique at high concentrations of reactants without occurring aggregation. [68]

Several research groups investigated this mechanism and introduced improvements for the native chemical ligation system: Tilman M. Hackeng *et al.* [69] investigated this reaction with all 20 amino acids at the C-terminal peptide and showed that all of them are suitable but Valine, Isoleucine, and Proline possessed slow ligation rates. A systematic study of the environmental thiol additives for the catalysis of the transthioesterification was performed by Erik C.B. Johnson and Stephen B.H. Kent. [70] In there, various thiol compounds (e.g. 3-mercaptobenzoic acid, 3-mercaptophenol, thiophenol, benzyl mercaptan) were investigated and showed different ligation rates. The results showed that 4-mercaptophenylacetic acid was faster than the commonly used thiophenol/benzyl mercaptan or sodium-2-mercaptoethanesulfonate. Wen Hou *et al.* [71] introduced a thiol acid capture strategy to combine multiple peptides step by step. Anne C. Conibear *et al.* [72] gave an overview of novel techniques to combine synthesised and expressed proteins. In there, the authors described the kinetic control of this reaction, unmasking of thioester precursors, acryl hydrazides as masked thioesters, and acetamidomethyl/thioazolidine/selenazolidine as protection groups. Further improvements of the introduction of thioesters were investigated by Dillon T. Flood *et al*. [73] There, first a hydrazide was introduced at the carboxylic acid which reacted with acetyl acetone in order to form acyl pyrazole. This is a good leaving group and was easily exchanged by thiol compounds under mild conditions followed by native chemical ligation. The thiol compounds for the transthioesterification show a very good reactivity for native chemical ligation but are also toxic which was highlighted by Heike Rohde *et al*. [74] who wanted to overcome this problem. The research group performed successful reactions with tris(2-carboxyethyl)phosphine to prevent disulfide formation and replaced the thiol compounds by sodium ascorbate. Additionally, the non-toxic and highly water soluble sodium ascorbate acted as a radical scavenger preventing tris(2-carboxyethyl)phosphine from desulfurisation of cysteine as side reaction. Matthias Kuhlmann and Michael Schmitz transferred the native chemical ligation from peptides to synthetic polymers. Matthias Kuhlmann [52] modified polyglycidols with side chains carrying N-terminal cysteine residues for peptide binding. The same method was used by Michael Schmitz [75] with polyoxazolines. Bi-Huang Hu *et al.* [76] used native chemical ligation with polymers for hydrogel formation. The research group modified the end groups of four-arm star-PEG either with N-terminal cysteine or thioester groups. They could show that a hydrogel was formed *via* native chemical ligation when both kinds of star-PEGs were combined. This

technique was also used by Kristel W.M. Boere *et al.* [77] who worked with PEG and hyaluronic acid as precursor polymers. They used linear PEG as a terminal bifunctional macroinitiator with bound azo based initiators to copolymerise in a radical way *N*-isopropylacrylamide with cysteine functionalised 2-hydroxypropyl methacrylamide. The thioester groups were introduced at the chain ends of a liner PEG and at the side groups of hyaluronic acid. Hydrogels could be formed by the addition of cysteine functionalised PEG either with thioester functionalised PEG or thioester functionalised hyaluronic acid.

One method to overcome the problem with the released toxic thiol compound after the native chemical ligation is the use of the cyclic form of the thioester: the thiolactone. [78, 79] Zhiping Fan *et al.* [10, 80] functionalised the side groups of poly(γ-glutamic acid) with homocysteine thiolactone hydrochloride and ε-polylysin with cysteine *via* amidation reaction. By combining both functionalised polymers, hydrogels were obtained *via* native chemical ligation. The improved effect by the absence of the free toxic thiol group was shown by the very high cell viability of the cytotoxicity tests.

Another interesting cyclic compound is vinyl azlactone which was used by Samantha K. Schmitt *et al.* [11, 81] The authors copolymerised this monomer with oligo(ethylene glycol) methyl ether methacrylate/glycidyl methacrylate and bound this polymer on a polycarbonate/silicon surface *via* the epoxide functionality. Afterwards, cysteine functionalised peptides at the N-terminal were added and could be bound *via* native chemical ligation in water without the release of any toxic side products. The successful binding was proven by cell tests as the cells remained on the coating which carried the cell binding peptide sequence RGD. But the general disadvantage of azlactone is its very high reactivity with all nucleophiles which are competitive to the cysteine in the native chemical ligation reaction. Therefore the choice of the solvent is also important for this reaction. Julia Liebscher [82] introduced the functional group azlactone on the side chains of polyoxazolines in two steps: First, poly(2-ethyl-2-oxazoline-*co*-2-butenyl-2-oxazoline) was functionalised with *N*-(3-mercapto-1-oxopropyl)-2-methylalanine *via* thiol-ene chemistry. In a second step, the ring closure of the attached compound led to azlactone which was used successfully for native chemical ligation in dry DMSO. Figure 2.2.2-2 shows the linear thioester, cyclic thioester/thiolactone, and azlactone groups for native chemical ligation which will be investigated in this work in OEGMEA based copolymers which have not been reported in literature yet.

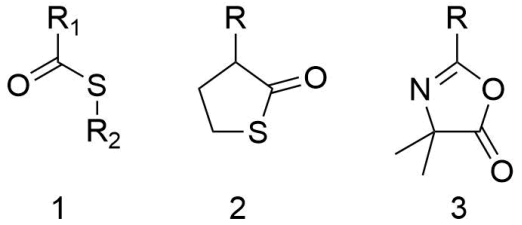

Figure 2.2.2-2: Linear thioester (1), cyclic thioester/thiolactone (2) and azlactone (3) groups for native chemical ligation. Modified with permission from reference [76] (1), [78] (2) and [11] (3). 1: Copyright 2009 American Chemical Society. 2: Copyright 2013 American Chemical Society 3: Copyright 2015 WILEY-VCH, Verlag GmbH & Co. KGaA, Weinheim.

Native chemical ligation is a growing research field over the past 25 years and shows much potential for the modification of peptides with various and promising applications. Researchers are provided with the newest and important synthetic methods [83] and protocols [84] from 2019 for studying protein functions, developing novel therapeutics and designing new materials in the future.

2.4 Hydrogels

2.4.1 Definition and characteristics

A hydrogel is a three-dimensional network consisting of hydrophilic polymers, which swells in water or aqueous solutions and can retain large amounts of solution while maintaining its three dimensional structure *via* chemical or physical crosslinks of the polymers. [85]The formed networks can be classified in four categories based on the preparation method of the respective hydrogel: A homopolymeric network consists of one type of monomer based polymers while copolymeric systems contain at least two different monomers. A semi-interpenetrating network consists of at least two polymers whereas one acts as a stable network and contains the other free non-crosslinked polymer, which loosely interacts with the network. In case of an interpenetrating network, the second incorporated polymer is also crosslinked with itself. [86] The applied polymers can be distinguished between natural and modified natural polymers (e.g. alginate, gelatine and modified cellulose) as well as purely synthetic polymers (polyacrylamide, poly(ethylene glycol), poly(vinyl alcohol)). [87] Based on the used polymers, the hydrogel's properties like swelling, stiffness, shape memory behaviour, self-healing, and stimuli-responsiveness towards pH, electric or magnetic fields, light or temperature can be tuned in wide ranges. For example, the swelling behaviour can be controlled by the crosslinking density of the polymers and the stimuli-responsiveness by the choice of functional monomers. [88, 89] The hydrogel's ability to keep large amounts of water combined with the excellent biocompatibility of the used polymers, render hydrogels

important candidates for the development of implantable biomaterials. [90] For these applications properties, like degradability, injectability, pore size, sterilisability, and incorporation of living cells as well as the release of active drugs substances, became important topics for the current hydrogel investigations. [91]

2.4.2 Crosslinking methods

For hydrogels, there exist two main types of crosslinking methods: Chemical and physical network formation. [92] The chemical crosslinking describes the covalent and quite stable linkage of polymers e.g. either with solely functional monomers or with additional crosslinkers *via* e.g. radical, addition or condensation reactions. [93] Remaining chemical and eventually toxic crosslinking agents have to be removed properly from the hydrogel before they can be applied e.g. for biomedical applications. They may also affect the chemical integrity of entrapped substances, like drugs, proteins or cells, and thereby change their bioactivity and cellular behaviour. [93] In order to overcome this problem, physical crosslinking methods were chosen in this work. The physical crosslinking describes the noncovalent linkage of polymers *via* reversible physical interactions which is important e.g. for rendering hydrogels stimuli-responsive, self-healing, and injectable, which is possible due to the reversible intermolecular interactions. [94] Various physical crosslinking methods have been explored, which include: ionic interactions, crystallisation, hydrogen bonds, hydrophobic interactions (π–π-stacking, host-guest-complex), metal coordination, and mixed systems forming hydrogen bonds and hydrophobic interactions, like coil-coil and antigen-antibody binding. [93, 94]

2.4.2.1 Electrostatic interactions

Polymers which carry positive or negative charges are called polyelectrolytes and form complexes *via* electrostatic interactions with oppositely charged polymer. [95] These charges can be at the polymer side chain and/or polymer main chain/backbone generated by polymerisation of charged monomers or charge functionalisation after polymerisation. [96] They are either permanent (e.g. quaternary amines) or non-permanent depending on the pH-value of the solution (e.g. carboxylic acid, primary amine) and enable a high-water solubility of the polymer due to the high solvation of water molecules around the charge. Another characteristic of these types of polymers is their intra- and intermolecular repulsion due to the similar charges resulting in an extended and stretched appearance instead of a random coil structure of the polymer chain in the solution. [97] This behaviour can be altered by increasing of the ionic strength of the solution by the addition of salts but a too high salt concentration leads to a precipitation of the polymer due to the charge screening from water molecules. [98] Polyelectrolytes which carry both charges are called zwitterionic and possess a very high dipole moment causing a very high polar host matrix with a strong solvation for the incorporation of polar/ionic guest molecules in solution. [99] Electrostatic interactions are good for hydrogel stabilisation but permanently charged compounds may also be harmful for cells and act antibacterial. [100]

Nitrogen based aromatic monomers became interesting for researches as these are able to undergo multiple interactions for stabilisation: Hydrogels based on poly(*N*-vinyl imidazole) were investigated in various protonated states/pH-values exhibiting different swelling behaviour due to the changes in hydrogen bond strengths. [101, 102] Imidazole can also form metal complexes by the coordination of the nitrogen with metal ions like zinc and give shape memory properties to hydrogels. [103] Additionally, these moieties can be stacked due to their partial hydrophobic character and the interaction of the molecular orbitals of the aromatic rings. [104] Besides these (meth)acrylate/vinyl based polymers, the introduction of imidazolium groups at the biocompatible poly(ethylene glycol) was of great interest. [105] In there, the authors modified poly(epichlorhydrin) with 1-methylimidazole and obtained a cationic polyether based on the positive charge of the quaternary nitrogen atom stabilised with various counter anions. So far, linear polyglycidols carrying imidazolium groups were not reported and will be investigated in this work.

In terms of negatively charged monomers, phosphonate based compounds became important due to their high occurrence in nature and role in biochemical processes. [106] It possesses

two acidic protons with $pK_{a,1}$ = 1.1-2.3 and $pK_{a,2}$ = 5.3-7.2 depending on the functional group next to the phosphorus. [107] Benjamin Canniccioni *et al.* [108] showed that the polymerisation of protected as well as deprotected phosphonate based methacrylate monomers was possible *via* RAFT. Poly(vinylphosphonic acid) and hyaluronic acid were used as negatively charged precursor polymers for the hydrogel formation with chitosan as a precursor polymer carrying positive charges *via* the primary amine groups. [109] Zwitterionic copolymer systems based on vinyl phosphonic acid/acrylamide, [106, 110] vinyl phosphonic acid/*N*-isopropyl acrylamide [111], and sulfobeatine methacrylate/methacryloyloxymethyl phosphonic acid [112] showed promising applications as hydrogels for cell adhesion and coatings for anti-fouling applications. Hassan Srour *et al.* [113] introduced phosphonate groups at the chain ends of polyacrylates with pendant imidazole groups (Figure 2.3.2.1) to form hydrogels. So far, the only reported linear polyglycidol with pendant phosphonate groups was reported by Jens Köhler *et al.* [114] who modified the hydroxyl groups of the polymer with diethyl vinyl phosphonate *via* base catalysed Michael addition with subsequent deprotection. Therefore the aim of this work is to introduce the imidazolium/phosphonate groups at allyl functionalised polyglycidols and investigate their hydrogel formation behaviour which have not been reported in literature yet.

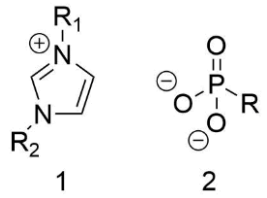

Figure 2.3.2.1: Positively charged imidazole (1) and negatively charged phosphonate (2) group. Modified with permission from reference [113]. Copyright 2014 WILEY-VCH Verlag GmbH & Co. KGaA, Weinheim.

2.4.2.2 π-π Stacking interactions

π–π Stacking interactions describe the arrangement of two or more organic compounds with π-electrons driven by their quadrupole moments and dispersion interactions. [115] These compounds can be aromatic like benzene-derivatives, non-aromatic like quinone-derivatives and non-cyclic like tetracyanoethylene. [116]The strength of the π–π stacking interactions depends on the distribution of the π-electrons which again depends on the substituents of the compounds and the solvent. These factors polarise the π-electrons and lead to compounds being called electron rich and electron poor. [117] The distance and angle between the π-systems also have an influence as the quadrupole-moments will interact with different strengths. [118] Multiple π-conjugated systems lead to layer-by-layer π–π stacking, higher

stabilisation exhibiting fast charge transport and ion conductivity but a too bad solubility in common organic solvents due to their rigid structure. [119] Mechanical dynamic simulations and quantum mechanical calculations are important methods to determine interaction energies of π–π stacked systems [115] and in order to understand phenomena like porphyrin aggregation, conformation of diarylnaphthalenes/phenylacetylene macrocycles, strength of aromatic based polyamides, catalytic hydroformylation/formation of elastomeric polypropylene, asymmetric *cis* dihydroxylation of olefins, recognition of drugs in proteins, and stabilisation of the DNA. [120] Pyrene and naphthalene diimide moieties (Figure 2.3.2.2.) became interesting for the formation of hydrogels as these compounds possess a high driving force for π–π stacking at very low concentrations. [121, 122] These low molecular weight gelators form fibrous structures and can be used solely or be attached at the side chains of polymers to self-assemble.

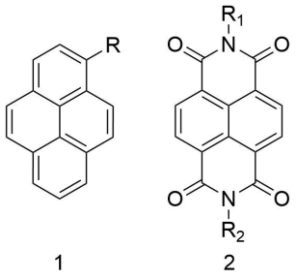

Figure 2.3.2.2: Pyrene (1) and naphthalene diimide (2) group. Modified with permission from reference [123]. Copyright 2010 The Royal Society of Chemistry.

Srinivasa Rao Nelli *et al.* [121] modified pyrene moieties with one of the single amino acids glutamic acid, lysine, serine, or aspartic acid and obtained fibre based hydrogels at very low concentrations (3 wt-%) due the multiple interactions π–π stacking, hydrogen bonds, and electrostatic interactions. In order to increase the water solubility of such low molecular weight gelators, hydrophilic building blocks (bis-ethylene oxy, succinic acid) were introduced into pyrene modified phenyl alanine compounds. [124, 125] The pyrene groups were also transferred to polymers: Poly(ethylene imine) was modified with pyrene groups at the polymer side chain which interacted with carbon nanotubes and formed layers. A promotion of redox-reactions with enzymes could be measured on these surfaces. [126] Xia Yang *et al.* [127] modified hyaluronic acid with pyrene groups at the side chains which could form nanoparticles by the π–π-stacking of the hydrophobic moieties in the core surrounded by the water soluble hyaluronic acid in the shell. Furthermore, hyperbranched poly(ethylene glycol) was end-capped with pyrene moieties whereas two stacked groups formed a guest molecule for γ-cyclodextrin and subsequently a hydrogel. [128]

In contrast to pyrene, the naphthalene diimide compounds were mostly used as low molecular weight gelators for fibre formation with amine acids as building blocks: Modified lysine moieties showed a β-sheet self-assembly at low concentrations (1.5 wt-%) by the intermolecular π–π stacking. [122] A pH-dependency of lysine and serine modified groups was investigated by Ling Huang-Hsu *et al.* [129] and showed that the fibre width, gelation temperature, and storage/loss modulus could be tuned. Niloptal Singha *et al.* [130] modified naphthalene diimide a hydrophobic *n*-hexyl chain and a cell adhesion sequence (RGDS) with hydrophilic groups. Aggregates were formed *via* π–π stacking, hydrogen bonds, and hydrophobic chain interactions which were cell permeable without any toxic side effects. Additionally, due to the naphthalene diimide's fluorescent properties, the cells could be labelled by this technique. In order to further increase the aromatic compound's water solubility, Priya Rajdev *et al.* [131] modified naphthalene diimide with tris(ethylene glycol) groups. Additionally, they varied the linkage group and observed different behaviours: An ester group led to micelles and an amide group led to a hydrogel due to the additional hydrogen bonds.

Besides the mentioned π–π stackings between the same aromatic species, self-assembly behaviour between different ones is also very interesting. Pyrene and naphthalene diimide show congruent overlaps of the molecular orbitals [123] forming stable charge transfer complexes: Srinivasa Rao Nelli *et al.* [132] modified the pyrene and naphthalene diimide moieties with one of the single amino acids serine, aspartic acid, glutamic acid, or lysine. The combination of functionalised pyrene and naphthalene diimide compounds led to fibre based hydrogels at very low concentrations (3 wt-%). Their properties could be tuned *via* the pH-value and cytotoxicity tests showed cell viability between 60-100 % for concentrations in the range 10-100 μM. Self-healing materials based on this mixed π–π stacking were developed by Stefano Burattini *et al.* [133] There, the authors synthesised copolymers possessing naphthalene diimide at the backbone and polyamides terminated with pyrene groups giving together a stable material due to π–π-stacking. After damaging, the material recovered up to 100 % by heating to 87 °C. Lewis R. Hart *et al.* [134] modified linear and branched poly(ethylene glycol) with terminal pyrene groups and polymers containing bis-ethylene oxy and naphthalene diimide groups at the backbone. Due to their viscosity they could be used as materials for 2D inkjet printing and gave fluorescent properties to the printed material. Therefore the aim of this work is to introduce the pyrene and naphthalene diimide groups at allyl functionalised polyglycidols which should form hydrogels by π–π stacking. The synthetic route for this and the hydrogel formation have not been reported in literature yet.

3 Results and discussion

3.1 Polymers with peptide binding units

3.1.1 Polymer synthesis via RAFT polymerisation

In this chapter, the synthesis and characterisation of oligo(ethylene glycol) methyl ether acrylate (OEGMEA) based copolymers with different peptide binding units is described. RAFT polymerisation was chosen in order to control the polymer chain length. Short polymers with $M_n < 10$ kDa were targeted because ^{1}H NMR analysis is suitable in order to identify the end groups properly which are necessary for calculating the polymer's molecular weight.

Three different peptide binding units were introduced: linear thioester, cyclic thioester (thiolactone) and azlactone. The linear thioester group was generated in two steps. First, OEGMEA was copolymerised with 2-hydroxyethyl acrylate (HEA) in order to obtain a hydroxyl group which was used in the next step for a Steglich esterification with a thioester compound containing a carboxyl group (chapter 4.1.2). The linear thioester group shall be the reference for the native chemical ligation as a toxic thiol compound will be released after binding of the peptide. In case of the thiolactone and azlactone groups, the monomers thiolactone acrylamide (TLA) and vinyl azlactone (VAL) were used directly for the polymerisation. These functional groups were described for native chemical ligation by Zhiping Fan *et al.* [10, 80] and Samantha K. Schmitt *et al.* [11, 81] which are interesting candidates to substitute the linear thioester in order to avoid the release of a toxic thiol compound.

The copolymerisations (Scheme 4.1.1-1) were successful and the polymers were characterised *via* ^{1}H NMR, IR, RAMAN spectroscopy and GPC.

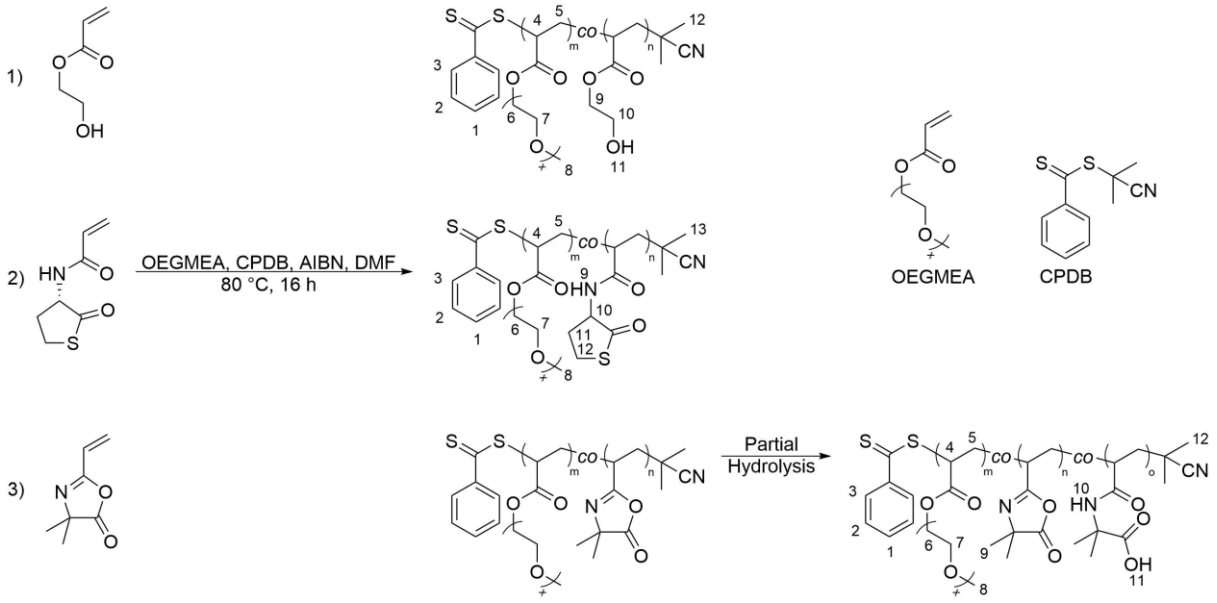

Scheme 4.1.1-1: Copolymerisation of OEGMEA with HEA (1), TLA (2) and VAL (3) *via* RAFT.

The ^{1}H NMR (Figure 4.1.1-1) shows the signals of the dithiobenzoate group of the RAFT Z-group H-1 – H-3 in the range 7.96-7.39 ppm. The signals of the cyanopropyl RAFT R-group H-12 for copolymers containing HEA/VAL and H-13 for copolymers containing TLA appear at 1.35 and 1.30 ppm. H-4 and H-5 represent the protons of the polymer backbone and are visible in the region 2.50-1.54 ppm. The methylene group H-6 of the first repeating unit of the monomer OEGMEA can be seen at 4.19 ppm and the protons of the residual repeating units overlap with the methylene group H-7 in the range 3.77-3.52 ppm. The methoxy group H-8 of OEGMEA appears at 3.37 ppm.

P(OEGMEA-*co*-HEA) shows the signals of the ethylene group H-9 at 4.19 ppm, H-10 in the range 3.77-3.52 ppm and the hydroxyl group H-11 in the range 2.60-1.54 ppm. P(OEGMEA-*co*-TLA) shows the signals of the thiolactone ring the single proton H-10 at 4.64 ppm and the methylene groups H-11 in the range 2.60-1.58 ppm and H-12 in the range 3.65-3.52 ppm. H-9 of the amide group is not visible. P(OEGMEA-*co*-VAL) shows the proton of the methyl groups H-9 at 1.49 ppm.

In order to calculate the monomer ratio and M_n, the integral of the signals of the dithiobenzoate group of the RAFT Z-group H-1 – H-3 were set to 5. Then, the integral of the methoxy group H-8 of OEGMEA was determined and divided by 3. For P(OEGMEA-*co*-HEA) the area of H-6/H-9 was determined and with a known amount of OEGMEA, the amount of the methylene groups of H-9 of HEA was calculated. For P(OEGMEA-*co*-TLA) the integral of the single proton of the thiolactone ring H-10 was taken to determine the

amount of TLA. For P(OEGMEA-*co*-VAL) the amount of VAL was calculated by the difference of the backbone signals. A detailed summary of the calculation is shown in table 4.1.1-1 and the integral of the isotopic signal of the oligo(ethylene glycol) group which overlaps with the methoxy group was neglected.

Table 4.1.1-1: Calculation of the repeating units of the copolymers.

Polymer	**P(OEGMEA-*co*-HEA)**	**P(OEGMEA-*co*-TLA)**	**P(OEGMEA-*co*-VAL)**
Integral of methoxy group H-8	23.84	19.44	20.34
Calculation	23.84 : 3 = 7.95	19.44 : 3 = 6.48	20.34 : 3 = 6.78
Units of OEGMEA	8	6	7
Integral of specific signals	H-6/H-9: 20.62	H-10: 2.19	H-4/H-5/H-9/H-12: 40.06
Calculation	(H-6/H-9 – 8 • H-6) : 2 = (20.62 – 8 • 2) : 2 = 2.31	H-10 : 1 = 2.19 : 1 = 2.19	(H-4/H-5/H-9/H-12 – H-12 – 7 • H-4/H-5) : (H-9 + H-4/H-5) = (40.06 – 6 – 7 • 3) : (6 + 3) = 1.45
Units of HEA/TLA/VAL	2	2	1
M_n/g mol^{-1}	8 • 480 + 2 • 116 = 4,072	6 • 480 + 2 • 171 = 3,222	7 • 480 + 1 • 139 = 3,499

Therefore the copolymers have the following composition and number average molecular weights: P(OEGMEA-*co*-HEA) = 4,072 g mol^{-1} with OEGMEA:HEA = 8:2, P(OEGMEA-*co*-TLA) = 3,222 g mol^{-1} with OEGMEA:TLA = 6:2 and P(OEGMEA-*co*-VAL) = 3,499 g mol^{-1} with OEGMEA:VAL = 7:1. GPC analysis in DMF (Figure 4.1.1-2, Table 4.1.1-2) shows that the polymers possess a narrow distribution with low dispersities (1.10-1.16) meaning that the polymerisation was undertaken *via* RAFT successfully. These values fit with literature values for polymers containing OEGMEA synthesised *via* RAFT. [135-137] The calculated values for M_n *via* ^{1}H NMR are bigger than the obtained values for M_n *via* GPC meaning that the hydrodynamic volume of the synthesised polymers is as big as the one from PEG with a smaller molecular weight. The reason for this is P(OEGMEMA)s partial hydrophobic part in the polymer backbone that is less polar than the polar OEGMEA side chains leading to dense coils in the polar DMF solvent. In contrast to this, the polar PEG chains that are used as standards interact better with the polar DMF solvent causing a less dense coil with a higher hydrodynamic volume.

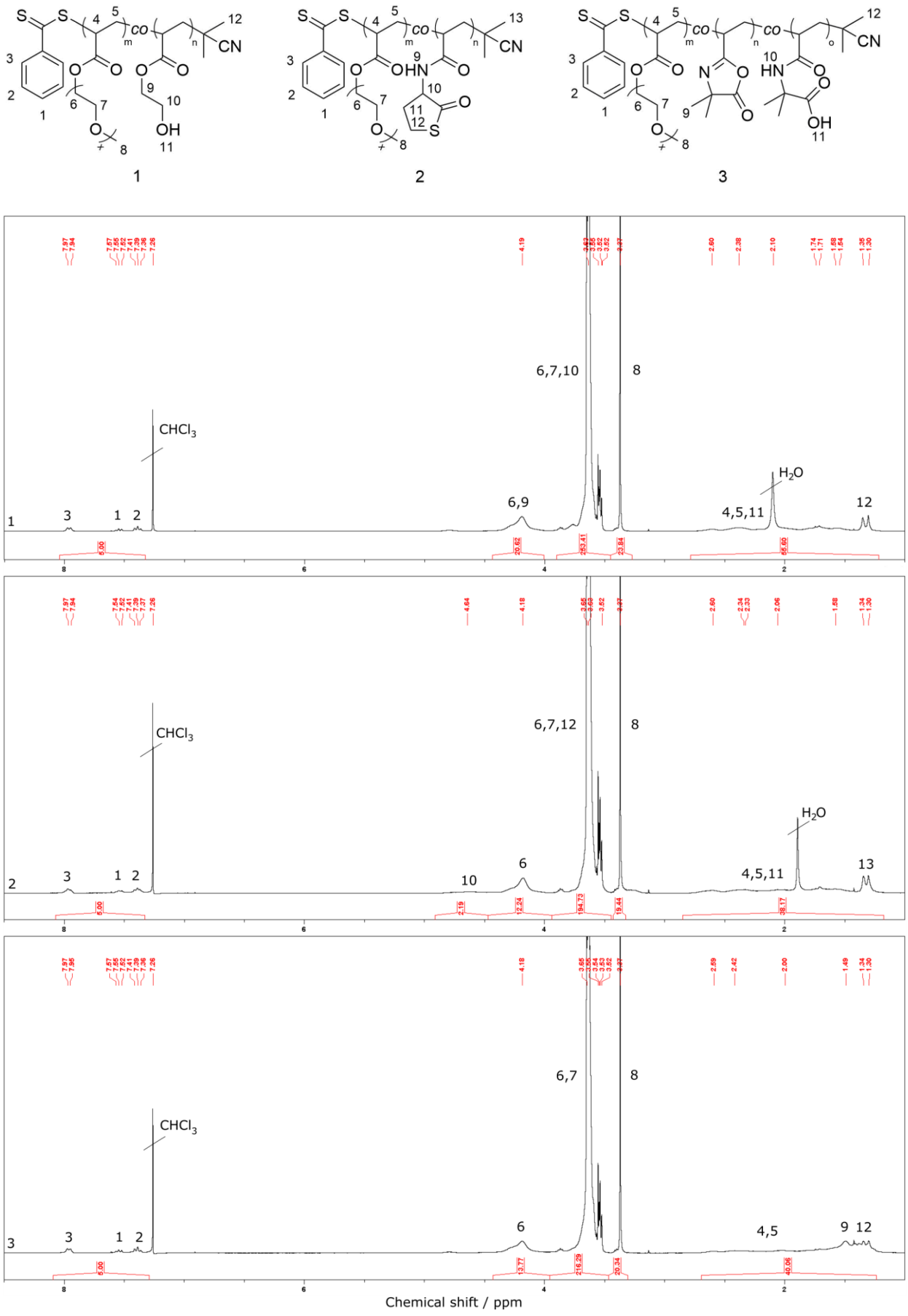

Figure 4.1.1-1: ^{1}H NMR spectra of P(OEGMEA-*co*-HEA) (1), P(OEGMEA-*co*-TLA) (2) and P(OEGMEA-*co*-VAL) (3) in $CDCl_3$.

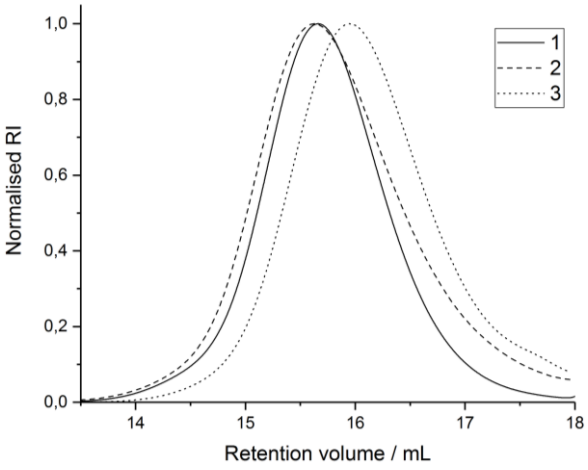

Figure 4.1.1-2: GPC traces of P(OEGMEA-*co*-HEA) (1), P(OEGMEA-*co*-TLA) (2) and P(OEGMEA-*co*-VAL) (3) in DMF (RI).

Table 4.1.1-2: GPC data of of P(OEGMEA-*co*-HEA) (1), P(OEGMEA-*co*-TLA) (2) and P(OEGMEA-*co*-VAL) (3) in DMF (RI).

Run	**1**	**2**	**3**
M_n/Da	2,157	2,001	1,747
M_w/Da	2,372	2,321	1,996
Đ	1.10	1.16	1.14

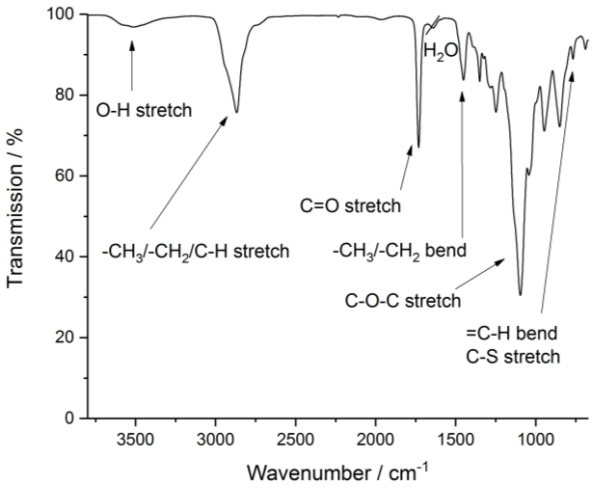

Figure 4.1.1-3: IR spectrum of P(OEGMEA-*co*-HEA).

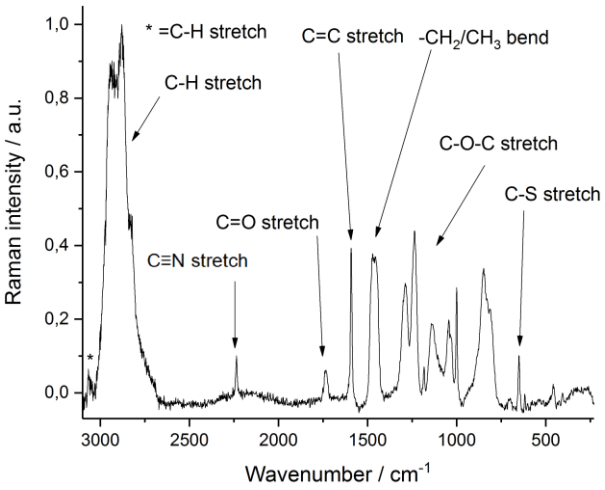

Figure 4.1.1-4: RAMAN spectrum of P(OEGMEA-*co*-HEA).

IR-spectra (Figure 4.1.1-3, 4.1.1-5 and 4.1.1-7) shows the following vibrations which all three copolymers have in common: -CH_3/-CH_2/C-H stretch (2868 cm^{-1}) and -CH_3/-CH_2 bend (1451 cm^{-1}) are visible from the RAFT agent, the polymer back bone and the side groups. The C=O stretch (1732 cm^{-1}) belongs to the all monomers as it appears in the ester group of OEGMEA and the amide/thiolactone group of TLA. The C-O-C stretch (1350-850 cm^{-1}) belongs to the ether side chain of OEGMEA and the =C-H bend/C-S stretch (767 and 689 cm^{-1}) belong to the aromatic ring and dithiobenzoate group of the RAFT Z-group. P(OEGMEA-co-HEA) has additionally the broad O-H stretch vibration of the hydroxyl group of HEA at 3514 cm^{-1}. P(OEGMEA-*co*-TLA) shows the N-H stretch and N-H bend vibrations of the amide group of TLA at 3524 and 1535 cm^{-1}. P(OEGMEA-*co*-VAL) shows the C=O

and C=N stretch vibrations of the azlactone group of VAL at 1819 and 1673 cm^{-1}. C-N stretch vibrations of TLA and VAL are overlapping with C-O-C ones. A partial hydrolysis of the moisture sensitive VAL can be seen as additional signals of N-H stretch and N-H bend vibrations from the formed amide groups are visible at 3424 and 1530 cm^{-1}. The partial ring opening could come from surrounded moisture during the storage of the polymer at -20 °C. RAMAN spectra (Figure 4.1.1-4, 4.1.1-6 and 4.1.1-8) show the following vibrations which all three copolymers have in common: The =C-H stretch (3057 cm^{-1}) belongs to the aromatic ring of the RAFT Z-group. The C-H stretch (2944/2880 cm^{-1}), -CH_2 bend (1465 cm^{-1}) and C-C bend (459-312 cm^{-1}) are visible from the RAFT agent, the polymer back bone and the side groups. TheC≡N stretch (2227 cm^{-1}) of the nitrile group of the RAFT R-group, The C=C stretch (1592 cm^{-1}) of the aromatic ring of the RAFT Z group and the C-S stretch of the dithioester group (650 cm^{-1}) of the RAFT agent can be seen. The C=O stretch (1736 cm^{-1}) belongs to the all monomers as it appears in the ester group of OEGMEA, the amide/thiolactone group of TLA and the azlactone group of VAL. OEGMEA has the C-O-C stretch (1289-854 cm^{-1}) due to the ether side chain. Additionally, P(OEGMEA-*co*-TLA) shows more C-S stretch vibrations of the thiolactone group of TLA (686-630 cm^{-1}) and P(OEGMEA-*co*-VAL) shows one more C=N stretch vibration of the azlactone group of VAL (1673 cm^{-1}).

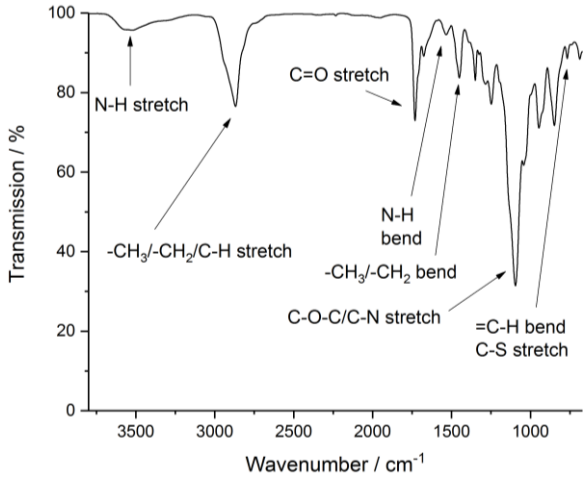

Figure 4.1.1-5: IR spectrum of P(OEGMEA-*co*-TLA).

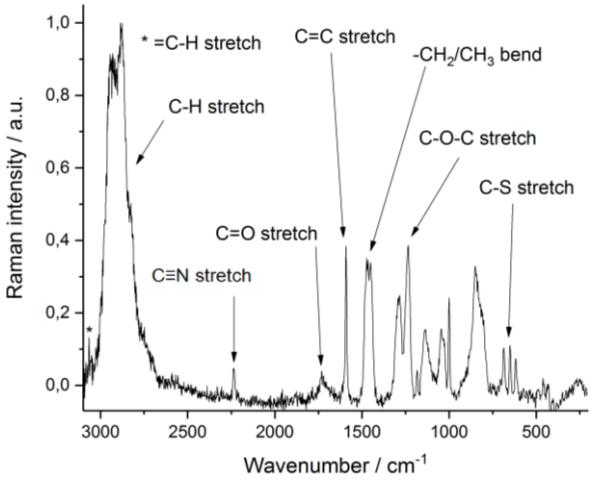

Figure 4.1.1-6: RAMAN spectrum of P(OEGMEA-*co*-TLA).

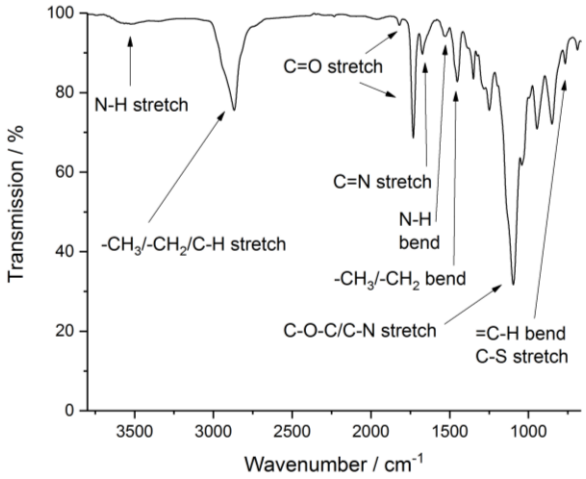

Figure 4.1.1-7: IR spectrum of P(OEGMEA-*co*-VAL).

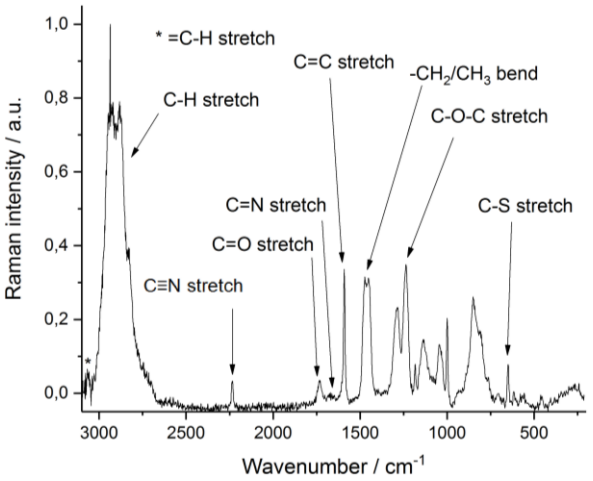

Figure 4.1.1-8: RAMAN spectrum of P(OEGMEA-*co*-VAL).

3.1.2 Thioester-linker synthesis and modification of P(OEGMEA-co-HEA)

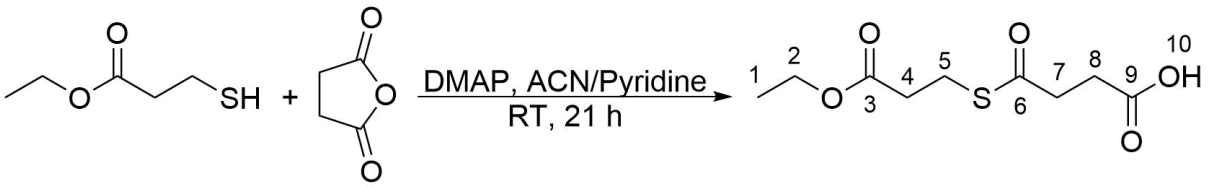

Scheme 4.1.2-1: Synthesis of ethyl 3-mercaptopropionate-succinic acid.

The thioester-linker EMP-SA (Scheme 4.1.2-1) was synthesised according to literature procedure [76] with a slight modification and was isolated with a yield of 70 %. The product was obtained as a clear liquid and was analysed *via* ^{1}H, ^{13}C NMR, IR and RAMAN spectroscopy and mass spectrometry.

^{1}H NMR spectrum (Figure 4.1.2-1) shows the ethyl group with H-1 (1.25 ppm) and H-2 (4.15 ppm). The methylene groups H-4 – H-8 are visible in the range 3.14-2.61 ppm. H-10 is not visible. ^{13}C NMR spectrum (Figure 4.1.2-2) shows the ethyl group with C-1 (14.30 ppm) and C-2 (60.97 ppm). The methylene groups C-4/5/7/8 appear in the range 38.18-24.18 ppm. Additionally, the carbon atoms from the carbonyl groups C-3/6/9 are visible in the range 197.44-171.76 ppm. MS-ASAP (Figure 4.1.2-3) shows a peak at 233.0484 which matches to the calculated value $[M-H]^{-}$ = 233.0484. IR-spectrum (Figure 4.1.2-4) shows the typical vibrations of the product: The O-H stretch (3043 cm^{-1}) and C=O stretch (1372-1311 cm^{-1}) belong to the carboxylic group. The ethyl ester group shows C-O-C stretch (1245-873 cm^{-1}) and the thioether/thioester group show C-S stretch (792-773 cm^{-1}). The ethyl and ethylene groups possess $-CH_3$, $-CH_2$ & C-H stretch (2980-2920 cm^{-1}), $-CH_2$ & C-H stretch (2712-2361 cm^{-1}) and $-CH_3$ & $-CH_2$ bend (1430-1411 cm^{-1}). C=O stretch (1733-1673 cm^{-1}) belong

to the ester and thioester group. , , and The typical vibrations of the product are also visible in the RAMAN-spectrum (Figure 4.1.2-5): The C-H stretch (2952-2923 cm^{-1}), -CH_2 & -CH_3 bend (1435-1416 cm^{-1}) and C-C bend (530-185 cm^{-1}) belong to the ethyl and ethylene groups. The ester/thioester and carboxyl group show the C=O stretch (1737-1676 cm^{-1}). The ethyl ester possess the C-O-C stretch (1279-796 cm^{-1}) and the thioester the C-S stretch (776-647 cm^{-1}).

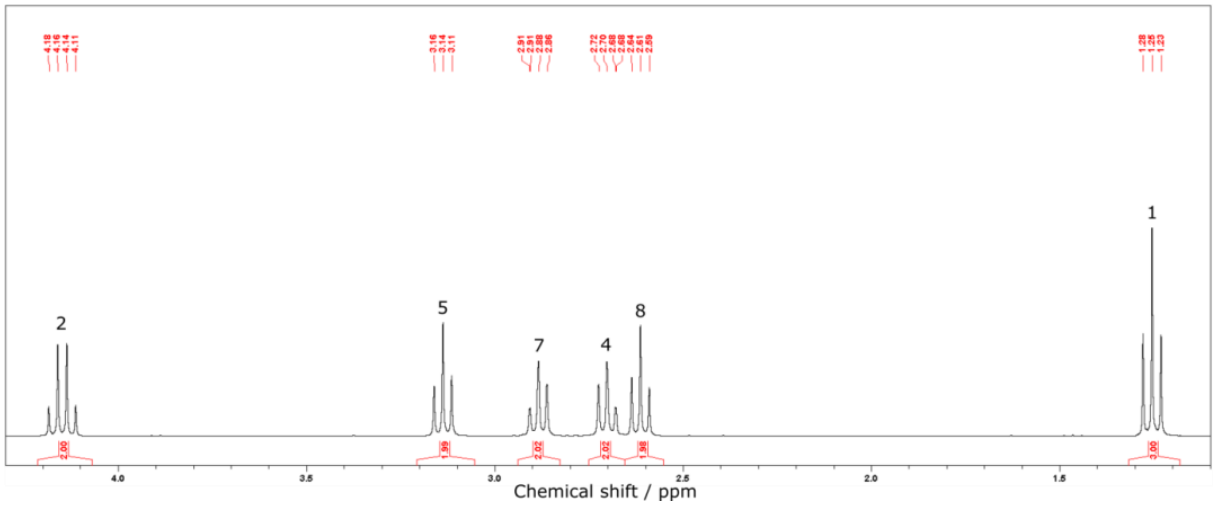

Figure 4.1.2-1: ^{1}H NMR spectrum of EMP-SA in $CDCl_3$.

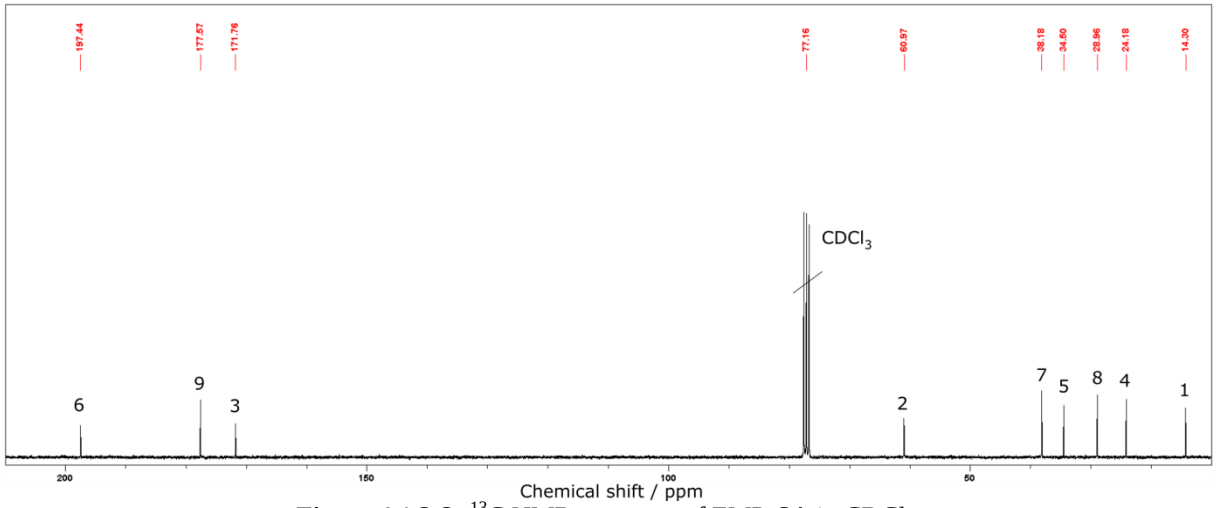

Figure 4.1.2-2: ^{13}C NMR spectrum of EMP-SA in $CDCl_3$.

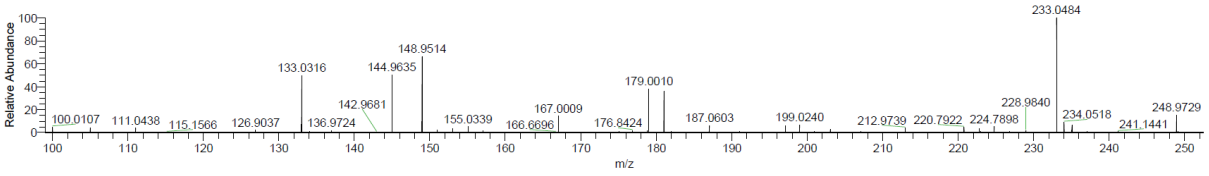

Figure 4.1.2-3: ASAP-MS spectrum of EMP-SA.

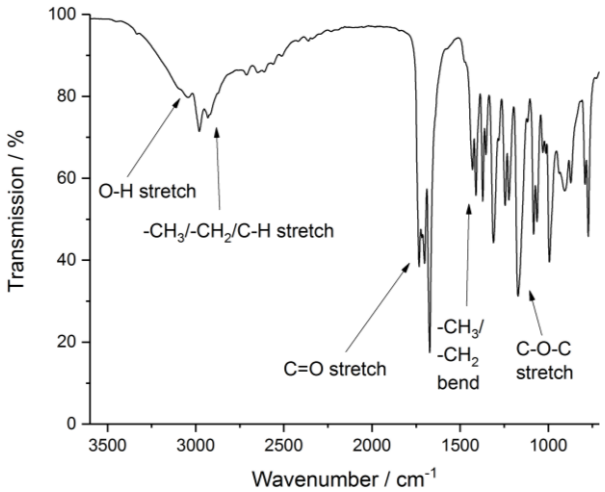

Figure 4.1.2-4: IR spectrum of EMP-SA.

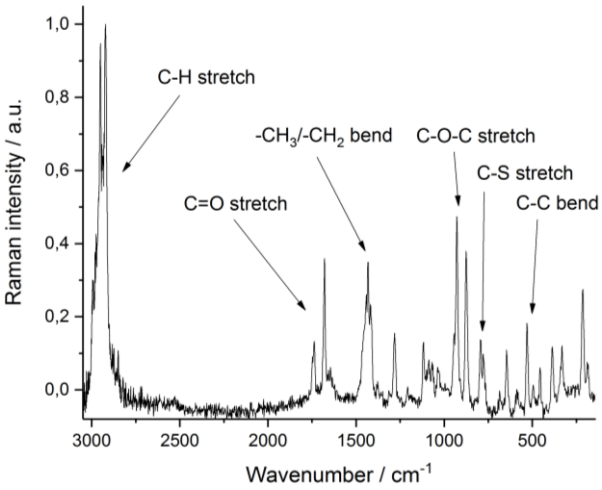

Figure 4.1.2-5: RAMAN spectrum of EMP-SA.

P(OEGMEA-*co*-HEA) was esterified with EMP-SA (Scheme 4.1.2-2) in a typical Steglich esterification using DCC and DMAP according literature procedure [138]. The product was isolated and characterised *via* ^{1}H NMR, IR, RAMAN spectroscopy and GPC.

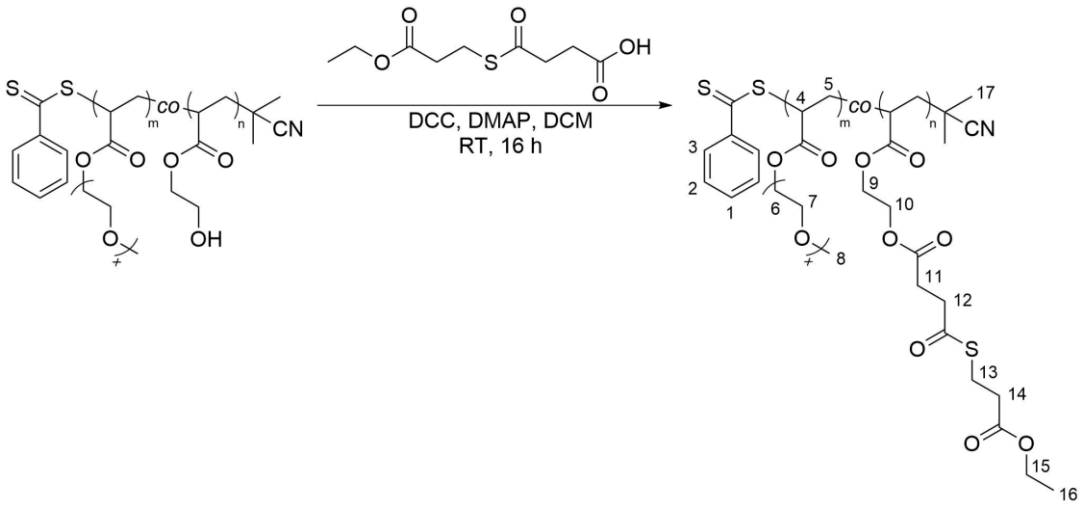

Scheme 4.1.2-2: Modification of P(OEGMEA-*co*-HEA) with EMP-SA.

The ^{1}H NMR spectrum (Figure 4.1.2-6) shows the same signals from the parent polymer additionally those of the thioester linker EMP-SA: H-1 – H-3 of the RAFT Z-group are visible in the range 7.96-7.39 ppm but with less than five protons because the amine compounds of the esterification split the dithiobenzoate group in a side reaction. H-17 of the RAFT R-group can be seen at 1.35/1.30 ppm and the polymer backbone appears in the region 2.35-1.54 ppm. The methylene groups of the first repeating units of OEGMEA/HEA H-6 and H-9 appear at 4.26-4.18 ppm and the residual ones H-6/H-7/H-10 at 3.65-3.52 ppm. The methoxy group H-8 of OEGMEA is visible at 3.37 ppm. The protons of the thioester-linker appear at 4.15 ppm (H-15), 3.12 ppm (H-13), 2.89 ppm (H-12), 2.68 ppm (H-14), 2.60 ppm (H-11) and 1.25 ppm (H-16). The ratio of the methylene groups H-12/H-13 to the methoxy

group H-8 show a 58 % conversion of the OH-groups of HEA after the esterification, with OEGMEA:HEA = 8:2 = 4:1 gives with factor 2 for methylene group:

[(H-12/13 : 2)] : [H-8 : 3 : 4 • 2] = [((2.26 + 2.34) : 2)] : [23.83 : 3 : 4 • 2] = 0.58 = 58 %

This conversion is reasonable as the agents for the esterification underwent a side reaction with the RAFT-Z group (cleavage through the amines) so that less amount of DCC/DMAP was left for the esterification reaction. In order to prevent this in future experiments, one could cleave the Z-group before the esterification or use more DCC/DMAP.

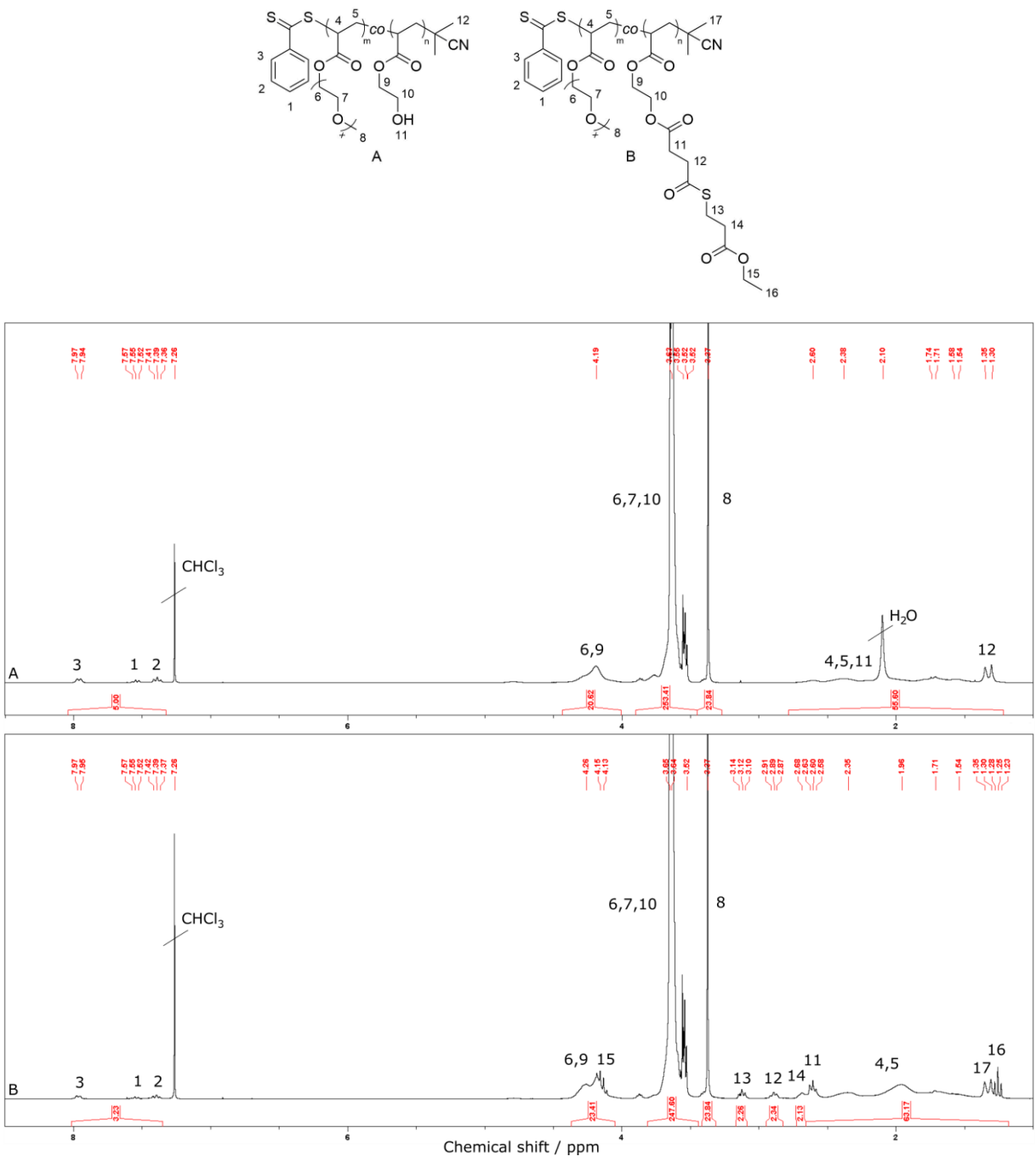

Figure 4.1.2-6: ^{1}H NMR spectra of P(OEGMEA-*co*-HEA) (A) and P(OEGMEA-*co*-EMP-SA) (B) in $CDCl_3$.

GPC analysis in DMF (Figure 4.1.2-7, Table 4.1.2-1) shows a shift of the polymer distribution to higher molecular weights compared to the parent polymer which can occur due to intermolecular stacking of the hydrophobic side chains of EMP-SA and cause a broadening at the same time. The dispersity increased slightly from 1.10 to 1.22.

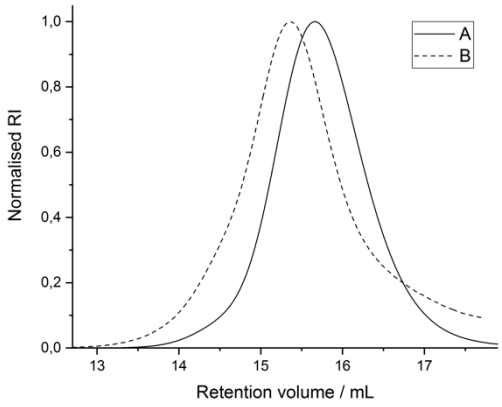

Figure 4.1.2-7: GPC traces of P(OEGMEA-*co*-HEA) (A) and P(OEGMEA-*co*-EMP-SA) (B) in DMF (RI).

Table 4.1.2-1: GPC data of of P(OEGMEA-*co*-HEA) (A) and P(OEGMEA-*co*-EMP-SA) (B) in DMF (RI).

Run	**A**	**B**
M_n/Da	2,157	2,193
M_w/Da	2,372	2,682
Đ	1.10	1.22

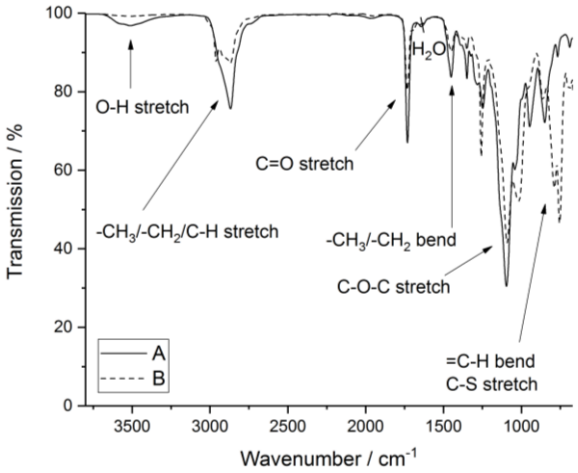

Figure 4.1.2-8: IR spectra of P(OEGMEA-*co*-HEA) (A) and P(OEGMEA-*co*-EMP-SA) (B).

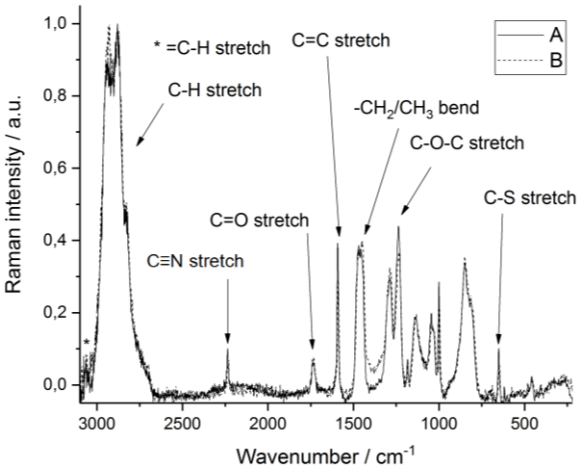

Figure 4.1.2-9: RAMAN spectra of P(OEGMEA-*co*-HEA) (A) and P(OEGMEA-*co*-EMP-SA) (B).

IR spectrum (Figure 4.1.2-8) shows the following vibrations which the parent polymer and modified polymer have in common: The -CH_2 & C-H stretch (3002/2904 cm^{-1}), -CH_3 stretch (2960/2870 cm^{-1}), -CH_2 & C-H stretch (2748 cm^{-1}) and -CH_2/-CH_3 bend (1451/1388 cm^{-1}) belong to the RAFT agent, the polymer back bone and the side chains. The C=O stretch (1733/1693 cm^{-1}) belongs to the ester group of the side chains. OEGMEA possess theC-O-C stretch (1350-862 cm^{-1}) due to its ether side chain. The RAFT Z group shows the =C-H bend/C-S stretch (788-665 cm^{-1}) from the aromatic ring and the dithioester group which overlaps with the C-S stretch from the thioester group from the thioester linker. The only difference that is visible is the decrease of the O-H stretch vibration after the esterification. The vibrations in the RAMAN spectrum (Figure 4.1.2-9) are before and after the esterification the same: The =C-H stretch (3057 cm^{-1}) and C=C stretch (1589 cm^{-1}) belong to the aromatic ring of the RAFT Z-group. The dithioester group shows the C-S stretch (647 cm^{-1}) of the RAFT Z-group. From the RAFT R-group, the nitrile group with C≡N stretch (2230 cm^{-1}) is

visible. OEGMEA shows its C-O-C stretch (1288-849 cm^{-1}) from the ether side chain and the ester/thioester groups from the side chains show the C=O stretch (1733 cm^{-1}). The residual C-H stretch (2927-2880 cm^{-1}), -CH_2 bend (1458 cm^{-1}) and C-C bend (458/285 cm^{-1}) belong to the RAFT group, polyethylene backbone and aliphatic side chains.

3.1.3 RAFT Z-group cleavage and native chemical ligation

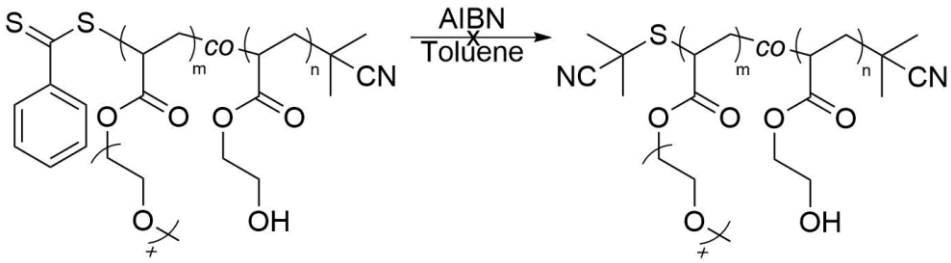

Scheme 4.1.3-1: RAFT Z-group cleavage of P(OEGMEA-*co*-HEA).

In order to prevent side reactions between the model peptide CGGGF and the RAFT Z-group during the peptide conjugation (nucleophilic attack of amine at the dithioester), we attempted to remove the RAFT Z-group (Scheme 4.1.3-1) *via* radical reaction with AIBN according literature procedure with the ratio AIBN:end group = 20:1 [139] and even with 40:1. This step was not successful; even after variation of reaction parameters like reaction time, temperature, concentration and equivalents only 30 % of the RAFT Z-group could be removed. The reason for that could be that the polymers are too short and therefore not suitable for this reaction procedure. In literature, this method was applied for polymers in the range of 8.8 – 48.5 kDa with the ratio AIBN:end group = 20:1. [139] On one hand, the reactants need to have a certain concentration in order to react with each other properly but on the other hand; the concentration of radicals should not be too high because they favour the recombination reaction instead of the reaction with other molecules in viscous solvents (cage effect). [140] Further alternative Z-group cleavage methods like aminolysis [135] and oxidative hydrolysis [141] cannot be applied because with these methods also the peptide binding units will react the cleaving compounds and cannot be used for native chemical ligation anymore. In future experiments, one could synthesise longer polymer chains with M_n ~ 10 kDa so that end group analysis with ^{1}H NMR is still possible and at the same time the polymer chains are long enough for the Z-group removal procedure. From that point on, the decision was made to try the peptide conjugation with polymers still carrying the RAFT Z-group and see if the native chemical ligation at the chain side groups still would occur.

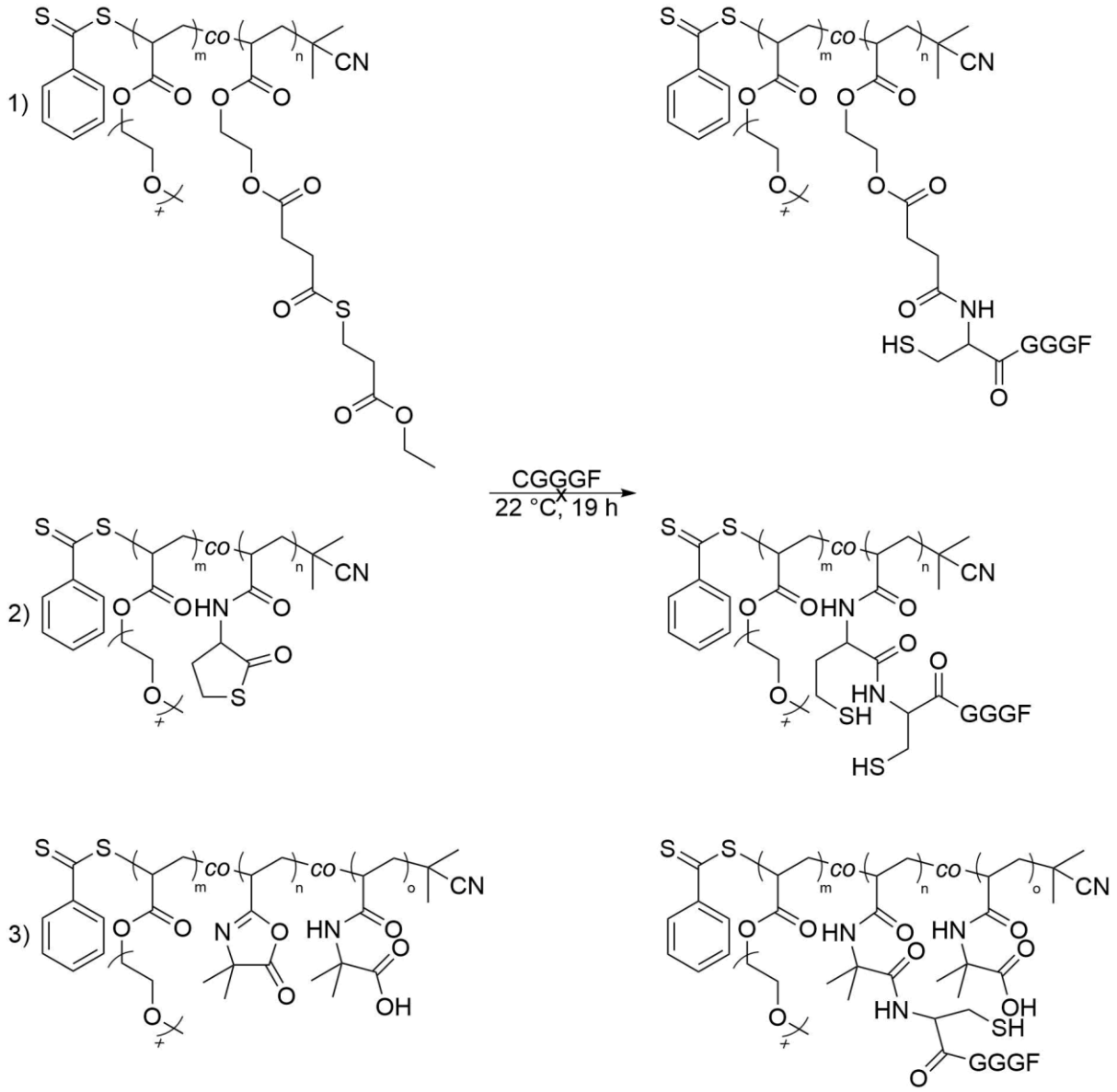

Scheme 4.1.3-2: Reaction of P(OEGMEA-co-EMP-SA) (1), P(OEGMEA-co-TLA) (2) and P(OEGMEA-co-VAL) (3) with CGGGF.

The peptide conjugation (Scheme 4.1.3-2) was also not successful because as expected the peptide underwent an aminolysis reaction with the RAFT Z-group. It can be excluded that the Z-group was removed by the surrounded water because it is a too weak nucleophile for this reaction. [142, 143] In the ^{1}H NMR spectrum (Figure 4.1.3-1) one can see that the intensity of signals of the aromatic region decreased from 5 to around two to three. The methoxy group of OEGMEA was used as reference. Additionally, the OEGMEA side chains may be too long which could shield the co-monomers and prevent native chemical ligation with CGGGF or the thioester compounds need additional thiol additives for catalysis of the native chemical ligation. Polymers with reverse side chain lengths facilitate this reaction. [82] Therefore in future experiments OEGMEA could be used with three ethylene glycol units which are shorter and may shield less the native chemical addition. Additionally, the peptide binding

units may be modified with a spacer so that they are approximately long as the OEGMEA chains and could react better with the peptides. In these experiments, each polymer has only 1-2 peptide binding units which could also be increased for a higher binding ability of peptides standing in accordance with former experiments in literature. [82] Other reaction conditions are also important and may be changed for future experiments in order to bind the peptides, e.g. increase of concentration of polymer, peptide and the reaction temperature. From that point on the decision was made to synthesise OEGMEA based copolymers *via* free radical polymerisation and try peptide conjugation on these systems in order to check primarily the effect of missing RAFT Z-groups on the native chemical ligation.

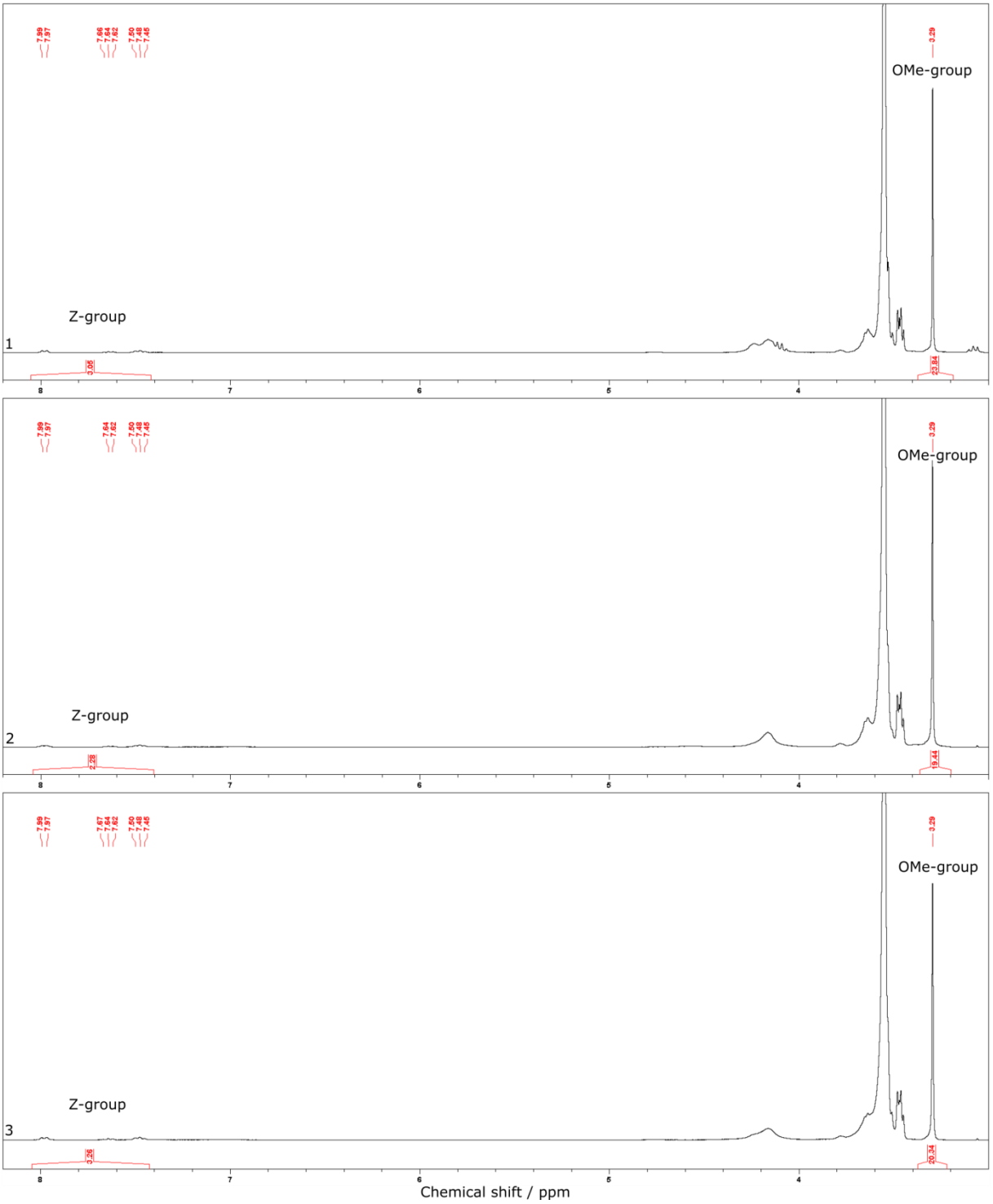

Figure 4.1.3-1: ^{1}H NMR spectra of P(OEGMEA-*co*-EMP-SA) (1), P(OEGMEA-*co*-TLA) (2) and P(OEGMEA-*co*-VAL) (3) in MeCN-d_3 after reaction with CGGGF.

3.1.4 Polymer synthesis *via* free radical polymerisation

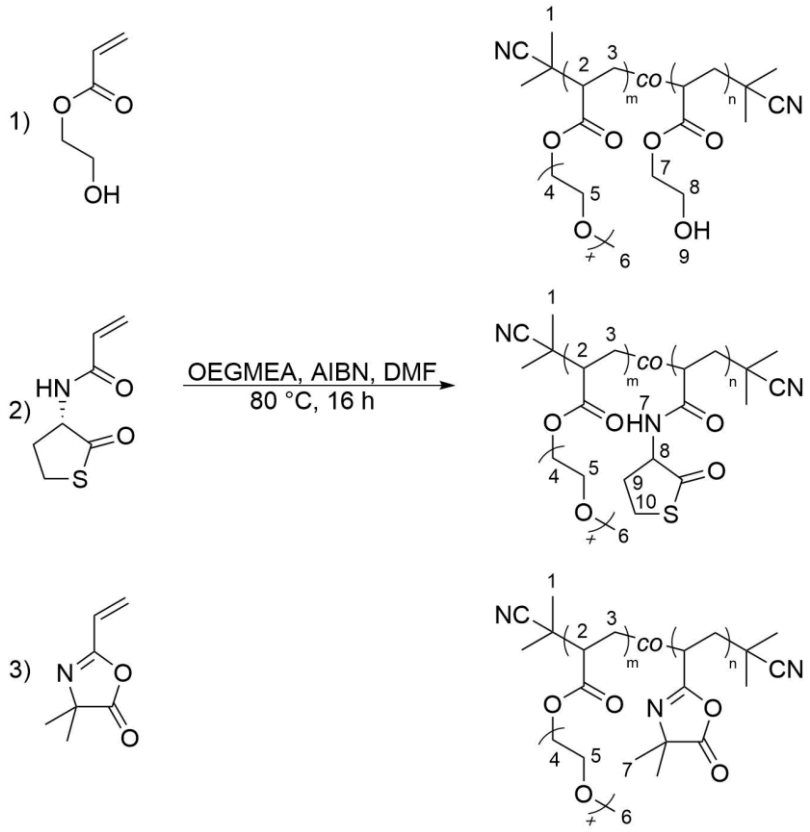

Scheme 4.1.4-1: Copolymerisation of OEGMEA with HEA (1), TLA (2) and VAL (3) *via* free radical polymerisation. For simplicity, only recombined polymers will be shown for all reactions.

OEGMEA was copolymerised *via* free radical polymerisation with each of the monomers for peptide binding: HEA, TLA and VAL (Scheme 4.1.4-1). The syntheses were successful and the polymers were characterised *via* ^{1}H NMR, IR, RAMAN spectroscopy and GPC.

^{1}H NMR spectrum (Figure 4.1.4-1) shows the following protons which all three copolymers have in common: H-1 (1.35/1.30 ppm) of the methyl end groups, H-2/3 of the polymer backbone (2.33-1.64 ppm), the first repeating unit of OEGEMA H-4 (4.19 ppm), the residual methylene groups of OEGMEA H-4/5 (3.65-3.53 ppm) and the methoxy group H-6 (3.37 ppm). P(OEGMEA-*co*-HEA) has additionally H-7/8 of HEA which overlap with H-4 and H-5. H-9 appears in the region of the polymer backbone. In the spectrum of P(OEGMEA-*co*-TLA), signals of TLA can be seen: H-7 (6.97 ppm) of the amide group, H-8 (4.56 ppm) of the single proton and the methylene groups H-9/10 appear in the region 2.53-1.49 ppm and 3.63-3.45 ppm. P(OEGMEA-*co*-VAL) has additionally the methyl groups of VAL H-7 (1.36 ppm).

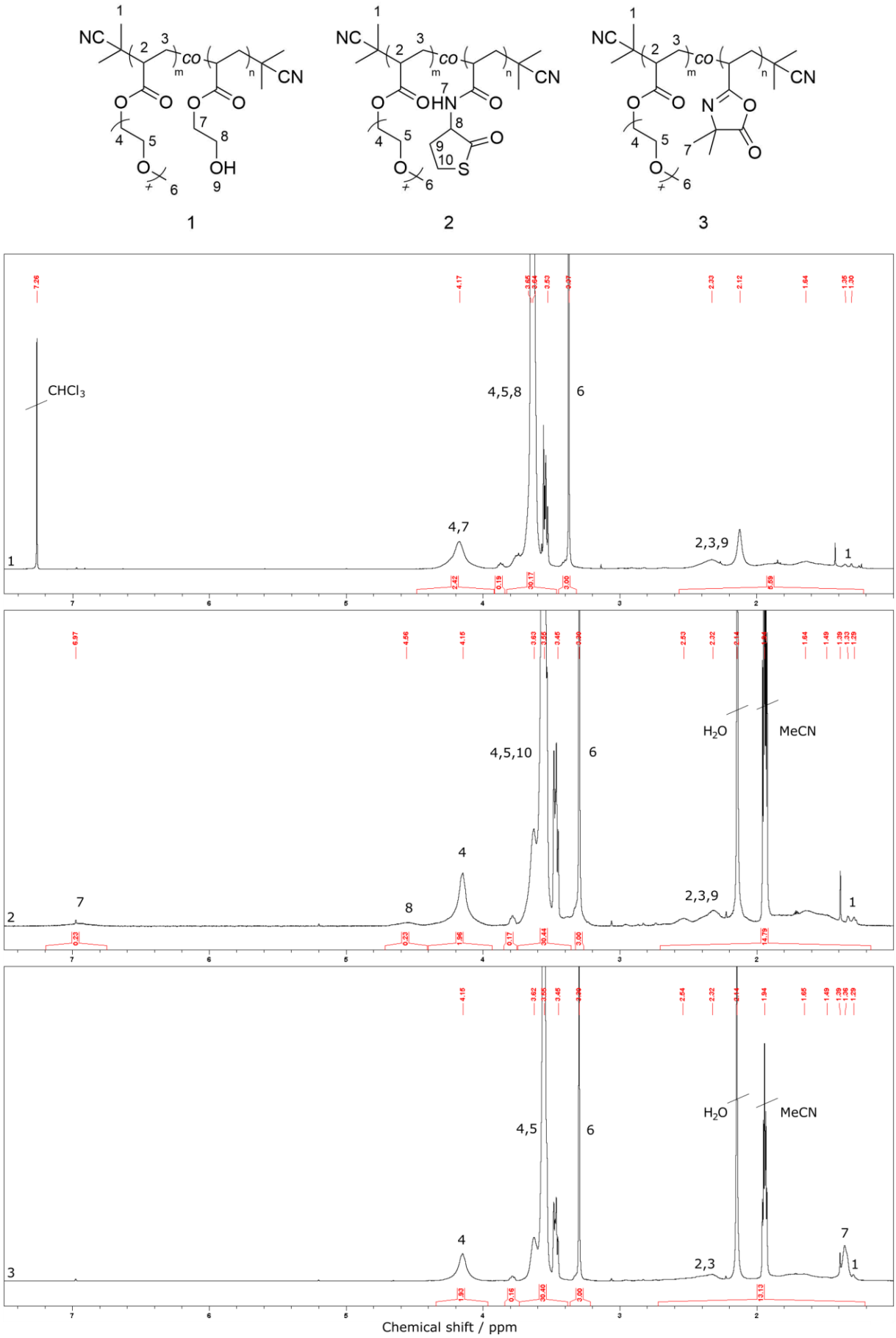

Figure 4.1.4-1: ^{1}H NMR spectra of P(OEGMEA-*co*-HEA) (1) in $CDCl_3$, P(OEGMEA-*co*-TLA) (2) and P(OEGMEA-*co*-VAL) (3) in MeCN-d_3.

The ratio of OEGMEA:HEA can be calculated *via* ^{1}H NMR from the methoxy group H-6 and the methylene groups H-4/7. The satellite signals of OEGMEA were considered:

OEGMEA: H-6 – satellite = 3.00 – 0.19 = 2.81 equivalent 3 protons. That means the value 1.87 is equivalent 2 protons.

OEGMEA/HEA overlap H-4/7: H-4/7 – 2 protons of OEGMEA = 2.42 – 1.87 = 0.55 protons of HEA. Units of HEA = 0.55 : 2 = 0.28 (divided by 2 because 2 protons at the methylene group). OEGMEA:HEA-ratio = 2.81:0.28 = 10:1.

The calculation of the ratio OEGMEA:TLA and OEGMEA:VAL in the polymer will be explained later in chapter 4.1.6. The direct determination of the monomer-ratios in the polymer is not possible *via* ^{1}H NMR because the signals of TLA and VAL are overlapping with the polymer backbone. Therefore, they will be reacted with benzylamine which performs the nucleophilic ring opening of TLA and VAL. The ratio of the monomers will be then determined via ^{1}H NMR via the signals of the aromatic compound and the methoxy group of OEGMEA.

GPC analysis in DMF (Figure 4.1.4-2, Table 4.1.4.-1) shows broad distributions and dispersities in the range 2.03-2.77 which is common for polymers synthesised *via* free radical polymerisation: Three fractions can be seen (11.0 min, 12.8 min, 14.5 min) which come from the three termination products via recombination (11.0 min) and disproportionation (12.8 min, 14.5 min) after the polymerisation. According Schulz-Flory, the GPC should show one broad distribution [144] but the chosen column set is separating the fractions well. Additionally, the slope of the fraction at 11.0 min is higher than of the other two ones meaning that the exclusion limit for the GPC measurement was reached there.

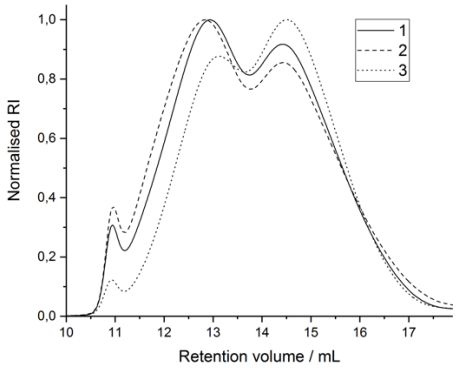

Figure 4.1.4-2: GPC traces of P(OEGMEA-*co*-HEA) (1), P(OEGMEA-*co*-TLA) (2) and P(OEGMEA-*co*-VAL) (3) in DMF (RI).

Table 4.1.4-1: GPC data of P(OEGMEA-*co*-HEA) (1), P(OEGMEA-*co*-TLA) (2) and P(OEGMEA-*co*-VAL) (3) in DMF (RI).

Run	**1**	**2**	**3**
M_n/Da	4,759	4,729	4,396
M_w/Da	11,959	13,083	8,907
Đ	2.51	2.77	2.03

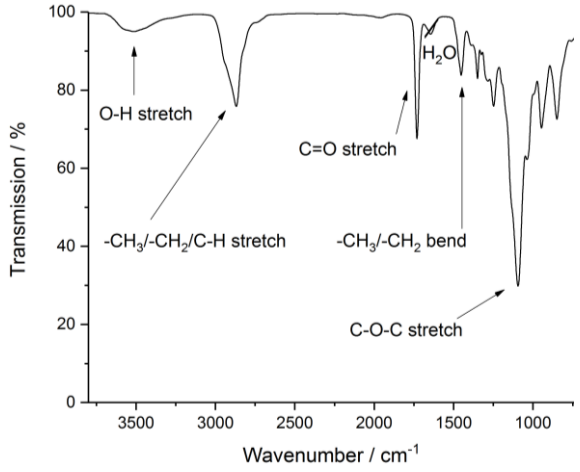

Figure 4.1.4-3: IR spectrum of P(OEGMEA-*co*-HEA).

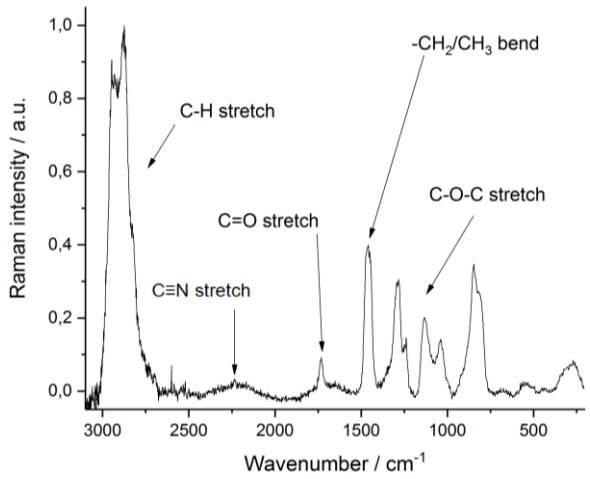

Figure 4.1.4-4: RAMAN spectrum of P(OEGMEA-*co*-HEA).

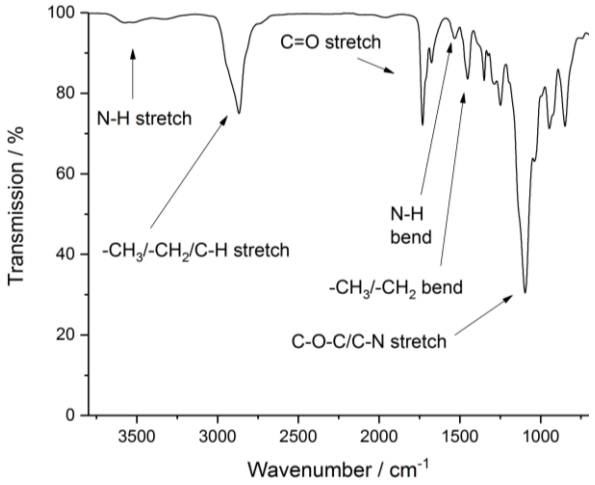

Figure 4.1.4-5: IR spectrum of P(OEGMEA-*co*-TLA).

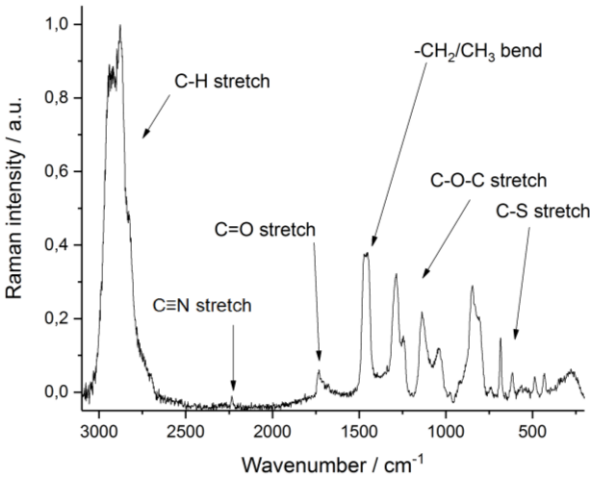

Figure 4.1.4-6: RAMAN spectrum of P(OEGMEA-*co*-TLA).

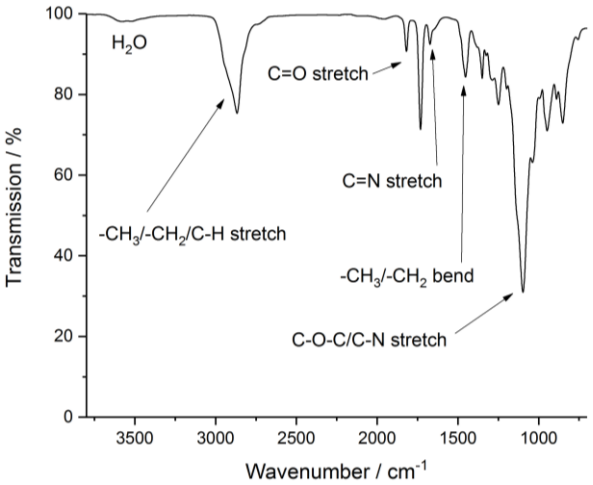

Figure 4.1.4-7: IR spectrum of P(OEGMEA-*co*-VAL).

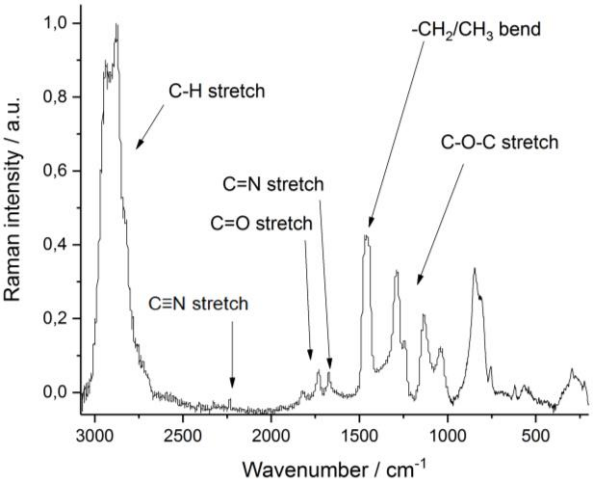

Figure 4.1.4-8: RAMAN spectrum of P(OEGMEA-*co*-VAL).

IR spectra (Figure 4.1.4-3, Figure 4.1.4-5, Figure 4.1.4-7) show the following vibrations which all three copolymers have in common: The -CH_2 & C-H stretch (2869 cm^{-1}), -CH_3 & -CH_2 bend (1453 cm^{-1}), -CH_3 bend (1388 cm^{-1}) and -CH_2 bend (759 cm^{-1}) belong to the methyl end groups, polyethylene backbone and the aliphatic side chains. The side groups possess the C=O stretch (1731 cm^{-1}) from the ester of the OEGMEA and amide/thiolactone group of TLA. C-O-C stretch (1350-850 cm^{-1}) belongs to the ether side chain of OEGMEA. P(OEGMEA-*co*-HEA) shows additionally the O-H stretch vibration at 3511 cm^{-1} from the hydroxyl group of HEA. P(OEGMEA-*co*-TLA) shows vibrations from TLA: N-H stretch (3570 cm^{-1}) and N-H bend (1532 cm^{-1}) belong to the amide group. Its C-N stretch is overlapping with C-O-C stretch (1350-1038 cm^{-1}) and the C-S stretch belongs to the thiolactone group. Additionally, -CH_2 bend (742 cm^{-1}) is visible which belongs to the polyethylene backbone and aliphatic side groups. In the spectrum of P(OEGMEA-*co*-VAL) one can find additionally C=O (1818 cm^{-1}), C=N (1673 cm^{-1}) and C-N (1350-1039 cm^{-1}, overlapping with C-O-C) stretch vibrations of the azlactone group of VAL. O-H stretch vibrations at 3500 cm^{-1} are also visible but come from incorporated water molecules in the polymer and not from N-H stretch vibrations due to possible hydrolysed VAL because there is no corresponding N-H bend vibration at 1535 cm^{-1} to be seen. RAMAN spectra (Figure 4.1.4-4, Figure 4.1.4-6, Figure 4.1.4-8) shows the following vibrations which all three copolymers have in common: C-H stretch (2932/2873 cm^{-1}), -CH_3 & -CH_2 bend (1461 cm^{-1}) and C-C stretch/bend (683-284 cm^{-1}) belong to the methyl end groups, polyethylene backbone and aliphatic side chains. C≡N stretch (2234 cm^{-1}) is visible from the nitrile end group. The C=O stretch (1732 cm^{-1}) belongs to the ester group of OEGMEA, amide/thiolactone group of TLA and azlactone group of VAL. OEGMEA shows C-O-C stretch (1295-818 cm^{-1}) from its ether side chain. P(OEGMEA-*co*-TLA) has additionally a C-S stretch vibration (686 cm^{-1}) from the thiolactone group of TLA and P(OEGMEA-*co*-VAL) has the C=O stretch (1826 cm^{-1}) and C=N stretch vibrations (1671 cm^{-1}) from the azlactone group of VAL.

3.1.5 Modification of P(OEGMEA-*co*-HEA) with thioester-linker

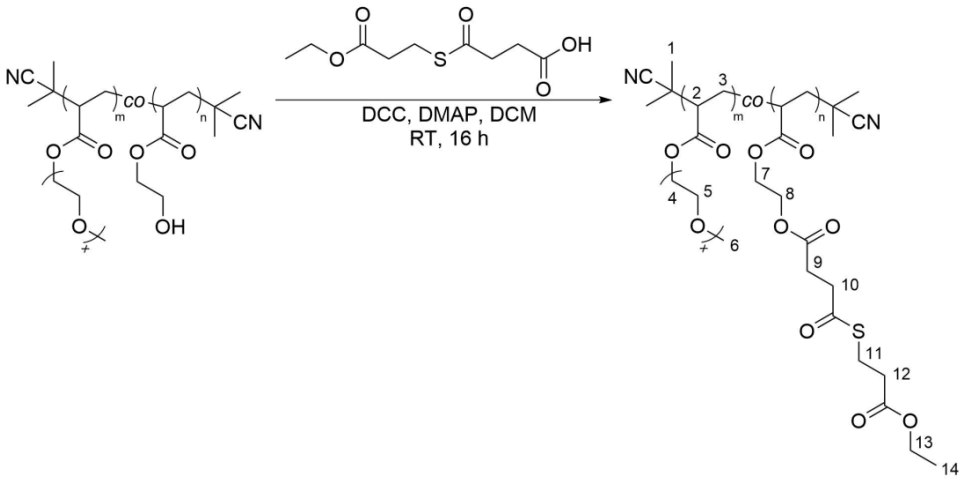

Scheme 4.1.5-1: Modification of P(OEGMEA-*co*-HEA) with EMP-SA.

P(OEGMEA-*co*-HEA) was esterified with EMP-SA (Scheme 4.1.5-1) in a typical Steglich esterification using DCC and DMAP according literature procedure [138]. The product was isolated and characterised *via* ^{1}H NMR, IR, RAMAN spectroscopy and GPC.

The product and the parent polymer have the following signals in common in the ^{1}H NMR spectrum (Figure 4.1.5-1): H-1 from the methyl end groups (1.35/1.28 ppm), H-2/3 from the polymer backbone (2.32-1.44 ppm), H-4 from the first repeating unit of OEGMEA and first methylene group of HEA (4.18 ppm), H-4/5/7 from the residual methylene groups of OEGMEA/HEA (3.64-3.52 ppm) and H-6 from the methoxy group (3.37 ppm). The esterified product additionally shows the signals of the ethyl and ethylene groups of the thioester-linker: H-13 (4.15 ppm), H-11 (3.12 ppm), H-10 (2.89 ppm), H-12 (2.68 ppm), H-9 (2.60 ppm) and H-14 (1.25 ppm). The OH-groups of HEA were esterified with 100 % conversion and can be calculated in the following way:

OEGMEA: H-6 – satellite = 11.35 – 1 = 10.35 equivalent to 3 protons of the methoxy group. 2 protons of the thioester-linker for a 100 % conversion with OEGMEA:HEA = 10:1 would give: 10.35 : (3 • 10) • 2 = 0.69 which was found in average of H-10/11 in the ^{1}H NMR spectrum. A higher conversion for the esterification compared to the RAFT polymers is reasonable as here are no end groups which can undergo side reactions with the Steglich esterification agents DCC and DMAP.

GPC measurement in DMF does not show significant changes (Figure 4.1.5-2, Table 4.1.5-1) except one polymer distribution which shifted from 13 min to 13.5 min due to possible hydrophobic interactions of the esterified side chains.

IR spectrum (Figure 4.1.5-3) shows the following vibrations which the parent polymer and modified ones have in common: The $-CH_2$ & C-H stretch (2932 cm^{-1}), $-CH_3$ stretch (2869 cm^{-1}) and $-CH_2$ bend (1452 cm^{-1}) belong to the methyl end groups, polyethylene backbone and aliphatic side chains. The C=O stretch (1941/1731 cm^{-1}) is visible from the ester group of OEGMEA and ester/thioester groups of the bound thioester linker., OEGMEA has additionally C-O-C stretch (1349-850 cm^{-1}) from its ether side chain. The only visible difference is the decrease of the O-H stretch vibration at 3500 cm^{-1} after the esterification but is still present due to incorporated water molecules in the polymer. RAMAN spectrum (Figure 4.1.5-4) also shows the same vibrations like the parent polymer: The C-H stretch (2933/2879 cm^{-1}), $-CH_3$ & $-CH_2$ bend (1467/1453 cm^{-1}) and C-C stretch/bend (546/272 cm^{-1}) belong to the methyl end group, polyethylene backbone and the aliphatic side chains. The C≡N stretch (2360 cm^{-1}) is visible from the nitrile end group. The ester groups of OEGMEA, HEA and thioester linker are visible as C=O stretch (1734 cm^{-1}). OEGMEA shows additionally the C-O-C stretch (1287-848 cm^{-1}) from the ether side chain.

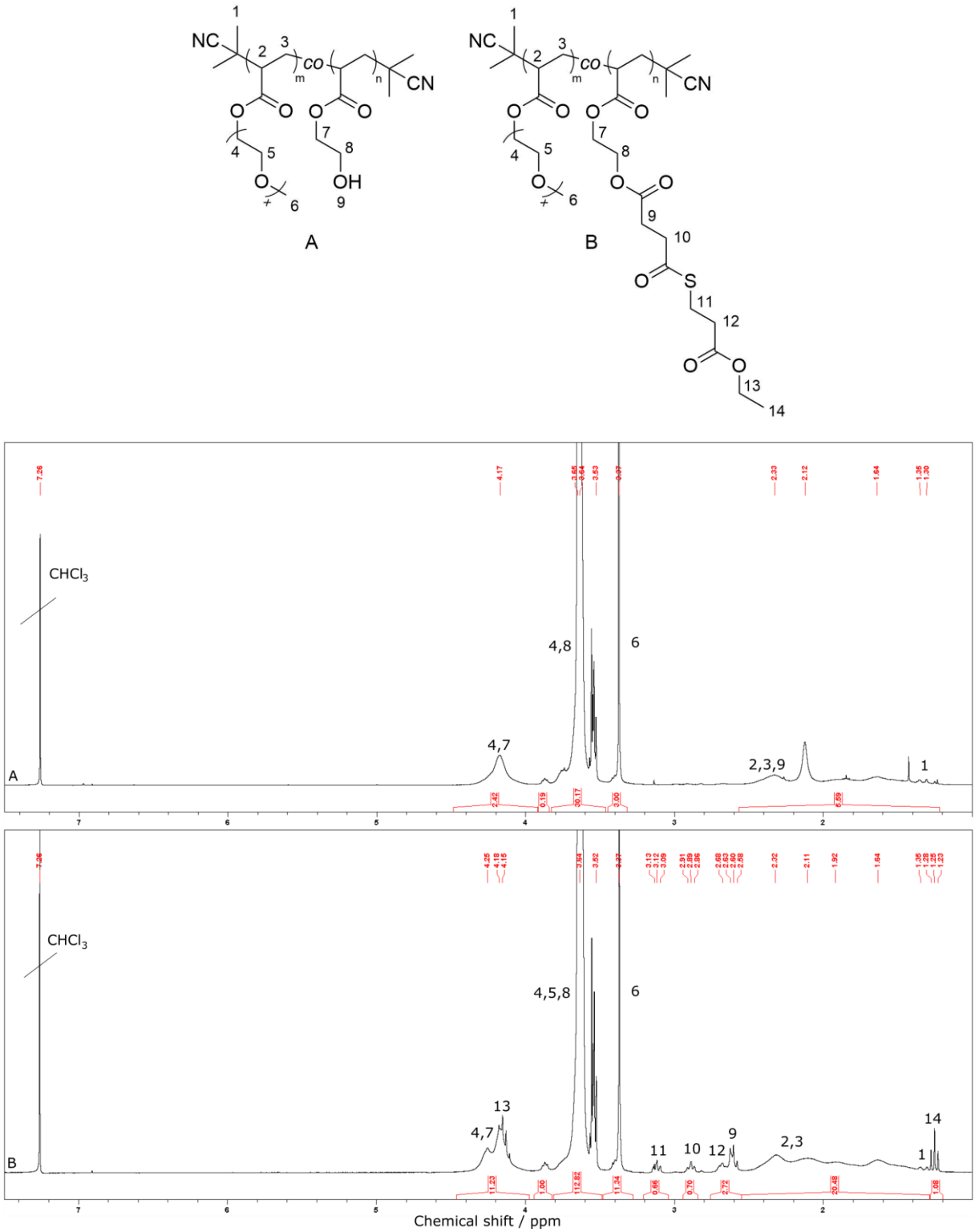

Figure 4.1.5-1: ^{1}H NMR spectra of P(OEGMEA-*co*-HEA) (A) and P(OEGMEA-*co*-EMP-SA) (B) in $CDCl_3$.

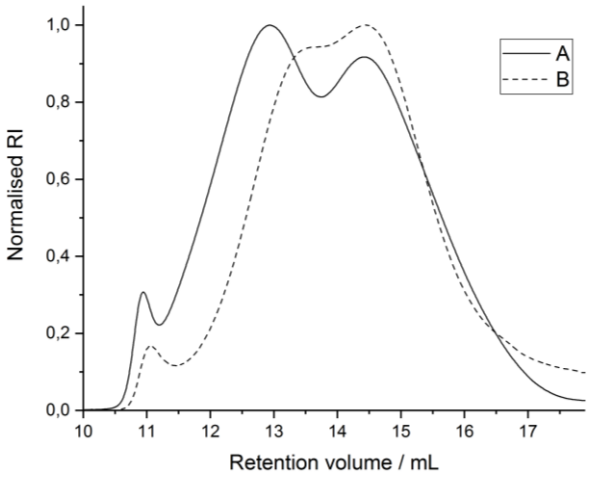

Figure 4.1.5-2: GPC traces of P(OEGMEA-*co*-HEA) (A) and P(OEGMEA-*co*-EMP-SA) (B) in DMF (RI).

Table 4.1.5-1: GPC data of P(OEGMEA-*co*-HEA) (A) and P(OEGMEA-*co*-EMP-SA) (B) in DMF (RI).

Run	**A**	**B**
M_n/Da	4,759	3,824
M_w/Da	11,959	8,233
Đ	2.51	2.15

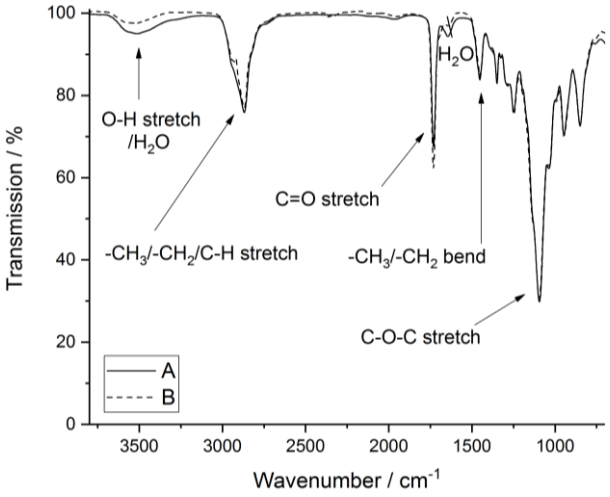

Figure 4.1.5-3: IR spectra of P(OEGMEA-*co*-HEA) (A) and P(OEGMEA-*co*-EMP-SA) (B).

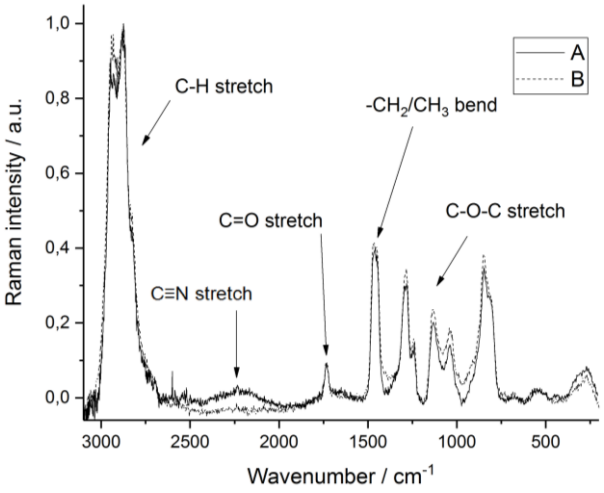

Figure 4.1.5-4: RAMAN spectra of P(OEGMEA-*co*-HEA) (A) and P(OEGMEA-*co*-EMP-SA) (B).

3.1.6 Determination of the monomer ratios

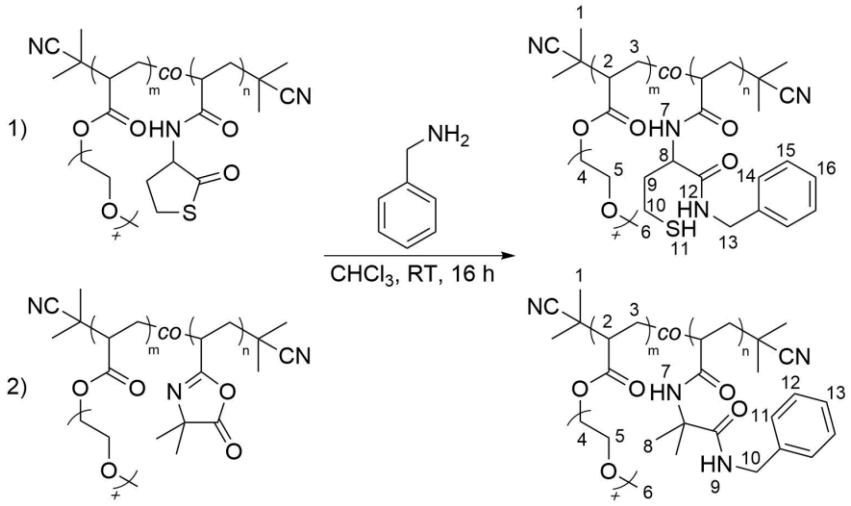

Scheme 4.1.6-1: Modification of P(OEGMEA-*co*-TLA) (1) and P(OEGMEA-co-VAL) (2) with benzylamine.

In order to determine the ratios OEGMEA:TLA and OEGMEA:VAL, the copolymers were reacted with benzylamine (Scheme 4.1.6-1) so that the ratio could be calculated from the ^{1}H NMR spectra from the signals of the aromatic ring and the methoxy group. The procedure was performed according literature procedure with some changes. [100, 145] The products were successfully synthesised and characterised *via* ^{1}H NMR, IR, RAMAN spectroscopy and GPC.

^{1}H NMR spectrum (Figure 4.1.6-1) shows the following same signals of P(OEGMEA-*co*-TLA) before and after reaction with benzylamine: H-1 (1.29/1.27 ppm) from the propyl end groups, H-2/3 (2.54-1.64 ppm) from the polymer backbone, H-4 (4.15 ppm) of the first repeating unit of OEGMEA, H-4/5 (3.63-3.45 ppm) of the residual methylene groups of OEGMEA, H-6 of the methoxy group (3.30 ppm), H-7 (6.93 ppm) of the amide group/H-8 (4.51 ppm) of the single proton and H-9 (overlap with polymer backbone) of TLA. After the reaction with benzylamine, the methylene group H-13 (4.36 ppm) and aromatic ring H-14 – H-16 (7.29 ppm) of this compound are visible.

Calculation OEGMEA:TLA-ratio:

TLA: Aromatic region is set to five protons equivalent to ove TLA unit

OEGMEA: Methoxy group H-6 – satellite = 20.68 – 1.02 = 19.66

19.66 divided by 3 gives OEGMEA units: 19.66 : 3 = 6.55

That means OEGMEA:TLA = 6.55:1

IR spectrum (Figure 4.1.6-5) shows the following same vibrations of the parent and modified polymer: The N-H stretch (3524 cm^{-1}) and N-H bend (1535 cm^{-1}) belong to the amide groups. The -CH_2 & C-H stretch (2868 cm^{-1}) and -CH_3 & -CH_2 bend (1452 cm^{-1}) are from the methyl end groups, polyethylene backbone and aliphatic side chains. The ester group of OEGMEA and the amide/thiolactone group show the C=O stretch (1731/1671 cm^{-1}). The C-N stretch from the amide groups/the C-O-C stretch from OEGMEA's ether side chain (1349-849 cm^{-1}) and C-S stretch from the thiolactone/=C-H bend (801-701 cm^{-1}) from the aromatic ring of the bound benzylamine are overlapping. RAMAN spectrum (Figure 4.1.6-6) shows the following same vibrations of the parent and modified polymer: The C-H stretch (2923/2881 cm^{-1}), -CH_3 & -CH_2 bend (1470/1449 cm^{-1}) and C-C bend (487-275 cm^{-1}) belong to the methyl end groups, polyethylene backbone and the aliphatic side chains. The nitrile end groups are visible as C≡N stretch (2235 cm^{-1}). The ester group of OEGMEA and amide groups of TLA appear as C=O stretch (1734 cm^{-1}). OEGMEA has additionally the ether side chain with C-O-C stretch (1285-811 cm^{-1}). The C-S stretch (685/617 cm^{-1}) belongs to the thiolactone/thiol group of the closed and opened TLA. The product has new vibrations from the aromatic ring of the bound benzylamine (=C-H stretch: 3060 cm^{-1} and C=C stretch: 1608 cm^{-1}) and from the thiol group of the opened thiolactone ring (S-H stretch: 2575 cm^{-1}). GPC measurement in DMF (Figure 4.1.6-3, Table 4.1.6-1) does not show significant changes.

^{1}H NMR spectrum (Figure 4.1.6-2) shows the following same signals of P(OEGMEA-*co*-VAL) before and after reaction with benzylamine: H-1 of the methyl end groups (1.29/1.27 ppm), H-2/3 of the polymer backbone (2.31-1.62 ppm), H-4 of the methylene groups of the first repeating unit of OEGMEA (4.14 ppm), H-4/5 of the residual methylene groups of OEGMEA (3.62-3.45 ppm) and the methoxy group H-6 (3.29 ppm). After the reaction with benzylamine, the methyl groups of VAL shifted from to 1.36 ppm to 1.44 ppm and signals of the bound compound can be found: methylene group H-10 (4.35 ppm), aromatic protons H-11 – H-13 (7.28 ppm) and amide bonds H-7/9 (6.90 ppm).

Calculation OEGMEA:VAL-ratio:

VAL: Aromatic region is set to five protons equivalent to one VAL unit

OEGMEA: Methoxy group H-6 – satellite = 9.85 – 0.83 = 9.85

9.85 divided by 3 gives OEGMEA units: 9.85 : 3 = 3.28

That means OEGMEA:VAL = 3.28:1

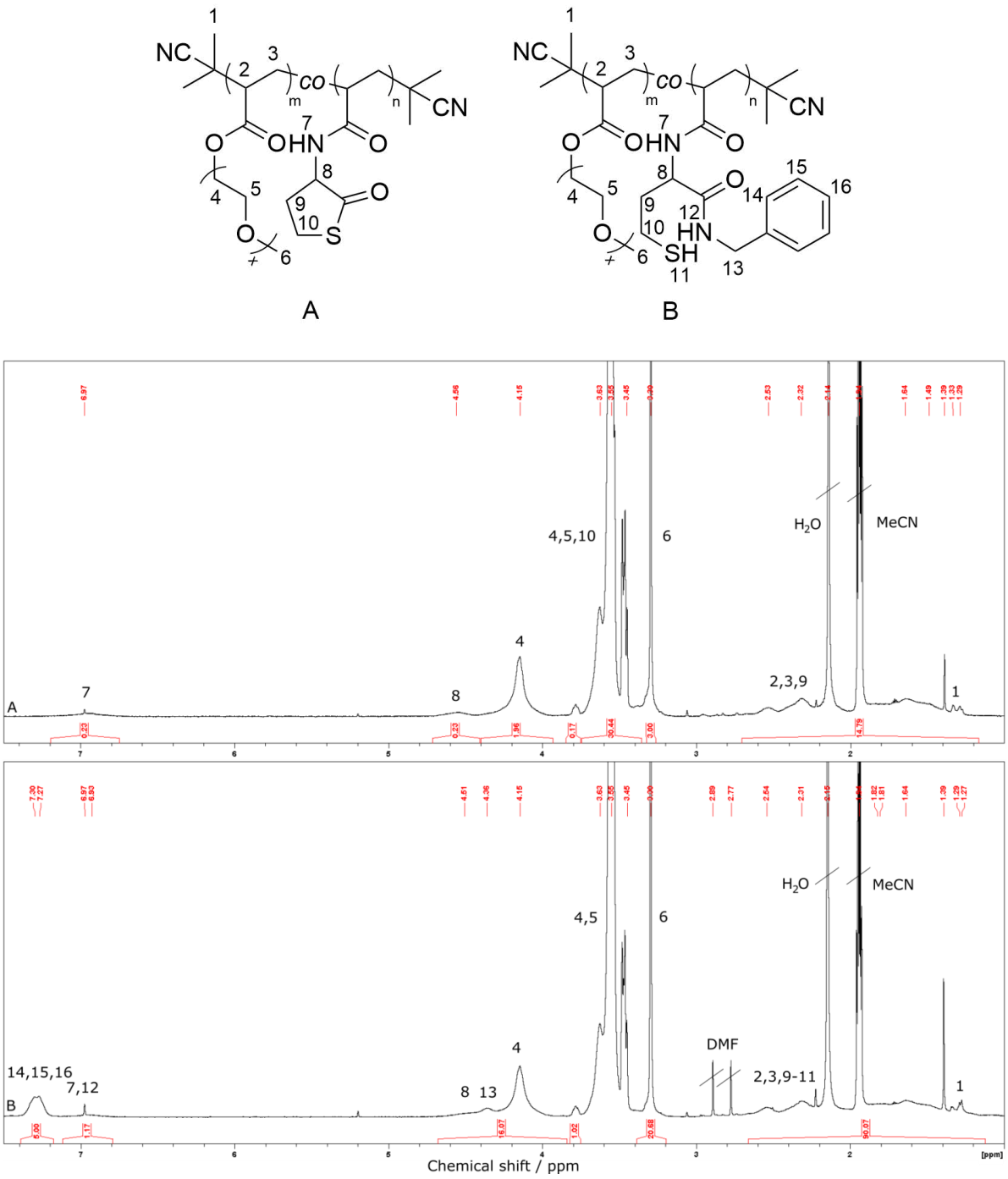

Figure 4.1.6-1: ^{1}H NMR spectra of P(OEGMEA-*co*-TLA) in MeCN-d_3 before (A) and after (B) reaction with benzylamine.

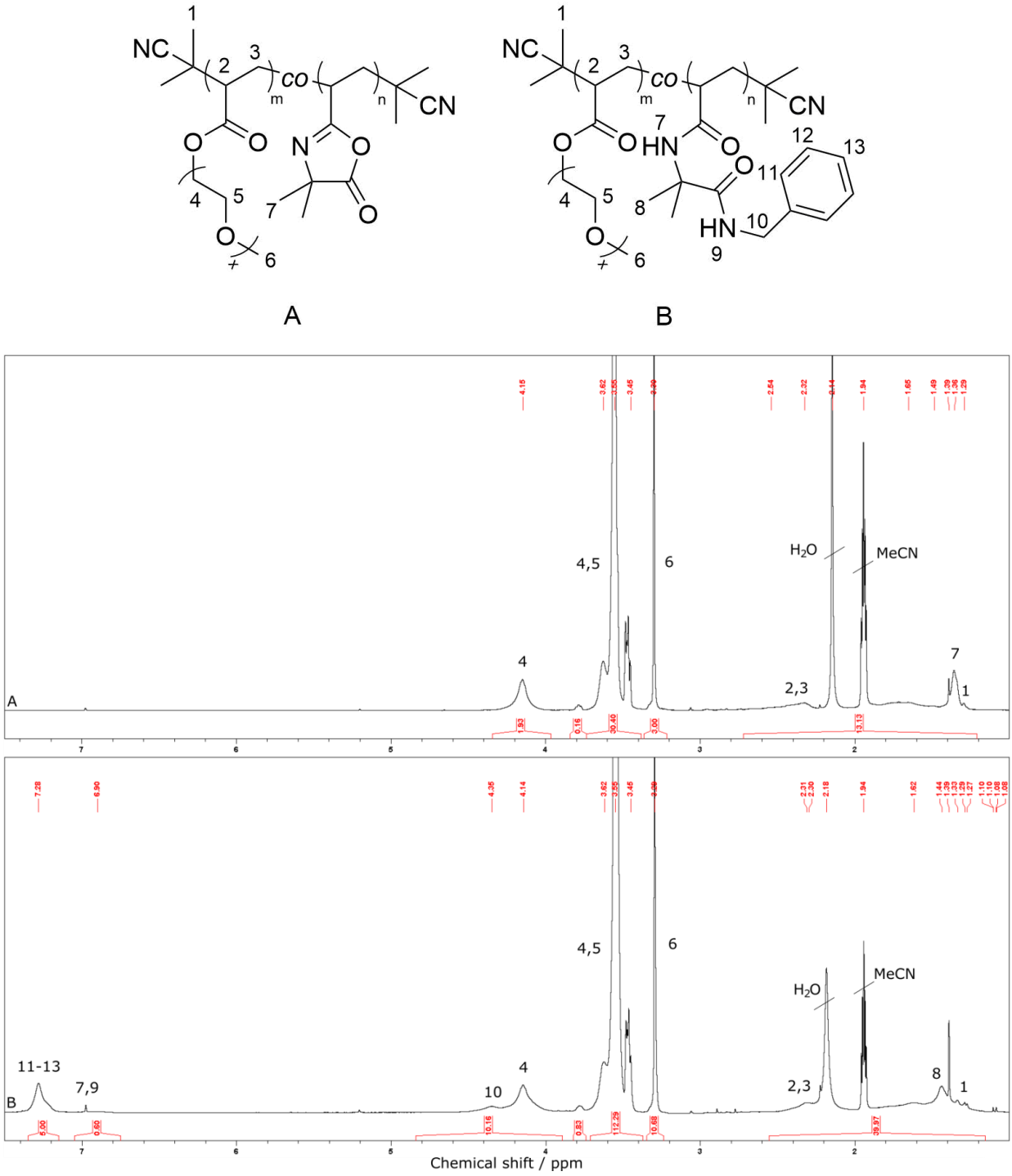

Figure 4.1.6-2: ^{1}H NMR spectra of P(OEGMEA-*co*-VAL) in MeCN-d_3 before (A) and after (B) reaction with benzylamine.

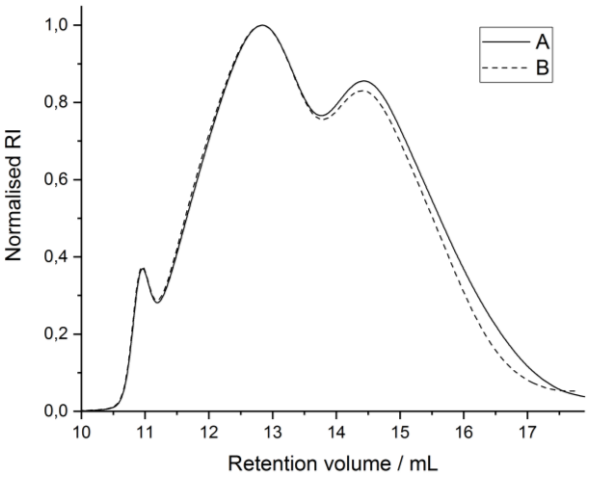

Figure 4.1.6-3: GPC traces of P(OEGMEA-*co*-TLA) before (A) and after (B) reaction with benzylamine in DMF (RI).

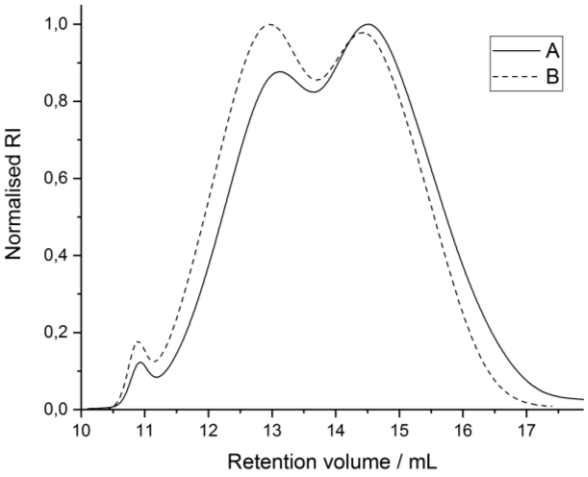

Figure 4.1.6-4: GPC traces of P(OEGMEA-*co*-VAL) before (A) and after (B) reaction with benzylamine in DMF (RI).

Table 4.1.6-1: GPC data of of P(OEGMEA-*co*-TLA) and P(OEGMEA-*co*-VAL) before and after reaction with benzylamine in DMF (RI).

Polymer	**P(OEGMEA-*co*-TLA)**		**P(OEGMEA-*co*-VAL)**	
	Without benzyl-amine	**With benzyl-amine**	**Without benzyl-amine**	**With benzyl-amine**
M_n/Da	4,729	5,218	4,396	5,226
M_w/Da	13,083	13,619	8,907	11,066
Đ	2.77	2.61	2.03	2.12

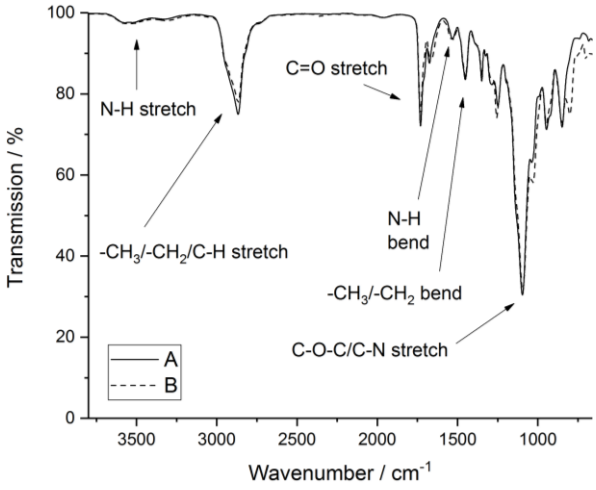

Figure 4.1.6-5: IR spectra of P(OEGMEA-*co*-TLA) before (A) and after (B) reaction with benzylamine.

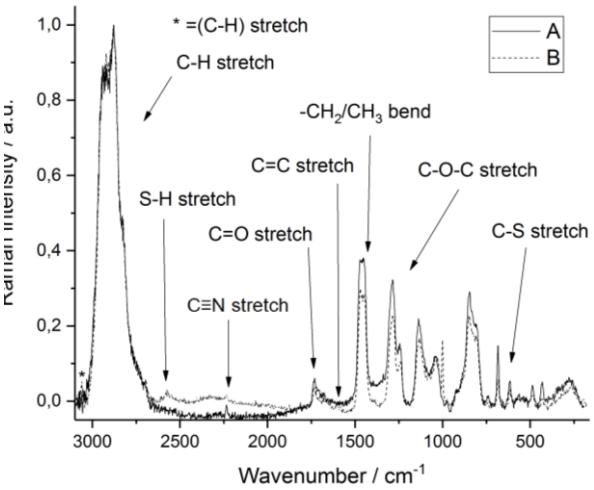

Figure 4.1.6-6: RAMAN spectra of P(OEGMEA-*co*-TLA) before (A) and after (B) reaction with benzylamine.

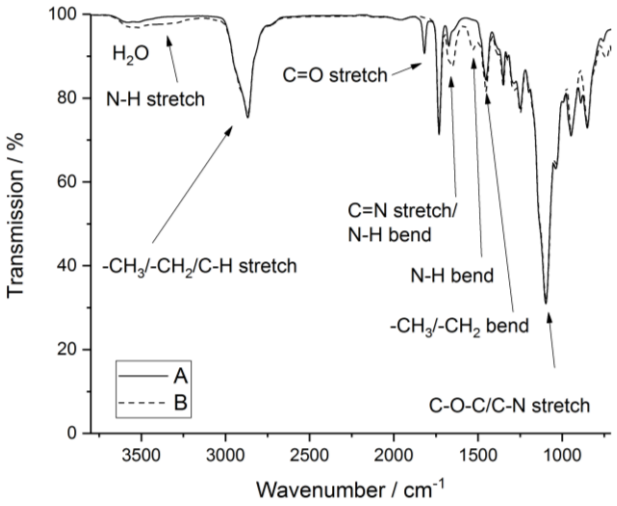

Figure 4.1.6-7: IR spectra of P(OEGMEA-*co*-VAL) before (A) and after (B) reaction with benzylamine.

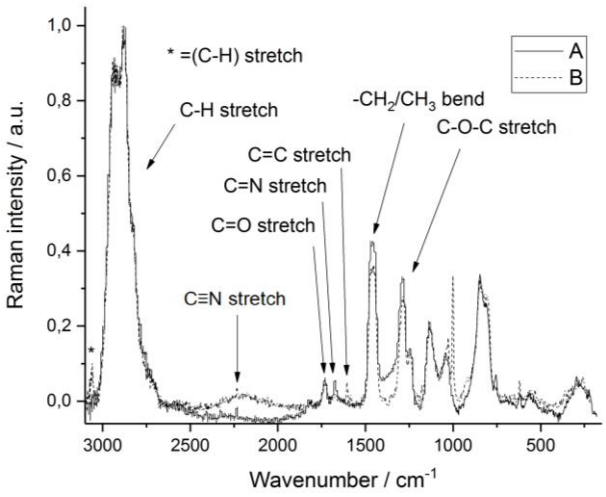

Figure 4.1.6-8: RAMAN spectra of P(OEGMEA-*co*-VAL) before (A) and after (B) reaction with benzylamine.

IR spectrum (Figure 4.1.6-7) shows the following vibrations which the parent and modified polymer have in common: The $-CH_2$ & C-H stretch (2868 cm^{-1}) and $-CH_2/-CH_3$ bend (1453/1384 cm^{-1}) belong to the methyl end groups, polyethylene backbone and the aliphatic/aromatic side chains. The C=O stretch (1731 cm^{-1}) is visible from the ester of OEGMEA. OEGMEA's ether side chain C-O-C stretch and closed/opened VAL C-N stretch (1350-850 cm^{-1}) are overlapping. After the reaction with benzylamine, the vibrations of the newly formed amid bonds can be found: N-H stretch (3524 cm^{-1})/N-H bend (1651/1531 cm^{-1}) belong to the new amide bond and the C=O stretch vibration (1818 cm^{-1}) of the azlactone from VAL disappeared after the reaction. =C-H bend vibrations of the aromatic ring of the bound benzylamine are also additionally visible (751/701 cm^{-1}). RAMAN spectrum (Figure 4.1.6-8) shows the following vibrations which the parent and modified polymer have in common: The C-H stretch (2930/2876 cm^{-1}), $-CH_3$ & $-CH_2$ bend (1461 cm^{-1}) and C-C bend (620-260 cm^{-1}) belong to the methyl end groups, polyethylene backbone and the aliphatic/aromatic side chain. The nitrile end groups C≡N stretch (2233 cm^{-1}) are also visible. The ester group of OEGMEA can be seen with C=O stretch (1730 cm^{-1}) and its ether side chain with C-O-C stretch (1288-807 cm^{-1}). After the reaction with benzylamine, the =C-H stretch (3060 cm^{-1}) and C=C stretch (1606 cm^{-1}) vibrations of the aromatic ring are visible and the C=N stretch vibration (1671 cm^{-1}) from the azlactone ring disappeared. GPC measurement in DMF (Figure 4.1.6-4, Table 4.1.6-1) does not show significant changes.

3.1.7 Reaction of copolymers with CGGGF

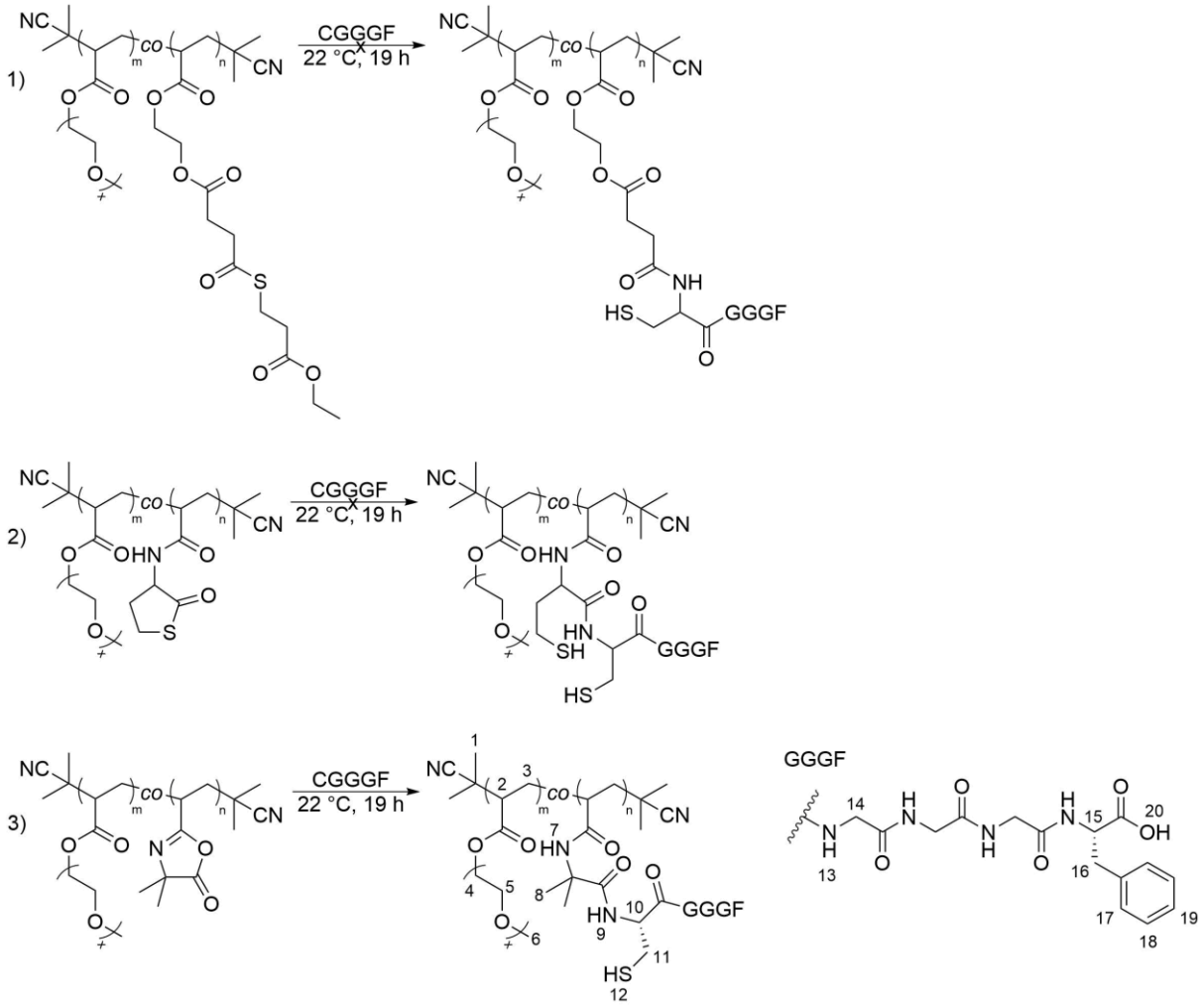

Scheme 4.1.7-1: Reaction of P(OEGMEA-*co*-EMP-SA) (1), P(OEGMEA-*co*-TLA) (2) and P(OEGMEA-*co*-VAL) (3) with CGGGF.

The copolymers, carrying peptide binding units, were mixed with the model peptide CGGGF (Scheme 4.1.7-1) in different solvents and analysed afterwards: (1) PBS, (2) NaAsc PBS, (3) NaAsc PBS with TCEP·HCl and (4) dry DMF. (1) was chosen as reference, (2) and (3) in order to prevent oxidation of the model peptide's thiol group with ascorbic acid and (4) to prevent the competitive nucleophilic attack of water on the peptide binding units. P(OEGMEA-*co*-EMP-SA) and P(OEGMEA-*co*-TLA) do not show any binding of CGGGF. The reason could be the too stable thioester bonds which still need the commonly used activation agents in a typical native chemical ligation process or OEGMEA's shielding of the peptide binding units. P(OEGMEA-*co*-VAL) shows different degrees of substitution: (1) 0 % as the ring of VAL could react faster with water than with CGGGF. (2) and (3) show some binding (15 %) where the reductive agents show an effect that the thiol group of CGGGF could be prevented from oxidation and be able to bind on VAL. Water molecules are

nonetheless competitive on that reaction. (4) shows a binding of 19 % although a dry solvent was used. An improvement of the binding compared to aqueous solvent is given but still too far away from 100 %. The reason for the low degree could be that water molecules which are around OEGMEA chains react faster with VAL than CGGGF. Additionally, the OEGMEA side chains may be too long which could shield the co-monomers and prevent native chemical ligation with CGGGF. Polymers with reverse side chain lengths facilitate this reaction. [82] OEGMEA with shorter chains, e.g. three units could be used or a spacer for the peptide binding units so that they are not shielded and could react better with the peptides. Further parameters like higher amount of peptide binding units, higher concentrations of polymer/peptide and higher reaction temperatures could be tried out in future experiments in order to improve the binding of the peptides.

The product of (4) is shown as an example for the analysis of ^{1}H NMR, IR, RAMAN spectroscopy and GPC. ^{1}H NMR analysis (Figure 4.1.7-1) shows the following signals which the parent and modified polymer have in common: The methyl end groups H-1 (1.34/1.29 ppm), the polymer back bone H-2/3 (3.32-1.63 ppm), the methylene group of the first repeating unit of OEGMEA H-4 (4.15 ppm), the residual methylene groups of OEGMEA H-4/5 (3.63-3.45 ppm) and the methoxy group H-6 (3.30 ppm). After the reaction with CGGGF, the methyl groups of VAL shifted from 1.36 ppm to 1.43 ppm. Additional signals of the peptide are visible: H-17 – H-19 from the aromatic ring (7.27 ppm), amide bonds H-7/9/13 (7.00 ppm) and H-15 of phenyl alanine (4.57 ppm). Other signals are overlapping. IR spectrum (Figure 4.1.7-3) shows the following vibrations which the parent and modified polymer have in common: The -CH_2 & C-H stretch (2868 cm^{-1}) and -CH_2/-CH_3 bend (1453/1385 cm^{-1}) belong to the methyl end groups, polyethylene backbone and aliphatic side chains. OEGMEA's C=O stretch (1731 cm^{-1}) from the ester group is visible and its ether chain, C-O-C stretch is overlapping with the C-N stretch (1350-850 cm^{-1}) of VAL. Additional signals of CGGGF are visible: N-H stretch (3511/3336 cm^{-1}) of the amine group from the opened VAL, C=C stretch (1671 cm^{-1}) of the aromatic ring from phenylalanine, N-H bend (1531 cm^{-1}) from CGGGF's amide bonds and =C-H/C-S stretch (702 cm^{-1}) from the aromatic ring of phenylalanine overlapping with the thiol group from cysteine. Also the C=O stretch vibration (1818 cm^{-1}) of VAL completely disappeared after the reaction with CGGGF. RAMAN spectrum (Figure 4.1.7-4) shows the following vibrations which the parent and modified polymer have in common: The C-H stretch (2936/2879 cm^{-1}), -CH_3 & -CH_2 bend (1459 cm^{-1}) and C-C stretch/bend (548/276 cm^{-1}) belong to the methyl end groups, polyethylene backbone and aliphatic side chains. OEGMEA's ester group with C=O stretch

(1737 cm^{-1}), and ether chain with C-O-C stretch (1293-807 cm^{-1}) are visible. Additionally, the S-H stretch (2649 cm^{-1}) of the thiol group from the bound cysteine is visible. GPC measurement in DMF (Figure 4.1.7-2, Table 4.1.7-1) shows a broadening and higher dispersity (from 2.03 to 2.49). Additionally, the three polymer fractions shifted to higher retention volumes which could come from intramolecular hydrogen bond formation of the amide groups leading to smaller hydrodynamic volumes of the polymers.

Calculation for the degree of substitution: The aromatic region H-17 – H-19 shows 0.27 protons and the methoxy group H-6 with the satellite show three protons. Reaction of benzylamine with P(OEGMEA-*co*-VAL) showed that five protons of the benzylamine led to 10.68 protons of the methoxy group H-6 with the satellite.

That means for the ratios: H-17 – H-19 : H-6 = 0.27 : 3.00 = 0.96 : 10.68

0.96 protons of the aromatic region of the peptide are bound and five are possible as the maximum: DS = 0.96 : 5 = 0.19 = 19 %

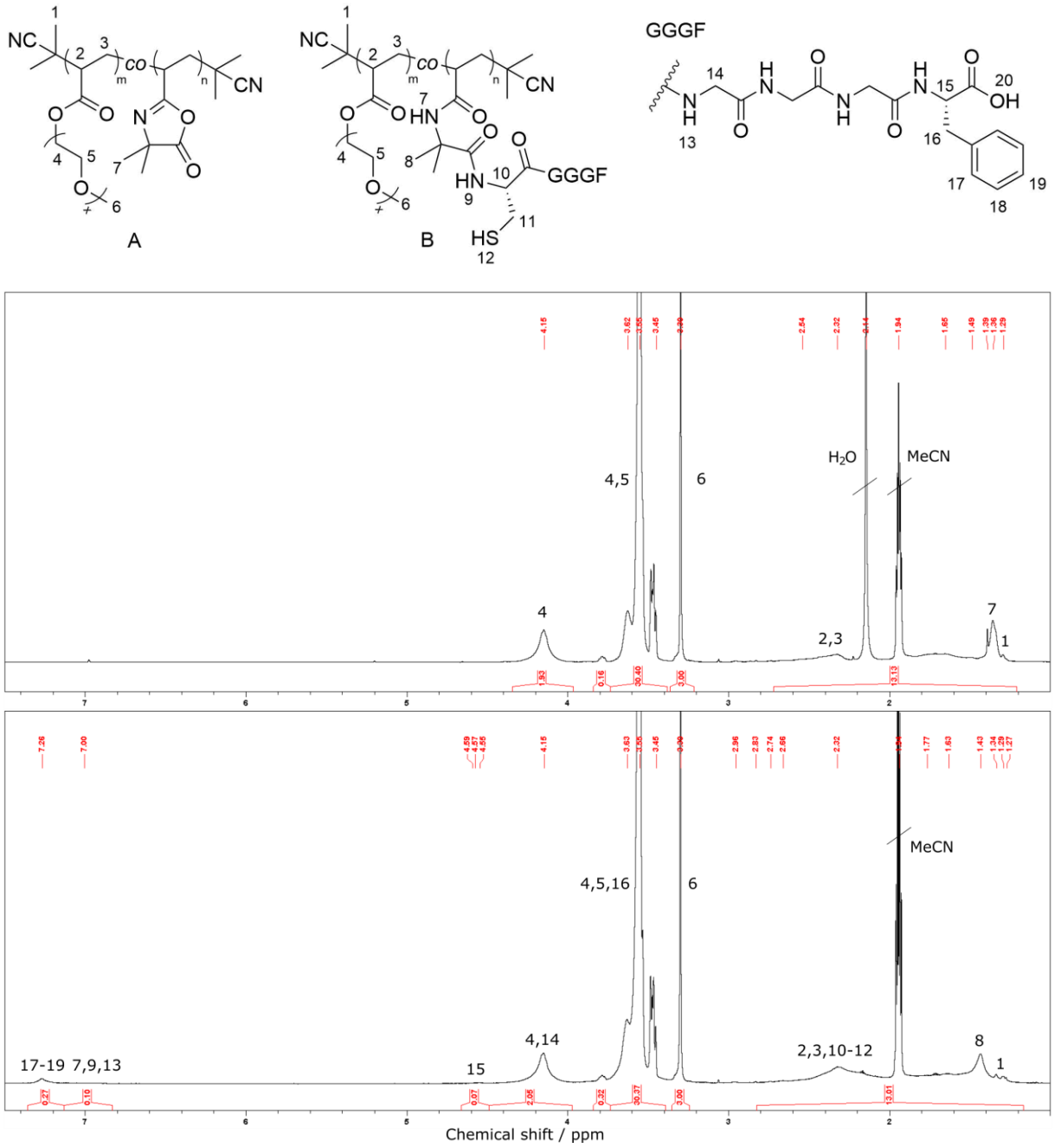

Figure 4.1.7-1: ^{1}H NMR spectra of P(OEGMEA-*co*-VAL) in MeCN-d_3 before (A) and after (B) reaction with CGGGF.

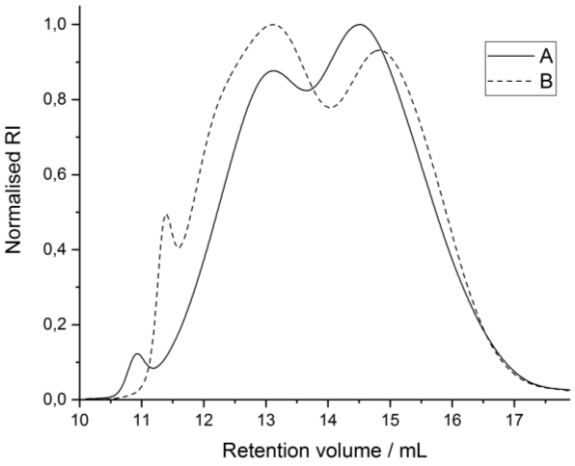

Figure 4.1.7-2: GPC traces of P(OEGMEA-*co*-VAL) before (A) and after (B) reaction with CGGGF in DMF (RI).

Table 4.1.7-1: GPC data of P(OEGMEA-*co*-VAL) before (A) and after (B) reaction with CGGGF in DMF (RI).

Run	**A**	**B**
M_n/Da	4,396	**5,771**
M_w/Da	8,907	**14,383**
Đ	2.03	**2.49**

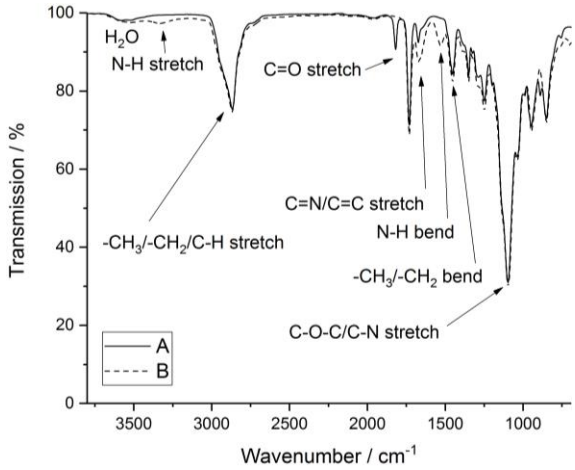

Figure 4.1.7-3: IR spectra of P(OEGMEA-*co*-VAL) before (A) and after (B) reaction with CGGGF.

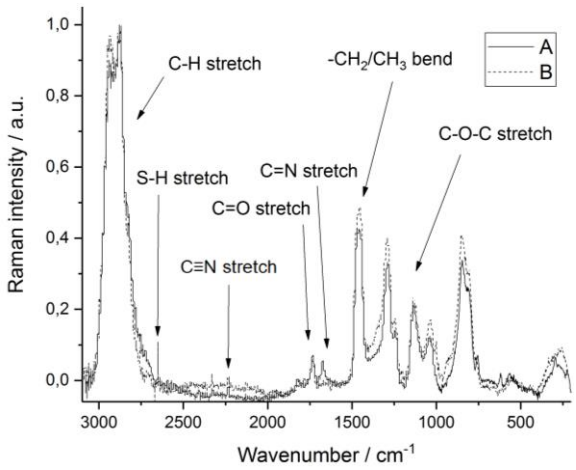

Figure 4.1.7-4: RAMAN spectra of P(OEGMEA-*co*-VAL) before (A) and after (B) reaction with CGGGF.

3.1.8 Hydrolysis stability tests

The experiments of the copolymers with CGGGF have shown that either the peptide could not be bound (P(OEGMEA-*co*-EMP-SA), P(OEGMEA-*co*-TLA)) or being bound with a low degree of substitution (P(OEGMEA-*co*-VAL). The following experiments were performed to check the stability of the thioester and azlactone compounds in water to find out if the hydrolysis (Scheme 4.1.8-1) is competitive to the native chemical ligation or if the thioester bonds are too stable. The experiments were performed in water at 22 °C for 19 h and the reaction conditions were not varied.

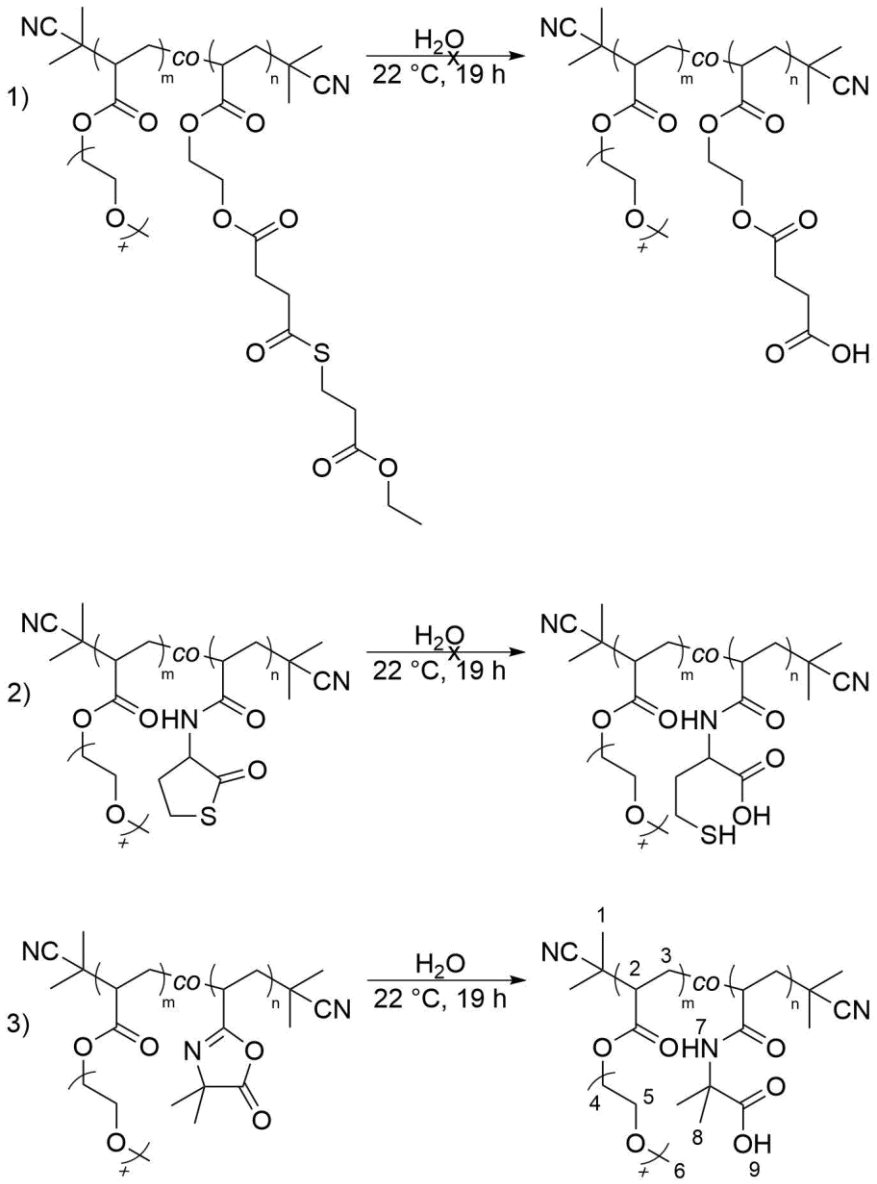

Scheme 4.1.8-1: Hydrolysis of P(OEGMEA-*co*-EMP-SA) (1), P(OEGMEA-*co*-TLA) (2) and P(OEGMEA-*co*-VAL) (3).

P(OEGMEA-*co*-EMP-SA) and P(OEGMEA-*co*-TLA) do not show any reaction with water. In comparison to that, P(OEGMEA-*co*-VAL) is really unstable in aqueous solution and confirms that water is a competitive reagent to the peptide. The hydrolysed product was characterised *via* ^{1}H NMR, IR RAMAN spectroscopy and GPC.

^{1}H NMR analysis (Figure 4.1.8-1) shows the following signals which the parent and modified polymer have in common: The methyl end groups H-1 (1.33/1.30 ppm), the polymer back bone H-2/3 (2.54-1.57 ppm), the methylene group of the first repeating unit of OEGMEA H-4 (4.15 ppm), the residual methylene groups of OEGMEA H-4/5 (3.63-3.45 ppm) and the methoxy group H-6 (3.30 ppm). After hydrolysis, the methyl groups of VAL have shifted from 1.36 ppm to 1.43 ppm, the new amide bond H-7/carboxyl group H-9 appears at 7.54 ppm/9.06 ppm. IR spectrum (Figure 4.1.8-3) shows the following vibrations which the

parent and modified polymer have in common: The -CH_2 & C-H stretch (2868 cm^{-1}) and -CH_2 bend (1453 cm^{-1}) belong to the methyl end groups, polyethylene backbone and aliphatic side chains. OEGMEA's ester group C=O stretch (1731 cm^{-1}) and ether chain with C-O-C (1350-1039 cm^{-1}) and C-O-C stretch (996-850 cm^{-1}) are visible overlapping with C-N stretch from VAL. Additionally, after hydrolysis the N-H stretch (3518 cm^{-1}), N-H bend (1657/1531 cm^{-1}) and C=O stretch (1389 cm^{-1}) from the formed amide group vibrations are visible of the open VAL compound. At the same time, the C=O stretch (1818 cm^{-1}) vibration of the VAL compound disappeared. RAMAN spectrum (Figure 4.1.8-4) shows the following vibrations which the parent and modified polymer have in common: The C-H stretch (2930 cm^{-1}/ 2883 cm^{-1}), -CH_3 & -CH_2 bend (1474/1459 cm^{-1}) and C-C stretch/bend (567/435-271 cm^{-1}) belong to the methyl end groups, polyethylene backbone and aliphatic side chains. The nitrile's C≡N stretch (2236 cm^{-1}) is visible and OEGMEA's ester group C=O stretch (1737 cm^{-1}) and ether chain C-O-C stretch (1289-813 cm^{-1}) can be seen. After hydrolysis, the C=N stretch (1671 cm^{-1}) vibration disappeared and the C=O stretch vibration of VAL shifted from 1826 cm^{-1} to 1669 cm^{-1}. GPC analysis in DMF (Figure 4.1.8-2, Table 4.1.8-1) shows that the dispersity decreased from 2.03 to 1.55 and that all 3 polymer fractions shifted to lower retention volumes which may come from intramolecular hydrogen bond formation due to the carboxyl group of the hydrolysed VAL leading to smaller hydrodynamic volumes.

In conclusion, EMP-SA and TLA are stable in water at 22 °C for 19 h. That means that the peptide binding, as assumed, was not successful due to the competitive nucleophilic attack of water, but is just too stable under the chosen reaction conditions. The thioester group needs reaction agents for activation which are commonly used for native chemical ligation. AZL is not stable at 22 °C for 19 h. That means that the peptide binding was low due to the competitive nucleophilic attack of the water. In order to improve the degree of substitution, one could increase the amount of AZL units in the polymer. Furthermore, one could increase the spacer between the polymer backbone and the AZL unit because the OEGMEA side chains may be too long which could shield the co-monomers and prevent native chemical ligation with CGGGF. Polymers with reverse side chain lengths facilitate this reaction. [82] Furthermore, the concentration of the polymers/peptides and the reaction temperature could be increased to improve the binding efficiency.

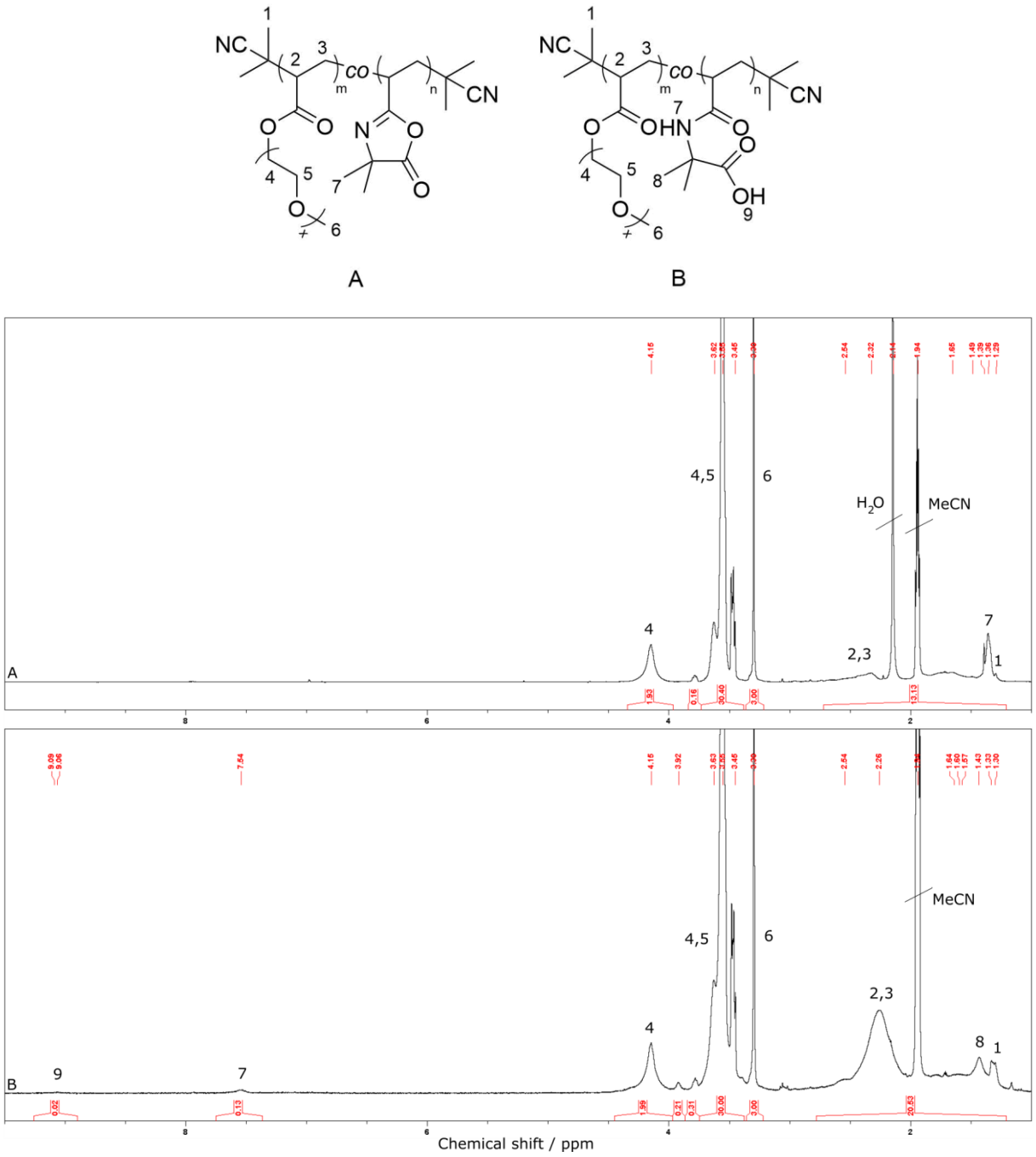

Figure 4.1.8-1: ^{1}H NMR spectrum of P(OEGMEA-*co*-VAL) in MeCN-d_3 before (A) and after (B) hydrolysis.

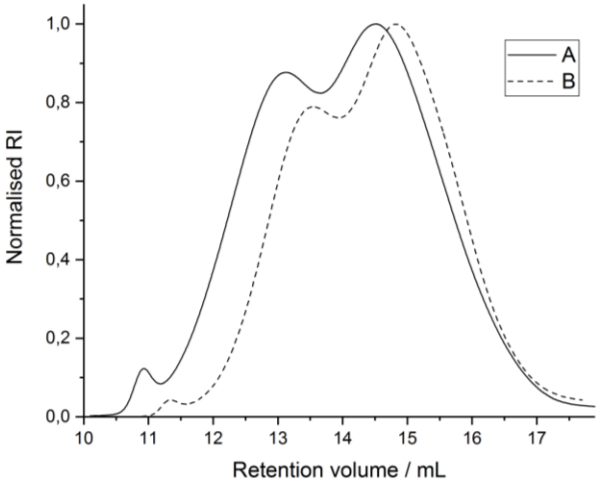

Figure 4.1.8-2: GPC traces of P(OEGMEA-*co*-VAL) before (A) and after (B) hydrolysis in DMF (RI).

Table 4.1.8-1: GPC data of P(OEGMEA-*co*-VAL) before (A) and after (B) hydrolysis in DMF (RI).

Run	**A**	**B**
M_n/Da	4,396	**4,500**
M_w/Da	8,907	**6,993**
Đ	2.03	**1.55**

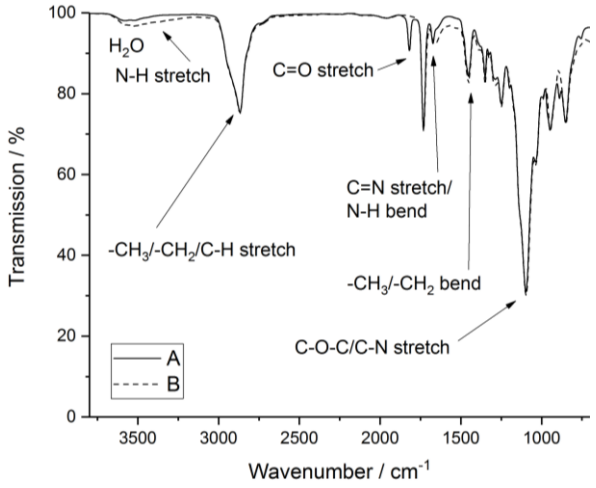

Figure 4.1.8-3: IR spectra of P(OEGMEA-*co*-VAL) before (A) and after (B) hydrolysis.

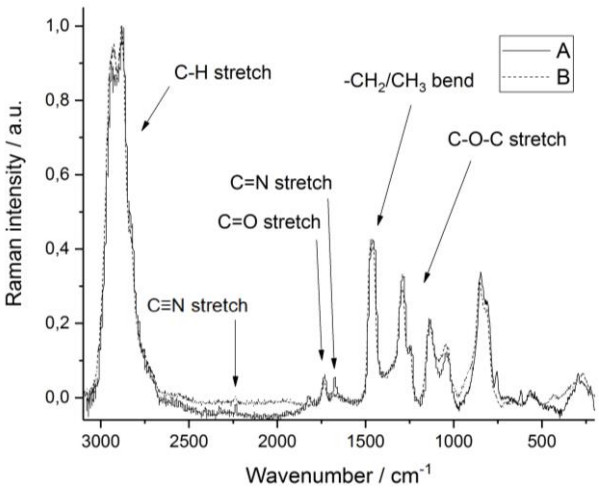

Figure 4.1.8-4: IR spectra of P(OEGMEA-*co*-VAL) before (A) and after (B) hydrolysis.

3.2 Low molecular weight polyglycidols

Besides OEGMEA, the biocompatible polyglycidol (PG) was investigated in this work. This linear analogue to PEG possesses additional side chains for further functionalisation and the polymers were investigated in terms of synthesis, modification and characterisation for hydrogel formation.

3.2.1 Monomer and polymer synthesis

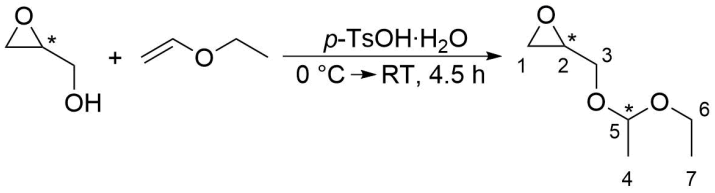

Scheme 4.2.1-1: Synthesis of EEGE.

The monomer ethoxy ethyl glycidyl ether (EEGE, Scheme 4.2.1-1) was synthesised according literature procedure [146] and was isolated with a yield of 57 %. ^{1}H, ^{13}C NMR, IR spectroscopy and mass spectrometry confirm the structure of the product. The ring protons of the epoxide appear in the ^{1}H NMR spectrum (Figure 4.2.1-1) in the region 3.05-2.47 ppm (H-1, H-1', H-2)$^{\#}$ and the carbon atoms appear at 44.35/44.30 ppm (C-1)$^{\#}$ and 50.73/50.62 ppm (C-2)$^{\#}$ in the ^{13}C NMR spectrum (Figure 4.2.1-2). The methylene groups with the protons H-3 and H-6 are visible in the region 3.72-3.27 ppm with its corresponding carbon atoms at 65.68/65.02 ppm (C-3)$^{\#}$ and 60.78 ppm (C-6). The residual protons/carbon atoms of the acetal group are to be seen at 1.22-1.18 ppm (H-4)$^{\#}$/19.61/19.49 ppm (C-4)$^{\#}$, 4.64 ppm (H-5)/99.55/99.53 ppm (C-5)$^{\#}$ and 1.08 ppm (H-7)/15.11 (C-7). $^{\#}$Splitting is due to the enantiomeric mixture. Mass spectrometry (Figure 4.2.1-3) confirms the molecular weight of the monomer with the found value m/z = 145.0855 which is in accordance with the calculated one $[M-H]^{-}$ = 145.0855. The fragment at 131.1064 (M – 14.9871) could be generated due to the loss of a methyl group. IR spectrum (Figure 4.2.1-4) shows the C-H/-CH_2/-CH_3 stretch vibrations (3053-2841 cm^{-1}) and the -CH_2 & -CH_3 bend vibrations (1483-1384 cm^{-1}), which belong to the oxirane ring, methylene side group and acetale protecting group. The ether from the oxirane ring and protecting group is visible as C-O-C stretch vibrations (1338-855 cm^{-1}). No O-H vibration of the free glycidol is visible confirming the fully protected product.

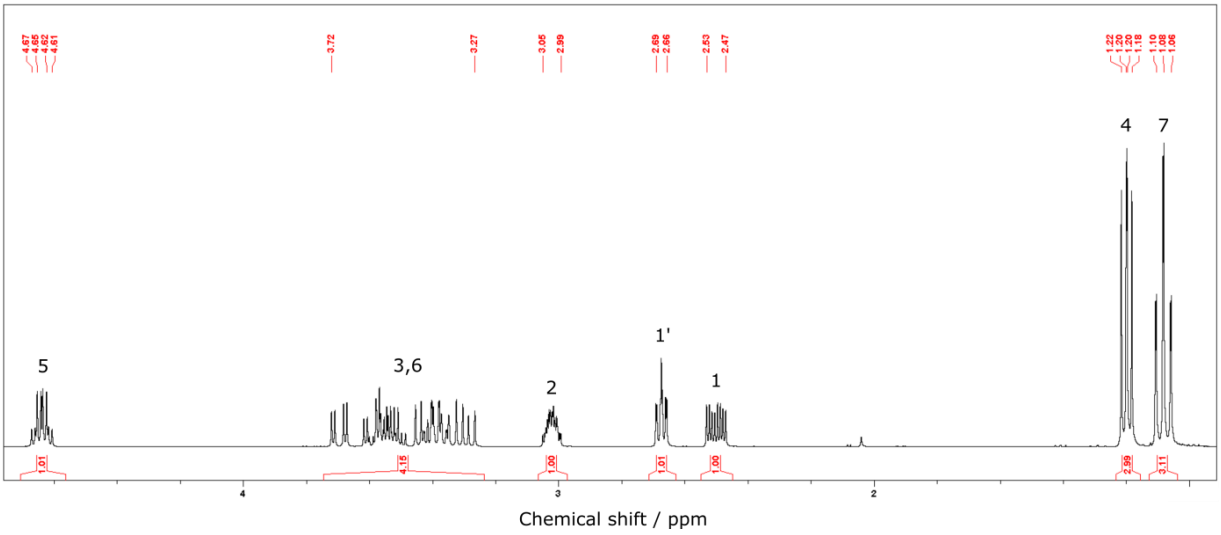

Figure 4.2.1-1: ^{1}H NMR spectrum of EEGE in $CDCl_3$.

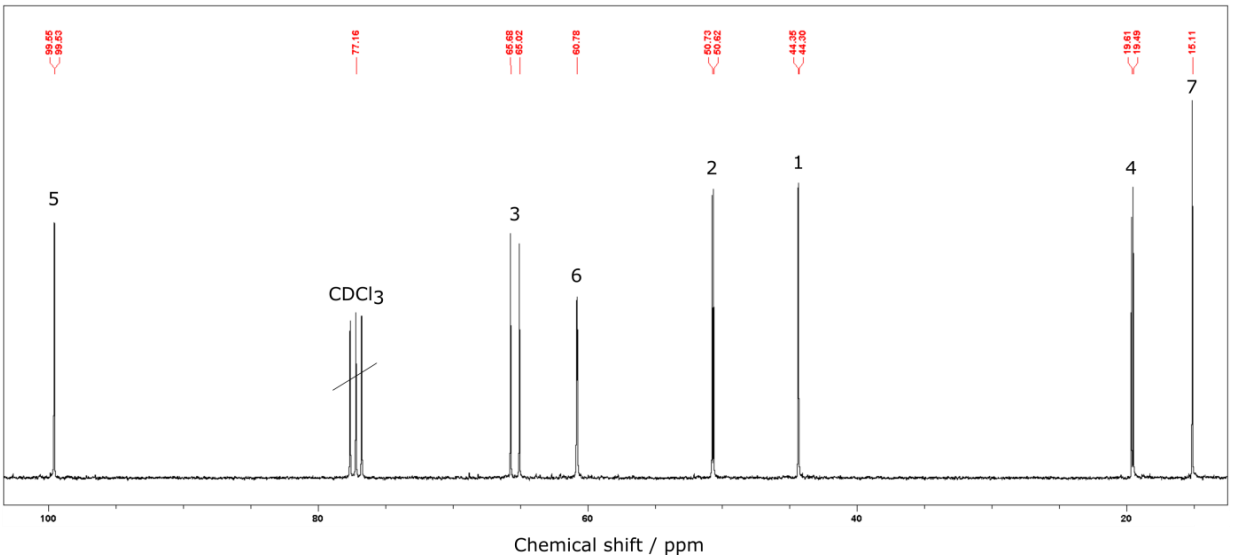

Figure 4.2.1-2: ^{13}C NMR spectrum of EEGE in $CDCl_3$.

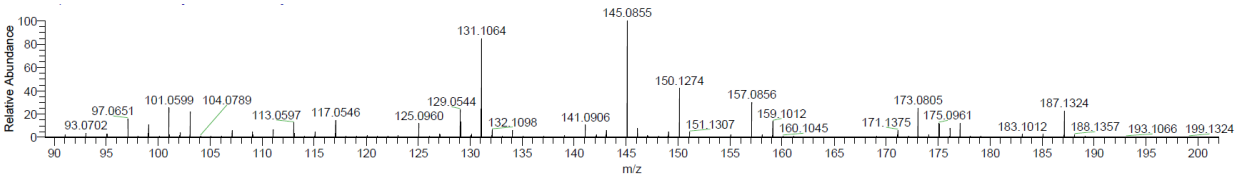

Figure 4.2.1-3: Mass spectrum of EEGE.

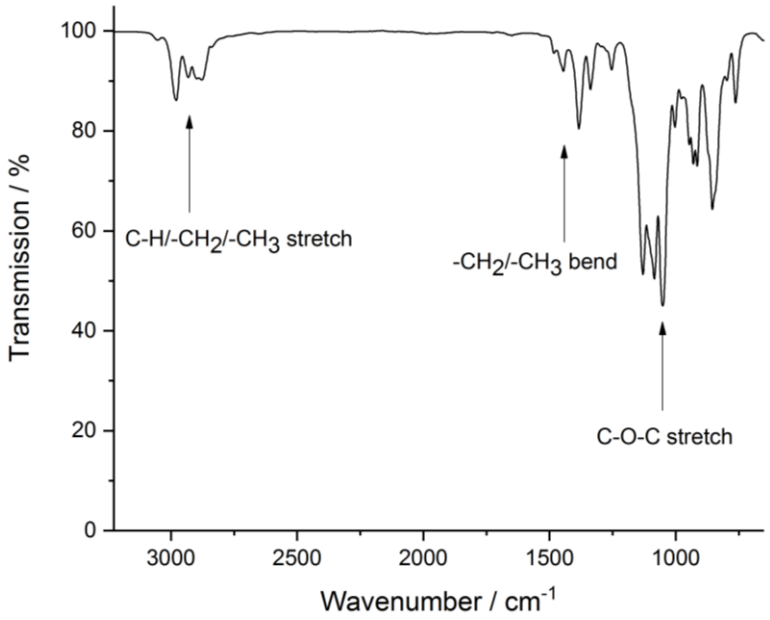

Figure 4.2.1-4: IR spectrum of EEGE.

Scheme 4.2.1-2: Synthesis of P(EEGE-*co*-AGE).

Afterwards, EEGE was copolymerised with the monomer allyl glycidyl ether (AGE) initiated by the base KO^{t}Bu (Scheme 4.2.1-2) according to literature procedure [53] in different ratios m/n = 57/3 (1), 54/6 (2), 51/9 (3) and 48/12 (4) in order to investigate the influence of the degree of functionalisation on the polymer's properties after functionalisation. The amount of AGE in the polymer was 5 % (1), 10 % (2), 15 % (3) and 20 % (4). The numbers 1-4 will be kept for all further functionalised polymers in this work referring to the initial ratio of EEGE:AGE. ^{1}H NMR, IR, RAMAN spectroscopy and GPC confirm the structure of the isolated products. Spectroscopic analysis will be explained for m/n = 54/6 as an example. In the ^{1}H NMR spectrum (Figure 4.2.1-7), the end group with the proton H-1 overlaps with the signal of H-8 at 1.18 ppm. The polymer backbone with the protons H-2 and H-3 give a broad multiplet with the methylene groups H-4 and H-7 in the range 3.69-3.40 ppm. The methyl group with H-5 is to be seen at 1.28 ppm and H-6 appears at 4.69 ppm which overlaps with the end group H-13. The allyl group is to be seen in the region 5.94-5.81 ppm (H-10), 5.25 ppm (H-12), 5.15 ppm (H-11) and 3.98 ppm (H-9). All four polymerisations reached

100 % monomer conversion in a crude ^{1}H NMR (spectra not shown) indicated by the disappearance of the ring protons of EEGE and AGE in the range 3.05-2.47 ppm. IR spectrum (Figure 4.2.1-8) shows the C-H/-CH_2/-CH_3 stretch vibrations (2977-2874 cm^{-1}) and the -CH_2 & -CH_3 bend vibrations (1456-1379 cm^{-1}) which belong to the ^{t}butyl group, polyether backbone, methylene side group, acetale protecting group and allyl group. Additionally, the C-O-C stretch vibrations (1340-816 cm^{-1}) from the polyether backbone, acetale and allyl side groups are visible. RAMAN spectrum (Figure 4.2.1-9) shows the C-H stretch vibration (2980-2801 cm^{-1}), -CH_2 & -CH_3 bend vibration (1455-1401 cm^{-1}) and C-C stretch/bend vibrations (670-271 cm^{-1}) which belong to the ^{t}butyl group, polyether backbone, methylene side group, acetale protecting group and allyl group. The C=C stretch vibration (1646 cm^{-1}) from the allyl group is also visible. Additionally, the C-O-C stretch vibrations (1276-753 cm^{-1}) from the polyether backbone, acetale and allyl side groups can be seen. GPC measurements in DMF (Figure 4.2.1-5, Table 4.2.1-1) show similar curve shapes which are all bimodal due to the side reaction with KO^{t}Bu (chapter 2.1.3.1) causing a minor polymer fraction in the range 13.0-14.7 mL besides the main polymer distribution in the range 14.7-18.0 mL. Despite that fact, the polymers' dispersities are very low (1.12-1.15) which is characteristic for a controlled living polymerisation and they are comparable with literature values of polyglycidols. [52-56] No significant changes were observed in the elution behaviour of polyglycidols containing different amounts of AGE which might be due to the too low stepwise changes of AGE amounts. These hydrophobic units do not show a significant influence on the hydrodynamic volume which is majorly determined by the hydrophobic co-monomer EEGE being in a majority in the polymer.

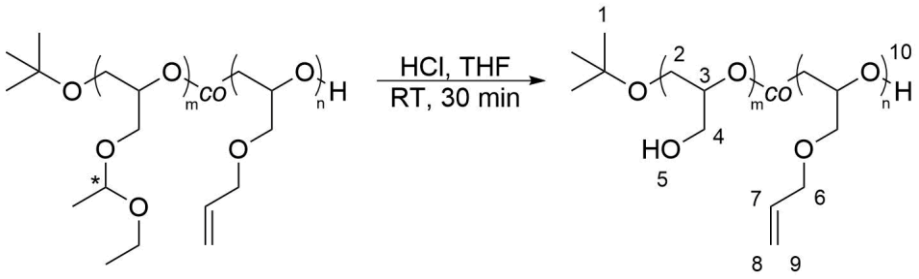

Scheme 4.2.1-3: Synthesis of P(G-*co*-AGE).

Acidic treatment of P(EEGE-*co*-AGE) leads to removal of the acetal group (Scheme 4.2.1-3) in order to obtain the water soluble P(G-*co*-AGE). ^{1}H NMR, IR, RAMAN spectroscopy and GPC confirm the structure of the isolated products. In the ^{1}H NMR spectrum (Figure 4.2.1-7), the end group with H-1 is to be seen at 1.12 ppm, the polymer backbone protons H-2 and H-3 overlap with the methylene group H-4 in the range of 3.54-3.37 ppm and the signals of the

acetal group from P(EEGE-*co*-AGE) (H-5 – H-8) completely disappeared. Thus a new signal from the hydroxyl group H-5 appears at 4.50 ppm which overlaps with the end group H-10. The allyl group signals remain unchanged: 3.95 ppm (H-6), 5.94-5.81 ppm (H-7), 5.14 ppm (H-8), 5.25 ppm (H-9). IR spectrum (Figure 4.2.1-8) shows the appearance of the new broad characteristic O-H stretch vibration (3363 cm^{-1}) which is characteristic for the deprotected glycidol with the free alcohol group. The -CH_2 & C-H stretch vibrations (2923-2875 cm^{-1}) and -CH_2 bend vibration (1451-1409 cm^{-1}) from the ^{t}butyl group, polyether backbone, methylene side group and allyl group remain unchanged. The same applies for the C-O-C stretch vibrations (1348-853 cm^{-1}) from the polyether backbone and allyl group. RAMAN spectrum (Figure 4.2.1-9) shows that the major signals remain unchanged: C-H stretch vibration (2933-2879 cm^{-1}), -CH_2 & -CH_3 bend vibration (1463-1413 cm^{-1}) and C-C stretch/bend vibrations (751-473 cm^{-1}) belong to the the ^{t}butyl group, polyether backbone, methylene side group and allyl group. , The allyl group shows the C=C stretch vibration (1643 cm^{-1}) and the C-O-C stretch vibration (1287-850 cm^{-1}) belongs to the polyether backbone and allyl group. GPC measurements in DMF (Figure 4.2.1-6, Table 4.2.1-1) show similar curve shapes among 1-4 and also compared to the protected polymers 1-4. The bimodal curve shows the minor polymer fraction in the range 12.5-13.7 mL due to the side reaction with KO^{t}Bu (chapter 2.1.3.1) and the main one in the range 13.7-16.0 mL. The polymers' dispersities are still low (1.09-1.25) as well. The deprotected polymers have smaller retention volumes compared to the protected ones although the protected ones possess a higher molecular weight and should have theoretically also a smaller retention time. The reason for this is the different coiling behaviour of the polymers in DMF which is a polar solvent. The interaction of the polar solvent with the nonpolar protected polymer chains lead to a strong coiling behaviour leading to a smaller hydrodynamic volume. In contrast to this, the interaction of the polar solvent with the polar deprotected polymer chains lead to a weak coiling behaviour leading to a higher hydrodynamic volume. [147] Additionally one can see that the retention time is increasing with higher amount of AGE which can be explained again *via* the coiling behaviour: More AGE units lead to a more hydrophobic polymer which is coiling denser in the polar solvent DMF. This in turn enables the polymer to flow through more pores of the GPC column and lead therefore to an increased retention time.

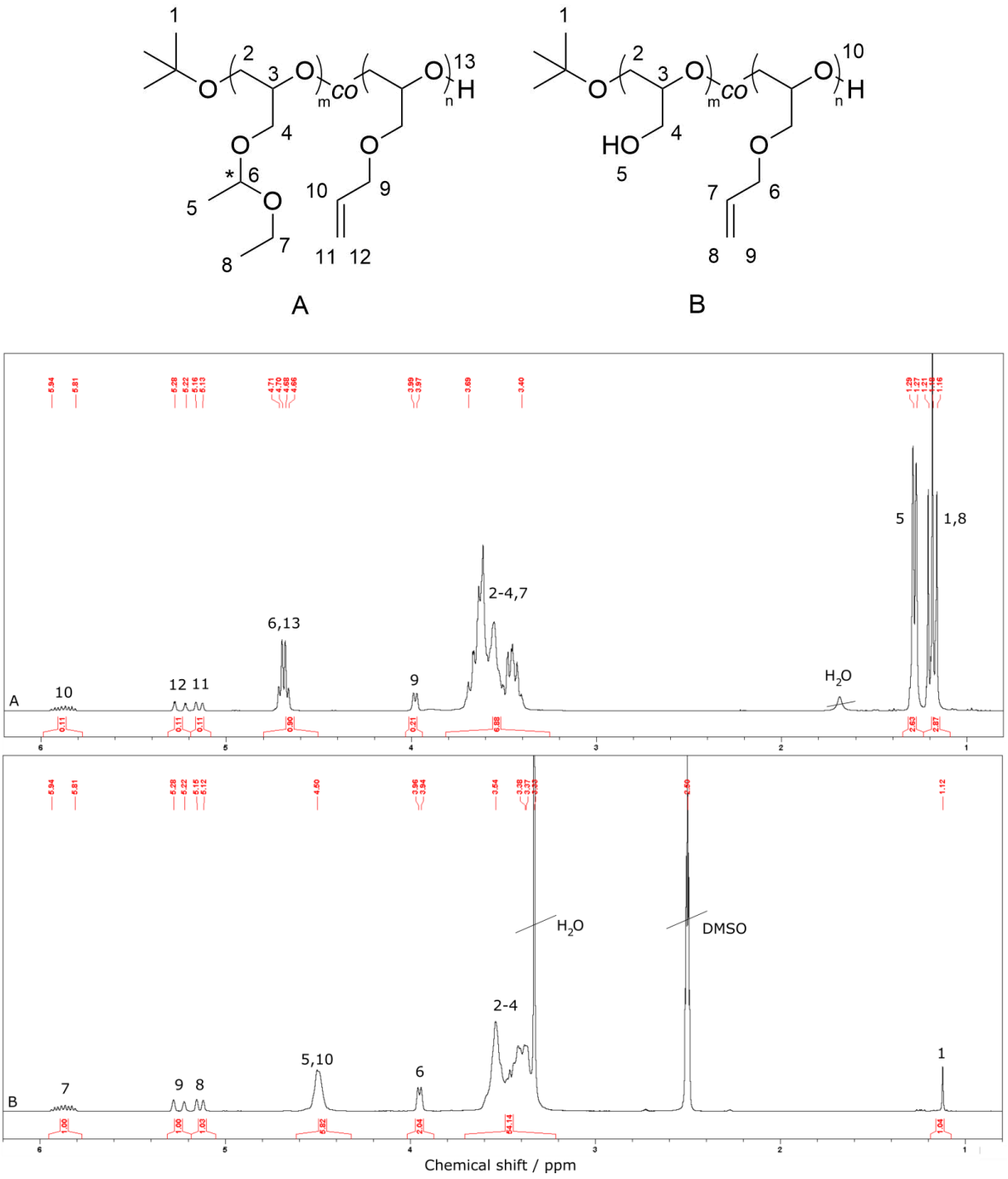

Figure 4.2.1-7: ^{1}H NMR spectra of P(EEGE-*co*-AGE) in $CDCl_3$ (A) and P(G-*co*-AGE) in DMSO-d_6 (B).

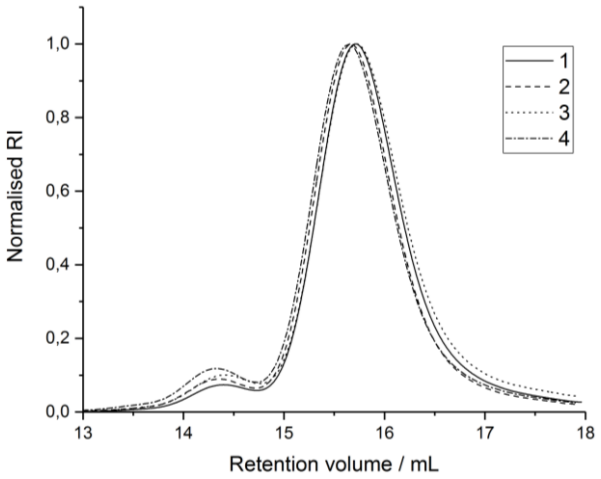

Figure 4.2.1-5: GPC traces of series of P(EEGE-*co*-AGE) in DMF (RI).

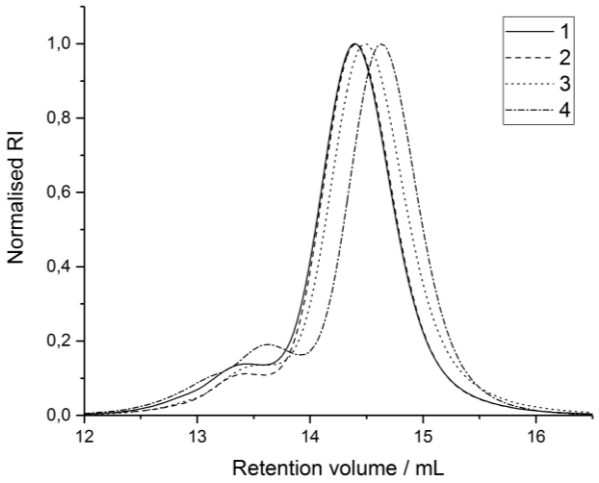

Figure 4.2.1-6: GPC traces of series of P(G-*co*-AGE) in DMF (RI).

Table 4.2.1-1: GPC data of series of P(EEGE-*co*-AGE) and P(G-*co*-AGE) in DMF (RI).

P(EEGE-*co*-AGE)	**1**	**2**	**3**	**4**
M_n/Da	2,061	2,142	2,020	2,173
M_w/Da	2,305	2,399	2,318	2,484
Đ	1.12	1.12	1.15	1.14
P(G-*co*-AGE)	**1**	**2**	**3**	**4**
M_n/Da	4,299	4,245	4,073	4,774
M_w/Da	5,380	4,641	4,452	5,443
Đ	1.25	1.09	1.09	1.14

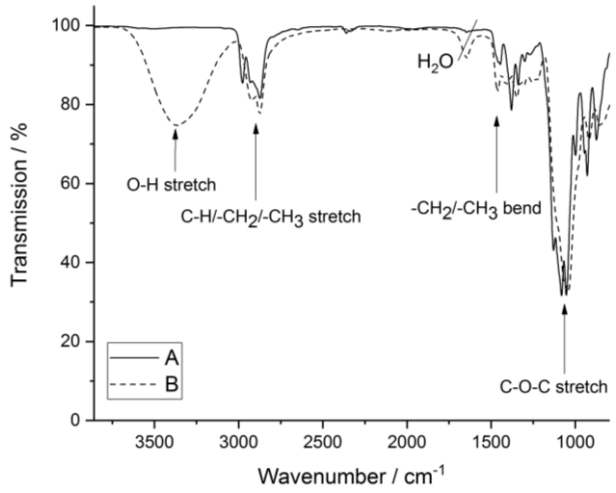

Figure 4.2.1-8: IR spectra of P(EEGE-*co*-AGE) (A) and P(G-*co*-AGE) (B).

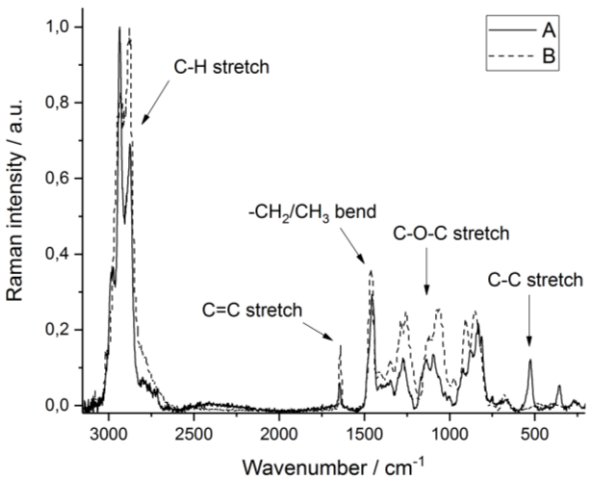

Figure 4.2.1-9: RAMAN spectra of P(EEGE-*co*-AGE) (A) and P(G-*co*-AGE) (B).

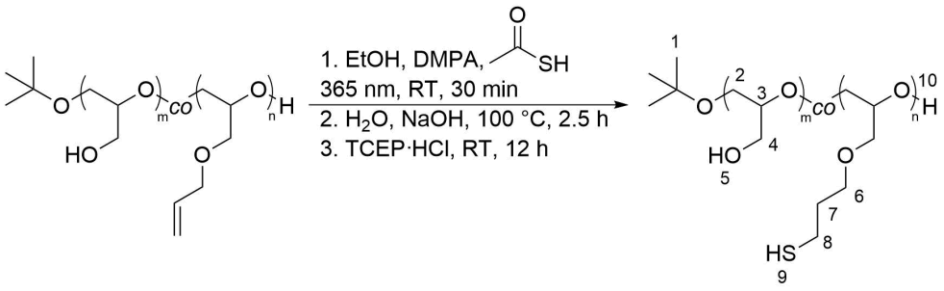

Scheme 4.2.1-4: Synthesis of P(G-*co*-SH).

In order to obtain thiol functionalised polyglycidols P(G-*co*-SH), the P(G-*co*-AGE) was modified in two steps according literature procedure (Scheme 4.2.1-4). [53] First, the allyl group reacted with thioacetic acid *via* thiol-ene reaction to generate a thioester group. Then, sodium hydroxide was used for the nucleophilic attack on the thioester to obtain thiol groups. P(G-*co*-SH) was successfully synthesised and its chemical structure was confirmed *via* ^{1}H NMR, IR, RAMAN spectroscopy and GPC in accordance with literature values. [53] In the ^{1}H NMR spectrum (Figure 4.2.1-10), the protons of the end groups H-1 (1.12 ppm)/H-10 (4.50 ppm), the polymer back bone H-2/H-3 and the methylene side chain H-4 (3.53-3.37 ppm) and the hydroxyl side group H-5 (4.50 ppm) remain unchanged after the thiol functionalisation. A complete consumption of the allyl group was performed as the corresponding protons H-6 – H-9 completely disappeared and new signals of the methylene groups appeared: H-7 (1.76 ppm) and H-8 (2.53 ppm). The proton H-9 of the thiol group is visible at 2.22 ppm. Proton H-6 shifted into the region 3.53-3.37 ppm. IR spectrum (Figure 4.2.1-11) shows the same unchanged signals of the O-H stretch (3372 cm^{-1}) from the alcohol group of the glycidol and the C-H/-CH_2/-CH_3 stretch (2921-2873 cm^{-1}) and -CH_2 bend (1460-1406 cm^{-1}) vibrations of the ^{t}butyl group, polyether backbone, methylene side group and the newly formed propylene side group. The C-O-C stretch (1348-855 cm^{-1}) vibrations of the polyether backbone and ether side group from the converted allyl group are also visible. A very weak signal of the S-H stretch vibration (2557 cm^{-1}) from the newly formed thiol group can be seen at. RAMAN spectrum (Figure 4.2.1-12) also shows the same unchanged signals of the C-H stretch (2926-2881 cm^{-1}), -CH_2/-CH_3 bend (1459 cm^{-1}) and C-C stretch/bend (655-493 cm^{-1}) vibrations from the ^{t}butyl end group, polyether backbone, the methylene and propylene side groups. The polyether backbone and ether side group shows the C-O-C stretch (1257-850 cm^{-1}) vibration. The complete consumption of the allyl group can be seen very well as the signal of the C=C stretch vibration (1643 cm^{-1}) completely disappears and the S-H stretch (2567 cm^{-1}) and C-S stretch (751 cm^{-1}) vibrations from the newly formed thiol group appear.

GPC measurement in DMF (Figure 4.2.1-13, Table 4.2.1-2) shows a broadening of the curve compared to P(G-*co*-AGE) and shift to higher retention volume. A change from 4,245 Da (Đ = 1.09) for P(G-*co*-AGE) to 3,418 Da (Đ = 1.32) for P(G-*co*-SH) and an increased intensity of the polymer fraction derived from the side reaction with KO^{t}Bu (see chapter 2.1.3.1) were observed. The reason for this could be intramolecular disulfide bond formation occurring during sample preparation and measurement leading to a smaller hydrodynamic volume.

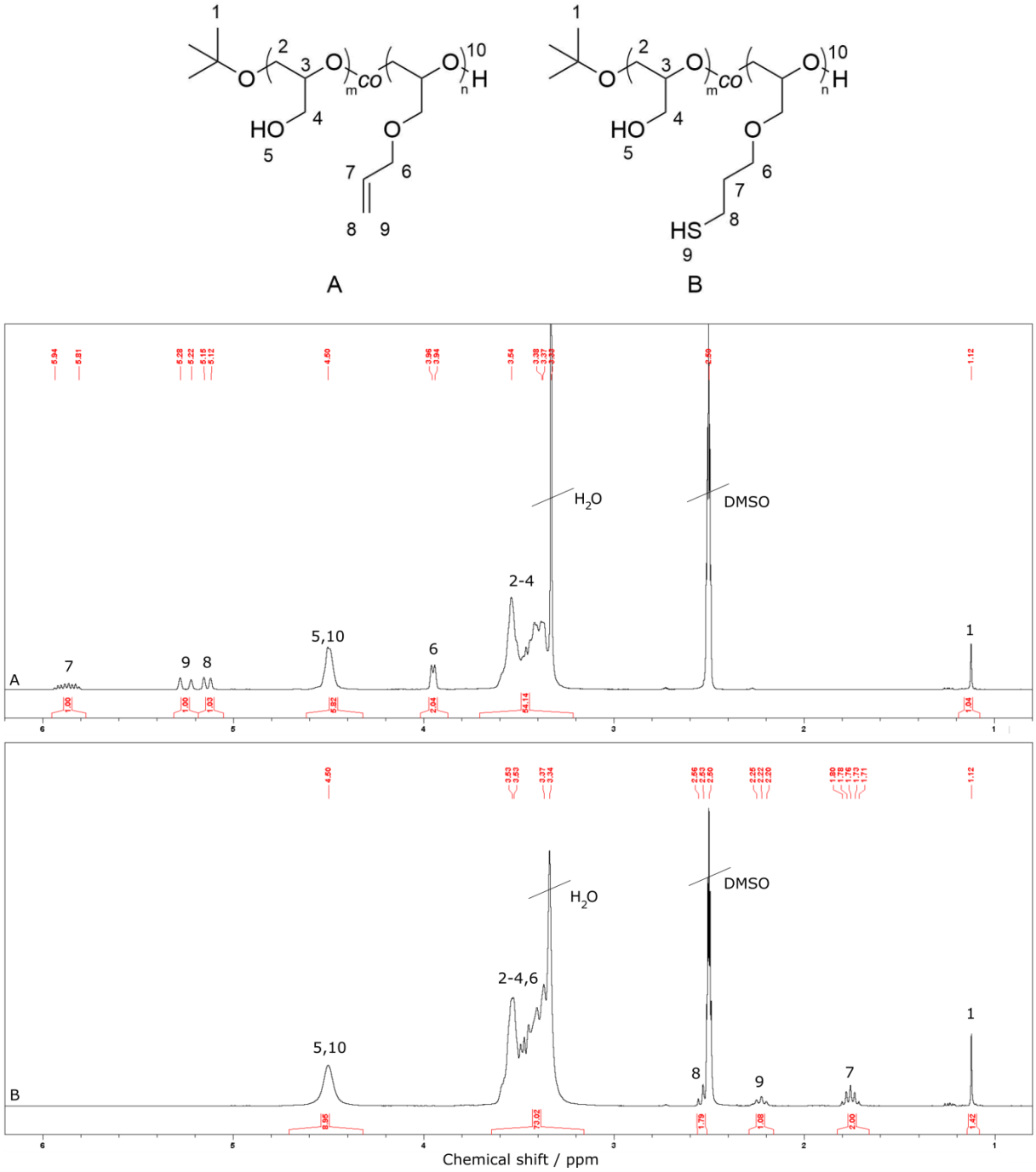

Figure 4.2.1-10: ^{1}H NMR spectra of P(G-*co*-AGE) (A) and P(G-*co*-SH) in DMSO-d_6 (B).

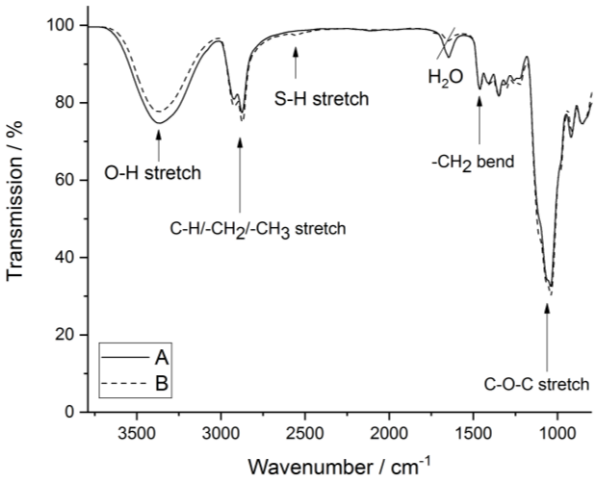

Figure 4.2.1-11: IR spectra of P(G-*co*-AGE) (A) and P(G-*co*-SH) (B).

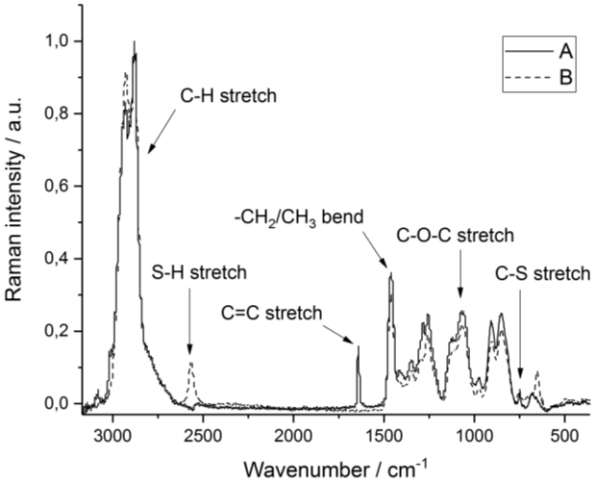

Figure 4.2.1-12: RAMAN spectra of P(G-*co*-AGE) (A) and P(G-*co*-SH) (B).

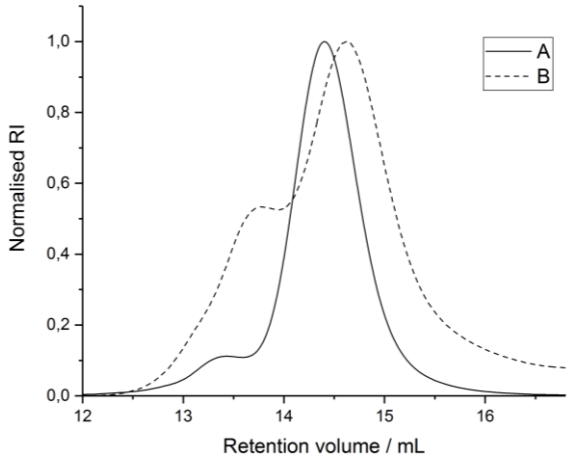

Figure 4.2.1-13: GPC traces of P(G-*co*-AGE) (A) and P(G-*co*-SH) (B) in DMF (RI).

Table 4.2.1-2: GPC data of P(G-*co*-AGE) (A) and P(G-*co*-SH) (B) in DMF (RI).

Run	**A**	**B**
M_n/Da	4,245	3,418
M_w/Da	4,641	4,504
Đ	1.09	1.32

3.2.2 Electrolyte functionalisation

3.2.2.1 Positively charged polymers

In general, there are three possibilities to synthesise polymers carrying charges: (1) The monomer is charged and will be used for the polymerisation [148], (2) a charged molecule will be attached onto the polymer [100] and (3) the charge will be generated at the polymer *via* reaction with an uncharged molecule [149] or the change of the pH value [150]. Method (1) is unpractical for polyglycidols because the negatively charged growing chain end and the positively charged monomer could interact electrostatically and hinder therefore the polymerisation. Method (2) and (3) were investigated by Bianca M. Blunden *et al.* [149] and both led to successful polymer modifications. Both methods will be attempted in this work (Scheme 4.2.2.1-1). For method (2), 1-methyl-3-(3-propanethiol)-imidazolium chloride shall be synthesised and bound to P(G-*co*-AGE) *via* thiol-ene reaction. For method (3), P(G-*co*-AGE) shall first be modified with 3-chloro-1-propanethiol *via* thiol-ene chemistry to obtain polyglycidol carrying chloride groups P(G-*co*-Cl) and then be modified with 1-methylimidazole to obtain polyglycidols carrying imidazolium groups P(G-*co*-Im). So far, polyglycidols with pendant imidazolium groups were not reported in literature. Only poly(epichlorhydrin) was modified with 1-methylimidazole to obtain a polyether carrying positive charges *via* the quaternary nitrogen atoms. [105]

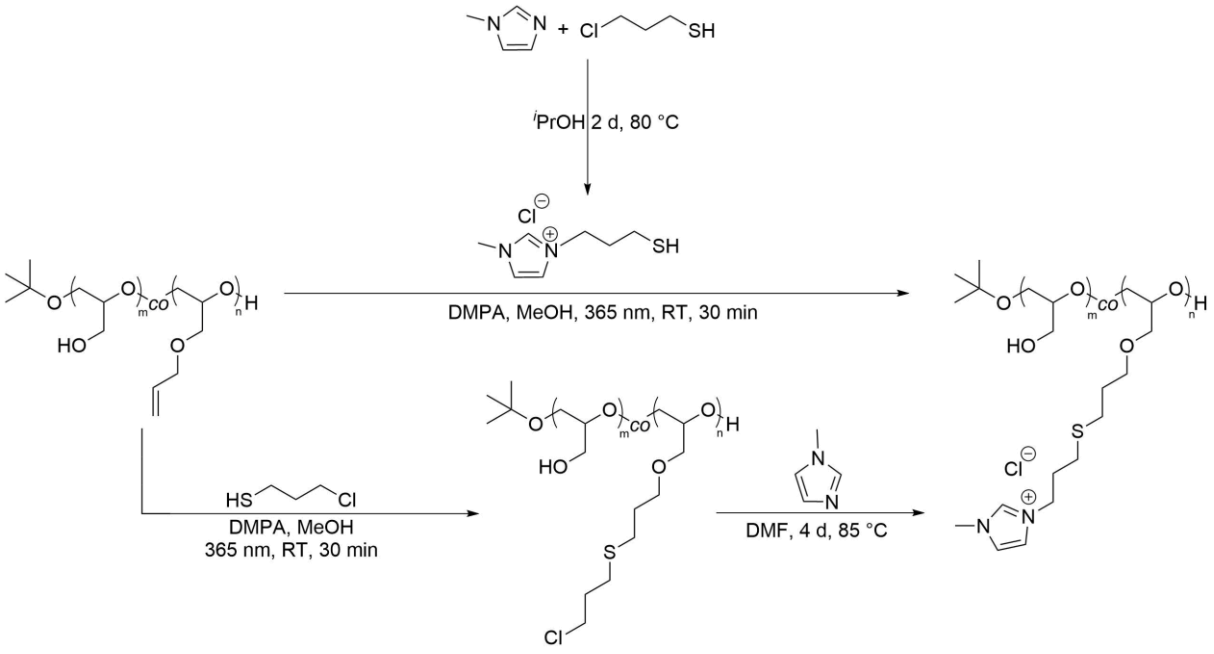

Scheme 4.2.2.1-1: Strategies for the synthesis of polyglycidols carrying imidazolium groups.

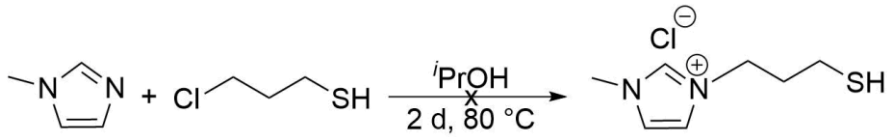

Scheme 4.2.2.1-2: Synthesis of 1-methyl-3-(3-propanethiol)-imidazolium chloride.

First, we attempted to synthesise 1-methyl-3-(3-propanethiol)-imidazolium chloride (Scheme 4.2.2.1-2) according literature procedure [151] in order to use method (2) to modify P(G-*co*-AGE) *via* thiol-ene chemistry but the compound could not be isolated. The reaction mixture showed the product and the starting compounds which could not be separated. Probably the solubility concentrations for the extraction were not good enough and could be improved in future experiments by varying the concentration or the solvent for extraction. Therefore the decision was made to perform method (3) and to modify P(G-*co*-AGE) first with 3-chloro-1-propanethiol to obtain polyglycidol carrying chloride groups P(G-*co*-Cl) and then with 1-methylimidazole to obtain polyglycidols carrying imidazolium groups P(G-*co*-Im). The products were successfully synthesised and characterised *via* ^{1}H NMR, IR, RAMAN spectroscopy and GPC.

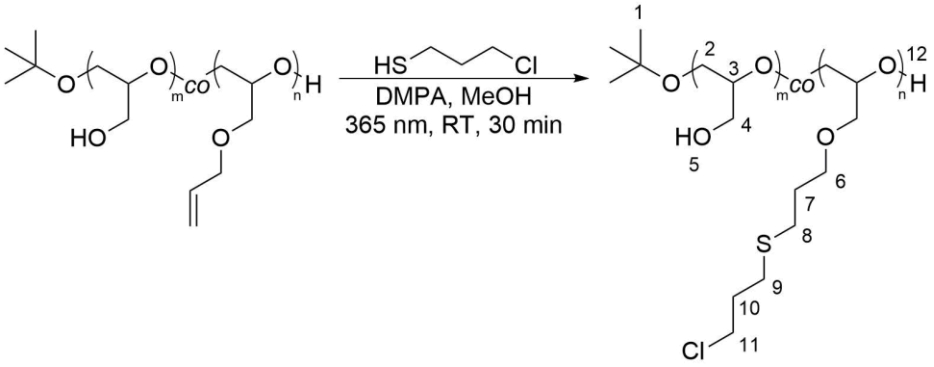

Scheme 4.2.2.1-3: Synthesis of P(G-*co*-Cl).

After the thiol-ene reaction (Scheme 4.2.2.1-3), the signals of the allyl group H-6 – H-9 (5.94-3.94 ppm) completely disappeared in the ^{1}H NMR spectrum (Figure 4.2.2.1-1) and new signals of the methylene groups are visible: H-7 (1.74 ppm), H-8/H-9 (2.58 ppm), H-10 (1.95 ppm) and H-11 (3.70 ppm). H-6 is overlapping with the signals of the polymer backbone and methylene side groups H-2 – H-4/H-6 (3.72-3.33 ppm). Signals from the hydroxyl groups H-5/H-12 (4.50 ppm) and ^{t}butyl group H-1 (1.12 ppm) remain unchanged. IR spectrum (Figure 4.2.2.1-2) does not show any changes in the vibrations: O-H stretch (3359 cm^{-1}) from the alcohol group of the glycidol, -CH_2 & C-H stretch (2931 cm^{-1}/ 2874 cm^{-1}) and -CH_2 bend (1458 cm^{-1}/1417 cm^{-1}) from the ^{t}butyl end group, polyether

backbone, methylene and propylene side groups. The polyether backbone and the ether side groups show the C-O-C stretch (1347-855 cm^{-1}). RAMAN spectrum (Figure 4.2.2.1-4) shows after the thiol-ene reaction the complete disappearance of the C=C stretch (1643 cm^{-1}) from the allyl group indicating a full conversion and an increase of the C-C overlapping with C-Cl (651 cm^{-1}) stretch vibration from the new chloride group. All other vibrations remain unchanged: C-H stretch (2922 cm^{-1}/2883 cm^{-1}), -CH_2 bend (1459 cm^{-1}/1421 cm^{-1}), C-C stretch (1348 cm^{-1}/1301 cm^{-1}) and C-C bend (474 cm^{-1}/226 cm^{-1}) from the ^{t}butyl end group, polyether backbone, methylene and propylene side groups. The polyether backbone and the ether side groups show the C-O-C stretch (1261-1064 cm^{-1}). GPC analysis in DMF (Figure 4.2.2.1-5, Table 4.2.2.1-2) shows an increase of M_n and aggregates in the region 11-13.5 mL which may come from the intermolecular stacking of the hydrophobic side chains. Additionally it was observed, that the polymer was no longer soluble in water after the thiol-ene reaction as the side chains are too hydrophobic.

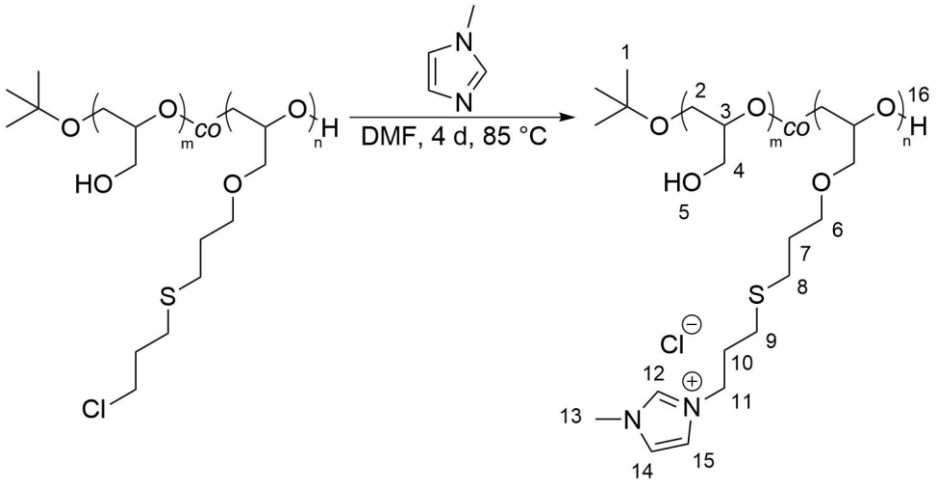

Scheme 4.2.2.1-4: Synthesis of P(G-*co*-Im).

Afterwards, the chloride group was replaced by the imidazolium group *via* nucleophilic substitution (Figure 4.2.2.1-4). The products were successfully synthesised and characterised *via* ^{1}H NMR, IR spectroscopy and GPC.

^{1}H NMR spectrum (Figure 4.2.2.1-1) shows the signals of the attached imidazolium group: H-12 (9.14 ppm), H-13 (3.85 ppm) and H-14/H-15 (7.79-7.71 ppm). A clear shift of the methylene group H-11 next to the chloride from 3.70 ppm to 4.31-4.24 ppm is visible due to the more electronegative withdrawn imidazolium group. The polymer backbone with methylene side groups H-2 – H-4/H-6 (3.54-3.37 ppm), the methylene side chains H-7 (1.75 ppm), H-8/H-9 (slight shift to 2.77-2.68 ppm), H-10 (2.05 ppm), ^{t}butyl end group H-1 (1.12 ppm) and hydroxyl groups H-5/H-16 (4.55 ppm) remain unchanged. The degree of

modification was calculated by the ratio of H-10 to H-7 whereas H-7 was set as 2 protons. With the chosen conditions, the degree of modification degreased with the lower amount of functional chloride groups from 97 to 40 % (Table 4.2.2.1). This is reasonable as the maximum polymer concentration in DMF for the reaction was kept the same and with lower functional chloride groups, the local chloride concentration for the nucleophilic substitution is decreasing as well. Therefore the substitution with imidazolium is decreasing, too. The degree of functionalisation of 97 % is comparable to the literature where poly(epichlorhydrin) was modified with 1-methylimidazole with similar reaction conditions [105].

Table 4.2.2.1-1: Degree of functionalisation for P(G-*co*-Im).

Polymer	Degree of functionalisation / %
1	40
2	67
3	92
4	97

The degree of modification may also increase as with higher amount of chloride groups, the introduced positive charges lead to repulsion which can further complicate the nucleophilic substitution reactions. Additionally, the polymer was again water soluble due to the introduced charges *via* the imidazolium group. IR spectrum (Figure 4.2.2.1-3) shows the following vibrations which the chloride and imidazolium modified polymer have in common: O-H stretch (3356 cm^{-1}) of the hydroxyl group from the glycidol and the -CH_2 & C-H stretch (2931 cm^{-1}/2872 cm^{-1}) and -CH_2 & -CH_3 bend (1460 cm^{-1}/1393 cm^{-1}) from the ^{t}butyl end group, polyether backbone, methylene/propylene side group and 1-metyl imidazolium group. The polyether backbone and ether side group shows the C-O-C stretch (1347-851 cm^{-1}). New vibrations are visible due to the imidazolium ring: =C-H stretch (3112 cm^{-1}) and aromatic ring (1597 cm^{-1}). C-N/C=C stretch vibrations from the 1-methyl imidazolium group are overlapping with the C-O-C/-CH_3 ones. GPC analysis in DMF (Figure 4.2.2.1-6, Table 4.2.2.1-2) shows higher aggregates (1,2) and smaller aggregates (3) and due to hydrogen bonds of hydroxyl and imidazolium groups. (4) also shows smaller aggregates and additional shifts to higher retention times probably due to intramolecular π–π stacking.

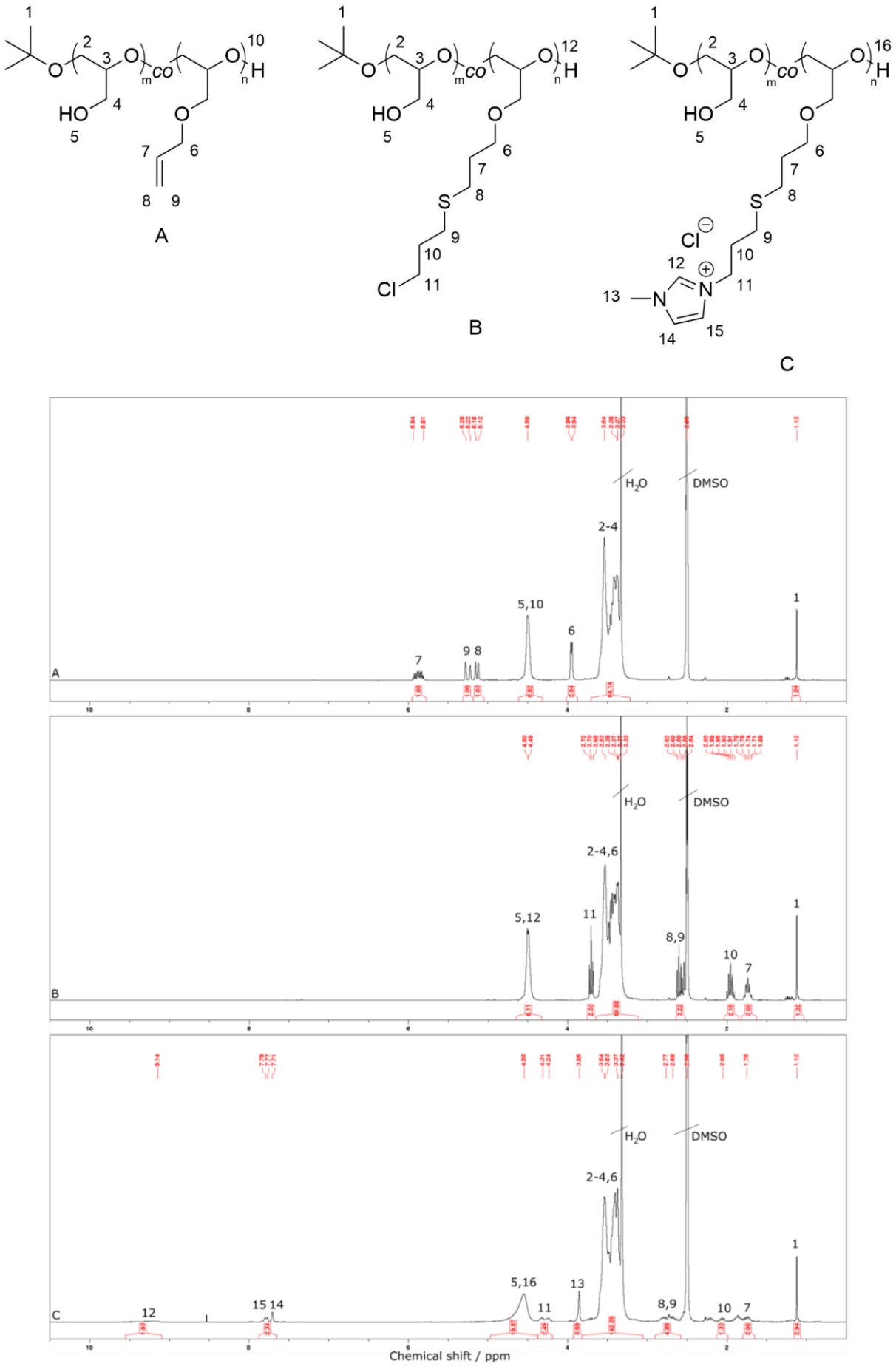

Figure 4.2.2.1-1: ^{1}H NMR spectra of P(G-*co*-AGE) (A), P(G-*co*-Cl) and P(G-*co*-Im) in DMSO-d_6.

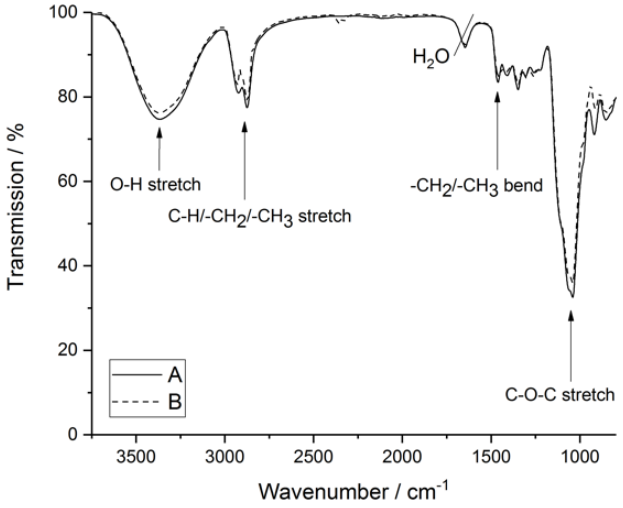

Figure 4.2.2.1-2: IR spectra of P(G-*co*-AGE) (A) and P(G-*co*-Cl) (B).

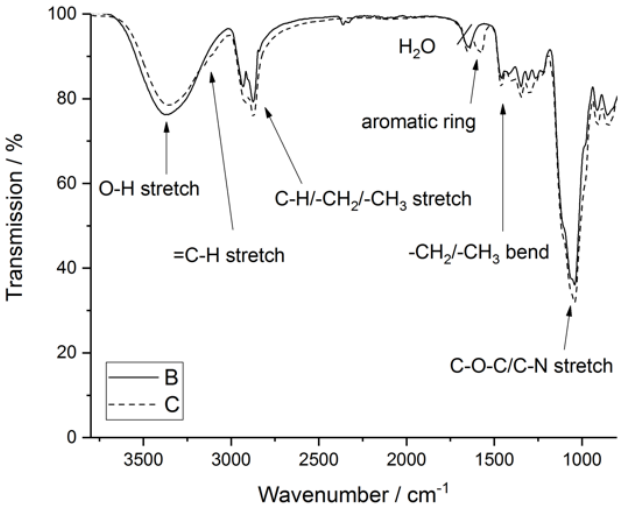

Figure 4.2.2.1-3: IR spectra of P(G-*co*-Cl) (A) and P(G-*co*-Im) (B).

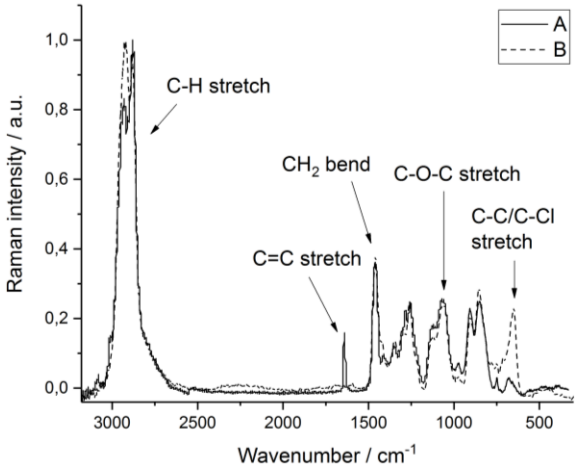

Figure 4.2.2.1-4: RMAN spectra of P(G-*co*-AGE) (A) and P(G-*co*-Cl) (B).

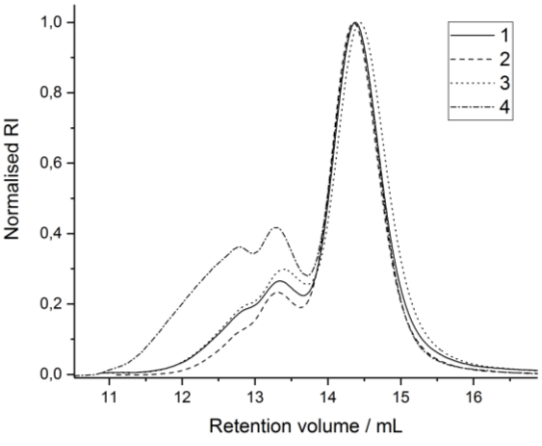

Figure 4.2.2.1-5: GPC traces of series of P(G-co-Cl) in DMF (RI).

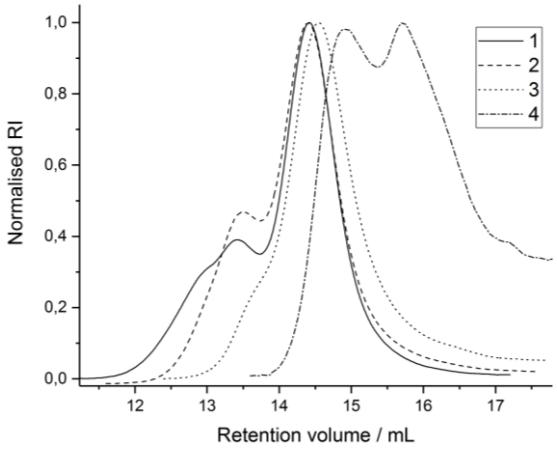

Figure 4.2.2.1-6: GPC traces of series of P(G-co-Im) in DMF (RI).

Table 4.2.2.1-2: GPC data of series of P(G-*co*-Cl) and P(G-*co*-Im) in DMF (RI).

P(G-*co*-Cl)	**1**	**2**	**3**	**4**
M_n/Da	4,543	4,622	4,525	5,633
M_w/Da	5,930	5,447	5,748	9,048
Đ	1.31	1.18	1.27	1.61
P(G-*co*-Im)	**1**	**2**	**3**	**4**
M_n/Da	4,560	3,955	3,308	1,824
M_w/Da	5,953	5,138	3,931	2,362
Đ	1.31	1.30	1.19	1.30

3.2.2.2 Negatively charged polymers

Here are also the same three methods for the modification of the polymers containing a charge possible (see chapter 3.2.2.1): In order to introduce negative charges at polyglycidol, method (1) was excluded because the OH groups of the phosphonamide group would disturb the polymerisation process. Diethylphosphonamides also do not work because they would undergo a nucleophilic attack with the growing polymer chain end. Method (2) was evaluated as efficient as method (3). Method (3) was chosen (Scheme 4.2.2.2-1) because several protected phosphonate derivatives containing a disulfide group were reported [152 140] which show a good solubility in solvents that were previously reported for redox and thiol-ene reactions of disulfide/thiol compounds and polyglycidols. [53, 54] Therefore, first bis(diethylphosphonamide)disulfide shall be synthesised and then reduced/bound *via* thiol-ene reaction to P(G-*co*-AGE). In the end, the diethyl groups shall be removed in order to obtain phosphonamide groups which deprotonate and carry negative charges.

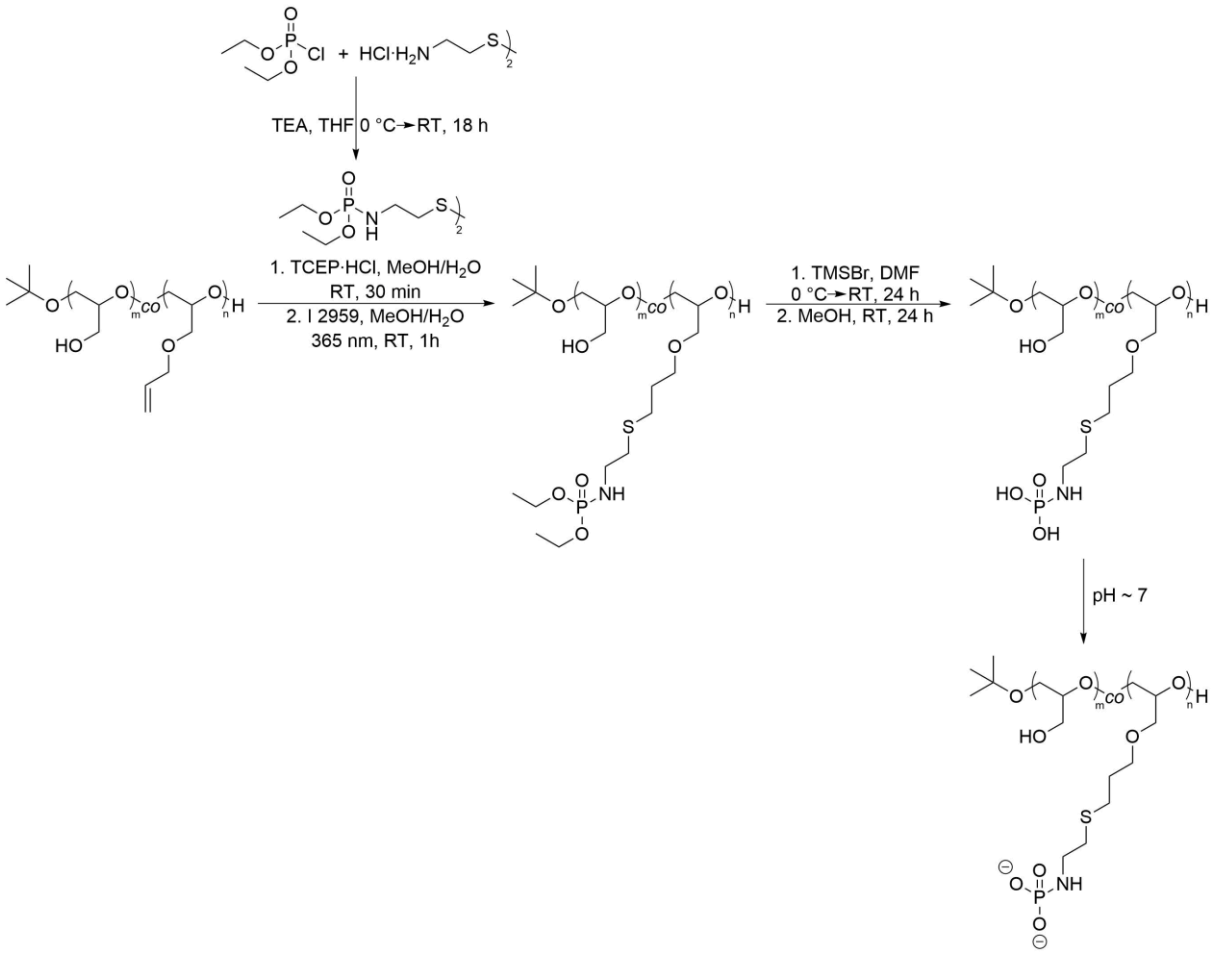

Scheme 4.2.2.2-1: Strategy for the synthesis of polyglycidols carrying phosphonamide groups.

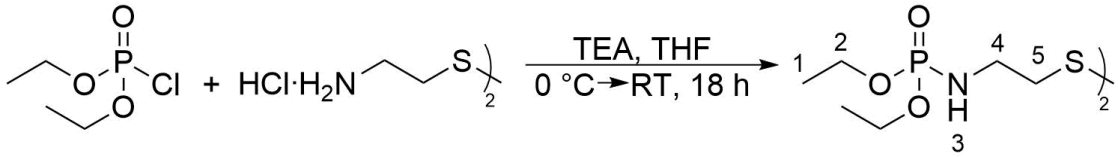

Scheme 4.2.2.2-2: Synthesis of bis(diethylphosphonamide)disulfide.

Bis(diethylphosphonamide)disulfide (protected phosphonamide linker, Scheme 4.2.2.2-2) was synthesised according to literature procedure [152] and characterised *via* ^{1}H, ^{13}C, ^{31}P{^{1}H} NMR, IR spectroscopy and mass spectrometry. It was obtained as a yellow solid with a yield of 71 %. The ^{1}H NMR spectrum (Figure 4.2.2.2-1) shows the signals of the ethyl group H-1/H-2 (1.21 ppm/3.90 ppm), the amide group H-3 (5.05 ppm) and the ethylene group H-4/H-5 (3.03 ppm/2.74 ppm). In the ^{13}C NMR spectrum (Figure 4.2.2.2-2) one can see the ethyl group C-1/C-2$^{\#}$ (16.13 ppm, 16.04 ppm/61.30 ppm, 61.23 ppm). C-4/C-5 are overlapping with the solvent speak (39.51 ppm). $^{\#}$Splitting is because of the partial hydrolysis. ^{31}P{^{1}H} NMR spectrum (Figure 4.2.2.2-3) shows a signal at 9.31 ppm and at 0.07 ppm$^{\#}$, whereas $^{\#}$ is the hydrolysed form (1.4 %). MS (ASAP, Figure 4.2.2.2-5) shows a peak at m/z = 425.1081 which stands in accordance with the calculated value $[M+H]^{+}$ = 425.1099. In the IR spectrum

(Figure 4.2.2.2-4) one can see the following vibrations: N-H stretch (3180 cm^{-1}), C-N & C-O-P stretch (1353 cm^{-1} /1293 cm^{-1}), P=O stretch (1226 cm^{-1}), C-N & C-O-P stretch (1179-1029 cm^{-1}), P-O stretch (961 cm^{-1}), C-O-P stretch (905 cm^{-1}/883 cm^{-1}), of the generated phosphonamide group. The C-S stretch (802 cm^{-1}) belongs to the thioether group of the disulfide and the -CH_2 & C-H stretch (2979 cm^{-1}/2905 cm^{-1}), -CH_2 bend (1463 cm^{-1}), -CH_3 bend (1396 cm^{-1}/1367 cm^{-1}) and -CH_2 bend (768 cm^{-1}) belong to the ethyl/ethylene groups.

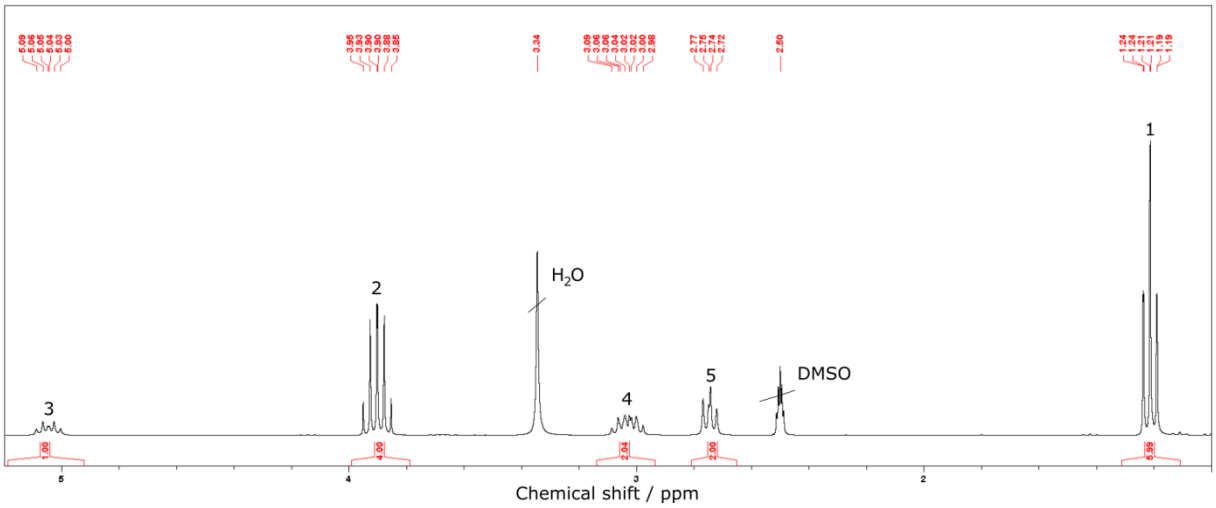

Figure 4.2.2.2-1: ^{1}H NMR spectrum of bis(diethylphosphonamide)disulfide in DMSO-d_6.

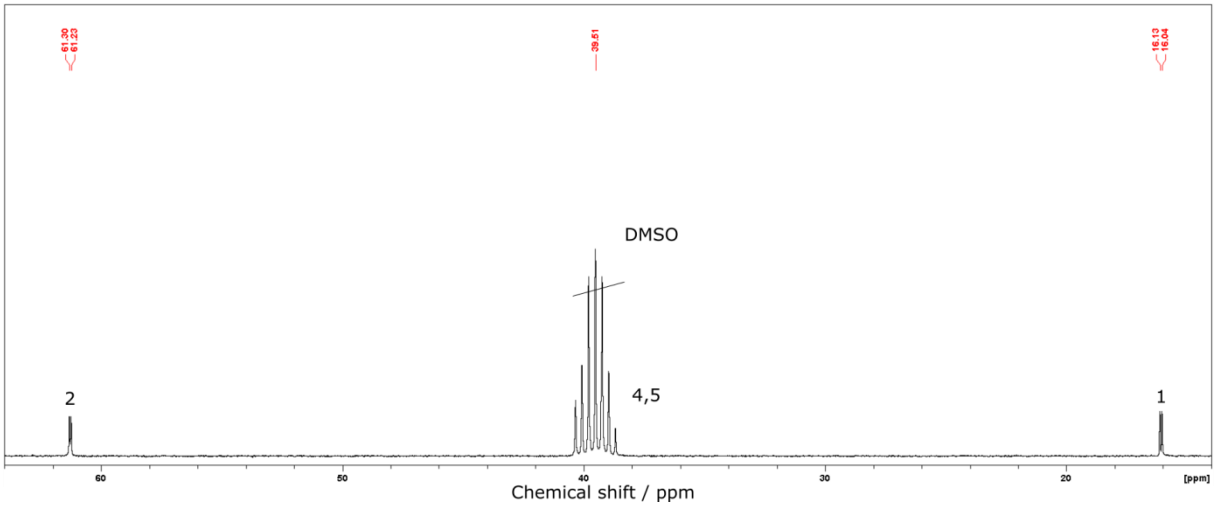

Figure 4.2.2.2-2: ^{13}C NMR spectrum of bis(diethylphosphonamide)disulfide in DMSO-d_6.

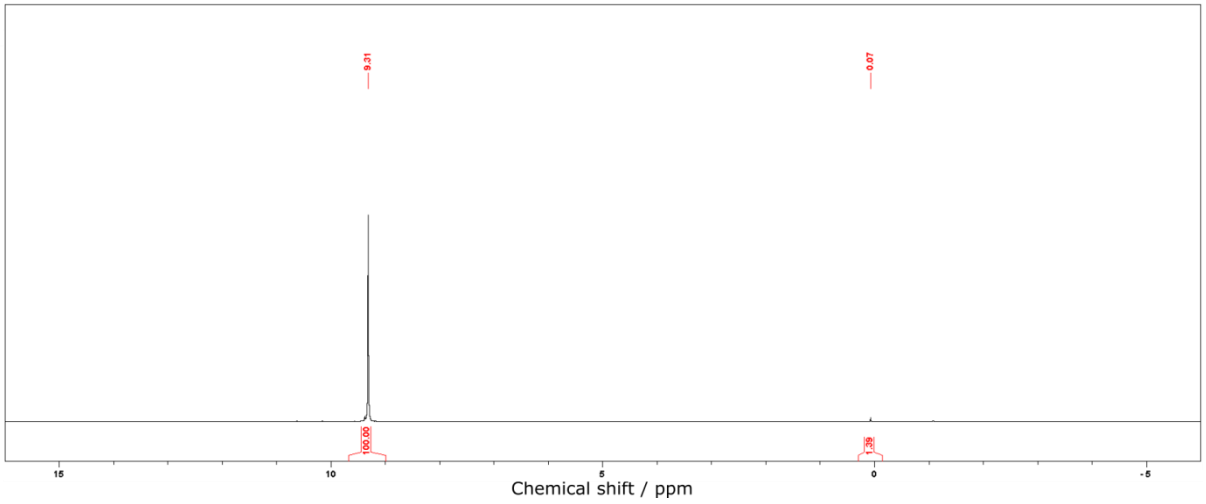

Figure 4.2.2.2-3: $^{31}P\{^{1}H\}$ NMR spectrum of bis(diethylphosphonamide)disulfide in DMSO-d_6.

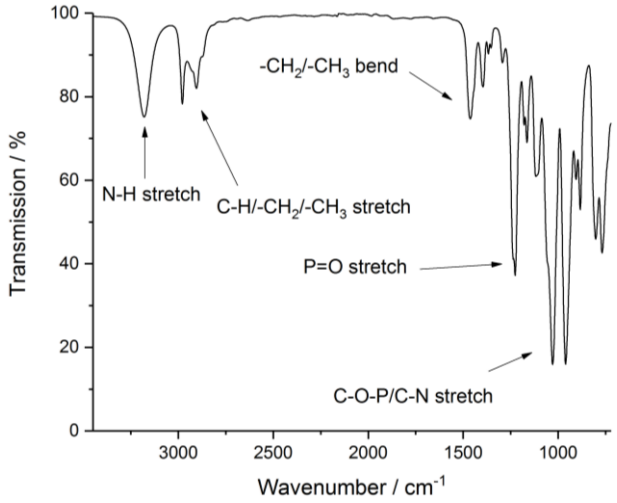

Figure 4.2.2.2-4: IR spectrum of bis(diethylphosphonamide)disulfide.

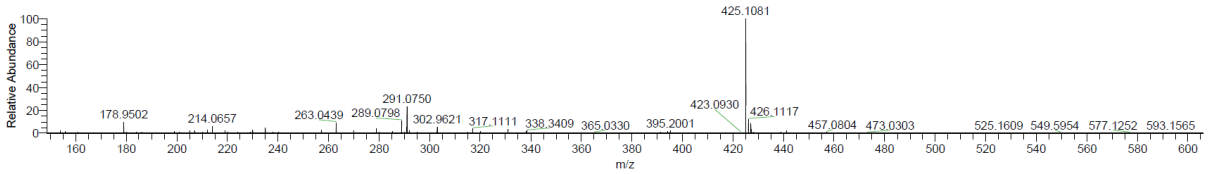

Figure 4.2.2.2-5: ASAP-MS spectrum of bis(diethylphosphonamide)disulfide.

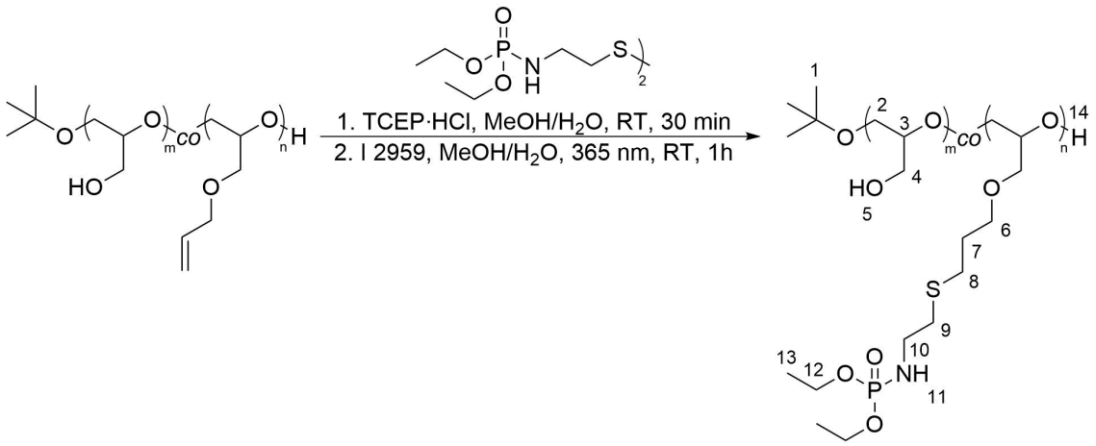

Scheme 4.2.2.2-3: Synthesis of P(G-*co*-POEt).

In the next step, the protected phosphonamide linker was first reduced with TCEP·HCl and then used for thiol-ene chemistry (Scheme 4.2.2.2-3) on P(G-*co*-AGE). The products were successfully synthesised and characterised *via* ^{1}H, ^{31}P{^{1}H} NMR, IR, RAMAN spectroscopy and GPC. ^{1}H NMR spectrum (Figure 4.2.2.2-6) shows the complete disappearance of the allyl group H-6 – H-9 (5.94-3.94 ppm) and the signals of the attached phosphonamide linker are visible: the ethylene group H-9 (2.53 ppm) overlapping with H-8 and solvent signal and H-10 (2.96-2.85 ppm), the amide group H-11 (4.99-4.91 ppm) and the ethyl group H-12/H-13 (3.95-3.85 ppm/1.21 ppm). The new methylene group H-7 can be seen at 1.73 ppm. The following signals remain unchanged: hydroxyl group H-5/H-14 (4.50 ppm), the polymer backbone with methylene side groups H-2 – H-4/H-6 (3.53-3.37 ppm) and the ^{t}butyl end group H-1 (1.12 ppm). The ^{31}P{^{1}H} NMR spectrum (Figure 4.2.2.2-7) shows a peak at 9.43 ppm which is similar to the unbound phosphonamide linker (9.31 ppm). In the IR spectrum (Figure 4.2.2.2-8) one cannot see many differences between the parent and modified polymer as some vibrations of the functional groups are overlapping: O-H & N-H stretch (3352 cm^{-1}) belong to the alcohol group of the free glycidol and the amide group of the bound phosphonamide compound. The-CH_2 & C-H stretch (2933 cm^{-1}/2875 cm^{-1}) and -CH_2 & -CH_3 bend (1457 cm^{-1}/1414 cm^{-1}/1394 cm^{-1}) are visible from the ^{t}butyl end group, polyether backbone, aliphatic side group and ethyl protecting groups. The C-O-C & C-N & C-O-P stretch (1349-797 cm^{-1}) belong to the polyether backbone and ether side group overlapping with the new bound phosphonamide group. A clear difference is to be seen at 1215 cm^{-1} which comes from the P=O stretch vibration of the bound phosphonamide compound. RAMAN spectrum (Figure 4.2.2.2-10) shows the complete disappearance of the C=C stretch (1643 cm^{-1}) vibration and the appearance of the C-S stretch (755 cm^{-1}) one confirming the full conversion of the allyl group and binding of the phosphonamide compound via a thioether

bond. The other vibrations remain unchanged: C-H stretch (2933 cm^{-1}/2884 cm^{-1}), -CH_2 & -CH_3 bend (1462 cm^{-1}/1421 cm^{-1}), C-C stretch (1352 cm^{-1}/1300 cm^{-1}), C-C stretch (684 cm^{-1}/656 cm^{-1}) and C-C bend (497-229 cm^{-1}) from the ^{t}butyl end group, polyether backbone and aliphatic side groups. C-O-C stretch (1261-859 cm^{-1}) belongs to the polyether backbone and ether side group. GPC analysis in DMF (Figure 4.2.2.2-11, Table 4.2.2.2) does not show formed aggregates and just the typical high molecular weight shoulder.

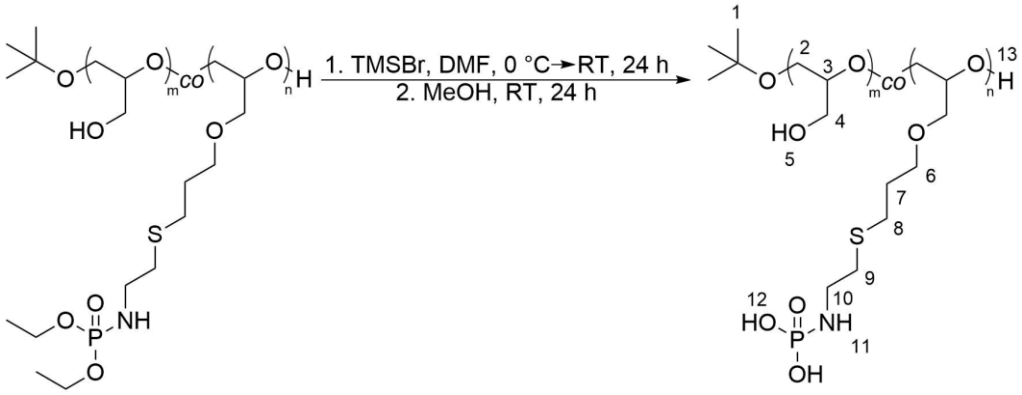

Scheme 4.2.2.2-4: Synthesis of P(G-*co*-POH).

In the next step, the protecting groups of the phosphonamide functionality were removed (Scheme 4.2.2.2-4). The products were successfully synthesised and characterised *via* ^{1}H, ^{31}P{^{1}H} NMR, IR spectroscopy and GPC. In the ^{1}H NMR spectrum (Figure 4.2.2.2-6), one can see the disappearance of the ethyl groups H-12/H-13 (3.95-3.85 ppm/1.21 ppm) and a shift of H-8/H-9 from 2.53 ppm to 2.57 ppm/2.69 ppm is visible due to the electronegative withdrawn hydroxyl groups. The residual signals remain unchanged: polymer back bone with methylene side groups H-2 – H-4/H-6 (3.54-3.37 ppm), methylene groups H-7 (1.75 ppm) and H-10 (2.96 ppm), hydroxyl groups H-12/H-13 overlapping with the amide group H-11 (4.52 ppm) and the ^{t}butyl end group H-1 (1.12 ppm). In the ^{31}P{^{1}H} NMR spectrum (Figure 4.2.2.2-7) one can see a shift from 9.43 ppm to -0.10 ppm which is reasonable as H_3PO_4 is used as internal standard for the ^{31}P{^{1}H} NMR spectroscopy and the phosphonamide group is chemically similar to that. Additionally this signal is broad which may be caused by interaction with residual water in the solvent. IR spectrum (Figure 4.2.2.2-9) shows the same signals and the polymer with the protected phosphonamide groups: O-H & N-H stretch (3347 cm^{-1}) of the alcohol group of the free glycidol and the phosphonamide group are visible. The -CH_2 & C-H stretch (2923/2874 cm^{-1}) and -CH_2 bend (1461/1412 cm^{-1}) belong to the ^{t}butyl end group polyether backbone and aliphatic side chains. The C-O-C & C-N stretch (1347-852 cm^{-1}) from the polyether backbone, ether side chain and phosphonamide group are also visible. The intensity of the P=O vibration (1215 cm^{-1}) of the phosphonamide group

decreased, which may come from the formed hydrogen bonds between the phosphonamide groups itself or the alcohol groups of the glycidols. GPC analysis in DMF (Figure 4.2.2.2-12, Table 4.2.2.1) shows that higher aggregates are formed in the region 10.5-12.0 mL which also may come from intermolecular hydrogen bonds. Additionally the polymer with the highest amount of phosphonamide groups (4) was no longer soluble in DMF anymore and GPC analysis was performed in water (Figure 4.2.2.2-13, Table 4.2.2.2) which shows the typical low molecular weight tailing due to interactions with the column. It is interesting to see that (4) is not soluble in DMF anymore as the content of the phosphonamide groups is too high leading the polymer being too polar.

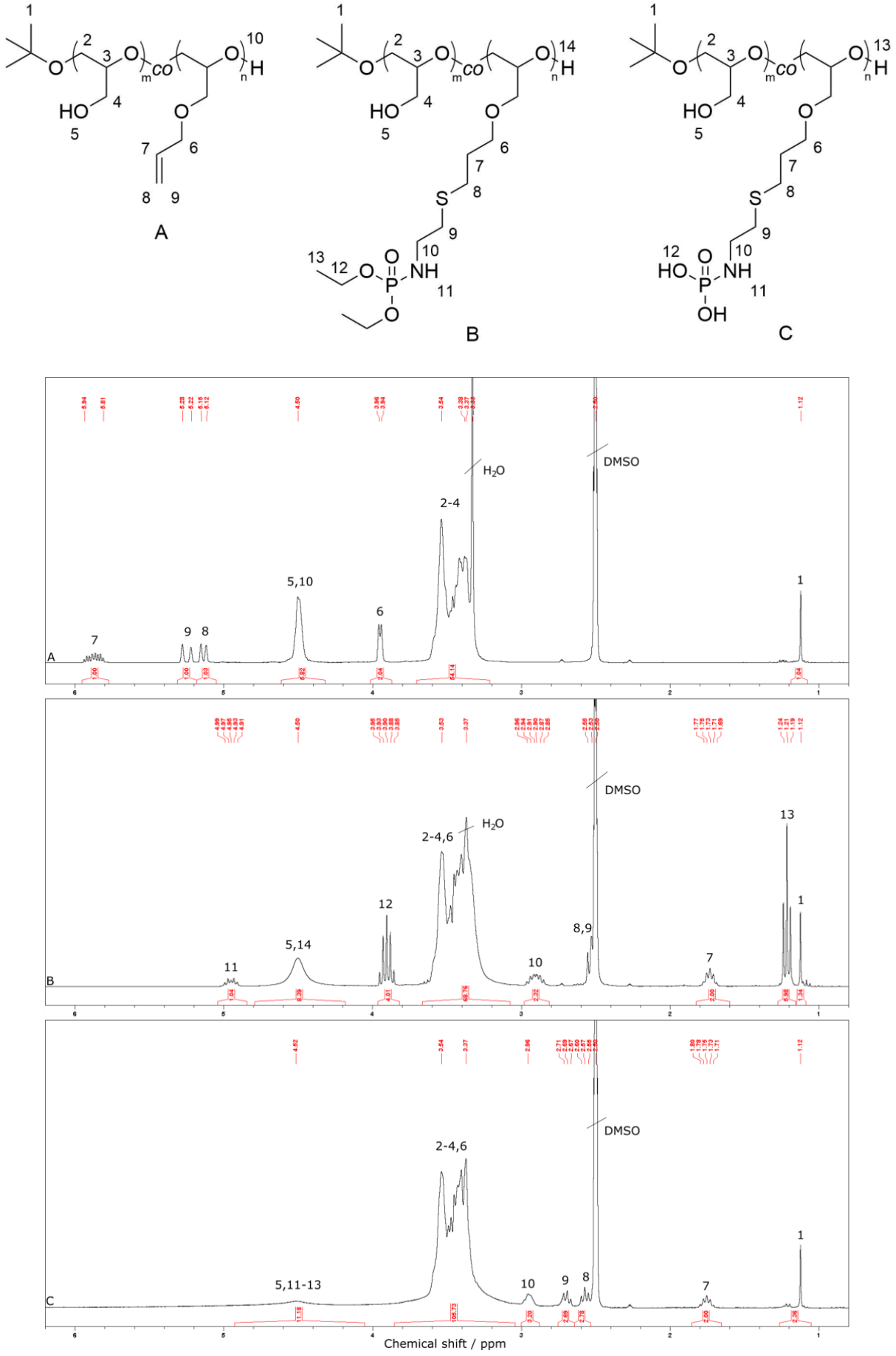

Figure 4.2.2.2-6: ^{1}H NMR spectra of P(G-*co*-AGE) (A), P(G-*co*-POEt) (B) and P(G-*co*-POH) (C) in DMSO-d_6.

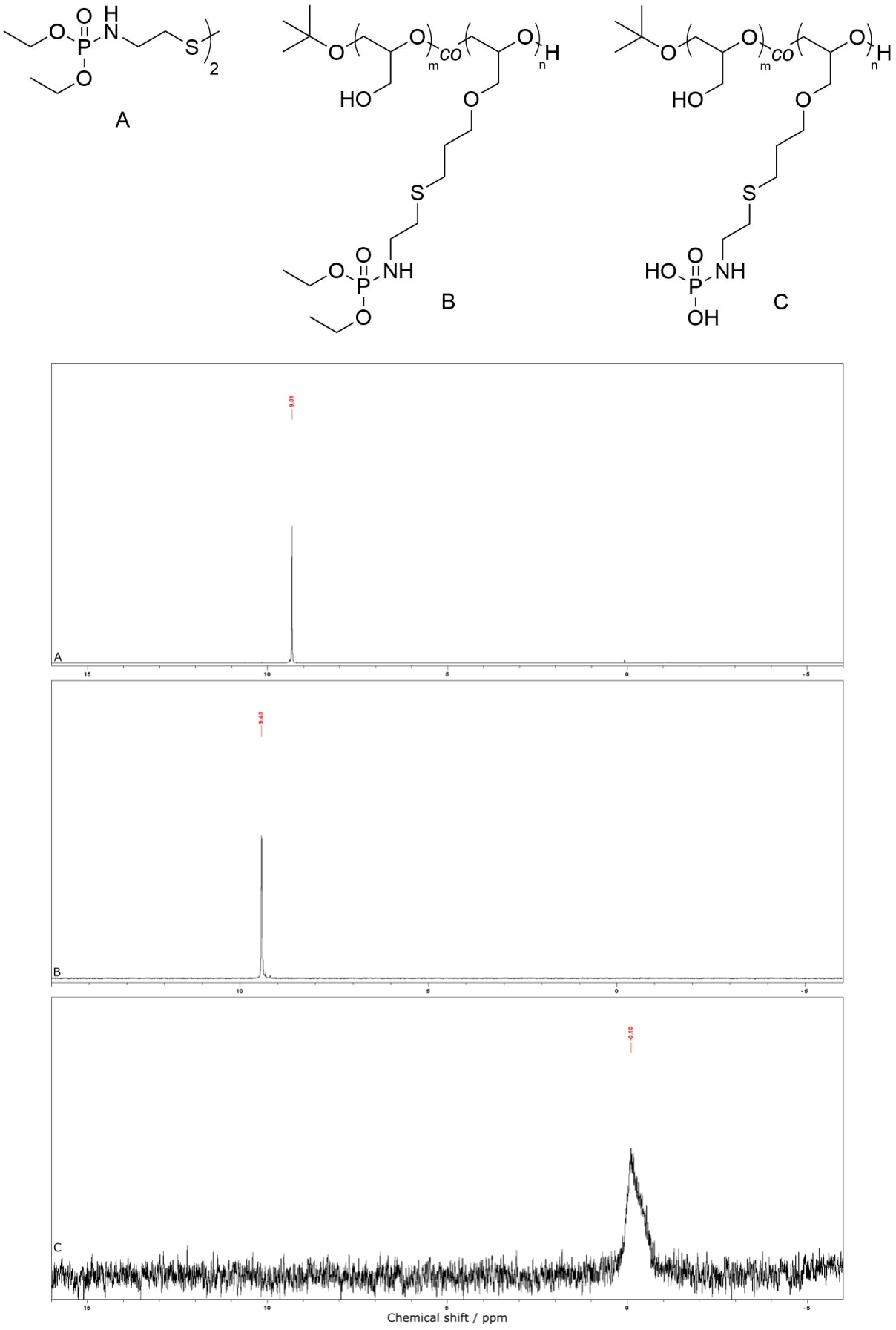

Figure 4.2.2.2-7: $^{31}P\{^{1}H\}$ NMR spectra of bis(diethylphosphonamide)disulfide (A), P(G-*co*-POEt) (B) and P(G-*co*-POH) (C) in DMSO-d_6.

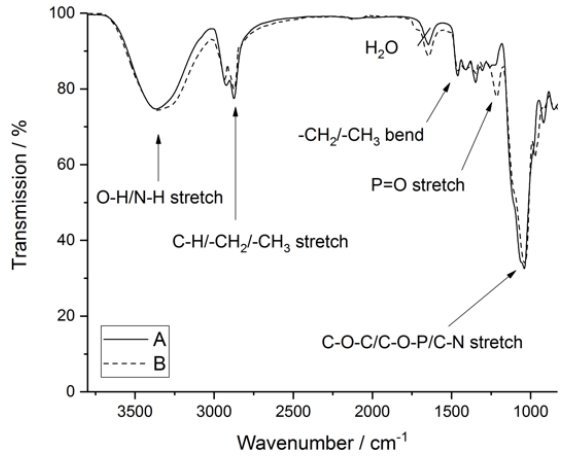

Figure 4.2.2.2-8: IR spectra of P(G-*co*-AGE) (A) and P(G-*co*-POEt) (B).

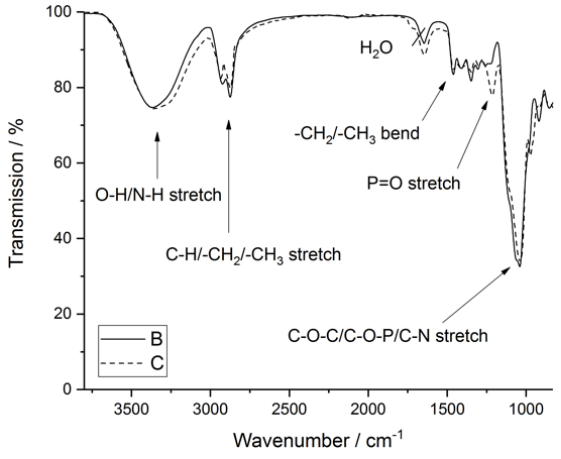

Figure 4.2.2.2-9: IR spectra of P(G-*co*-POEt) (A) and P(G-*co*-POH) (B).

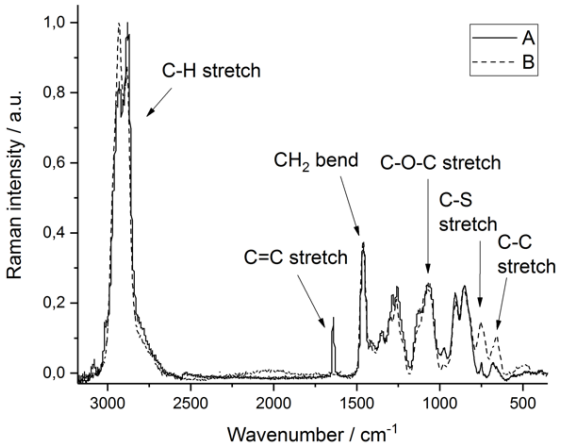

Figure 4.2.2.2-10: RAMAN spectra of P(G-*co*-AGE) (A) and P(G-*co*-POEt) (B).

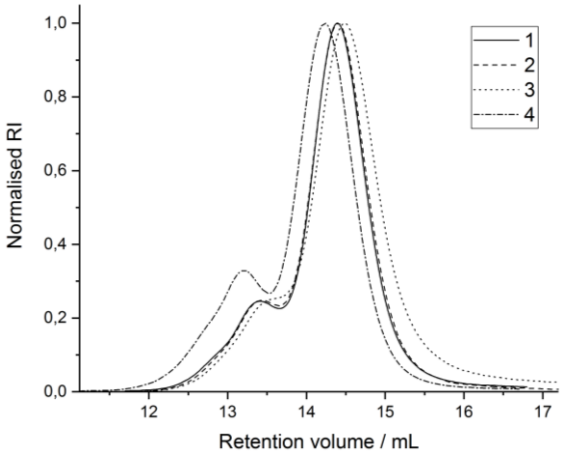

Figure 4.2.2.2-11: GPC traces of series of P(G-*co*-POEt) in DMF (RI).

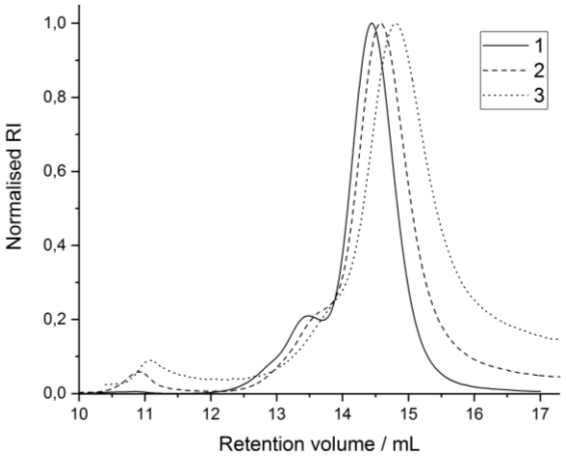

Figure 4.2.2.2-12: GPC traces of series of P(G-*co*-POH) in DMF (RI).

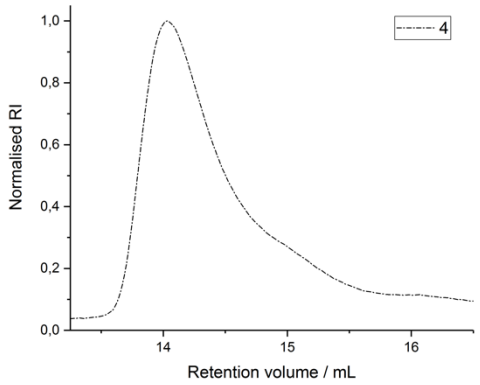

Figure 4.2.2.2-13: GPC trace of P(G-*co*-POH) in water (RI).

Table 4.2.2.2: GPC data of series of P(G-*co*-POEt) and P(G-*co*-POH) in DMF (RI, 1-3) and water (RI, 4).

P(G-*co*-POEt)	**1**	**2**	**3**	**4**
M_n/Da	4,355	4,283	3,960	5,026
M_w/Da	5,080	4,989	4,590	6,091
Đ	1.17	1.17	1.16	1.21
P(G-*co*-POH)	**1**	**2**	**3**	**4**
M_n/Da	4,282	3,582	2,850	2,440
M_w/Da	4,850	4,194	3,708	2,883
Đ	1.13	1.17	1.30	1.18

3.2.2.3 Gel tests

Figure 4.2.2.3: Solution of P(G-*co*-Im) (left), P(G-*co*-POH) (middle) and equimolar mixture of both (right) in PBS with G:Im = 48:11.6 and G:POH = 48:12 and 10 wt-% polymer in total.

For the gel tests, the positively and negatively charged polymers were dissolved separately in solutions with pH = 4.0, pH = 7.0, pH = 7.4 or pH = 10.0, stirred overnight and combined afterwards to give equimolar ratios of functional groups. The different pH values were chosen to find out how the hydrogel formation is dependent from the pH value due to the different

protonation/deprotonation possibilities of the phosphonamide/imidazolium groups. In these experiments, the amount of functional groups (5-20 %) and the polymer content (10-30 wt-%) was varied. For experiments with 20 and 30 wt-% only pH = 7.0 was tested. All of them remained as solutions and did not form a hydrogel (Figure 4.2.2.3). All of the buffer solutions except pH = 7.0 contained ions that additionally disturb the ionic interaction between the phosphonamide and imidazolium groups by charge compensation. Therefore, the gel test was also performed in a solution at pH = 7.0 without any ions in order to find out if the observed results derived from the nature of the solution or of the polymer. As here no hydrogels were formed either, in conclusion it must be the polymer's nature not forming a network. In order to improve this system, one could either increase the degree of functional groups or use polymers with longer chains for a better network formation. Compared to literature, Hassan Srour *et al.* [113] described a fully functionalised polyacrylate with imidazolium groups at the side chains and phosphonates at the chain ends which formed hydrogels. Their work stands in accordance with our observation that a too low degree of functionalisation and too short polymers are not enough for a hydrogel formation with these functional groups. In this work, also the synthesis and characterisation of high molecular weight polyglycidols will be investigated and modified to obtain polyelectrolytes to attempt forming hydrogels.

3.2.3 π–π Functionalisation

In general, π–π functionalisation of polymers can be reached *via* polymerisation of a π–π functionalised monomer [153] but is not suitable for this work because the kinetics of such pyrene modified glycidylether compounds is unknown and naphthalene diimide compounds are not stable in presence of nucleophiles like the active polymer chain end. Therefore the polymers have to be functionalised afterwards with these aromatic groups. Pyrene compounds can be modified with disulfide groups, [154] shall then be reduced and bound onto polyglycidols *via* thiol-ene chemistry. Also, pyrene compounds were bound *via* amidation onto polyglycidols before [155] and this technique also will be used in this work (Scheme 4.2.3-1). Naphthalene diimide functionalised polyglycidols have not been reported yet but there are three possibilities which will be attempted (Scheme 4.2.3-2, Scheme 4.2.3-3): First is the synthesis of a disulfide functionalised naphthalene diimide compound, not reported as well, which could be bound to polyglycidols *via* reduction of the disulfide group with subsequent thiol-ene chemistry with P(G-*co*-AGE). Second method is the synthesis of allyl functionalised naphthalene diimide compounds [156] which could be bound to P(G-*co*-SH)

via thiol-ene chemistry. Third method is adapted from Lewis R. Hart *et al.* [134] who worked with amine functionalised polymers and attached a naphthalene monoimide compound.

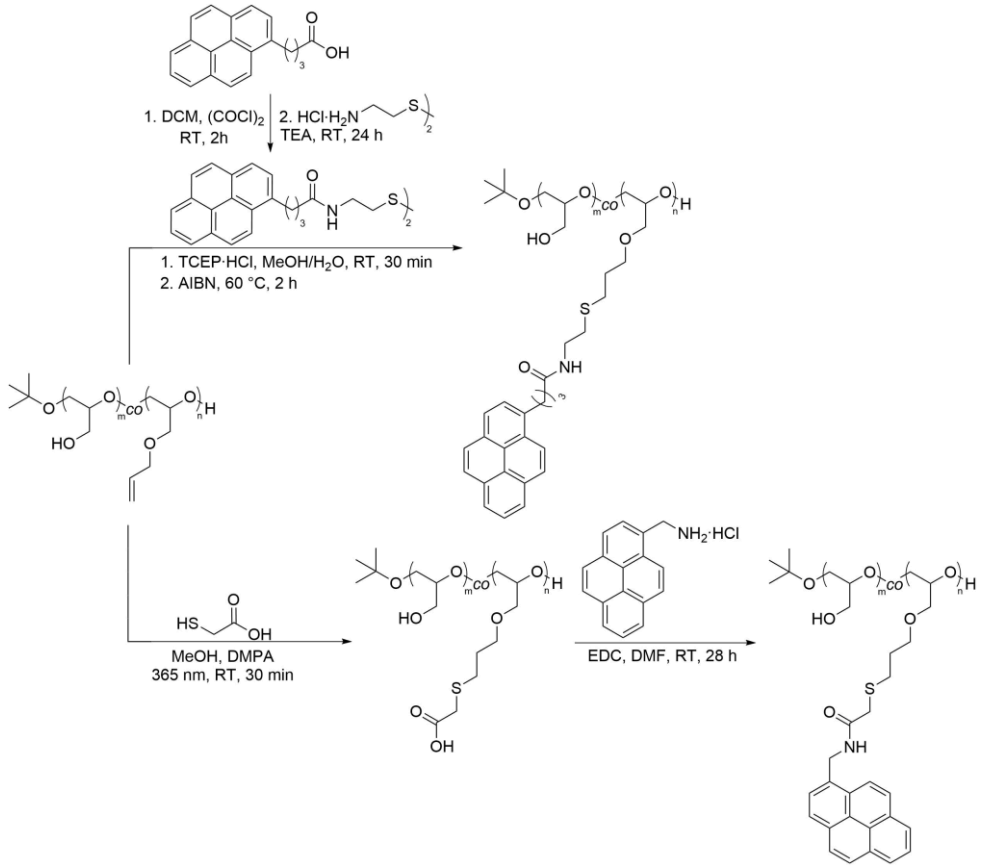

Scheme 4.2.3-1: Strategies for the synthesis of polyglycidols carrying pyrene groups.

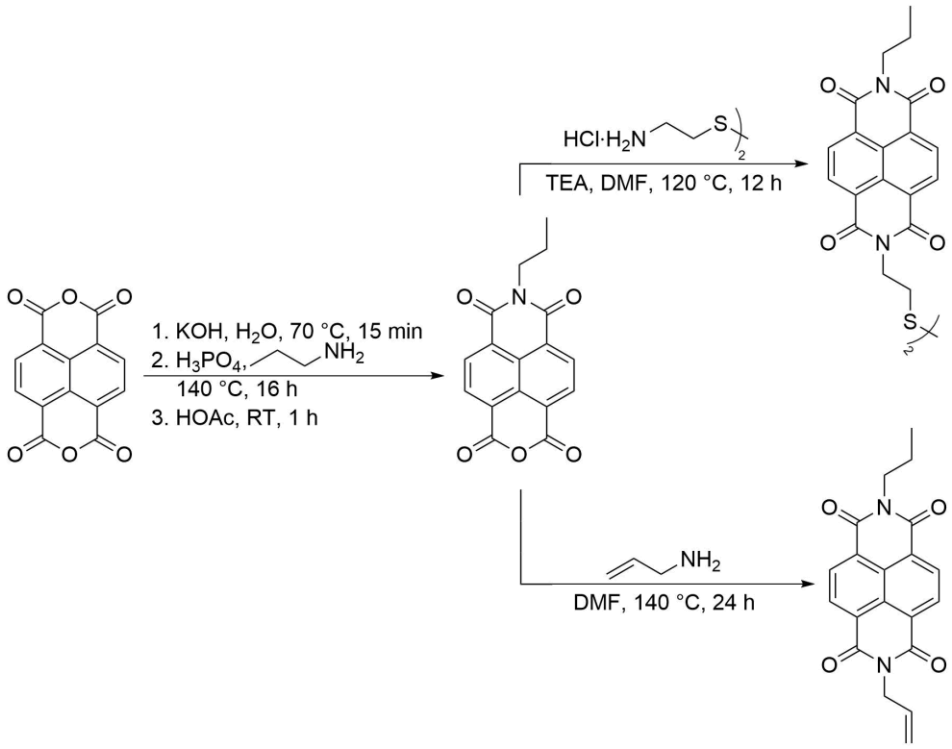

Scheme 4.2.3-2: Strategies for the functionalisation of 1,4,5,8-naphthalenetetracarboxylic dianhydride.

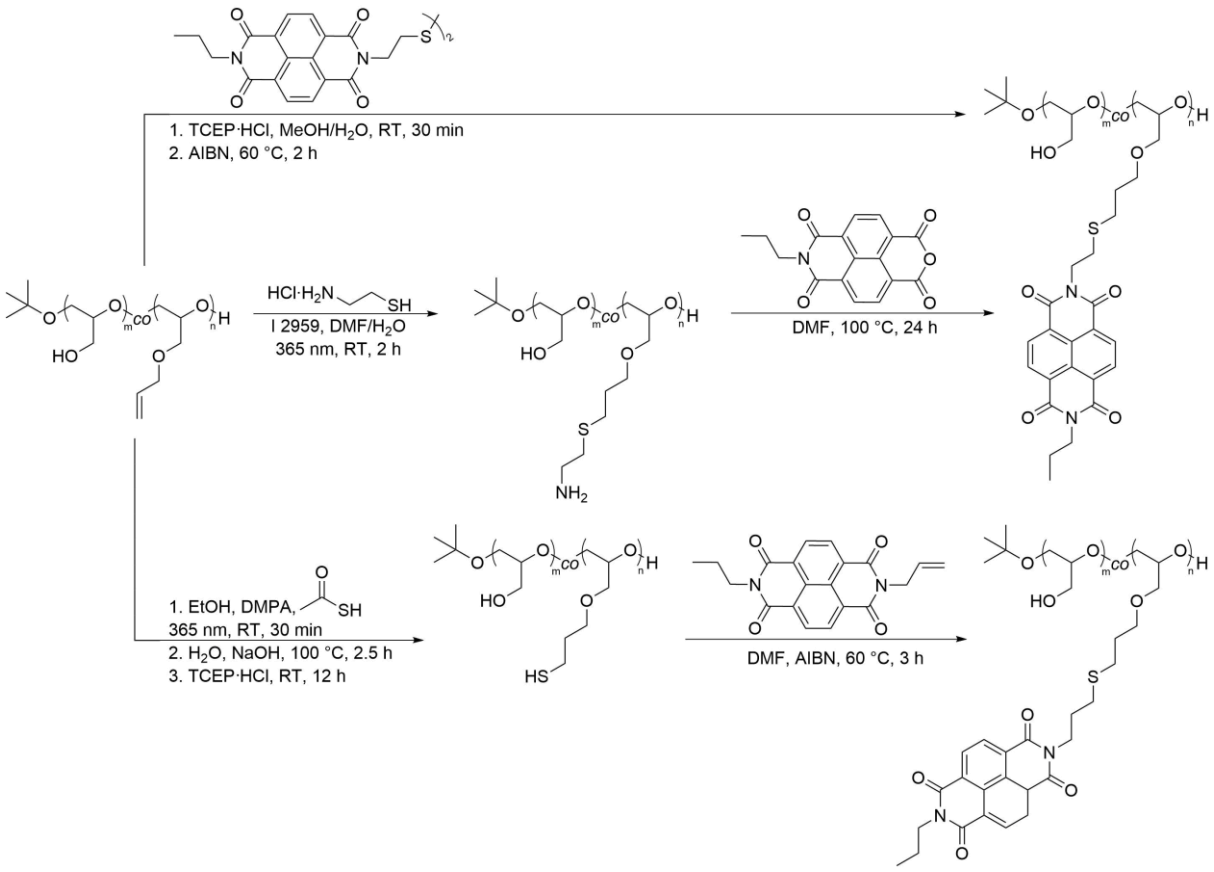

Scheme 4.2.3-3: Strategies for the synthesis of polyglycidols carrying naphthalene diimide groups.

3.2.3.1 Electron rich compound

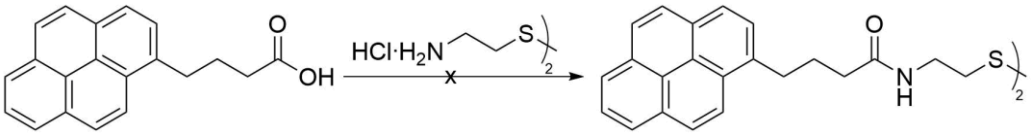

Scheme 4.2.3.1-1: Synthesis of bis(1-pyrenebutyric)cystamide.

We attempted to modify 1-pyrenebutyric acid with cystamine dihydrochloride (Scheme 4.2.3.1-1) using different activation agents for amidation: Oxalyl chloride, [154] CDI and DCC/DMAP. None of these pathways and purification *via* column chromatography with silica led to an isolated product. As silica is slightly acidic, it could have retained the product which is alkaline due to the amide bond leading to an unsuccessful separation. In future, alumina is a better choice because it is slightly alkaline and more suitable for alkaline products. From that point on, the decision was made to modify the polymers P(G-*co*-AGE) (G:AGE = 95:5 and 90:10) first with thioglycolic acid *via* thiol-ene chemistry to obtain carboxyl acid groups (Scheme 4.2.3.1-2) which can be used for amidation (Scheme 4.2.3.1-3) with amine functionalised pyrene compounds. The products were successfully synthesised and characterised *via* ^{1}H NMR, IR, RAMAN spectroscopy and GPC.

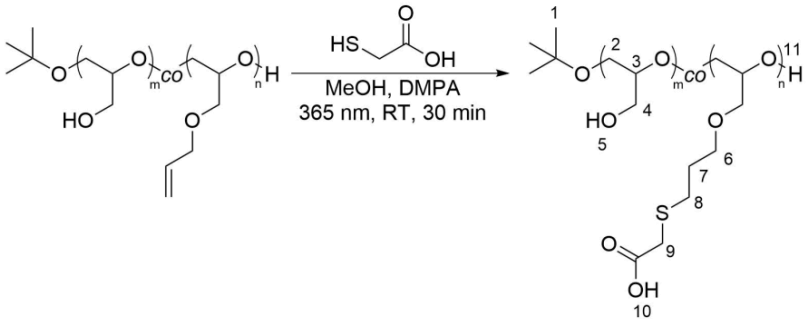

Scheme 4.2.3.1-2: Synthesis of P(G-*co*-COOH).

^{1}H NMR, IR and RAMAN analysis will be explained on G:AGE = 90:10 as an example: After the thiol-ene reaction, the signals of the allyl group H-7 – H-9 (5.94-5.12 ppm) and H-6 (3.95 ppm) disappeared in the ^{1}H NMR spectrum (Figure 4.2.3.1-1). New signals are visible from the formed propylene chain H-7 (1.75 ppm) and H-8 (2.61 ppm). The methylene group of the bound thioglycolic acid H-9 appears at 3.20 ppm. Signals of the other groups remain the same: hydroxyl groups H-5/H-11 (4.51 ppm), polymer backbone and first methylene side group H-2 – H-4/H-6 (3.54-3.37 ppm) and ^{t}butyl group H-1 (1.12 ppm). H-10 is not visible. IR spectrum (Figure 4.2.3.1-2) shows the following vibrations which the parent and modified polymer have in common: The O-H stretch (3364 cm^{-1}) from the alcohol group of the glycidol is visible and the -CH_2 & C-H stretch (2922 cm^{-1}), C-H stretch (2874 cm^{-1}) and -CH_2 bend

(1460 cm^{-1}/1405 cm^{-1}) belong to the ^{t}buyl end group, polyether backbone and aliphatic side chains. Additionally, the C-O-C stretch (1348-857 cm^{-1}) of the polyether backbone and side chain can be seen. New vibrations of the carboxylic group from the bound thioglycolic acid are visible: O-H stretch (2652 cm^{-1}) and C=O stretch (1717 cm^{-1}/1587 cm^{-1}). RAMAN spectrum (Figure 4.2.3.1-4) shows the following vibrations which the parent and modified polymer have in common: The O-H stretch (3046 cm^{-1}) from the alcohol group of the glycidol can be seen and the C-H stretch (2931 cm^{-1}/2883 cm^{-1}), -CH_2 bend (1462 cm^{-1}), C-C stretch (1347 cm^{-1}/1305 cm^{-1}/767-581 cm^{-1}) and C-C bend (465-214 cm^{-1}) from the ^{t}buyl end group, polyether backbone and aliphatic side chains are visible. Also here, the polyether polymer backbone's and ether side chain's C-O-C stretch (1259-855 cm^{-1}) can be seen. After the thiol-ene reaction, the C=C stretch vibration (1643 cm^{-1}) disappeared completely confirming a full consumption of the allylgroup and the C-S stretch vibration (675 cm^{-1}) appeared which confirms the successful binding of the thioglycolic acid. Additionally, the C=O stretch vibration (1712 cm^{-1}/1596 cm^{-1}) from the carboxylic acid of the thioglycolic acid is visible. GPC analysis in DMF (Figure 4.2.3.1-5, Table 4.2.3.1) shows a shift to smaller hydrodynamic volumes of the carboxylic modified polymers which can be explained by intramolecular formed hydrogen bonds of these functional groups. M_n of P(G-*co*-AGE) with G:AGE = 95:5 decreased from 4,299 Da to 2,926 Da and with G:AGE = 90:10 decreased from 4,245 Da to 2,103 Da.

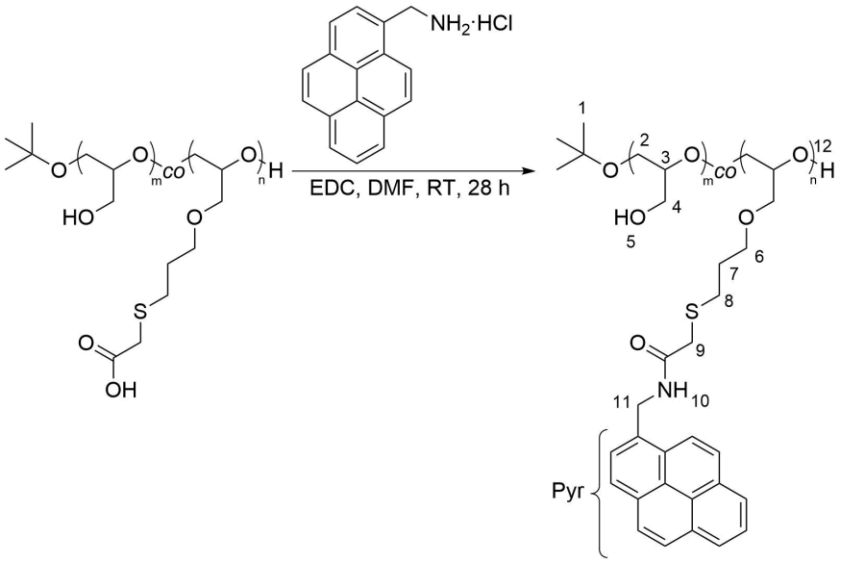

Scheme 4.2.3.1-3: Synthesis of P(G-*co*-Pyr).

After the amidation with 1-pyrenemethylamine hydrochloride, the bound pyrene group is visible in the ^{1}H NMR spectrum (Figure 4.2.3.1-1): H-Pyr (8.35-8.05 ppm) with its methylene group H-11 (5.02 ppm) and amide bond H-10 (8.66 ppm). Other signals of the polymer

remain the same: hydroxyl groups H-5/H-12 (4.50 ppm), polymer backbone and methylene side groups H-2 – H-4/H-6 (3.53-3.33 ppm), methylene group of the thioglycolic acid group H-9 (3.19 ppm), methylene side groups H-7/H-8 (1.71 ppm/2.59 ppm) and ^{t}butyl end group H-1 (1.12 ppm). H-7 was set as reference 2.00 protons and H-11 was used for calculation for degree of substitution. G:AGE = 95:5 has 100 % and G:AGE = 90:10 has 80 % conversion of carboxylic acid groups. Either sterical hindrance or competitive esterification with hydroxyl groups of the polymer have led to a lower degree of substitution. IR spectrum (Figure 4.2.3.1-3) shows the following vibrations which the carboxylic and pyrene functionalised polymer have in common: The O-H stretch (overlapping with N-H stretch from the amide group, 3359 cm^{-1}) belongs to the alcohol group of the glycidol. The -CH_2 & C-H stretch (2934 cm^{-1}), C-H stretch (2873 cm^{-1}) and -CH_2 bend (1457 cm^{-1}/1415 cm^{-1}) from the ^{t}buyl end group, polyether backbone and aliphatic side chains are visible. The C=O stretch (overlapping with C=C stretch of pyrene, 1726 cm^{-1}/1649 cm^{-1}) from the free/reacted thioglycolic acid can be seen.The C-O-C stretch (overlapping with C-N stretch of the amide bond, 1348-847 cm^{-1}) blongs to the polyether polymer backbone and ether side chain. New vibrations after binding of the pyrene ring are visible which confirm the successful binding of the pyrene moiety: =C-H stretch (3048 cm^{-1}) and =C-H bend (847 cm^{-1}/757 cm^{-1}) belong to the aromatic rings which show also a vibration at 1536 cm^{-1}.Additionally, the amide bond's N-H bend is visible. GPC analysis in DMF (Figure 4.2.3.1-6, Table 4.2.3.1) shows an increase of hydrodynamic volumes and dispersities of the pyrene modified polymers which can derive from the increased molecular weight due to the additional functionality and intermolecular π–π stacking in solution. M_n of P(G-*co*-AGE) with G:AGE = 95:5 increased from 2,926 Da to 5,692 Da and with G:AGE = 90:10 increased from 2,103 Da to 5,830 Da.

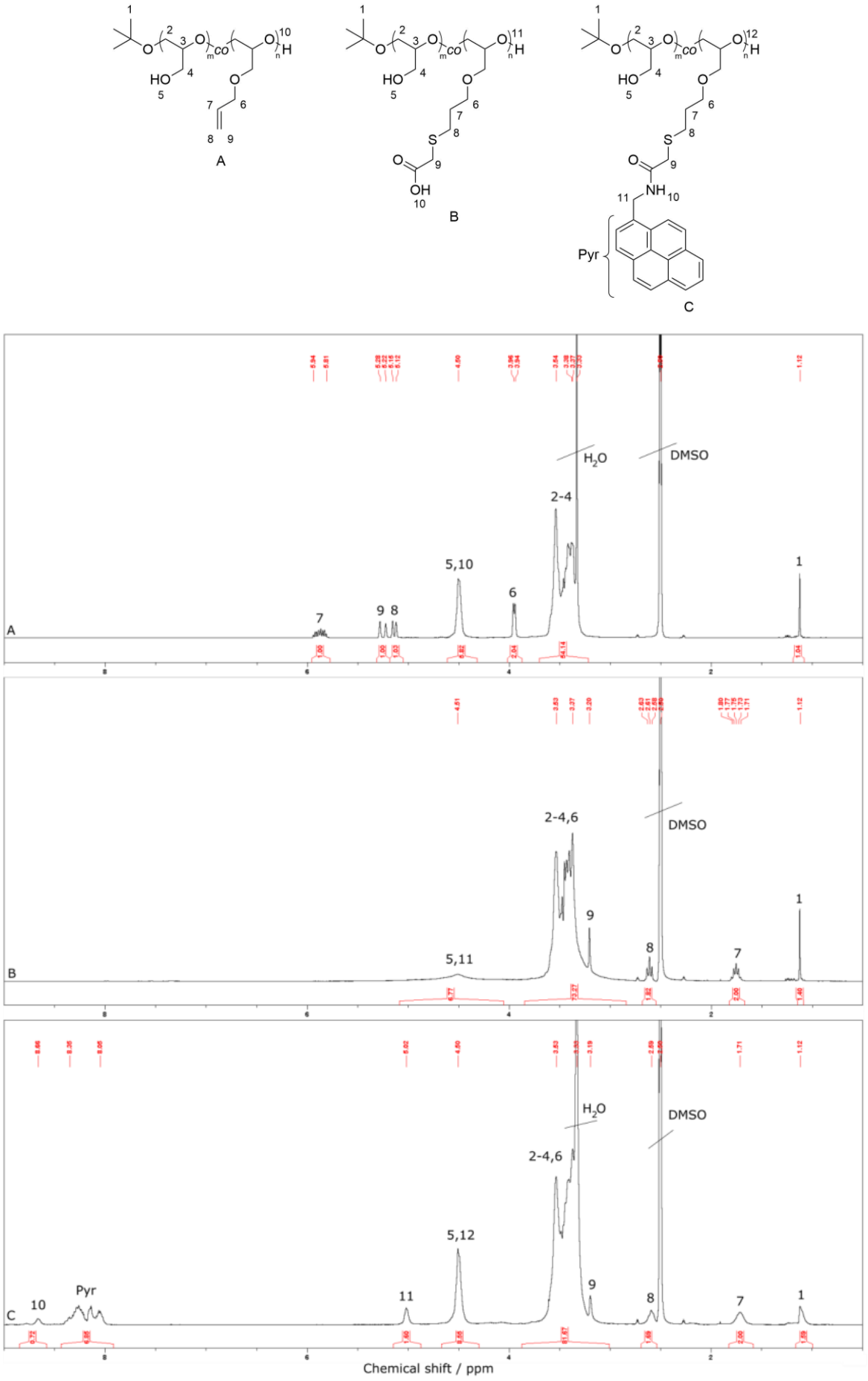

Figure 4.2.3.1-1: ^{1}H NMR spectra of P(G-*co*-AGE) (A), P(G-*co*-COOH) (B) and P(G-*co*-Pyr) (C) in DMSO-d_6.

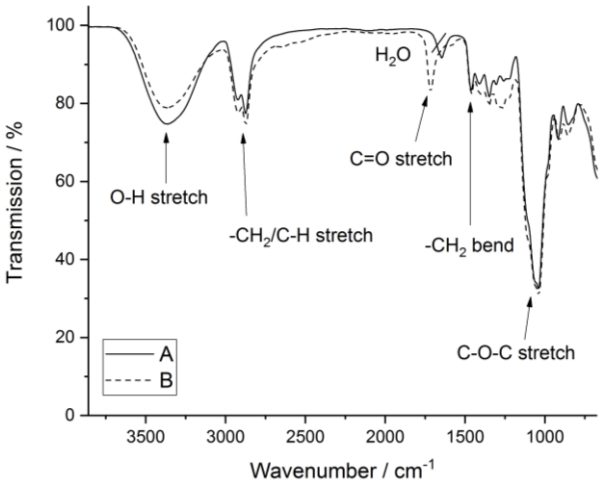

Figure 4.2.3.1-2: IR spectra of P(G-*co*-AGE) (A) and P(G-*co*-COOH) (B) with G:AGE = 90/10.

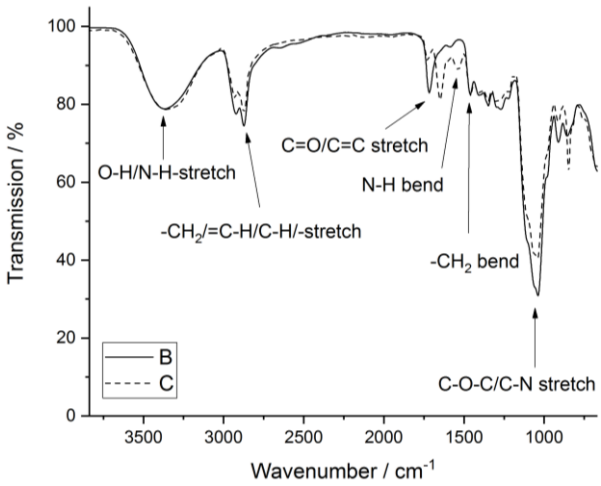

Figure 4.2.3.1-3: IR spectra of P(G-*co*-COOH) (A) and P(G-*co*-Pyr) (B) with G:AGE = 90/10.

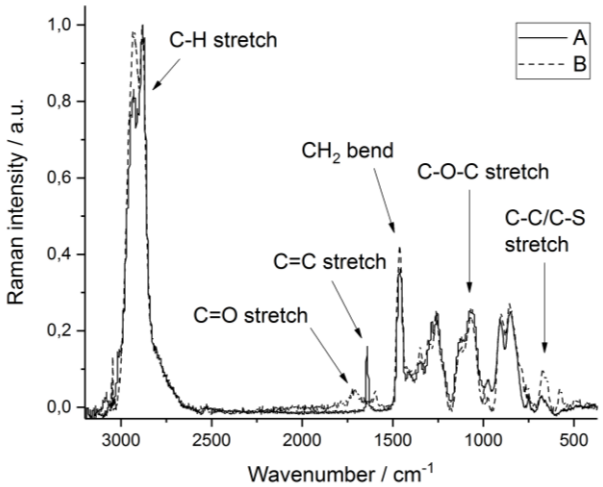

Figure 4.2.3.1-4: RAMAN spectra of P(G-*co*-AGE) (A) and P(G-*co*-COOH) (B) with G:AGE = 90/10.

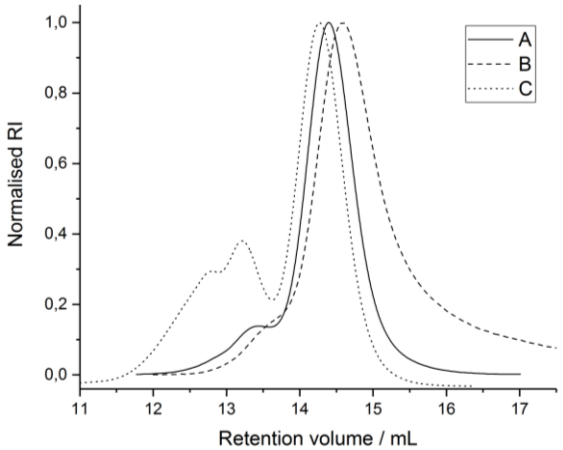

Figure 4.2.3.1-5: GPC traces of P(G-*co*-AGE) (A), P(G-*co*-COOH) (B) and P(G-*co*-Pyr) (C) with G:AGE = 95/5 in DMF (RI).

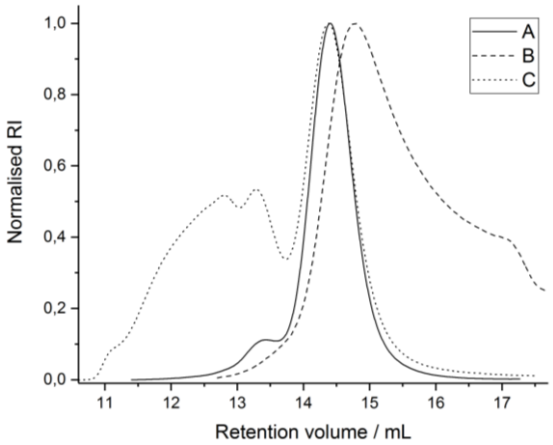

Figure 4.2.3.1-6: GPC traces of P(G-*co*-AGE) (A), P(G-*co*-COOH) (B) and P(G-*co*-Pyr) (C) with G:AGE = 90/10 in DMF (RI).

Table 4.2.3.1: GPC data of P(G-*co*-AGE) (A), P(G-*co*-COOH) (B) and P(G-*co*-Pyr) (C) with G:AGE = 95:5 (1) and G:AGE = 90:10 (2) in DMF (RI).

Run	A		B		C	
	1	2	1	2	1	2
M_n/Da	4,299	4,245	2,926	2,103	5,692	5,830
M_w/Da	5,380	4,641	3,629	2,795	8,551	10,922
Đ	1.25	1.09	1.24	1.33	1.50	1.87

3.2.3.2 Electron poor compound

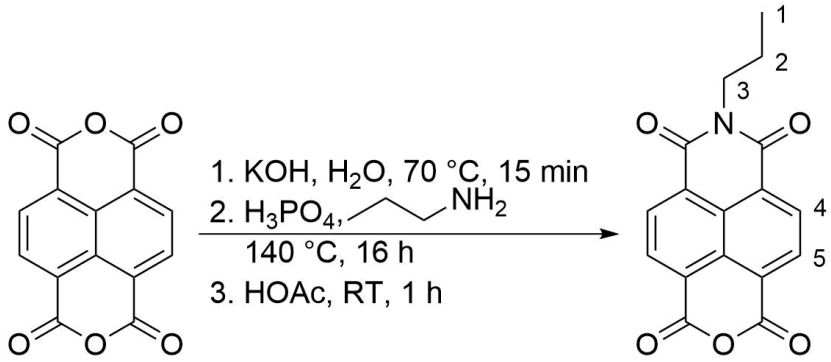

Scheme 4.2.3.2-1: Synthesis of *n*Pr-NMI.

*n*Pr-NMI was synthesised and isolated successfully (Scheme 4.2.3.2-1) according literature procedure by using *n*-propyl amine instead of *n*-butyl amine [157] and characterised *via* ^{1}H, ^{13}C NMR, IR and mass spectrometry. It was isolated with 57 % yield as a grey solid. ^{1}H NMR spectrum (Figure 4.2.3.2-1) shows the signals of the bound *n*-propyl group H-1 (0.93 ppm), H-2 (1.67 ppm) and H-3 (4.01 ppm). The ring protons are visible at 8.52 ppm (H-5) and 8.10 ppm (H-4). ^{13}C NMR spectrum (Figure 4.2.3.2-2) shows the signals of the *n*-propyl group C-1 (11.38 ppm), C-2 (20.81 ppm) and C-3 (overlapping with solvent signal, 39.52 ppm). The carbon atoms of the naphthalene ring are visible in the region 130.13-123.67 ppm, from the imide carbonyl at 163.04 ppm and from the anhydride carbonyl at 169.29 ppm. MS (ASAP, Figure 4.2.3.2-3) shows a signal at 310.0695 which stands well in accordance with the calculated value $[M+H]^+$: 310.0715. IR spectrum (Figure 4.2.3.2-4) shows the following vibrations of the product: The -CH_3 stretch (2964 cm^{-1}/2876 cm^{-1})/ -CH_3 bend (1374 cm^{-1}), -CH_2 & C-H stretch (2935 cm^{-1}), C-H stretch (2603 cm^{-1}/2532 cm^{-1}) and the -CH_2 & -CH_3 bend (1441 cm^{-1}) belong to the *n*-propyl group. . The aromatic ring's vibration (1561 cm^{-1}) and =C-H bend (822-680 cm^{-1}) can be seen. Also, the anhydride's and imide's C=O stretch (1700 cm^{-1}/1655 cm^{-1}) C-O-C/C-N stretch (1346-877 cm^{-1}) are visible.

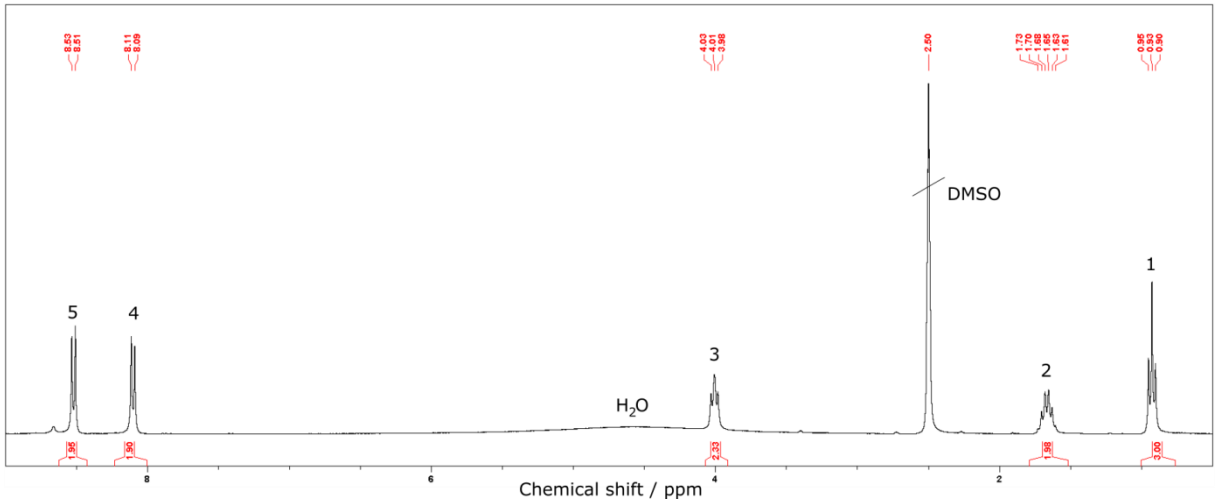

Figure 4.2.3.2-1: ^{1}H NMR spectrum of *n*Pr-NMI in DMSO-d_6.

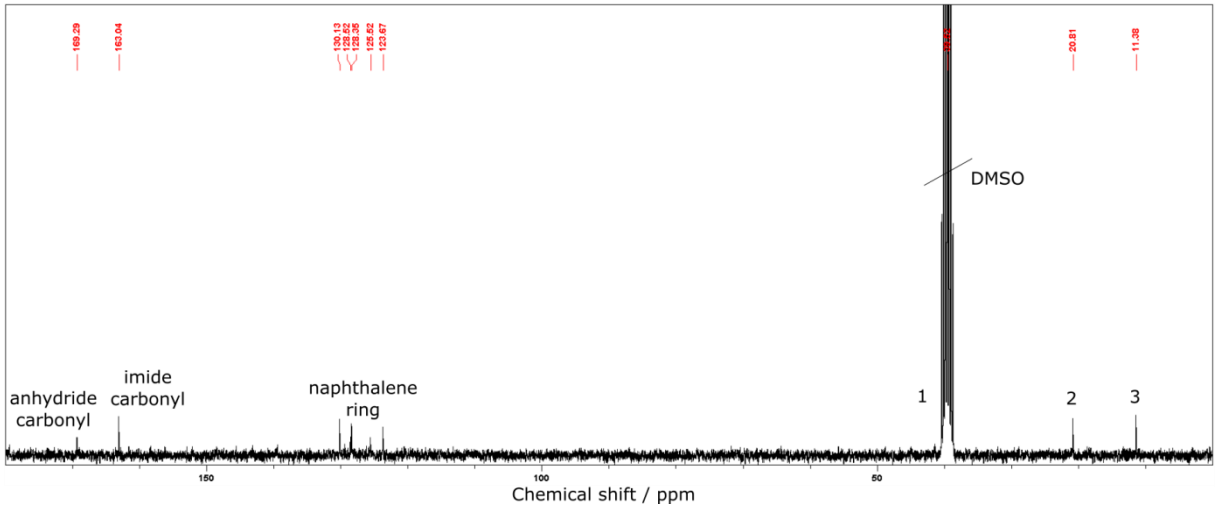

Figure 4.2.3.2-2: ^{13}C NMR spectrum of *n*Pr-NMI in DMSO-d_6.

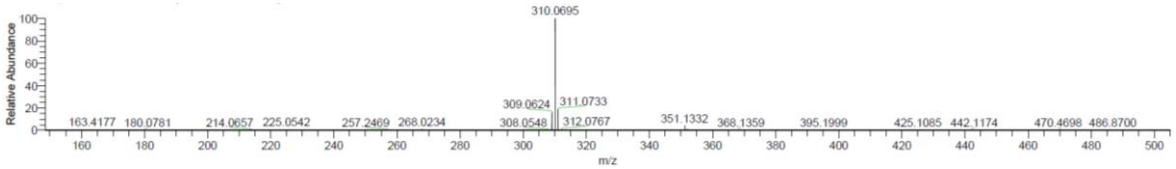

Figure 4.2.3.2-3: ASAP-MS spectrum of *n*Pr-NMI.

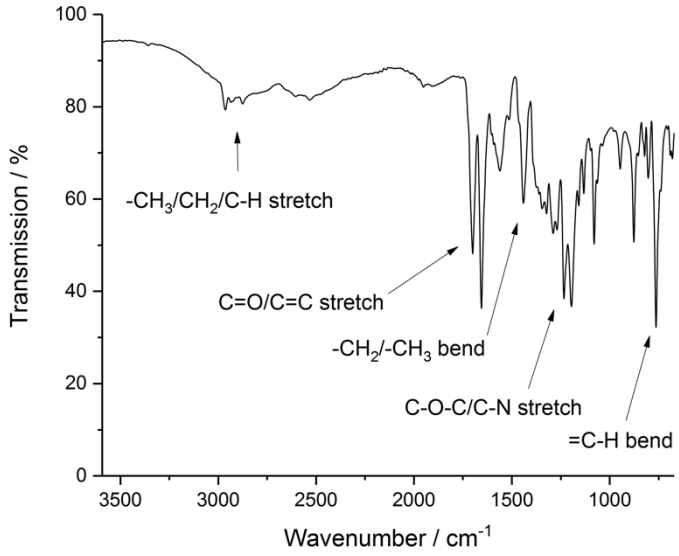

Figure 4.2.3.2-4: IR spectrum of *n*Pr-NMI.

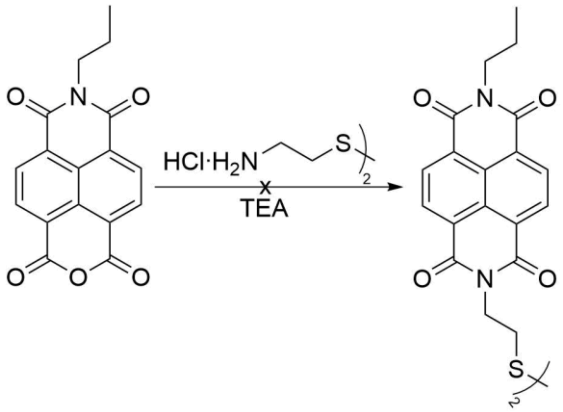

Scheme 4.2.3.2-2: Synthesis of *n*Pr-CA-NDI.

*n*Pr-NMI was modified with cystamin dihydrochloride without success (Scheme 4.2.3.2-2). The amine group may not be nucleophilic enough for this reaction because the electronegatively withdrawn sulphur is nearby. From that on, the decision was made to switch the functionalities: *n*Pr-NMI will be modified with allyl amine and tried to be bound to P(G-*co*-SH) *via* thiol ene-chemistry like Horak *et al.* modified thiol functionalised silica with allyl functionalised naphthalene. [156]

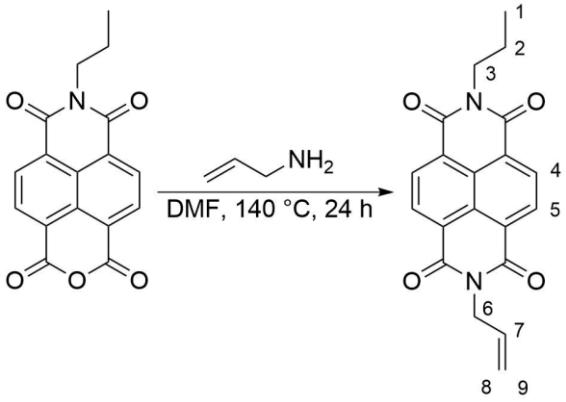

Scheme 4.2.3.2-3: Synthesis of *n*Pr-Allyl-NDI.

*n*Pr-Allyl-NDI was successfully synthesised (Scheme 4.2.3.2-3) and characterised *via* ^{1}H, ^{13}C NMR, IR spectroscopy and mass spectrometry. It was isolated with 43 % yield as a black solid. In the ^{1}H NMR spectrum (Figure 4.2.3.2-5), one can see the signals of the *n*-propyl chain H-1 (1.03 ppm), H-2 (1.77 ppm) and H-3 (4.17 ppm). The signals of the allyl group appear as H-6 (4.82 ppm), H-7 (5.99 ppm), H-8 (5.36 ppm) and H-9 (5.25 ppm). The ring protons H-4/H-5 are visible at 8.76 ppm. The ^{13}C NMR spectrum (Figure 4.2.3.2-6) shows the signals of the *n*-propyl chain with C-1 (11.60 ppm), C-2 (21.50 ppm) and C-3 (42.98 ppm) and the allyl group with C-6 (42.57 ppm), C-7 (126.61 ppm) and C-8/C-9 (118.60 ppm). The carbon atoms of the imide carbonyl are visible at 162.93 ppm/162.69 ppm and of the naphthalene ring in the region 131.19-126.89 ppm. MS (ASAP, Figure 4.2.3.2-7) shows a signal at 349.1168 which stands well in accordance with the calculated value $[M+H]^{+}$: 349.1188. IR spectrum (Figure 4.2.3.2-8) shows the vibrations of the functional groups of the product: The =C-H stretch (3089 cm^{-1}) and =C-H bend (881-680 cm^{-1}) belong to the naphthalene moiety and the aromatic ring shows a vibration (1579 cm^{-1}/1514 cm^{-1}). The *n*-propyl group's -CH_3/C-H stretch (2963 cm^{-1}), -CH_3/-CH_2/C-H stretch (2875 cm^{-1}) and -CH_2/-CH_3 bend (1451 cm^{-1}/1375 cm^{-1}) are visible. The C=O stretch (1702 cm^{-1}/1658 cm^{-1}), and C-N stretch (1330-930 cm^{-1}) belong to the anhydride and imide group.

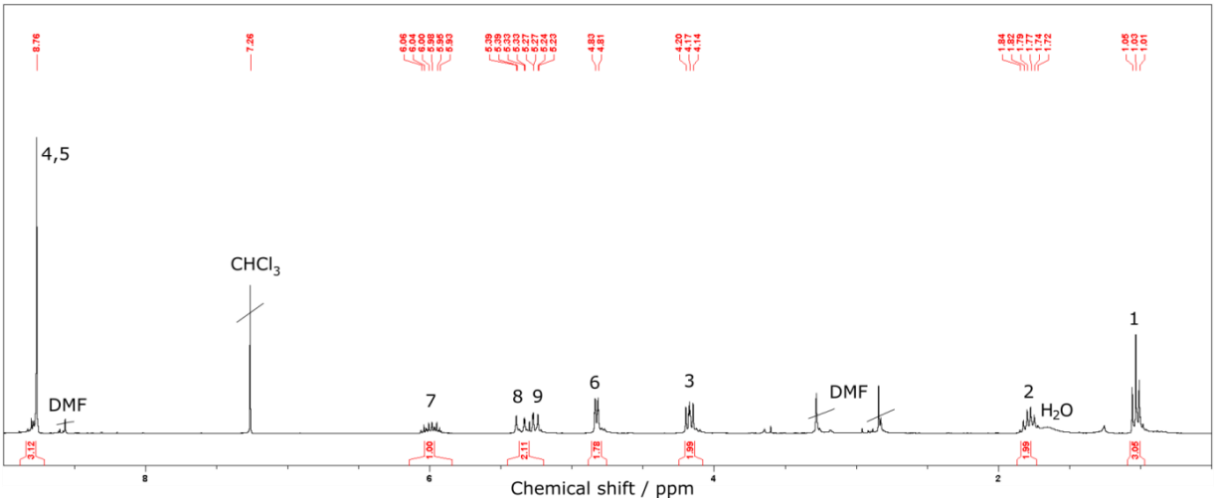

Figure 4.2.3.2-5: ^{1}H NMR spectrum of *n*Pr-Allyl-NDI in $CDCl_3$.

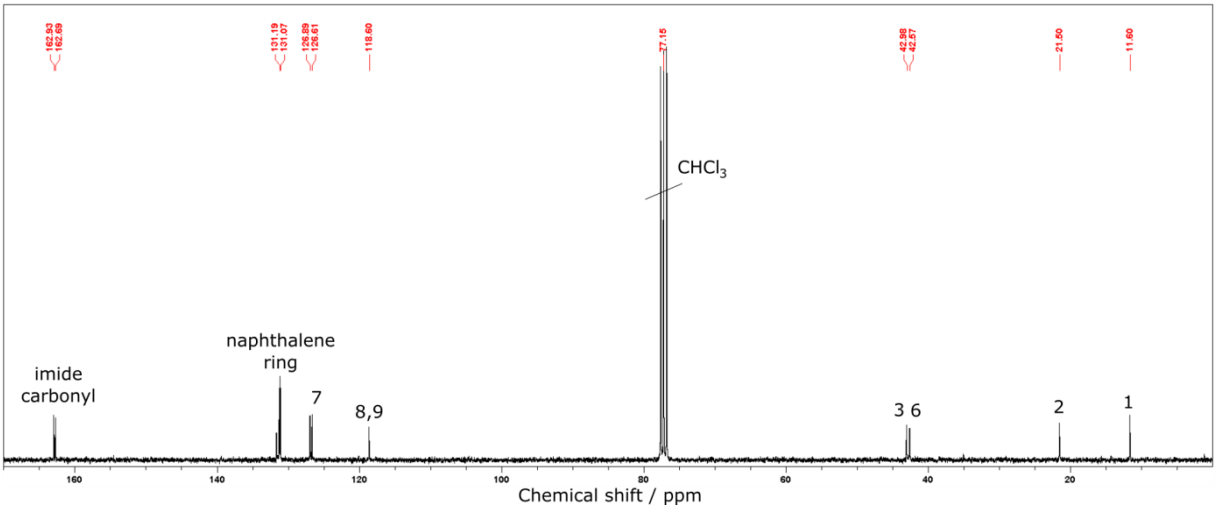

Figure 4.2.3.2-6: ^{13}C NMR spectrum of *n*Pr-Allyl-NDI in $CDCl_3$.

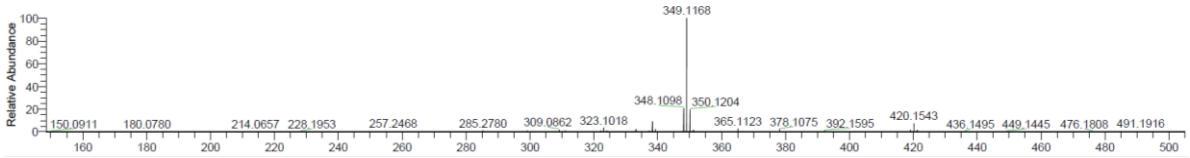

Figure 4.2.3.2-7: ASAP-MS spectrum of *n*Pr-Allyl-NDI.

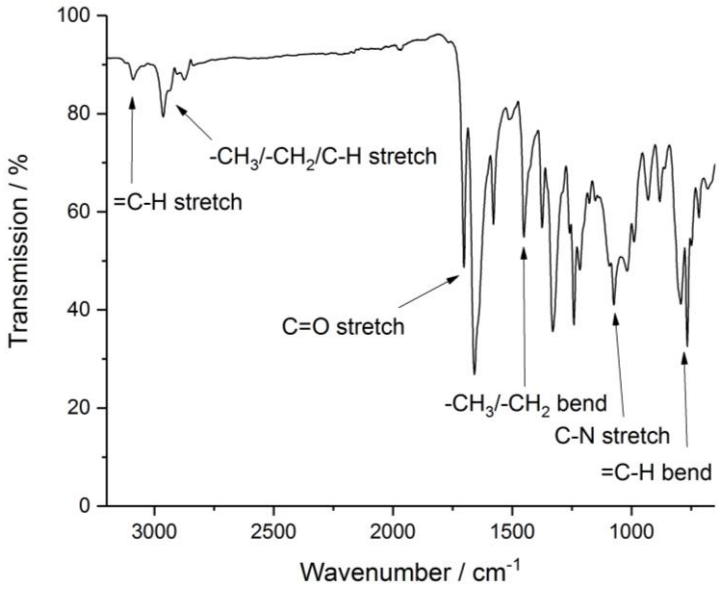

Figure 4.2.3.2-8: IR spectrum of *n*Pr-Allyl-NDI.

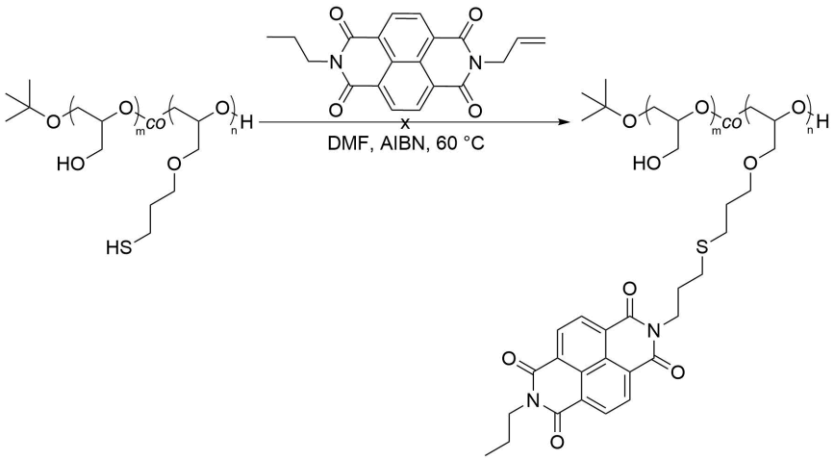

Scheme 4.2.3.2-4: Synthesis of P(G-*co*-*n*Pr-NDI).

In the next step, P(G-*co*-SH) was tried to be modified with nPr-Allyl-NDI [156] *via* thiol-ene chemistry (Scheme 4.2.3.2-4). Horak *et al.* mentioned the low reactivity of the allyl modified naphthalene but even longer reaction times (4 – 24 h) and higher amounts of this compound (SH:Allyl ratio from 1:1 to 1:3.9) did not lead to the desired product. Only a degree of substitution with maximum of 5 % (0.3 groups) was reached. The low reactivity could also be explained due to the neighbouring electronegatively withdrawn carbonyl groups which lead to an electron poor allyl group not being reactive enough for a thiol-ene reaction. [48, 51] Therefore, the decision was made to modify P(G-*co*-AGE) first with cysteamine hydrochloride (Scheme 4.2.3.2-5) to obtain amine groups which can react in a next step with *n*Pr-NMI, a method described by Lewis R. Hart. [134] The products were successfully synthesised and characterised *via* ^{1}H NMR, IR, RAMAN spectroscopy and GPC.

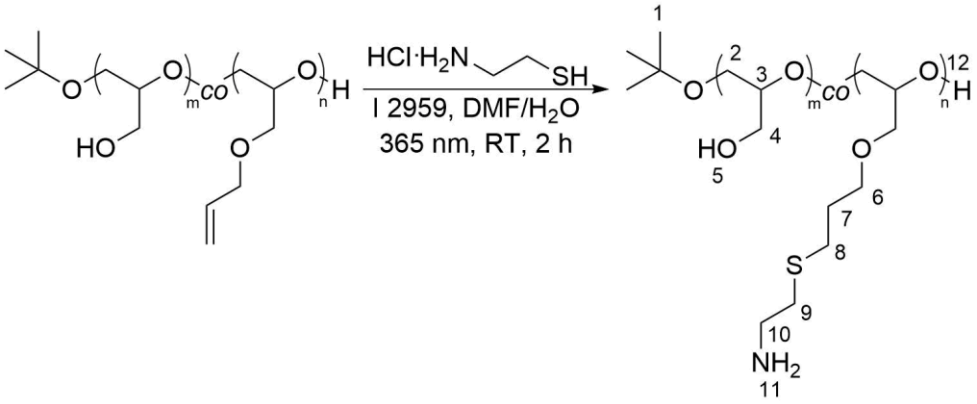

Scheme 4.2.3.2-5: Synthesis of P(G-*co*-NH_2).

After the thiol-ene reaction, the signals of the allyl group completely disappeared in the 1H NMR spectrum (Figure 4.2.3.2-9, H6 – H9, 3.94-5.94 ppm) and new methylene groups are visible: H-7 (1.75 ppm), H-8 (2.57 ppm), H-9 (2.70 ppm) and H-10 (2.94 ppm). H-6 is overlapping with the signals of the polymer backbone and side methylene groups H2 – H4 (3.53-3.37 ppm). Hydroxyl groups H-5/H-12 (4.52 ppm) and ^{t}butyl end group H-1 (1.12 ppm) remain the same. H-11 is not visible. IR spectrum (Figure 4.2.3.2-10) shows the following vibrations which the parent and modified polymer have in common: The O-H stretch (3349 cm^{-1}) belongs to the alcohol group of the glycidol and the -CH_2 & C-H stretch (2931 cm^{-1}), C-H stretch (2874 cm^{-1}), -CH_2 bend (1460 cm^{-1}/1411 cm^{-1}) belong to the ^{t}butyl end group, polyether backbone and aliphatic side chain. Additionally, the polyether backbone's and ether side chain's C-O-C stretch (1347-855 cm^{-1}) is visible. Some vibrations of the product are overlapping: N-H stretch from the amine group with O-H stretch, N-H bend with water signal and C-N/C-S stretch of the amine/thio ether group with C-O-C stretch. RAMAN spectrum (Figure 4.2.3.2-12) shows the following vibrations which the parent and modified polymer have in common: The O-H stretch (3150 cm^{-1}) belongs to the alcohol group of the glycidol and the C-H stretch (2927 cm^{-1}/2881 cm^{-1}), -CH_2 bend (1461 cm^{-1}), C-C stretch (1344 cm^{-1}/1307 cm^{-1}), C-C stretch (752 cm^{-1}) and C-C bend (493-243 cm^{-1}) belong to the ^{t}butyl end group, polyether backbone and aliphatic side chain. Additionally, the polyether backbone's and side chain's C-O-C stretch (1258-849 cm^{-1}) can be seen. After the thiol-ene reaction, the C=C stretch (1643 cm^{-1}) vibration of the allyl group completely disappeared and the C-S stretch (654 cm^{-1}) vibration of the formed thio ether group appeared confirming the full consumption of the allyl group. GPC analysis in DMF (Figure 4.2.3.2-13, Table 4.2.3.2) shows a decrease of the molecular weight (4,245 Da to 3,829 Da) which may come from hydrogen bonds between amine and hydroxyl groups causing a smaller hydrodynamic

volume. The dispersity increased (1.09 to 1.34) which may be caused by the interaction of the amine groups with the column material.

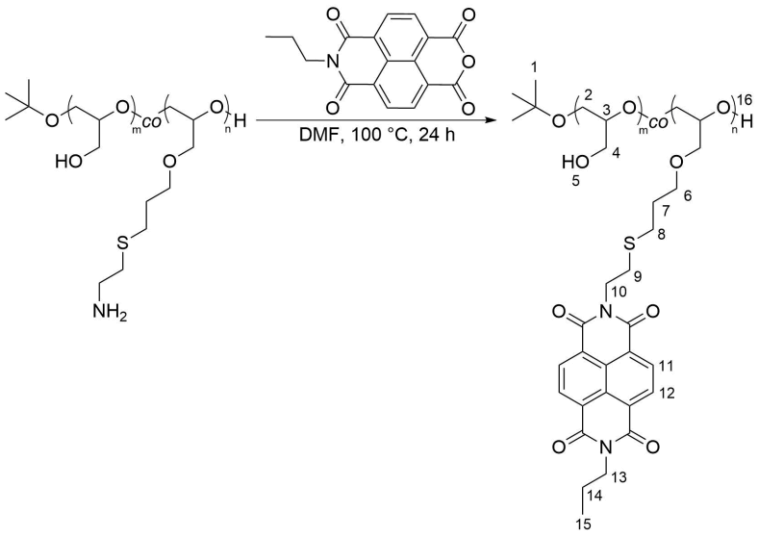

Scheme 4.2.3.2-6: Synthesis of P(G-*co*-*n*Pr-NDI).

Afterwards, P(G-*co*-NH_2) reacted with *n*Pr-NMI (Scheme 4.2.3.2-6) and could be isolated. The ^{1}H NMR spectrum (Figure 4.2.3.2-9) shows the following signals which the amine functionalised and NDI functionalised polymer have in common: ^{t}butyl group H-1 (1.12 ppm), polymer backbone with methylene side group H-2 – H-4/H-6 (3.53-3.33 ppm), the methylene side groups H-7 (1.82 ppm), H-8 (2.67 ppm), H-9 (2.79 ppm) and hydroxyl groups H-5/H-16 (4.49 ppm). The new signals of the attached *n*Pr-NDI group are visible at 8.69-8.12 ppm (H-11, H-12), 4.01 ppm (H-13), 1.67 ppm (H-14) and 0.95 ppm (H-15). The most characteristic signal for the successful binding of *n*Pr-NDI on the polymer is the methylene group H-10 next to the amine group which shifted from 2.94 ppm to 4.18 ppm due to the electronegatively withdrawn carbonyl groups nearby. IR spectrum (Figure 4.2.3.2-11) shows the following vibrations which the amine functionalised and NDI functionalised polymer have in common: The O-H stretch (3360 cm^{-1}) from the alcohol group of the glycidol is visible and the -CH_2 & C-H stretch (2932 cm^{-1}/2874 cm^{-1}) -CH_2 bend (1453 cm^{-1}) belong to the ^{t}butyl end group, polyether backbone and aliphatic side chain. The polyether backbone's and ether side chain's C-O-C stretch (1374-914 cm^{-1}) is overlapping with the imide's C-N stretch. Additionally, the product shows the C=O stretch (1705 cm^{-1}/1663 cm^{-1}) and =C-H stretch (882-765 cm^{-1}) from the naphthalene imide compound The aromatic ring (1580 cm^{-1}) shows additional vibrations. GPC analysis in DMF (Figure 4.2.3.2-13, Table 4.2.3.2) shows an increase of M_n (3,829 Da to 5,228 Da) which can derive from the increased molecular weight due to the additional functionality and the π–π stacking in solution forming higher aggregates possessing a larger hydrodynamic volume.

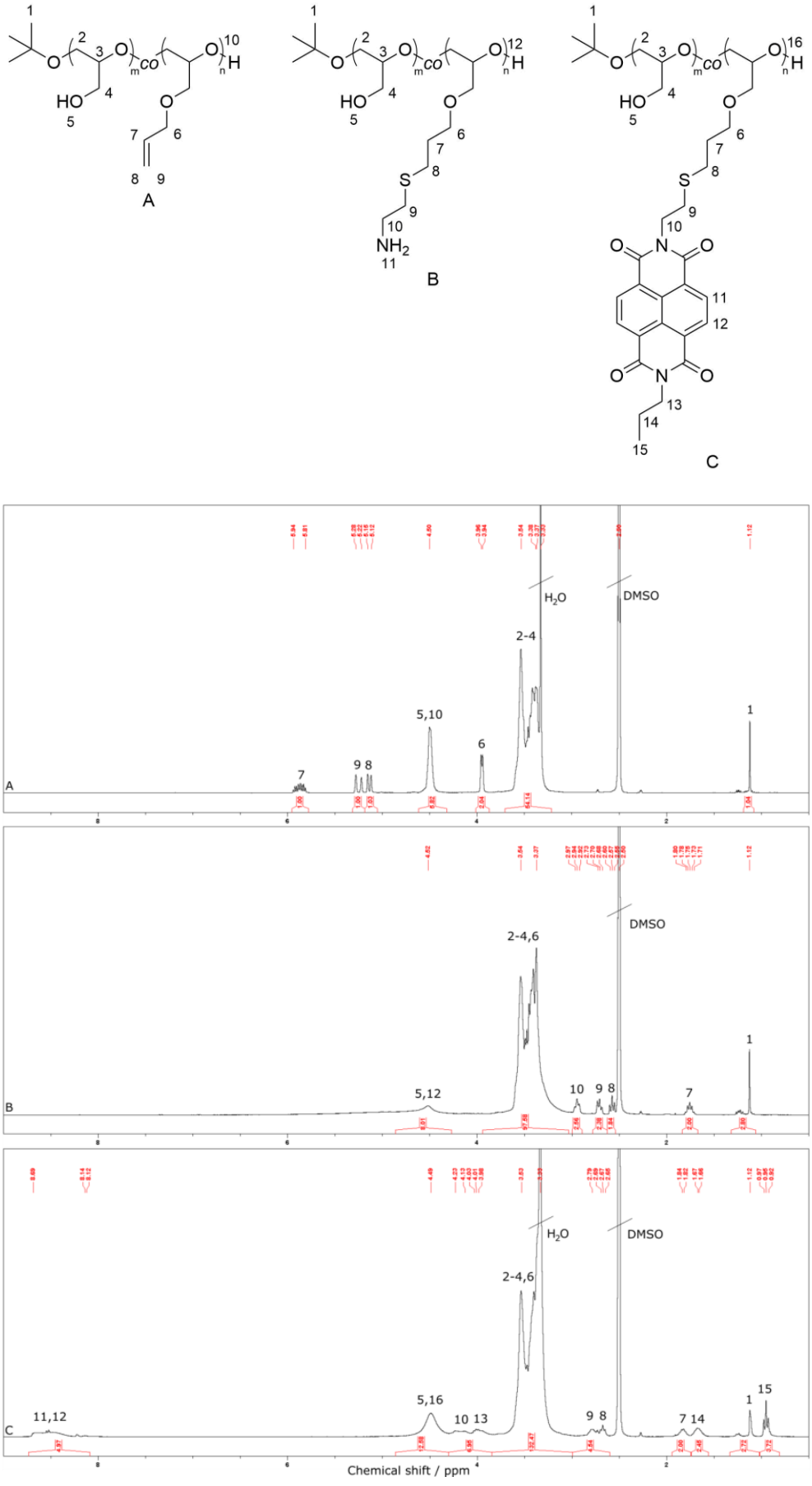

Figure 4.2.3.2-9: ^{1}H NMR spectra of P(G-*co*-AGE) (A), P(G-*co*-NH_2) (B) and P(G-*co*-nPr-NDI) (C) in DMSO-d_6.

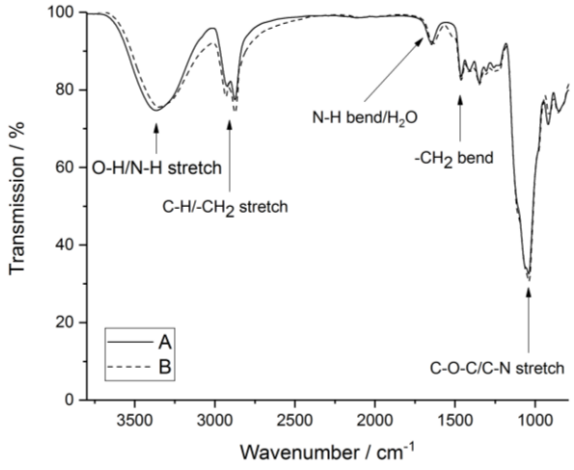

Figure 4.2.3.2-10: IR spectra of P(G-*co*-AGE) (A) and P(G-*co*-NH_2) (B).

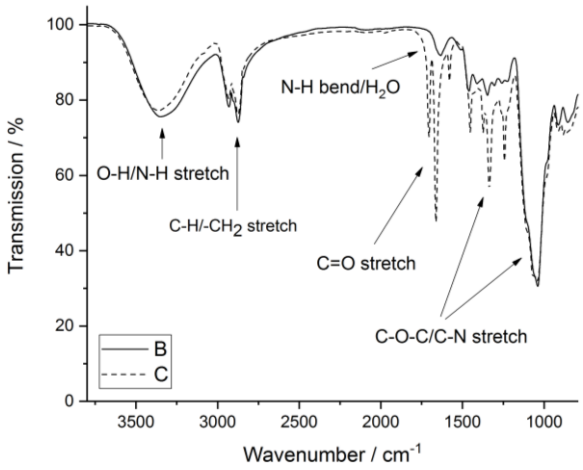

Figure 4.2.3.2-11: IR spectra of P(G-*co*-NH_2) (A) and P(G-*co*-*n*Pr-NDI) (B).

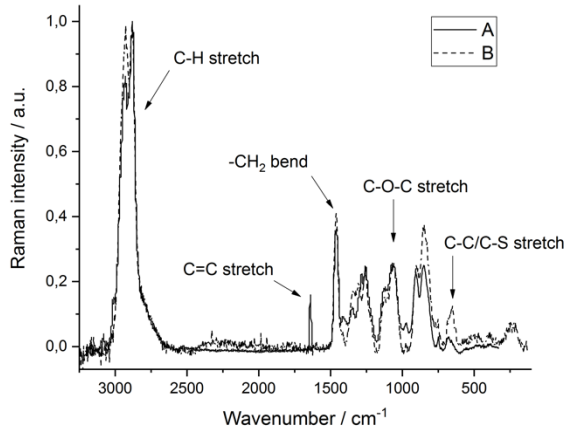

Figure 4.2.3.2-12: IR spectra of P(G-*co*-AGE) (A) and P(G-*co*-NH_2) (B).

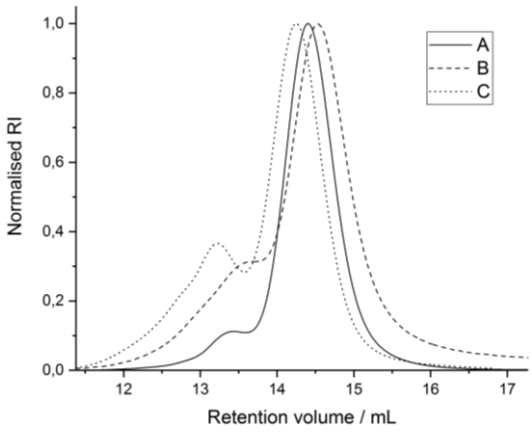

Figure 4.2.3.2-13: GPC traces of P(G-*co*-AGE) (A), P(G-*co*-NH_2) (B) and P(G-*co*-nPr-NDI) (C) in DMF (RI).

Table 4.2.3.2: GPC data of P(G-*co*-AGE) (A), P(G-*co*-NH_2) (B) and P(G-*co*-nPr-NDI) (C) in DMF (RI).

Run	**A**	**B**	**C**
M_n / Da	4,245	3,829	5,228
M_w / Da	4,641	5,140	6,677
Đ	1.09	1.34	1.28

3.2.3.3 Gel tests

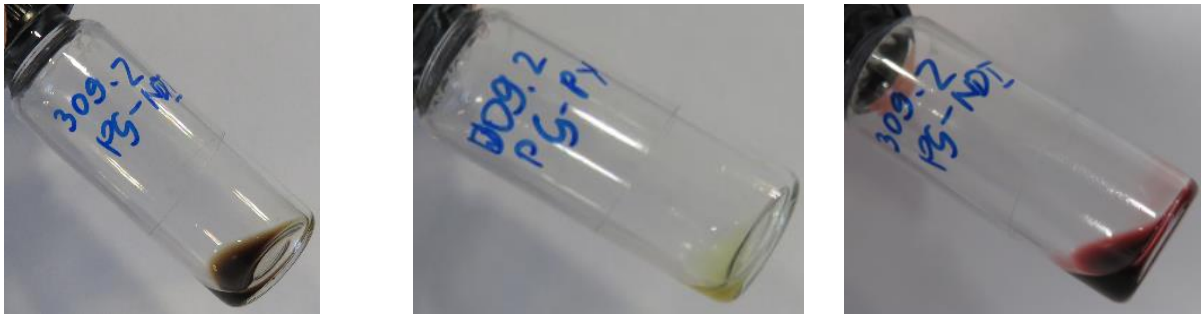

Figure 4.2.3.3-1: Solutions of P(G-*co*-NDI) (left), P(G-*co*-Pyr) (middle) and mixture of both (right) in water with G:Pyr = 57:3 and G:NDI = 54:6 with 10 wt-% polymer in total.

For a gel test, polymers carrying pyrene groups (RU (G:Pyr) = 57:3, yellow) and polymers carrying naphthalene diimide groups (RU (G:NDI) = 54:6, black) were dissolved in water (pH = 7.0). Both solutions were stirred at RT for 18 h, combined to give equimolar ratio of functional groups with a total amount of 10 mg of polymer (w/w (polymer) = 10 %) and stirred again at RT for 18 h. The final solution turned purple but did not form a hydrogel (Figure 4.2.3.3-1). UV-vis analysis (Figure 4.2.3.3-2, Table 4.2.3.3) shows the following transitions of the polymers/mixture:

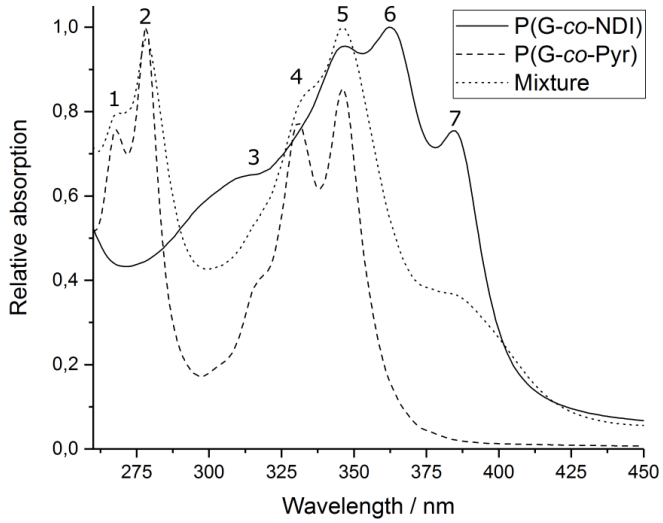

Figure 4.2.3.3-2: UV-Vis spectra of of P(G-*co*-NDI), P(G-*co*-Pyr) and mixture of both in water with c = 0.5 mg/mL.

Table 4.2.3.3: Wavelengths of P(G-*co*-NDI), P(G-*co*-Pyr) and the mixture.

Number	Wavelength / nm	P(G-*co*-NDI)	P(G-*co*-Pyr)	Mixture
1	267	-	Yes	Yes
2	278	-	Yes	Yes
3	315	Yes	Yes	Yes
4	331	-	Yes	Yes
5	347	Yes	Yes	Yes
6	364	Yes	-	Yes
7	387	Yes	-	Yes

The mixture shows that the relative intensity of the signals 1, 4 and 5 increased, the signals 3, 6 and 7 decreased and 2 remained. Increased/remained intensities stand for an intramolecular π-π*-transition of Pyr or NDI whereas decreased intensities are caused due to an intermolecular π(HOMO of Pyr)-π*(LUMO of NDI)-transition with a high overlapping of the molecular orbitals. [123] This shows that the functional aromatic groups are interacting but no hydrogel formation could be observed. This could be either explained due to the low amount of aromatic groups or the too low polymer content in the solution. The concentration of aromatic groups is similar to the previously reported low molecular gelators [87, 122, 132] but in there additional stabilisation of the gels was given *via* hydrogen bonds. Therefore the system in this work could be improved by increase of the functional aromatic groups. Additionally, one could increase the chain length of the polymers and the spacer between polymer back bone and aromatic group for a better network formation.

3.3 High molecular weight polyglycidols

3.3.1 Polymer synthesis

So far polyglycidols with short chain lengths were synthesised and did not show any network formation. For this reason it is proposed to increase the polymer chain length which may lead to the desired result because longer polymer chain lengths can carry more functional groups for the network stabilisation and they possess a higher capability of water incorporation. [158] The monomer-activated anionic ring opening polymerisation technique was used in order to achieve high molecular weight polyglycidols (Scheme 4.3.1-1). Therefore, the catalyst:initiator-ratio and total monomer concentration were varied according literature [41] to target number average molecular weights in the range 10-100 kDa (Table 4.3.1-1). In this

reference, the listed conditions were applied for a homopolymerisation of EEGE (1) and will be used in this work additionally for the homopolymerisation of AGE (2) and copolymerisation of EEGE and AGE (3) (step I). The polymers PEEGE and P(EEGE-*co*-AGE) were further treated under acidic conditions for deprotection of the glycidols (step II). For all products first the spectroscopic analysis will be discussed and then afterwards the GPC analysis.

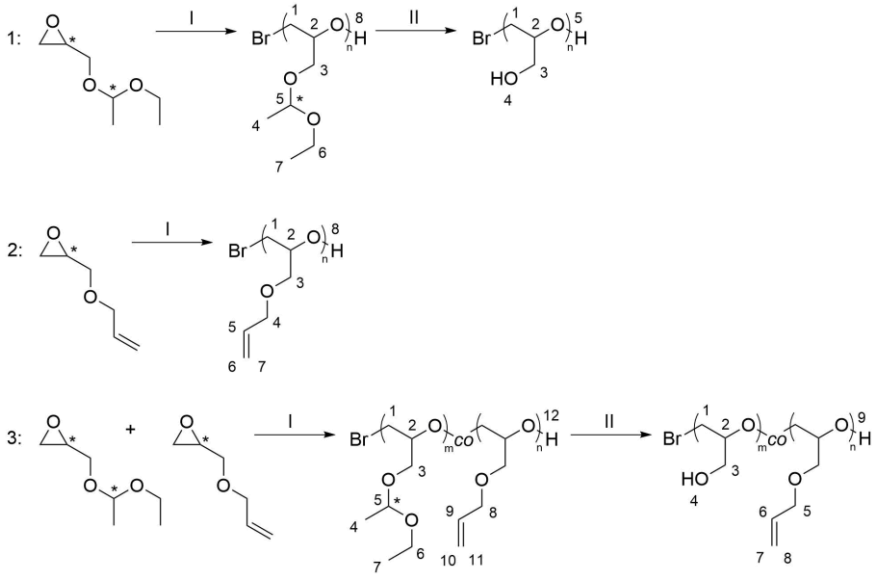

Scheme 4.3.1-1: Synthesis of high molecular weight polyglycidols: I: 1. $NOct_4Br$, Al^iBu_3, toluene, -20 °C → RT, 24 h. 2. EtOH, RT, 10 min. II: EtOH, HCl, RT, 4 h.

Table 4.3.1-1: Catalyst:initiator-ratio, total monomer concentration and theoretical number average molecular weight for 100 % conversion.

Run	$[Al^iBu_3]:[NOct_4Br]$	$[Monomer]_{total}$/M	$M_{n,theo}$/kDa
1	4:1	0.5	10
2	2:1	0.5	20
3	4:1	1	30
4	2:1	2	70
5	5:1	2	100

Crude ^{1}H NMR spectroscopy measurements (spectra not shown) reveals a monomer conversion of 100 % for polymers 1-3 and 5. Polymer 4 reached 88 % which may be caused by a too high viscosity during the polymerisation process what complicates monomers to be added on the growing polymer chain end (gel effect). [159] Clean ^{1}H NMR spectrum of PEEGE (Figure 4.3.1-1) shows the protons of the polymer backbone H-1/H-2, methylene side groups H-3/H-6 and end group H-8 in the region 3.69-3.43 ppm. Residual protons of the

acetal group are visible at 4.73 ppm (H-5), 1.26 ppm (H-4) and 1.17 ppm (H-7). After deprotection, the signals of the acetal group disappears and the signal of the hydroxyl side group (H-4), overlapping end group H-5, is visible at 4.51 ppm. Polymer backbone signals H-1/H-2 and methylene side group H-3 are slightly shifted due to another solvent for the ^{1}H NMR measurement (3.54-3.37 ppm). IR spectra (Figure 4.3.1-4) look similar with the difference that the deprotected polymers show the O-H stretch (3372 cm^{-1}) vibration of the alcohol group from the glycidol.. Residual vibrations of functional groups remain almost unchanged: The -CH_2/-CH_3/C-H stretch (2976-2875 cm^{-1})and -CH_2/-CH_3 bend (1460-1408 cm^{-1}) belong to the polyether backbone and aliphatic side chains. The polyether backbone shows additionally the C-O-C stretch (1340-853 cm^{-1}). RAMAN spectrum (Figure 4.3.1-5) shows no difference in the vibrations as well: The C-H stretch (2984-2803 cm^{-1}), -CH_2 & -CH_3 bend (1460 cm^{-1}) and C-C bend (532-363 cm^{-1}) belong to the polyether backbone and aliphatic side chains. The polyether's backbone C-O-C stretch (1275-816 cm^{-1}) and the end group's C-Br stretch (681 cm^{-1}) are visible.

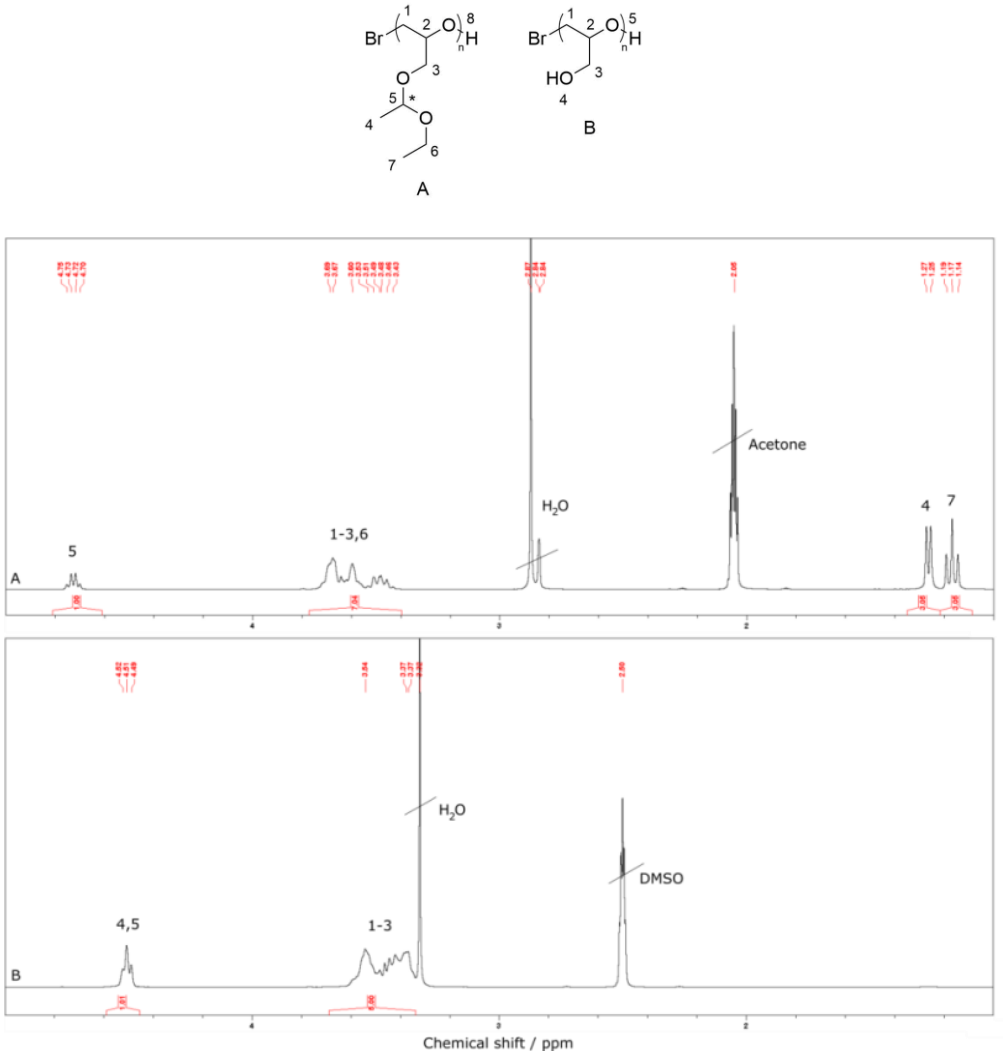

Figure 4.3.1-1: ^{1}H NMR spectra of PEEGE in acetone-d_6 (A) and PG in DMSO-d_6 (B).

The homopolymerisation of AGE reached 100 % for polymer 1-4 and 94 % for polymer 5 where latter ones may not have reached 100 % due to the gel effect. PAGE was successfully synthesised and characterised *via* ^{1}H NMR, IR and RAMAN spectroscopy and GPC. ^{1}H NMR spectrum (Figure 4.3.1-2) shows the polymer backbone signals H-1/H-2, the methylene side group H-3 and end group H-8 in the region 3.69-3.47 ppm. The allyl group is visible at 4.01 ppm (H-4), 5.99-5.86 ppm (H-5), 5.14 ppm (H-6) and 5.29 ppm (H-7). In the IR spectrum (Figure 4.3.1-6) one can see the -CH_2 & C-H stretch (2979-2865 cm^{-1}) and -CH_2 bend (1460-1350 cm^{-1}) vibrations from the polyether backbone/ether side chain and aliphatic side chains. Additionally, the polyether backbone's and ether side chain's C-O-C stretch (1302-920 cm^{-1}) vibrationsare visible. RAMAN spectrum (Figure 4.3.1-7) shows the =(C-H) stretch (3084-3013 cm^{-1}) and C=C stretch (1645 cm^{-1}) vibrations from the allyl group. The C-H stretch (2872 cm^{-1}), -CH_2 bend (1469-1422 cm^{-1}) and C-C bend (564 cm^{-1}) vibrations belong to the polyether backbone and aliphatic side chain. Additionally, the polyether backbone's/ether side chain's C-O-C stretch (1289-868 cm^{-1}) and end group's C-Br stretch (652 cm^{-1}) vibrations are visible.

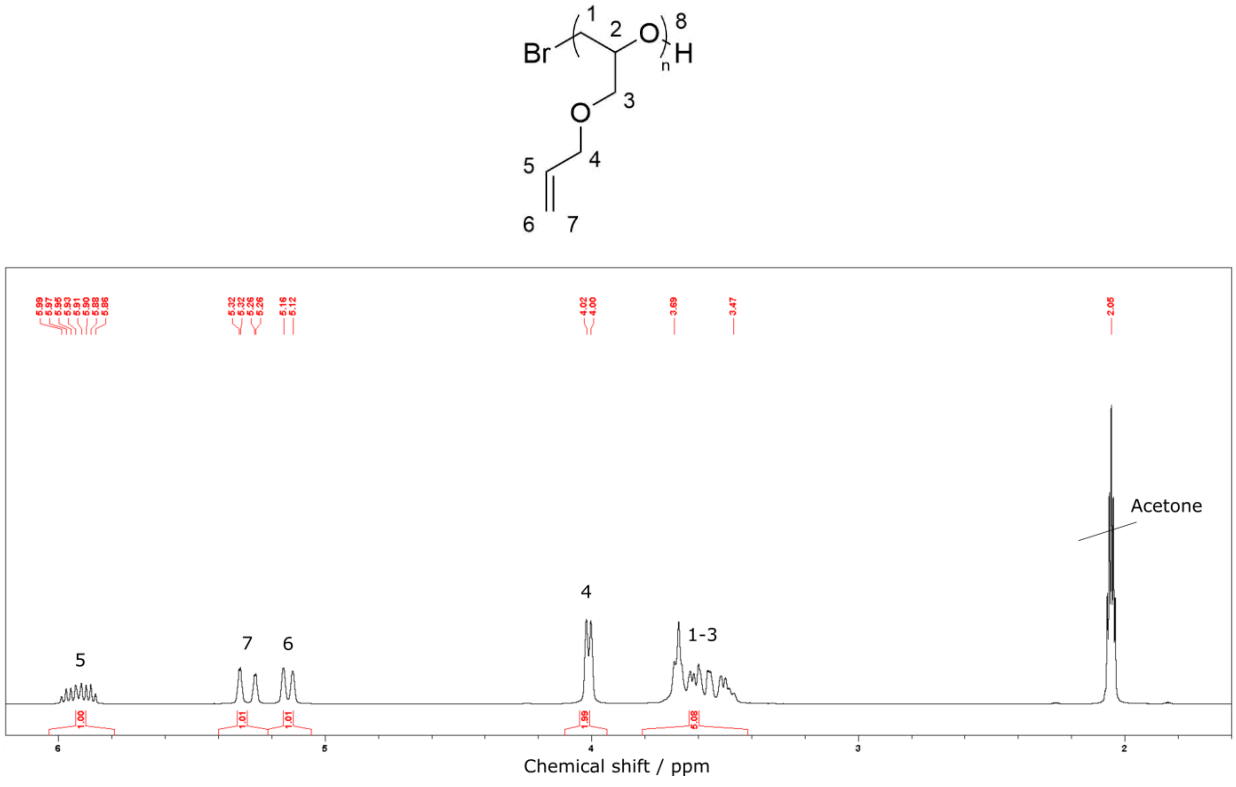

Figure 4.3.1-2: ^{1}H NMR spectrum of PAGE in acetone-d_6.

The copolymerisation of EEGE and AGE reached 100 % for polymer 1-3 and 5. Polymer 4 reached 98 % probably due to the gel effect. P(EEGE-*co*-AGE) was successfully synthesised and characterised *via* ^{1}H NMR, IR and RAMAN spectroscopy and GPC. ^{1}H NMR spectrum (Figure 4.3.1-3) shows the protons of the polymer backbone H-1/H-2, methylene groups H-3/H-6 and end group H-12 in the region 3.69-3.43 ppm. Further protons of the acetal group are visible at 4.73 ppm (H-5), 1.26 ppm (H-4) and 1.17 ppm (H-7). The protons of the allyl group appear at 6.00-5.87 ppm (H-9), 5.30 ppm (H-11), 5.15 ppm (H-10) and 4.02 ppm (H-8). After the deprotection, the protons of the acetal group are not visible anymore and a signal for the hydroxyl group H-4 overlapping with the end group H-9 appears at 4.50 ppm. Residual signals of the allyl group H-6 (5.94-5.81 ppm), H-8 (5.25 ppm), H-7 (5.14 ppm), H-5 (3.95 ppm), polymer backbone H-1/H-2 and methylene side group H-3 (3.54-3.37 ppm) remain in the same region and are shifted slightly due to measurement in another solvent. IR spectrum (Figure 4.3.1-8) shows similar signals for deprotected and protected polymer with C-H/-CH_2/-CH_3 stretch (2978-2875 cm^{-1}) and -CH_2/-CH_3 bend (1455-1380 cm-1) vibrations of the polyether backbone and aliphatic side chains. The C-O-C stretch (1240-814 cm^{-1}) vibration belongs to the polyether backbone and ether side group. After deprotection, the O-H stretch (3356 cm^{-1}) vibration of the alcohol group from glycidol is visible confirming the successful deprotection. RAMAN spectrum (Figure 4.3.1-9) shows no difference in the vibrations: The C-H stretch (2981-2770 cm^{-1}), -CH_2/-CH_3 bend (1453 cm^{-1}) and C-C bend (522-354 cm^{-1}) vibration belong to the polyether backbone and aliphatic side chains. Additionally, the C=C stretch (1644 cm^{-1}) vibration of the allyl group is visible. The polyether backbone's/ether side group's C-O-C stretch (1270-807 cm^{-1}) vibrations and the end group's C-Br stretch (665 cm^{-1}) vibration can be seen.

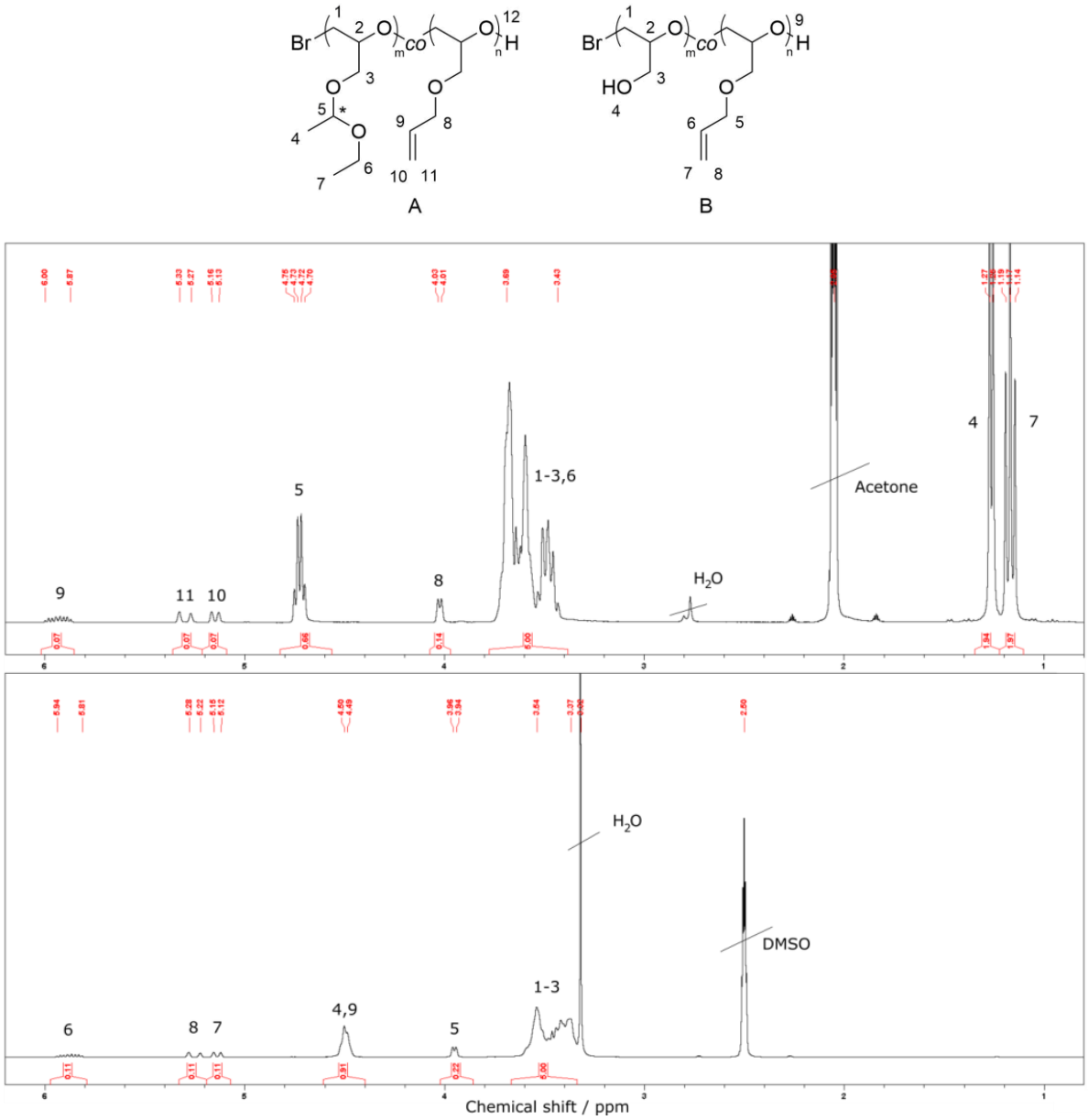

Figure 4.3.1-3: ^{1}H NMR spectra of P(EEGE-*co*-AGE) in acetone-d_6 (A) and P(G-*co*-AGE) in DMSO-d_6 (B).

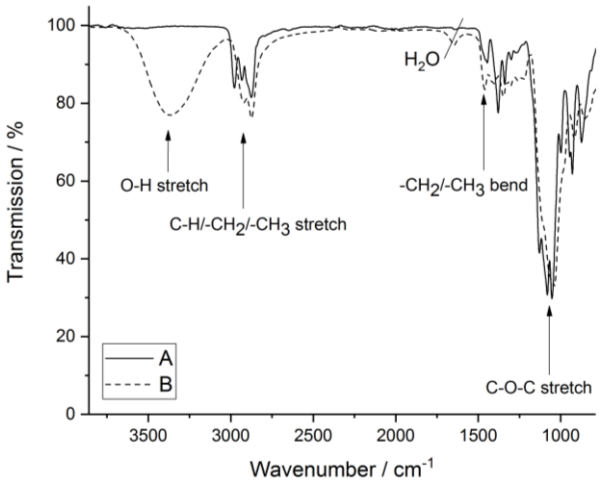

Figure 4.3.1-4: IR spectra of PEEGE (A) and PG (B).

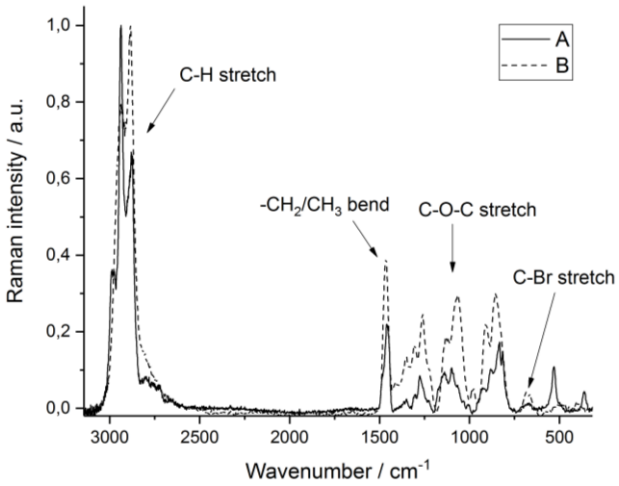

Figure 4.3.1-5: RAMAN spectra of PEEGE (A) and PG (B).

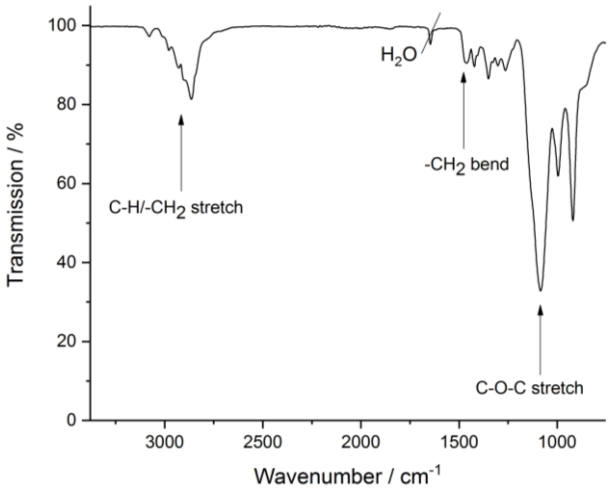

Figure 4.3.1-6: IR spectrum of PAGE.

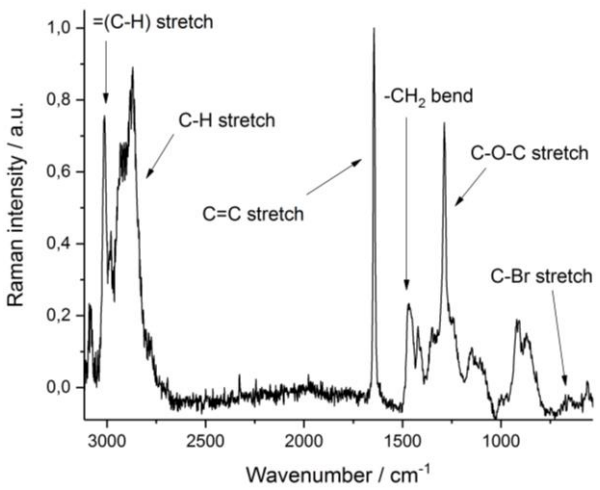

Figure 4.3.1-7: RAMAN spectrum of PAGE.

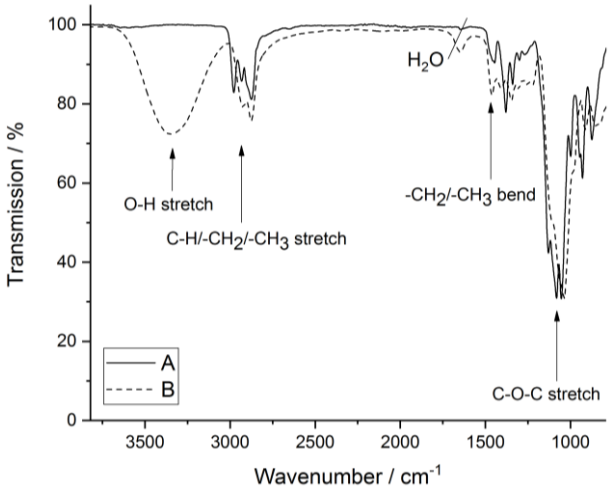

Figure 4.3.1-8: IR spectra of P(EEGE-*co*-AGE) (A) and P(G-*co*-AGE) (B).

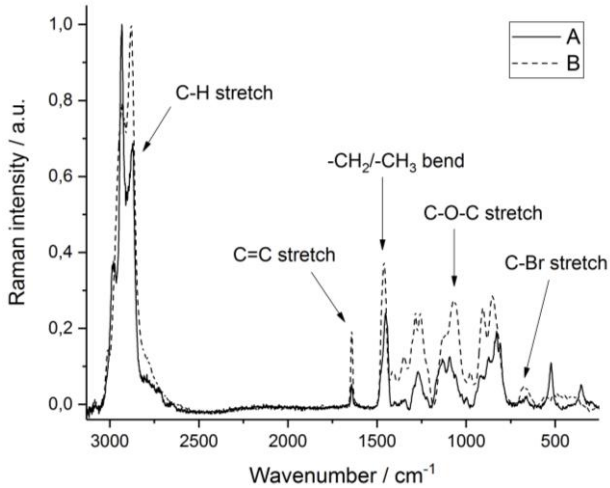

Figure 4.3.1-9: RAMAN spectra of P(EEGE-*co*-AGE) (A) and P(G-*co*-AGE) (B).

GPC measurement of the series of homopolymer PEEGE (Figure 4.3.1-10, Table 4.3.1-2) shows that traces 1-3 are monomodal possessing a low dispersity (1.11-1.30) representing a successful controlled living polymerisation. Trace 4 shows a very broad distribution with a high dispersity (2.44) indicating an unsuccessful monomer-activated anionic ring-opening polymerisation where polymer chains are growing unevenly fast. Trace 5 looks monomodal with a low molecular weight tailing and a high dispersity (2.15). After deprotection, the traces of PG remain slightly unchanged (Figure 4.3.1-11, Table 4.3.1-2) and the dispersities decreased (1.13-1.85). The reason why the polymerisations 4 and 5 were unsuccessful is the chosen initiating temperature at -20 °C which was not low enough as in literature lower temperatures are used for synthesising shorter polymer chain lengths. [47] Initiating at -30 °C would ensure that the polymerisation will be completed below 0 °C as above the complexation of the aluminium catalyst with the growing polymer chain end is not ensured anymore. This scenario could have happened by initiation at -20 °C. The dispersity and temperature effect applies also for the polymerisations 4 and 5 for PAGE and P(EEGE-*co*-AGE).

The homopolymer PAGE (Figure 4.3.1-12, Table 4.3.1-2) shows in total higher dispersities (1.30-3.41) compared to PEEGE and PG (Figure 4.3.1-15). The traces 1, 2 and 5 look monomodal with a low molecular weight tailing for trace 1 and with high molecular weight aggregations for trace 1, 2 and 5 where hydrophobic allyl groups may stack together and cause a higher hydrodynamic volume. Trace 3 and 4 look monomodal whereas trace 4 has a dispersity of 1.81 and trace 4 of PEEGE has 2.44 indicating that in this case for PAGE the catalyst:initiator-ratio is more appropriate for a controlled living polymerisation. The equivalents for the reactions were chosen the same intentionally in order to find out if there are differences in the homo and copolymerisation behaviour. More suitable catalyst:initiator-ratio and monomer concentrations for the homopolymerisation of AGE were found by Anne-Laure Brocas *et al*. [43] It is reasonable that the equivalents and concentrations for PAGE differ from PEEGE because the allyl group can interact additionally with aluminium [160] which influences the monomer activation for the polymerisation by a faster splitting of bromide from the aluminium complex.

The traces of the copolymer P(EEGE-*co*-AGE) (Figure 4.3.1-13, Table 4.3.1) are monomodal whereas 1-3 have low dispersities in the range 1.17-1.33. Traces 4 and 5 have a broadening with low molecular weight tailing and a dispersity of 2.08 and 2.26. Therefore 1-3 represent a successful controlled living polymerisation. These results show that the reaction conditions from the homopolymerisation of EEGE can be transferred to the copolymerisation of EEGE

and AGE. For 4 and 5, also lower initiation temperatures could improve the control of the polymerisation. After deprotection (Figure 4.3.1-14, Table 4.3.1-2), high molecular weight aggregates can be seen which may be caused by the intermolecular hydrogen bond formation of OH-groups [161] and lead to increased dispersities (Figure 4.3.1-16).

In a subsequent research, the polymerisation technique for the mentioned homo- and copolymerisations could be improved by control of the polymerisation temperature. In there, low dispersities with Đ < 1.15 (PEEGE), Đ < 1.55 (PAGE) and Đ < 1.35 (P(EEGE-*co*-AGE)) were obtained.

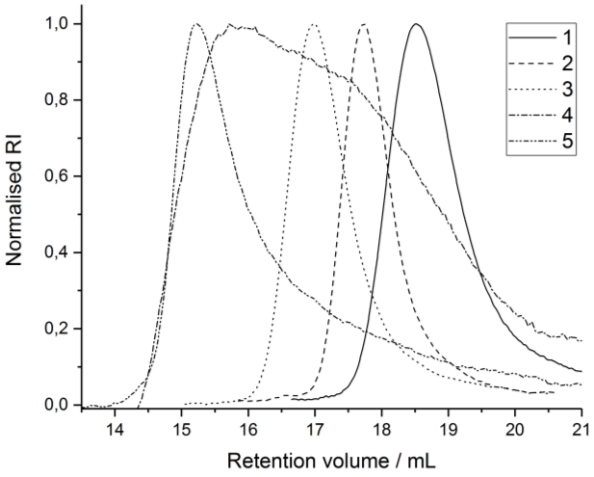

Figure 4.3.1-10: GPC traces of series of PEEGE in DMF (RI).

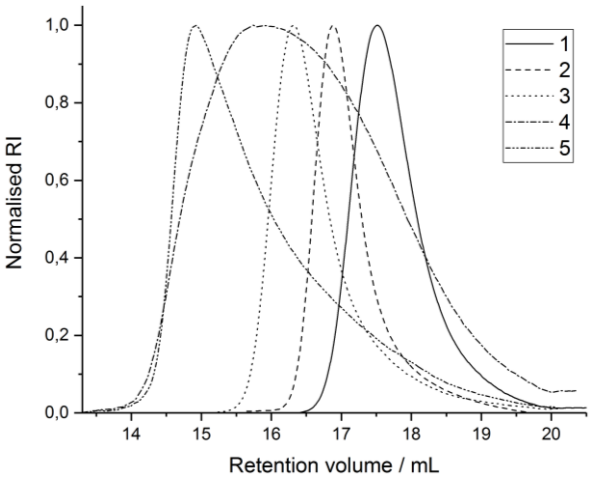

Figure 4.3.1-11: GPC traces of series of PG in DMF (RI).

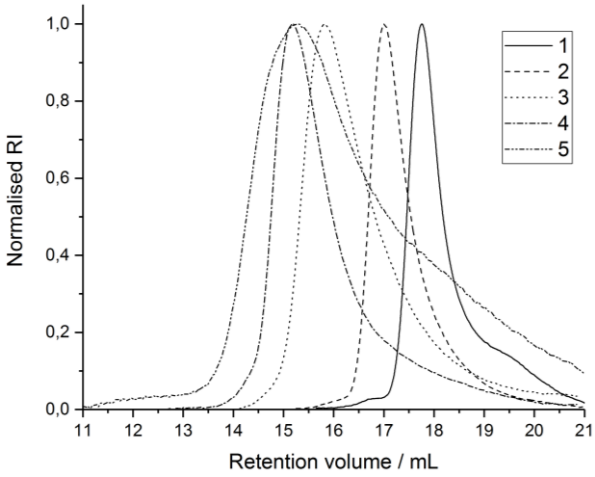

Figure 4.3.1-12: GPC traces of series of PAGE in DMF (RI).

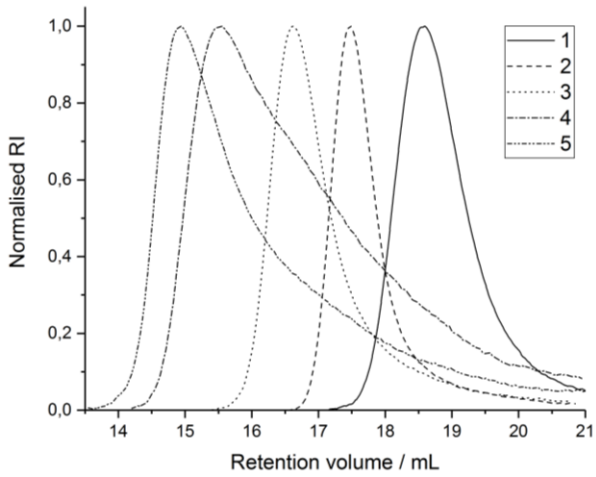

Figure 4.3.1-13: GPC traces of series of P(EEGE-*co*-AGE) in DMF (RI).

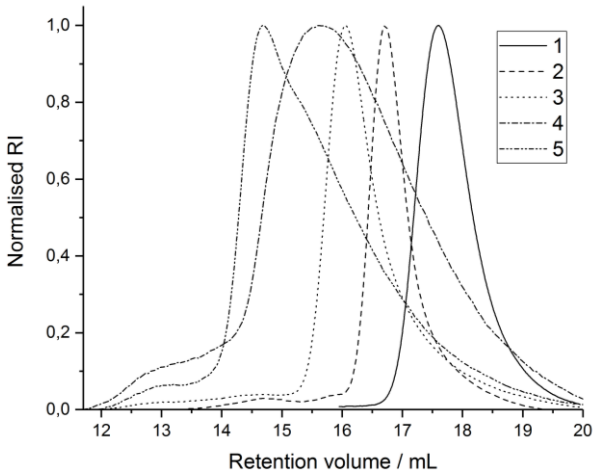

Figure 4.3.1-14: GPC traces of series of P(G-*co*-AGE) in DMF (RI).

Table 4.3.1-2: GPC data of series of PEEGE, PG, PAGE, P(EEGE-*co*-AGE) and P(G-*co*-AGE) in DMF (RI).

PEEGE	**1**	**2**	**3**	**4**	**5**
M_n/Da	4,750	8,841	11,776	11,104	19,008
M_w/Da	5,788	9,853	15,255	27,075	40,774
Đ	1.22	1.11	1.30	2.44	2.15
PG	**1**	**2**	**3**	**4**	**5**
M_n/Da	9,867	14,434	18,959	18,700	28,681
M_w/Da	11,161	16,345	23,179	34,664	49,860
Đ	1.13	1.13	1.22	1.85	1.74
PAGE	**1**	**2**	**3**	**4**	**5**
M_n/Da	6,293	11,076	18,091	27,144	14,257
M_w/Da	8,715	14,432	30,719	49,141	50,055
Đ	1.39	1.30	1.70	1.81	3.41
P(EEGE-*co*-AGE)	**1**	**2**	**3**	**4**	**5**
M_n/Da	4,628	9,669	13,997	15,088	21,829
M_w/Da	5,596	11,270	18,595	31,303	49,432
Đ	1.21	1.17	1.33	2.08	2.26
P(G-*co*-AGE)	**1**	**2**	**3**	**4**	**5**
M_n/Da	9,441	16,823	21,654	22,218	31,926
M_w/Da	10,597	25,636	45,055	72,736	79,256
Đ	1.12	1.52	2.08	3.27	2.48

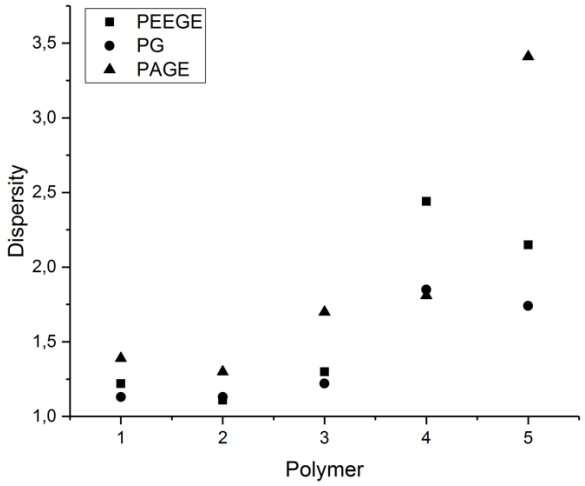

Figure 4.3.1-15: Dispersities of PEEGE, PG and PAGE in DMF (RI).

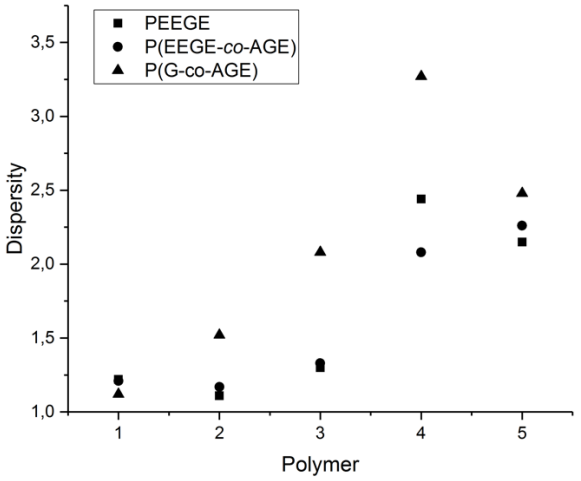

Figure 4.3.1-16: Dispersities of PEEGE, P(EEGE-*co*-AGE) and P(G-*co*-AGE) in DMF (RI).

3.3.2 Electrolyte functionalisation

Synthesis and analysis of these polymers were performed analogously to the low molecular weight ones (Scheme 4.3.2). Here, the parent polymer P(EEGE-*co*-AGE) with EEGE:AGE = 9:1 was used with targeted M_n = 30 kDa. Spectra and elugrams will not be explained, for those, see the previous chapter 4.2.2. Figures and table of analyses will be listed only (Figure 4.3.2-1 – Figure 4.3.2-13, Table 4.3.2).

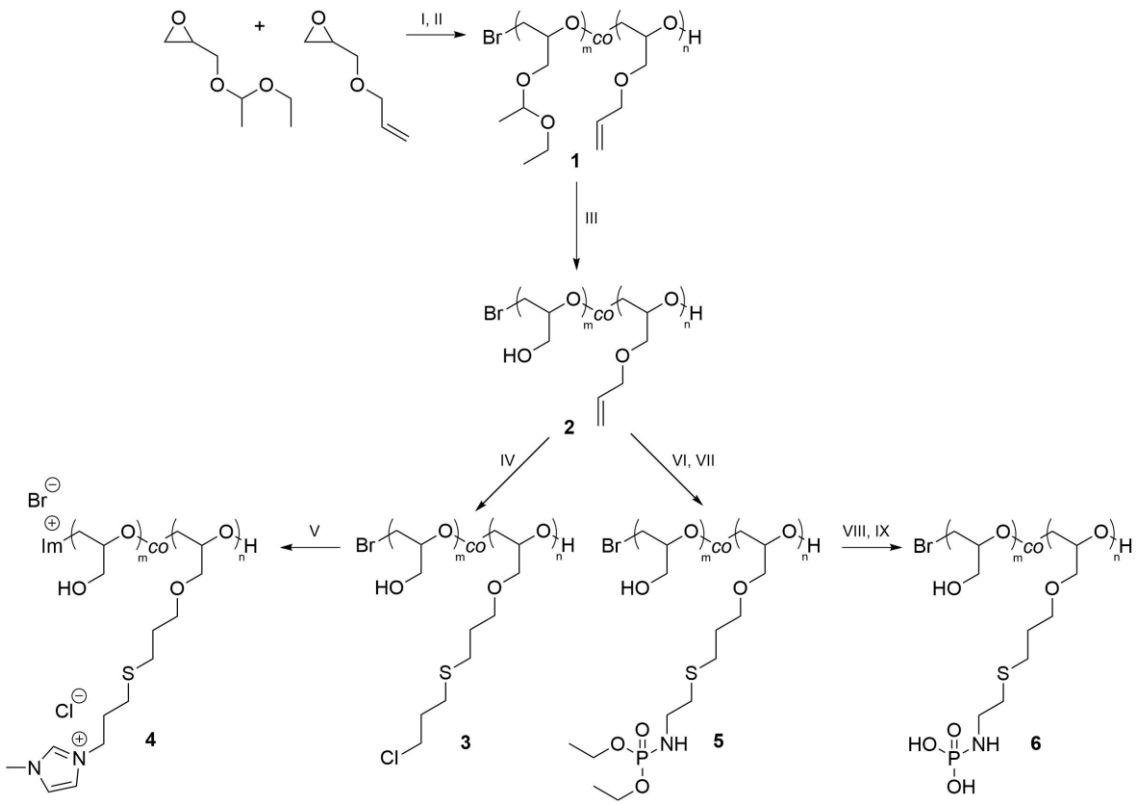

Scheme 4.3.2: Synthesis and modification of polyglycidols. I: $NOct_4Br$, Al^iBu_3, toluene, -20 °C → RT, 24 h. II: EtOH. III: HCl, EtOH, RT, 4 h. IV: 3-chloro-1-propanethiol, DMPA, MeOH, 365 nm, RT, 30 min. V: 1-methylimidazole, DMF, 85 °C, 4 d. VI: Protected phosphonamide-linker, TCEP·HCl, MeOH/H_2O, RT, 30 min. VII: I 2959, MeOH/H_2O, 365 nm, RT, 1 h. VIII: TMSBr, DMF, 0 °C → RT, 24 h. IX: MeOH, RT, 24 h.

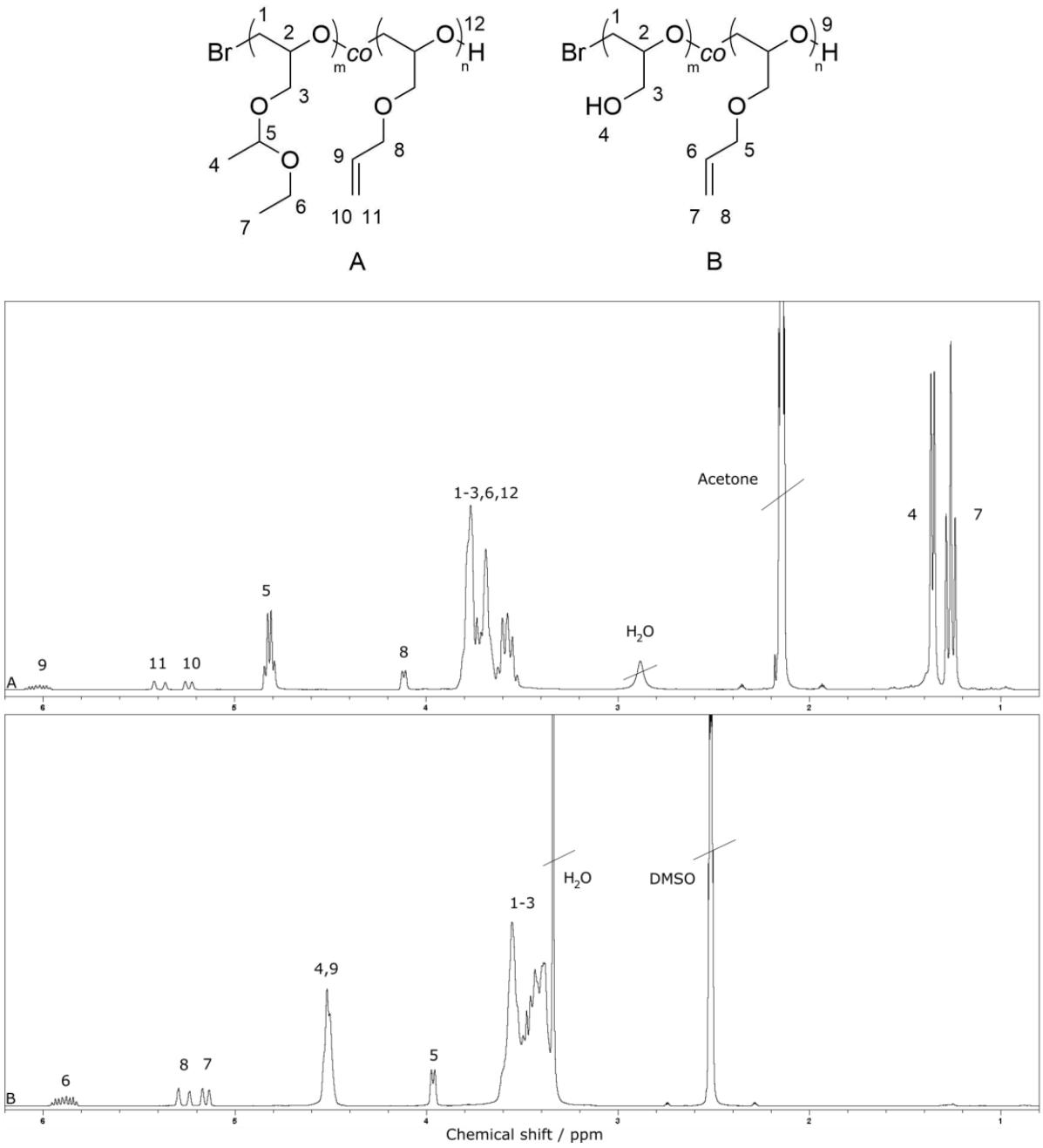

Figure 4.3.2-1: ^{1}H NMR spectra of P(EEGE-*co*-AGE) (A) in acetone-d_6 and P(G-*co*-AGE) (B) in DMSO-d_6.

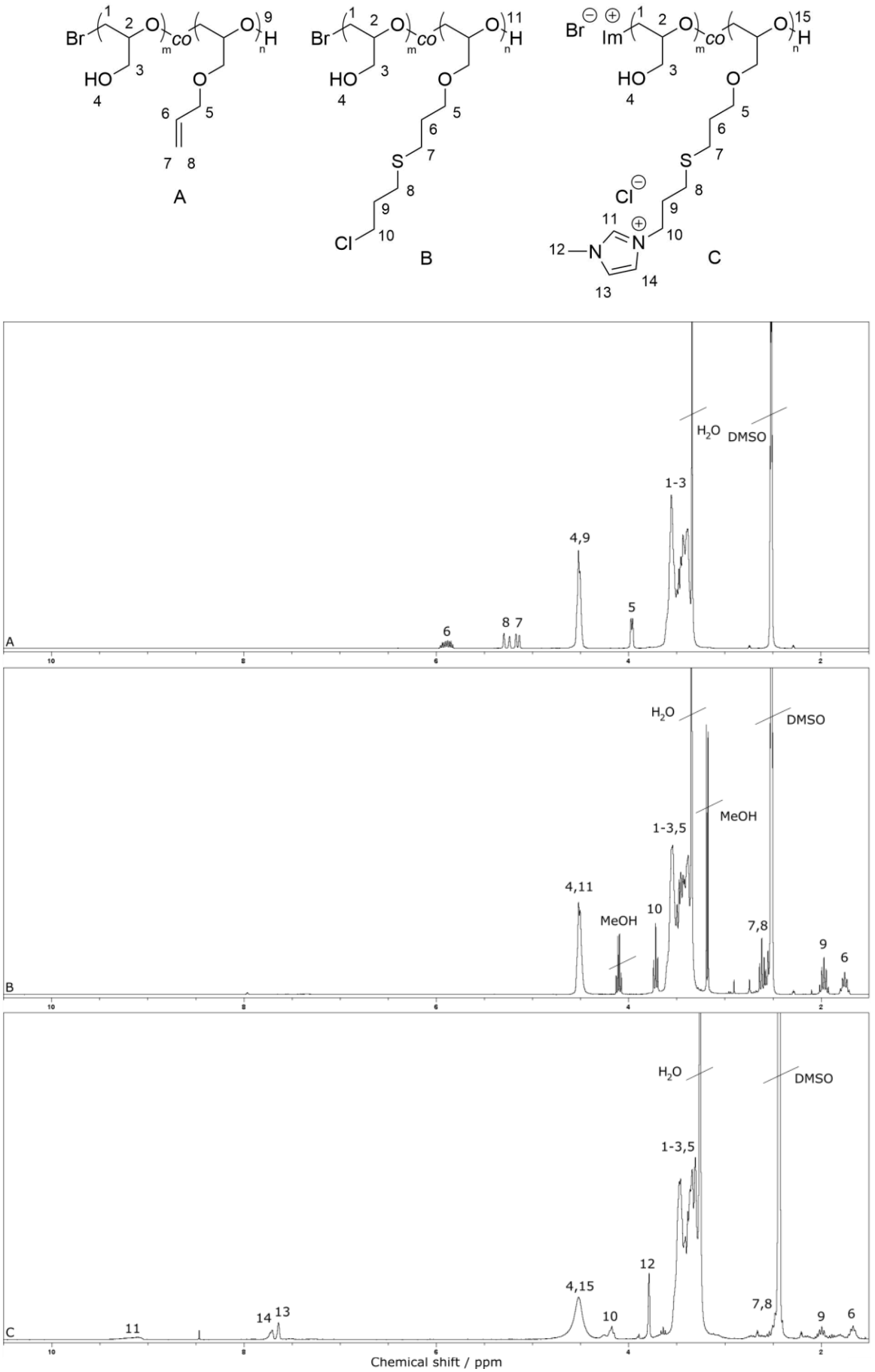

Figure 4.3.2-2: ^{1}H NMR spectra of P(G-*co*-AGE) (A), P(G-*co*-Cl) (B) and P(G-*co*-Im) (C, DS = 85 %) in DMSO-d_6.

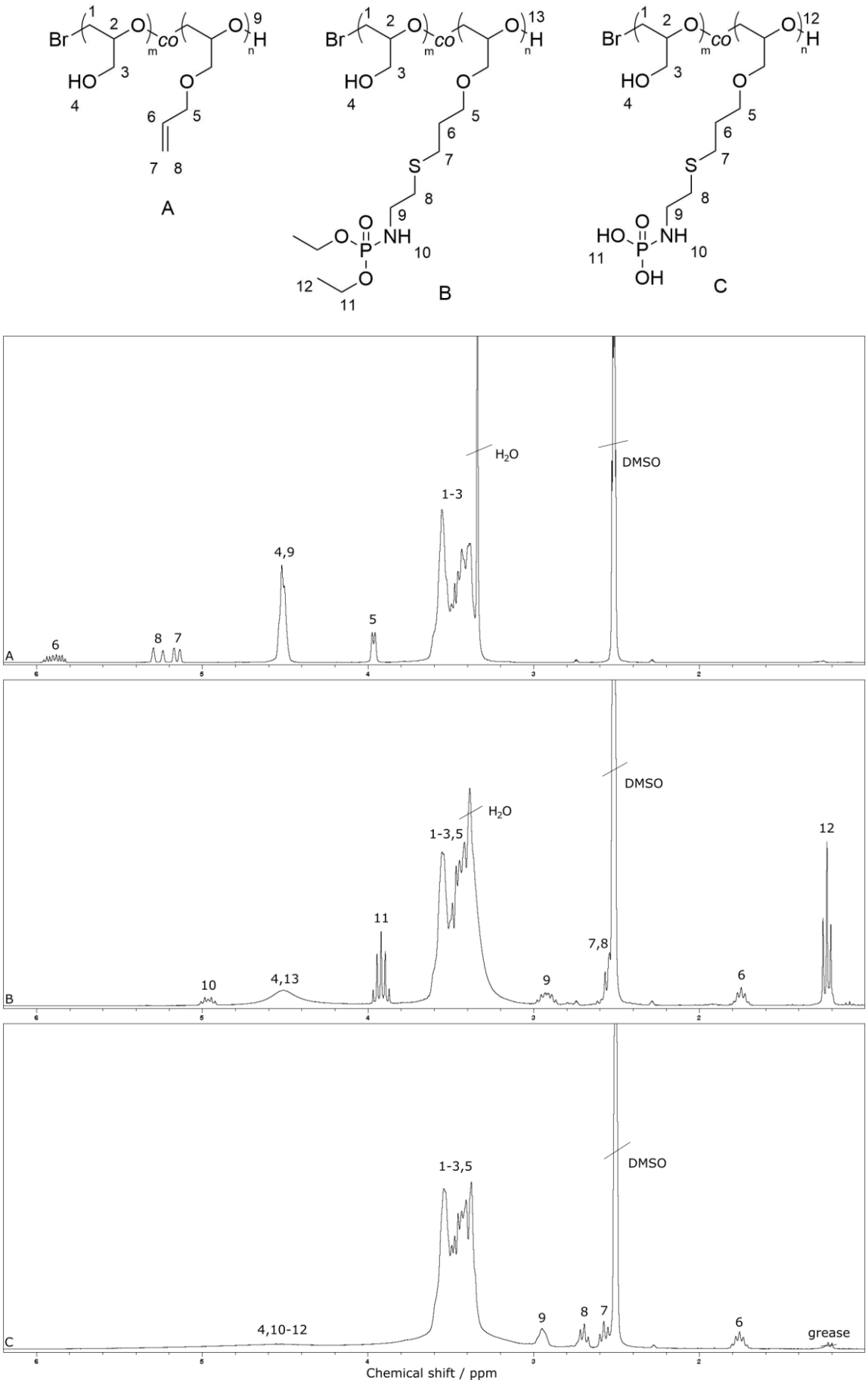

Figure 4.3.2-3: ^{1}H NMR spectra of P(G-*co*-AGE) (A), P(G-*co*-POEt) (B) and P(G-*co*-POH) (C) in DMSO-d_6.

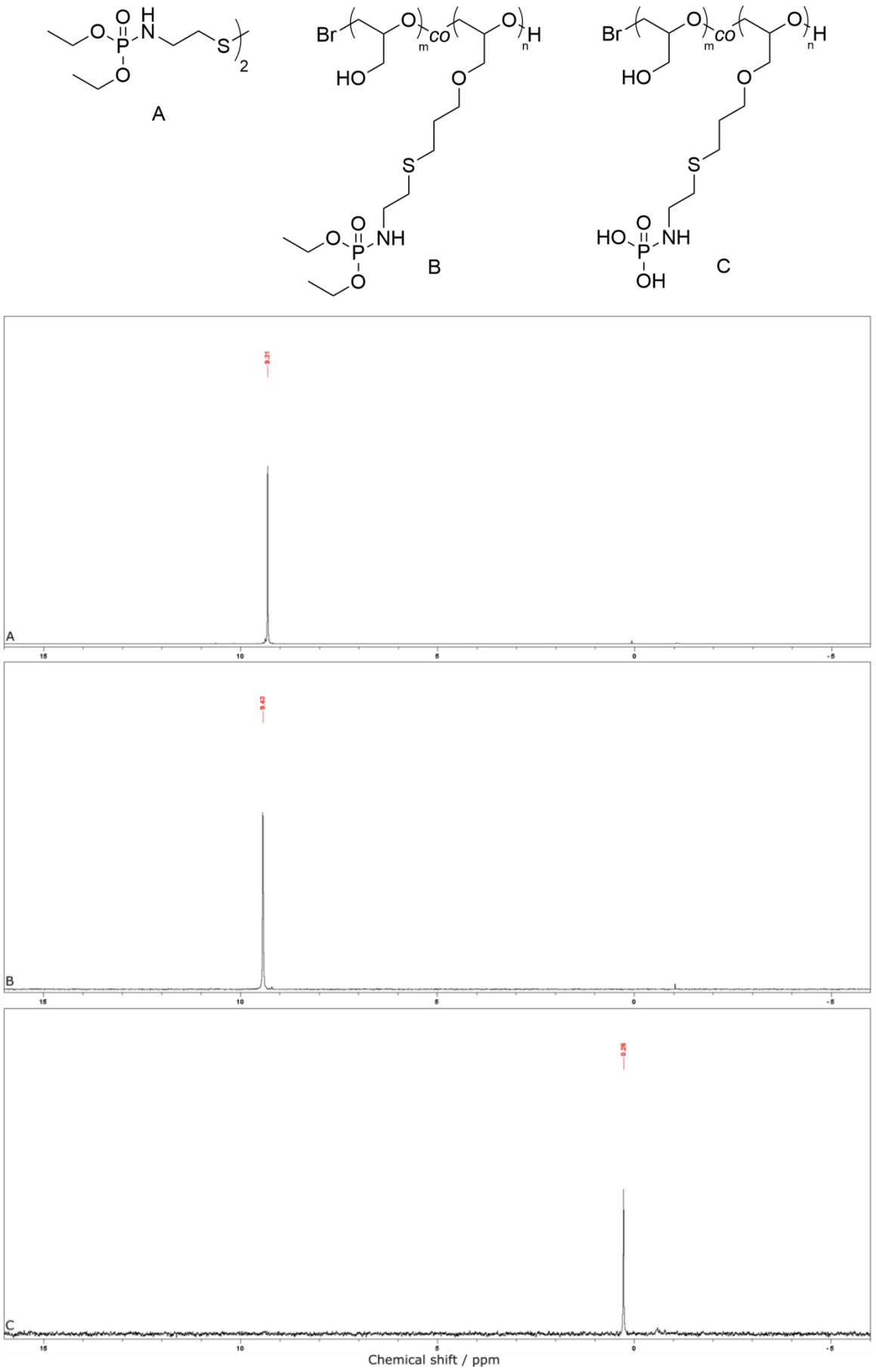

Figure 4.3.2-4: $^{31}P\{^{1}H\}$ NMR spectra of bis(diethylphosphonamide)disulfide (A), P(G-*co*-POEt) (B) and P(G-*co*-POH) (C) in DMSO-d_6.

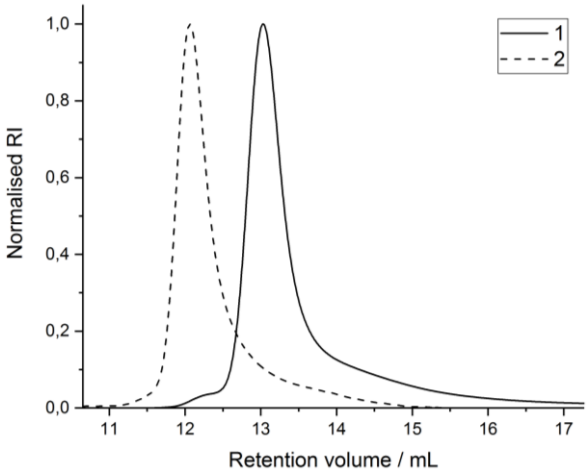

Figure 4.3.2-5: GPC traces of P(EEGE-*co*-AGE) (1) and P(G-*co*-AGE) (2) in DMF (RI).

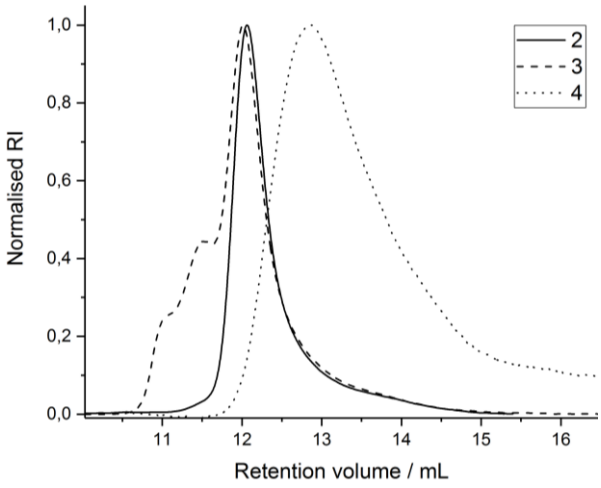

Figure 4.3.2-6: GPC traces of P(G-*co*-AGE) (2), P(G-*co*-Cl) (3) and P(G-*co*-Im) (4) in DMF (RI).

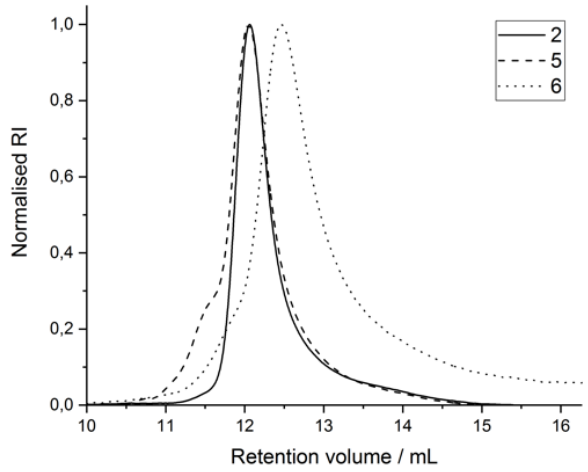

Figure 4.3.2-7: GPC traces of P(G-*co*-AGE) (2), P(G-*co*-POEt) (5) and P(G-*co*-POH) (6) in DMF (RI).

Table 4.3.2: GPC data of P(EEGE-*co*-AGE) (1), P(G-*co*-AGE) (2), P(G-*co*-Cl) (3), P(G-*co*-Im) (4), P(G-*co*-POEt) (5) and P(G-*co*-POH) (6) in DMF (RI).

Run	M_n/kDa	M_w/kDa	Đ
1	8.3	10.1	1.22
2	15.6	19.2	1.24
3	19.8	29.7	1.50
4	7.0	9.4	1.35
5	17.8	25.4	1.42
6	9.4	14.4	1.53

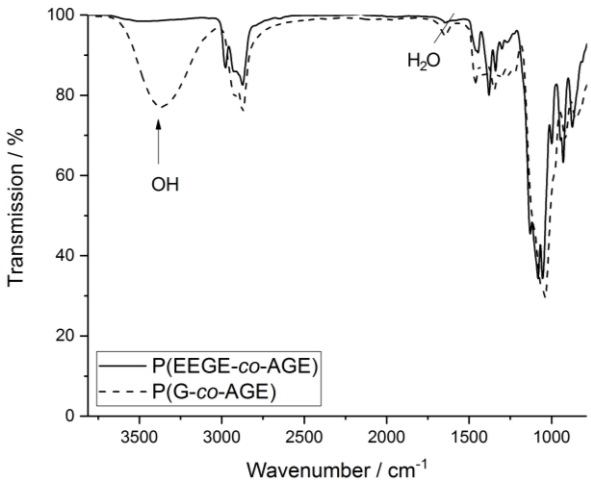

Figure 4.3.2-8: IR-spectra of P(EEGE-*co*-AGE) and P(G-*co*-AGE).

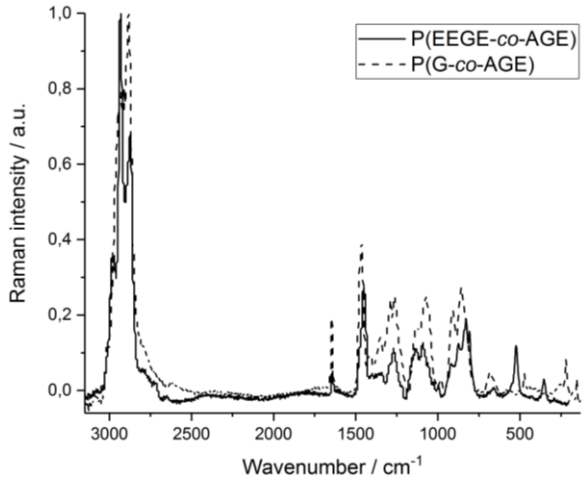

Figure 4.3.2-9: RAMAN-spectra of P(EEGE-*co*-AGE) and P(G-*co*-AGE).

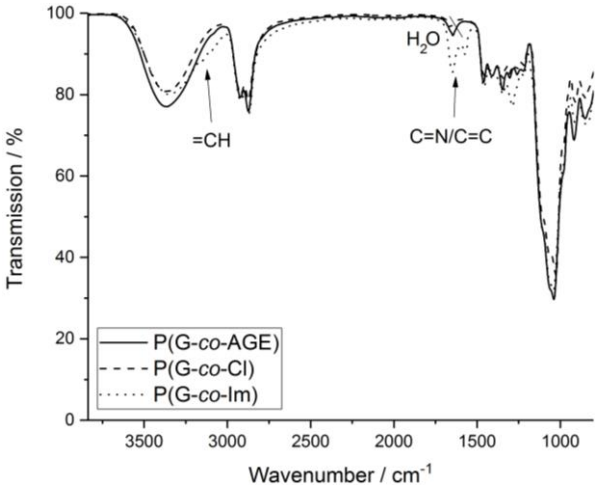

Figure 4.3.2-10: IR-spectra of P(G-*co*-AGE), P(G-*co*-Cl) and P(G-*co*-Im).

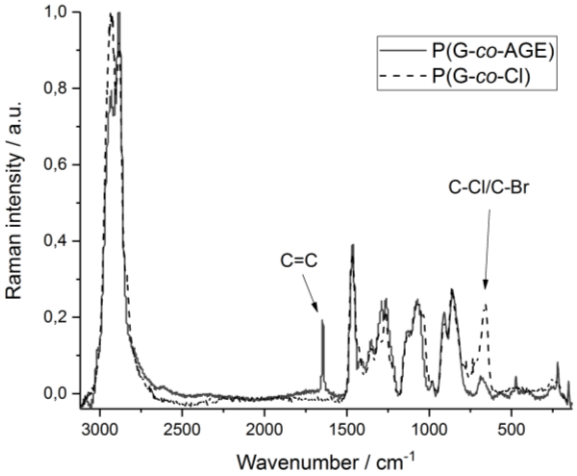

Figure 4.3.2-11: RAMAN-spectra of P(G-*co*-AGE) and P(G-*co*-Cl).

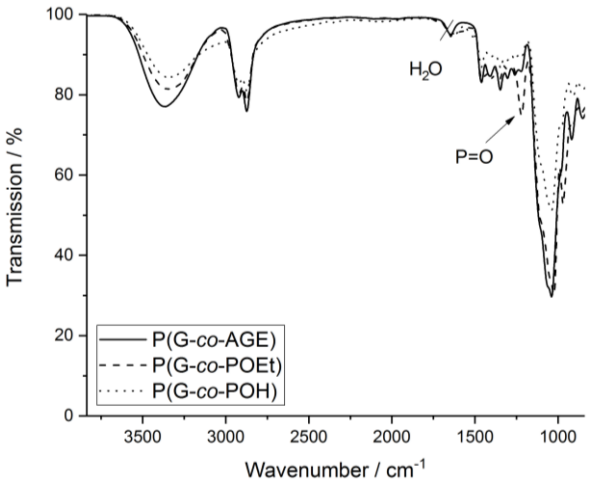

Figure 4.3.2-12: IR-spectra of P(G-*co*-AGE), P(G-*co*-POEt) and P(G-*co*-POH).

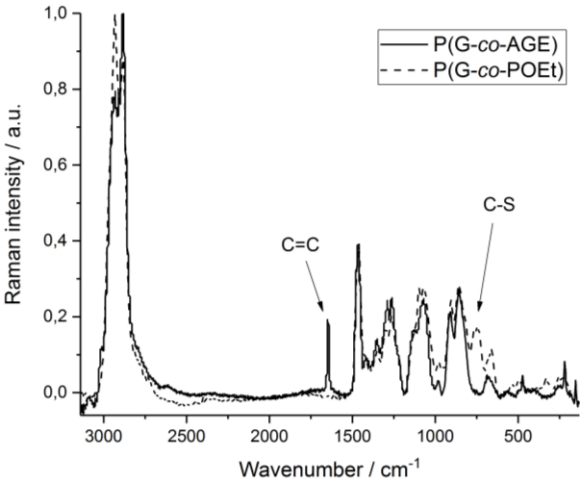

Figure 4.3.2-13: RAMAN-spectra of P(G-*co*-AGE) and P(G-*co*-POEt).

3.3.3 Gel tests

Afterwards, the synthesised polymers were used for three different systems:

1.) P(G-*co*-Im) with P(G-*co*-POH)

Polymers carrying phosphonamide groups were dissolved and polymers carrying imidazolium groups were dissolved. Both solutions were stirred at RT for 18 h, combined to give equimolar ratio of functional groups with a total amount of 10 wt-% polymer solution and stirred again at RT for 18 h. Solvent was varied: Water and buffer solutions with pH = 4, 7, 7.4 and 10.

2.) P(G-*co*-POH) with $CaCl_2$

P(G-co-POH) was dissolved in water and stirred at RT for 18 h. $CaCl_2$ solution was added and the solution was stirred again at RT for 18 h.

Table 4.3.3: Content of polymer and $CaCl_2$.

w/w (polymer) / %	V ($CaCl_2$ solution) / mL	w/v ($CaCl_2$ solution) / %
15	15	2, 4, 6, 8, 10
20	45	2, 10
30	20	2, 10

Figure 4.3.3: P(G-*co*-POH) in water (pH = 7.0, 15 wt-%) before (left) and after addition of $CaCl_2$ solution (4 w/v-%) (right).

3.) High molecular weight P(G-*co*-POH) with low molecular weight P(G-*co*-Im)

Polymers carrying phosphonamide groups (RU (G:POH) = 189:21) were dissolved and polymers carrying imidazolium groups (RU (G:Im) = 48:11.6) were dissolved. Both solutions were stirred at RT for 18 h, combined to give equimolar ratio of functional groups with a total amount of 10, 15, 20 and 30 wt-% of polymer in solution and stirred again at RT for 18 h.

The gel tests have shown, that in 1) with P(G-*co*-Im)/P(G-*co*-POH) the solution remained and did not form a hydrogel. Although the polymer chains were extended, the desired results could not be reached. But also in this case optimisations like longer polymer chains and higher degree of functionalisation could be performed. In the tests 2) with P(G-*co*-POH)/$CaCl_2$, also no hydrogels could be obtained by variation of the polymer content (Table 4.3.3), but an agglomerate formation could be observed (Figure 4.3.3). This could indicate that the phosphonamide groups interact with Ca^{2+} and lead to a precipitation by being shielded from the water molecules. Analytically, this could be investigated *via* $^{31}P\{^{1}H\}$ NMR in order to proof this interaction. These experiments could still be improved either by increasing the polymer chain length and increasing of the degree of phosphonamide groups for a higher intermolecular interaction of P(G-*co*-POH) with Ca^{2+}. The idea of the experiment 3) was that in case of an intramolecular interaction in 2), the cation may be replaced by a positively charged imidazolium group bound on a low molecular weight polyglycidol and could therefore lead to an intermolecular interaction. But also in this case the solutions remained and no hydrogel were formed. Here also the polymer chains may be too short and this set up could be improved by using polymers with higher molecular weights and higher degree of functionalisation.

4 Summary/Zusammenfassung

4.1 Summary

The **objective of this thesis** was the synthesis and characterisation of two linear multifunctional PEG-alternatives for bioconjugation and hydrogel formation: i) Hydrophilic acrylate based copolymers containing peptide binding units and ii) hydrophilic polyether based copolymers containing different functional groups for a physical crosslinking.

In **section 3.1** the successful synthesis of water soluble and linear acrylate based polymers containing oligo(ethylene glycol) methyl ether acrylate with either linear thioester functional 2-hydroxyethyl acrylate, thiolactone acrylamide, or vinyl azlactone *via* the living radical polymerisation technique Reversible Addition Fragmentation Chain Transfer (RAFT) and *via* free-radical polymerisation is described. The obtained polymers were characterized *via* GPC, ^{1}H NMR, IR and RAMAN spectroscopy.

The RAFT end group was found to be difficult to remove from these short polymer chains and accordingly underwent the undesired side reaction aminolysis with the peptide during the conjugation studies. Besides that, polymers without RAFT end groups did not show any binding of the peptide at the thioester groups, which can be improved in future by using higher reactant concentrations and higher amount of binding units at the polymer. Polymers containing the highly reactive azlactone group showed a peptide binding of 19 %, but unfortunately this function also underwent spontaneous hydrolysis before the peptide could even be bound. In all cases, oligo(ethylene glycol) methyl ether acrylate was used with a relatively high molecular weight (M_n = 480 Da) was used, which eventually was efficiently shielding the introduced binding units from the added peptide. In future, a shorter monomer with M_n = 300 Da or less or hydrophilic *N*,*N*'-dialkyl acrylamide based polymers with less steric hindrance could be used to improve this bioconjugation system. Additionally, the amount of monomers containing peptide binding units in the polymer can be increased and have an additional spacer to achieve higher loading efficiency.

The water soluble, linear and short polyether based polymers, so called polyglycidols, were successfully synthesized and modified as described in **section 3.2**. The obtained polymers were characterized using GPC, ^{1}H NMR, ^{31}P{^{1}H} NMR, IR, and RAMAN spectroscopy. The allyl groups which were present up to 20 % were used for radical induced thiol-ene chemistry for the introduction of functional groups intended for the formation of the physically crosslinking hydrogels. For the positively charged polymers, first a chloride group had to be

introduced for the subsequent nucleophilic substitution with the imidazolium compound. There, degrees of modifications were found in the range 40-97 % due to the repulsion forces of the charges, decreased concentration of active chloride groups, and limiting solution concentrations of the polymer for this reaction. For the negatively charged polymers, first a protected phosphonamide moiety was introduced with a deprotection step afterwards showing 100 % conversion for all reactions. Preliminary hydrogel tests did not show a formation of a three-dimensional network of the polymer chains which was attributed to the short backbone length of the used polymers, but the gained knowledge about the synthetic routes for the modification of the polymer was successfully transferred to longer linear polyglycidols. The same applies to the introduction of electron rich and electron poor compounds showing π–π stacking interactions by UV-vis spectroscopy.

Finally, long linear polyglycidyl ethers were synthesised successfully up to molecular weights of M_n ~ 30 kDa in **section 3.3**, which was also proven by GPC, ^{1}H NMR, IR and RAMAN spectroscopy. This applies to the homopolymerisation of ethoxyethyl glycidyl ether, allyl glycidyl ether and their copolymerisation with an amount of the allyl compound ~ 10 %. Attempts for higher molecular weights up to 100 kDa showed an uncontrolled polymerisation behaviour and eventually can be improved in future by choosing a lower initiation temperature. Also, the allyl side groups were modified *via* radical induced thiol-ene chemistry to obtain positively charged functionalities *via* imidazolium moieties (85 %) and negatively charged functionalities *via* phosphonamide moieties (100 %) with quantitative degree of modifications. Hydrogel tests have still shown a remaining solution by using long linear polyglycidols carrying negative charges with long/short linear polyglycidols carrying positive charges. The addition of calcium chloride led to a precipitate of the polymer instead of a three-dimensional network formation representing a too high concentration of ions and therefore shielding water molecules with prevention from dissolving the polymer. These systems can be improved by tuning the polymers structure like longer polymer chains, longer spacer between polymer backbone and charge, and higher amount of functional groups.

The **objective of the thesis** was partly reached containing detailed investigated synthetic routes for the design and characterisation of functional polymers which could be used in future with improvements for bioconjugation and hydrogel formation tests.

4.2 Zusammenfassung

Das **Ziel dieser Arbeit** war es zwei lineare multifunktionale PEG-Alternativen für die Bioconjugation und Hydrogelbildung herzustellen und zu charakterisieren: i) Wasserlösliche Acrylat-basierte Copolymere mit Peptidbindungseinheiten und ii) wasserlösliche Polyether-basierte Copolymere mit verschiedenen funktionalen Gruppen für eine physikalische Vernetzung.

In **Abschnitt 3.1** wurde die erfolgreiche Synthese von wasserlöslichen und linearen Acrylat-basierten Polymeren, die Oligo(ethylen glycol) methyl ether acrylat mit jeweils 2-Hydroxyethyl acrylate modifiziert mit linearem Thioester, Thiolactonacrylamid und Vinylazlacton enthielten, mittels der lebenden Polymerisationstechnik Reversible Additions-Fragmentierungs Kettenübertragung (RAFT) und mittels freier radikalischer Polymerisation durch GPC, ^{1}H NMR, IR und RAMAN Spektroskopie bewiesen. Es erwies sich als schwer die RAFT-Endgruppe von den kurzen Polymerketten zu entfernen und führte zur Nebenreaktion Aminolyse mit dem Peptid während des Konjugationsprozesses. Außerdem zeigten Polymere ohne RAFT-Endgruppen keine Peptidbindung an den Thioestergruppen, was durch höhere Konzentration der Reaktanten und größeren Anteil an Peptidbindungseinheiten am Polymer in Zukunft verbessert werden könnte. Polymere mit Azlaktongruppen zeigten eine Bindung von 19 %, wobei dies eine sehr reaktive Gruppe ist und vor der Peptidbindung noch hydrolysieren kann. In allen Fällen wurde Oligo(ethylen glycol) methyl ether acrylat mit M_n = 480 Da verwendet, welches die Peptidbindungsstellen abschirmen kann. Daher können in Zukunft Monomere mit M_n = 300 Da oder *N*,*N*'-Dialkylacrylamid-basierte Monomere mit weniger sterischer Hinderung für dieses System verwendet werden. Zusätzlich kann der Anteil an Monomeren mit Peptidbindungseinheiten im Polymer und zusätzlicher Seitenkette erhöht werden, um höhere Bindungseffektivitäten zu erreichen.

Die erfolgreiche Synthese und Modifikation von wasserlöslichen, linearen und kurzen Polyether-basierten Polymeren, sogenannten Polyglycidolen, konnte in **Abschnitt 3.2** mittels GPC, ^{1}H NMR, ^{31}P{^{1}H} NMR, IR und RAMAN Spektroskopie bewiesen werden. Die Allylgruppe, die bis zu 20 % vorhanden war, wurde für die radikalisch induzierte Thiol-En Chemie zur Einführung von funktionellen Gruppen verwendet. Für die positiv geladenen Polymere, wurde zuerst eine Chloridgruppe generiert, die anschließend für die nukleophile Substitution mit einer Imidazolkomponente verwendet wurde. Dabei wurden Substitutionsgrade von 40-97 % gefunden, was an den Abstoßungskräften der Ladungen,

verringerter Konzentration der aktiven Chloridgruppen und der begrenzten Löslichkeitskonzentration bei dieser Reaktion liegt. Für die negativ geladenen Polymere wurde zuerst eine geschützte Phosphonamidgruppe eingeführt, die anschließend entschützt wurde und bei allen Reaktionen einen Umsatz von 100 % zeigte. Vorläufige Hydrogeltests zeigten keine Bildung eines dreidimensionales Netzwerks der Polymerketten aber es wurden Erkenntnisse über die synthetischen Routen für die Modifikation der Polymere für den Transfer auf lange lineare Polyglycidole gewonnen. Das gleiche gilt für die Einführung von elektronreichen und elektronarmen Komponenten, die eine π–π Stapelwechselwirkung mittels UV-vis Spektroskopie zeigte.

Letztlich wurden lange lineare Polyglycidole bis zu Molmassen von M_n ~ 30 kDa erfolgreich in **Abschnitt 3.3** hergestellt und mittels GPC, ^{1}H NMR, IR and RAMAN Spektroskopie bewiesen. Dies gilt für die Homopolymerisation von Ethoxyethyl glycidyl ether, Ally glycidyl ether und deren Copolymerisation mit einem Anteil der Allylkomponente von ~ 10 %. Versuche um höhere Molekulargewichte bis zu 100 kDa zeigten ein unkontrolliertes Polymerisationsverhalten, welches durch eine niedrigere Initiierungstemperatur weiter verbessert werden kann. Ebenso wurden die Allylseitengruppen mittels radikalisch induzierter Thiol-En Chemie modifiziert, um positivgeladene Funktionalitäten durch Imidazolgruppen (85 %) und negativgeladene Funktionalitäten durch Phosphonamidgruppen (100 %) in quantitativen Umsätzen einzuführen. Hydrogeltests von langen linearen Polyglycidolen, die negativ geladene Gruppen haben, mit langen/kurzen linearen Polyglycidolen, die positiv geladene Gruppen haben, haben eine verbleibende Lösung gezeigt. Die Zugabe von Calciumchlorid führte zum Ausfall des Polymers anstatt zu einem dreidimensionalen Netzwerk repräsentiert durch eine zu hohe Ionenkonzentration. Dies führte zu einer Abschirmung der Wassermoleküle vom Polymer und verhinderte, dies aufzulösen. Das System kann verbessert werden, indem die Polymerstruktur variiert wird, z.B. durch längere Polymerketten, größere Abstände zwischen Polymerhauptkette und Ladung und einen größeren Anteil an funktionellen Gruppen.

Das **Ziel der Arbeit** wurde teilweise erreicht, welches detailliert untersuchte Syntheserouten für das Design und die Charakterisierung von funktionellen Polymeren beinhaltet, welche in Zukunft mit Verbesserungen für Bioconjuations- und Hydrogelformulierungstests verwendet werden können.

5 Experimental section

5.1 Materials and methods

5.1.1 Materials

Oligo(ethylene glycol) methyl ether acrylate (OEGMEA, M_n = 480 Da, Sigma Aldrich, ≥ 99.4 %), 2-hydroxyethyl acrylate (HEA, Sigma Aldrich, 96 %), ethyl 3-mercaptopropionate (EMP, Sigma Aldrich, 99 %), benzylamine (Sigma Aldrich, 99 %), (±)-glycidol (G, Sigma Aldrich, ≥ 96 %), ethyl vinyl ether (Sigma Aldrich, ≥ 99 %), potassium *tert*-butoxide in tetrahydrofuran solution (KO^{t}Bu, 1.0 M, Sigma Aldrich), thioacetic acid (Sigma Aldrich, 96 %), 1-methylimidazole (Alfa Aesar, 99 %), 3-chloro-1-propanethiol (Sigma Aldrich, 98 %), diethyl chlorophosphate (Alfa Aesar, > 97 %), triethylamine (TEA, Sigma Aldrich, ≥ 99.5 %), bromotrimethylsilane (TMSBr, Sigma Aldrich, 97 %), oxalyl chloride in methylene chloride solution (2.0 M, Sigma Aldrich), thioglycolic acid (Sigma Aldrich, ≥ 99 %), ortho-phosphoric acid (H_3PO_4, 85 %, Merck), *n*-propylamine (Sigma Aldrich, 98 %), acetic acid (HOAc, Sigma Aldrich, ≥ 99%), allylamine (Sigma Aldrich, 98 %), triisobutylaluminium in toluene (Al^{i}Bu$_3$, 25 wt-%, Sigma Aldrich), 2-cyano-2-propyl benzodithioate (CPDB, Sigma Aldrich, > 97 %), 2,2'-azobis(2-methylpropionitrile) (AIBN, Sigma Aldrich, 98 %), succinic acid (Sigma Aldrich, ≥ 99 %), 4-(dimethylamino)pyridine (DMAP, Sigma Aldrich, ≥ 99 %), *N*,*N*'-dicyclohexylcarbodiimide (DCC, Sigma Aldrich, ≥ 99 %), peptide sequence CGGGF (GeneCust, L-form of C/F, 95 %), *p*-toluenesulfonic acid monohydrage (p-TsOH·H_2O, Sigma Aldrich, ≥ 98.5 %), 2,2-dimethoxy-2-phenylacetophenone (DMPA, Sigma Aldrich, 99 %), tris(2-carboxyethyl)phosphine hydrochloride (TCEP·HCl, ABCR, 99 %), cystamine dihydrochloride (CA·2 HCl, Sigma Aldrich, 96 %), silica gel (SiO_2, Sigma Aldrich, average pore size 60 Å, 230-400 mesh particle size), 2-hydroxy-4'-(2-hydroxyethoxy)-2-methylpropiophenone (Irgacure 2959, I 2959, BASF), L-ascorbic acid (Sigma Aldrich, 99 %), 1-pyrenebutyric acid (Sigma Aldrich, 97 %), *N*-ethyl-*N'*-(3-dimethylaminopropyl)carbodiimide hydrochloride (EDC, Sigma Aldrich, ≥ 98 %), 1,4,5,8-naphthalenetetracarboxylic dianhydride (NTCDA, Alfa Aesar, 97 %), cysteamine hydrochloride (CeA·HCl, Sigma Aldrich, ≥ 98 %), tetraoctylammonium bromide (NOct$_4$Br, Sigma Aldrich, 98.0 %), sodium chloride (NaCl, Sigma Aldrich, ≥ 99.5 %) magnesium sulfate ($MgSO_4$, Sigma Aldrich, ≥ 99.5 %), sodium hydroxide (NaOH, Sigma Aldrich, ≥ 97.0 %), potassium hydroxide (KOH, Sigma Aldrich, ≥ 85 %), calcium chloride ($CaCl_2$, Sigma Aldrich, ≥ 97 %), sodium bicarbonate ($NaHCO_3$, Sigma Aldrich,

≥ 99.7 %), sodium sulfate (Na_2SO_4, Sigma Aldrich, ≥ 99.0 %), lithium bromide (LiBr, Sigma Aldrich, ≥ 99 %), sodium nitrate ($NaNO_3$, Sigma Aldrich, ≥ 99.0 %), sodium azide (NaN_3, Sigma Aldrich, ≥ 99.5 %), *N*,*N'*-dimethylformamide (DMF, Carl Roth, ≥ 99.8 %), tetrahydrofuran (THF, Fisher Scientific, 99.5 %), *n*-hexane (Carl Roth, ≥ 95 %), diethyl ether (Et_2O, Carl Roth, ≥ 95 %), acetonitrile (MeCN, Carl Roth, > 99 %), pyridine (Fisher Scientific, > 99 %), ethyl acetate (EtOAc, Fisher Scientific, > 99 %), concentrated hydrochloric acid (HCl, 32 %, Merck), dichloromethane (DCM, Fisher Scientific, > 99 %), methanol (MeOH, Carl Roth, ≥ 99 %), toluene (Carl Roth, ≥ 99.5 %), ethanol (EtOH, Sigma Aldrich, ≥ 99.8 %), isopropanol (Carl Roth, ≥ 99.9 %), buffer solutions (pH = 4.0 ± 0.1 containing potassium hydrogen phthalate, 10.0 ± 0.1 containing sodium bicarbonate/sodium carbonate, Sigma Aldrich), dimethylsulfoxid (DMSO, Carl Roth, ≥ 99.5 %), anhydrous *N*,*N'*-dimethylformamide (DMF, Sigma Aldrich, 99.8 %), anhydrous dichloromethane (DCM, Sigma Aldrich, ≥ 99.8 %), anhydrous chloroform ($CHCl_3$, Sigma Aldrich, ≥ 99 %), acetone (Merck, ≥ 99.5 %), chloroform-d ($CDCl_3$, Eurisotop, 99.8 %), acetone-d_6 (Deutero, 99.0 %), dimethylsulfoxid-d_6, (DMSO-d_6, Deutero, 99.8 %), acetonitrile-d_3 (Sigma Aldrich, 99.8 %) were used as received. Phosphate buffered saline (pH = 7.4 containing sodium chloride/potassium dihydrogen phosphate/sodium phosphate dibasic dodecahydrate/potassium chloride, Merck, ≥ 99 %) was kindly provided by my colleague Isabell Biermann. Thiolactone acrylamide (L-form) and vinyl azlactone were kindly provided by my colleague Julia Blöhbaum. Allyl glycidyl ether (AGE, Sigma Aldrich, ≥ 99 %) was dried over calcium hydride (CaH_2, ABCR, 92 %) and distilled. Water (H_2O) was purified *via* reverse osmosis (Sartorius Arium, 15.4 MΩ cm, pH = 7.0). Toluene (Carl Roth, ≥ 99.5 %) was distilled before usage (residual H_2O content of 3.0 ppm).

5.1.2 Methods

5.1.2.1 NMR spectroscopy

^1H NMR measurements were performed on a Bruker Fourier 300 at 300 MHz, ^{13}C NMR measurements on a Bruker Fourier 300 at 75 MHz and $^{31}P\{^1H\}$ NMR measurements on a Bruker 400 at 400 MHz. Tetramethylsilane was used for calibration for ^1H NMR and ^{13}C NMR measurements. The residual non-deuterated solvent signal was used as an internal reference for ^1H NMR measurements ($CDCl_3$ (7.26 ppm), acetone-d_6 (2.05 ppm), MeCN-d_3 (1.94 ppm) and DMSO-d_6 (2.50 ppm)) and for ^{13}C NMR measurements ($CDCl_3$ (77.16 ppm) and DMSO-d_6 (39.52 ppm)). Signals are abbreviated as: singlet (s), doublet (d), triplet (t),

quartet (q), quintet (quin), sextet (sext), broad (br) and multiplet (m). Samples were prepared with a concentration of 15 mg/0.6 mL.

5.1.2.2 GPC

GPC measurements were performed in DMF and in H_2O. Measurements in DMF containing 1 g/L LiBr were performed on Omnisec Resolve/Reveal (Malvern Panalytical) with a flow rate of 1 mL/min at 45 °C. Organic guard column (pre-column, Dguard) with D2000/D3000 columns in series for short polymers and D3000/D5000 columns in series for long polymers were used. Narrow linear PEG standards were used for calibration and a refractive index detector was used for analysis. Measurements in H_2O containing 0.1 M $NaNO_3$/0.02 % NaN_3 were performed on Viscotek SECmax (Malvern Instruments) with a flow rate of 0.7 mL/min at 35 °C. Columns A2000/A3000 columns in series for short polymers were used. Narrow linear PEG standards were used for calibration and a refractive index detector was used for analysis. Samples were prepared with a concentration of 5 mg/mL except for long polymers and polymers containing glycidols which were prepared with a concentration of 1 mg/mL. The polymers were dissolved in the GPC solvent for 12 hours and filtered over a PTFE membrane filter (0.45 μm pore size) before measurement.

5.1.2.3 FT-IR spectroscopy

FT-IR spectroscopy measurements were performed on a NICOLET iS spectrometer (Thermo Fisher Scientific) with an ATR unit.

5.1.2.4 RAMAN spectroscopy

RAMAN spectroscopy measurements were performed on a DXR RAMAN Microscope (Thermo Fisher Scientific) by using an excitation laser at 780 nm for the measurements.

5.1.2.5 ASAP-MS

ASAP-MS measurements were performed on an Exactive Plus Orbitrap Mass Spectrometer (Thermo Fisher Scientific).

5.1.2.6 UV-Vis spectroscopy

UV-vis measurements were performed on a Genesys 10S Bio spectrophotometer (Thermo Fisher Scientific). Samples were prepared with a concentration of 0.1 mg/mL.

5.1.2.7 Dialysis tubes

Dialysis procedures were performed against various solvents by using dialysis tubes with a molecular weight cut off of 1 kDa (pre-wetted regenerative cellulose tubing, Spectrum).

5.1.2.8 Lyophilisation

Lyophilisation was performed on an Alpha 1-2 LD (Christ) in order to remove water *via* freeze-drying.

5.1.2.9 UV-light

UV-light induced reactions with DMPA were performed with 3 UV LED cubes (365 nm, 77 mW cm^{-2}, Polymerschmiede) and reactions with I 2959 were performed with a UV handlamp (365 nm, 1 mW cm^{-2}, A. Hartenstein)

5.1.2.10 Karl-Fischer titration

Karl-Fischer titrations were performed on a coulometric Karl-Fischer Autotitrator (Mettler Toledo, C30S) with an InMotion Karl-Fischer Flex oven autosampler.

5.2 Acrylate based copolymers with peptide binding units

5.2.1 RAFT-copolymerisation

5.2.1.1 Poly(oligo(ethylene glycol) methyl ether acrylate-*co*-2-hydroxyethyl acrylate) (P(OEGMEA-*co*-HEA))

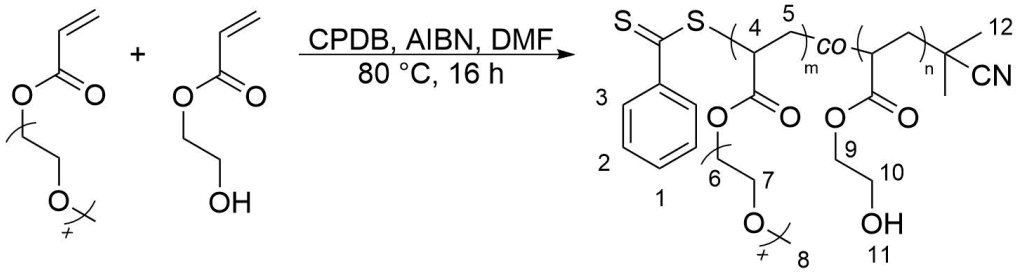

Scheme 5.2.1.1: Synthesis of P(OEGMEA-*co*-HEA).

OEGMEA (1.152 g, 2.40 mmol, 8 eq), HEA (70 mg, 0.60 mmol, 2 eq), CPDB (66.4 mg, 0.30 mmol, 1 eq) and AIBN (24.6 mg, 0.15 mmol, 0.5 eq) were dissolved in DMF (5 mL) and degassed *via* bubbling argon through the solution for 30 min. The reaction mixture was stirred at 80 °C for 16 h and the polymerisation was terminated by placing the vial in an ice-bath. The solvent was removed *via* rotary evaporator and the residue was dissolved in THF (2 mL). The polymer was precipitated in a mixture of *n*-hexane/diethyl ether (40 mL, v/v, 1/1) and dried at 60 °C under high vacuum for 1 day. A pink viscous liquid was obtained (913 mg).

^{1}H NMR (300 MHz, $CDCl_3$) δ/ppm = 7.96 (d, 2 H, H-3, *J* = 9 Hz), 7.55 (t, 1 H, H-1, *J* = 6 Hz), 7.39 (t, 2 H, H-2, *J* = 6 Hz), 4.19 (bt, 2(*m*+*n*)H, H-6 (first repeating unit), H-9), 3.77-3.52 (m, 4*m*xH, H-6, H-7; m, 2*n*H, H-10), 3.37 (s, 3*m*H, H-8), 2.60-1.54 (m, 3(*m*+*n*)H, H-4, H-5; bs, 1*n*H, H-11), 1.35/1.30 (2 s, 6 H, H-12). **GPC (DMF, RI):** M_n = 2,157 Da, M_w = 2,372 Da, Đ = 1.10. **FT-IR ν/cm^{-1} =** 3514 (b, O-H stretch), 2868 (m, -CH_3, -CH_2 & C-H stretch), 1732 (m, C=O stretch), 1451 (m, -CH_3 & -CH_2 bend), 1350 (m, C-O-C stretch), 1283 (m, C-O-C stretch), 1248 (m, C-O-C stretch), 1096 (s, C-O-C stretch), 1042 (m, C-O-C stretch), 947 (m, C-O-C stretch), 850 (m, C-O-C stretch), 767 (w, =C-H bend, C-S stretch), 689 (w, =C-H bend, C-S stretch). **RAMAN ν/cm^{-1} =** 3057 (w, =C-H stretch), 2944 (s, C-H stretch), 2880 (s, C-H stretch), 2227 (w, C≡N stretch), 1736 (m, C=O stretch), 1592 (m, C=C stretch), 1465 (m, -CH_3 and -CH_2 bend), 1289 (m, C-O-C stretch), 1236 (m, C-O-C stretch), 1185 (w, C-O-C & C=S stretch), 1139 (m, C-O-C stretch), 1043 (m, C-O-C stretch), 997 (m, C-O-C stretch), 854 (m, C-O-C stretch), 650 (w, C-S stretch), 459 (w, C-C bend), 312 (w, C-C bend).

5.2.1.2 Poly(oligo(ethylene glycol) methyl ether acrylate-*co*-thiolactone acrylamide) (P(OEGMEA-*co*-TLA))

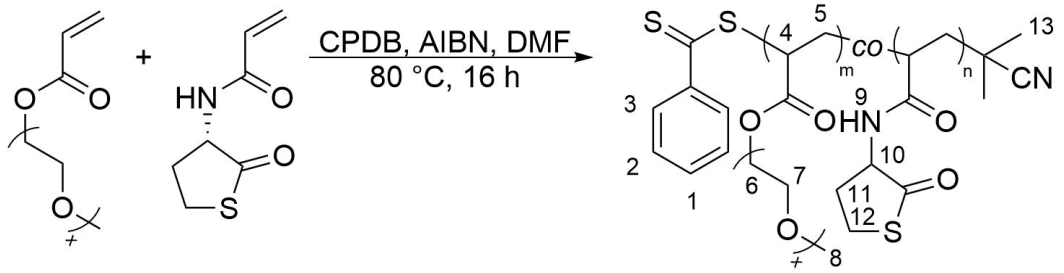

Scheme 5.2.1.2: Synthesis of P(OEGMEA-*co*-TLA).

OEGMEA (1.152 g, 2.40 mmol, 8 eq), TLA (102.7 mg, 0.60 mmol, 2 eq), CPDB (66.4 mg, 0.30 mmol, 1 eq) and AIBN (24.6 mg, 0.15 mmol, 0.5 eq) were dissolved in DMF (5 mL) and degassed *via* bubbling argon through the solution for 30 min. The reaction mixture was stirred at 80 °C for 16 h and the polymerisation was terminated by placing the vial in an ice-bath. The solvent was removed *via* rotary evaporator and the residue was dissolved in THF (2 mL). The polymer was precipitated in a mixture of *n*-hexane/diethyl ether (40 mL, v/v, 1/1) and dried at 60 °C under high vacuum for 1 day. A pink viscous liquid was obtained (758 mg).

^{1}H NMR (300 MHz, $CDCl_3$) δ/ppm = 7.96 (d, 2 H, H-3, *J* = 9 Hz), 7.54 (t, 1 H, H-1, *J* = 6 Hz), 7.39 (t, 2 H, H-2, *J* = 6 Hz), 4.64 (bs, 1nH, H-10), 4.18 (bt, 2*m*H, H-6 (first repeating unit)), 3.65-3.52 (m, 4*mx*H, H-6, H-7; m, 2*n*H, H-12), 3.37 (s, 3*m*H, H-8), 2.60-1.58 (m, 3(*m*+*n*)H, H-4, H-5; m, 2*n*H, H-11) 1.34/1.30 (2 s, 6 H, H-13), H-9 not visible. **GPC (DMF, RI):** M_n = 2,001 Da, M_w = 2,321 Da, Đ = 1.16. **FT-IR ν/cm^{-1} =** 3524 (b, N-H stretch), 2869 (m, -CH_3, -CH_2 & C-H stretch), 1731 (m, C=O stretch), 1676 (m, C=O stretch), 1535 (w, N-H bend), 1451 (m, -CH_3 & -CH_2 bend), 1350 (m, C-O-C & C-N stretch), 1284 (m, C-O-C & C-N stretch), 1248 (m, C-O-C & C-N stretch), 1095 (s, C-O-C & C-N stretch), 1043 (m, C-O-C & C-N stretch), 946 (m, C-O-C stretch), 849 (m, C-O-C stretch), 767 (w, =C-H bend, C-S stretch), 688 (w, =C-H bend, C-S stretch). **RAMAN ν/cm^{-1} =** 3052 (w, =C-H stretch), 2947 (s, C-H stretch), 2880 (s, C-H stretch), 2235 (w, C≡N stretch), 1730 (w, C=O stretch), 1591 (m, C=C stretch), 1475 (m, -CH_3 & -CH_2 bend), 1451 (m, -CH_3 & -CH_2 bend), 1285 (m, C-O-C stretch), 1234 (m, C-O-C stretch), 1181 (w, C-O-C & C=S stretch), 1135 (m, C-O-C stretch), 1046 (m, C-O-C stretch), 999 (m, C-O-C stretch), 847 (m, C-O-C stretch), 686 (w, C-S stretch), 648 (w, C-S stretch), 630 (w, C-S stretch), 462 (w, C-C bend), 269 (w, C-C bend).

5.2.1.3 Poly(oligo(ethylene glycol) methyl ether acrylate-*co*-vinyl azlactone) (P(OEGMEA-*co*-VAL))

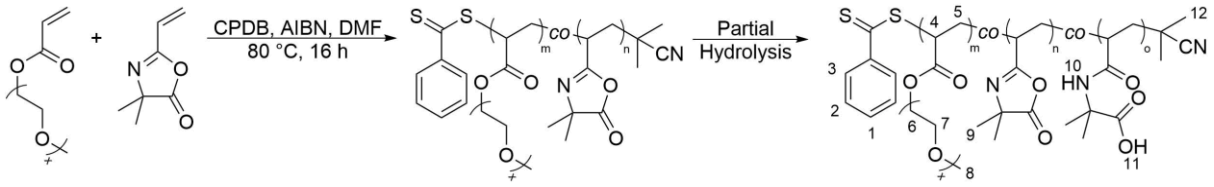

Scheme 5.2.1.3: Synthesis of P(OEGMEA-*co*-VAL).

OEGMEA (1.152 g, 2.40 mmol, 8 eq), VAL (84 mg, 0.60 mmol, 2 eq), CPDB (66.4 mg, 0.30 mmol, 1 eq) and AIBN (24.6 mg, 0.15 mmol, 0.5 eq) were dissolved in DMF (5 mL) and degassed *via* bubbling argon through the solution for 30 min. The reaction mixture was stirred at 80 °C for 16 h and the polymerisation was terminated by placing the vial in an ice-bath. The solvent was removed *via* rotary evaporator and the residue was dissolved in THF (2 mL). The polymer was precipitated in a mixture of *n*-hexane/diethyl ether (40 mL, v/v, 1/1) and dried at 60 °C under high vacuum for 1 day. A pink viscous liquid was obtained (644 mg).

^{1}H NMR (300 MHz, $CDCl_3$) δ/ppm = 7.96 (d, 2 H, H-3, *J* = 6 Hz), 7.55 (t, 1 H, H-1, *J* = 6 Hz), 7.39 (t, 2 H, H-2, *J* = 6 Hz), 4.18 (bt, 2*m*H, H-6 (first repeating unit)), 3.65-3.52 (m, 4*mx*H, H-6, H-7), 3.37 (s, 3*m*H, H-8), 2.59-1.30 (m, 3(*m*+*n*+*o*)H, H-4, H-5; 2 s, 6(*n*+*o*)H, H-9; 2 s, 6 H, H-12), H-10/H-11 not visible. **GPC (DMF, RI):** M_n = 1,747 Da, M_w = 1,996 Da, Đ = 1.14. **FT-IR ν/cm^{-1} =** 3524 (b, N-H stretch), 2868 (m, -CH_3, -CH_2 & C-H stretch), 1819 (w, C=O stretch), 1731 (m, C=O stretch), 1673 (m, C=N stretch), 1530 (w, N-H bend), 1452 (m, -CH_3 and -CH_2 bend), 1350 (m, C-O-C & C-N stretch), 1282 (m, C-O-C & C-N stretch), 1249 (m, C-O-C & C-N stretch), 1096 (s, C-O-C & C-N stretch), 1042 (m, C-O-C & C-N stretch), 946 (m, C-O-C & C-N stretch), 850 (m, C-O-C & C-N stretch), 767 (w, =C-H bend, C-S stretch), 689 (w, =C-H bend, C-S stretch). **RAMAN ν/cm^{-1} =** 3071 (w, =C-H stretch), 2927 (s, C-H stretch), 2881 (s, C-H stretch), 2235 (w, C≡N stretch), 1734 (w, C=O stretch), 1673 (w, C=N stretch), 1589 (m, C=C stretch), 1476 (m, -CH_3 & -CH_2 bend), 1450 (m, -CH_3 & -CH_2 bend), 1288 (m, C-O-C stretch), 1236 (m, C-O-C stretch), 1182 (mw, C-O-C & C=S stretch), 1137 (m, C-O-C stretch), 1044 (m, C-O-C stretch), 999 (m, C-O-C stretch), 847 (m, C-O-C stretch), 802 (m, C-O-C stretch), 648 (w, C-S stretch), 287 (w, C-C bend).

5.2.1.4 Ethyl 3-mercaptopropionate-succinic acid (EMP-SA)

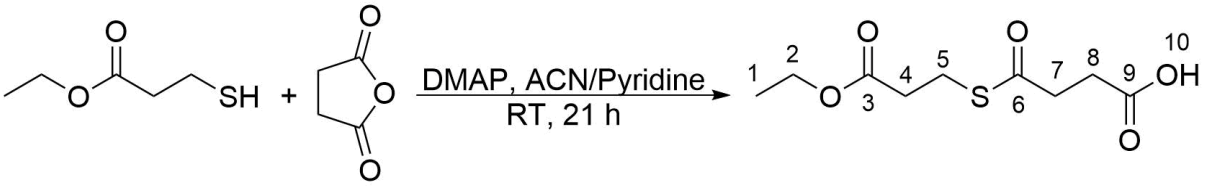

Scheme 5.2.1.4: Synthesis of EMP-SA.

Succinic acid (500 mg, 5.00 mmol, 1 eq) and DMAP (30.5 mg, 0.25 mmol, 0.05 eq) were dissolved in acetonitrile/pyridine (5.625 mL/0.625 mL, 9/1, v/v) and EMP (1.342 g, 1.266 mL, 10.00 mmol, 2 eq) was added dropwise. The solution was stirred at RT for 21 h. The solvent was removed *via* rotary evaporator and the residue was dried at RT for 1 day under high vacuum. The residue was dissolved in EtOAc (30 mL) and was washed with 0.1 M HCl (3 x 30 mL) and H_2O (3 x 30 mL). After drying over Na_2SO_4, the solvent was removed *via* rotary evaporator and the product was dried at RT for 1 day under high vacuum. The product was obtained as a clear liquid (814 mg, 3.475 mmol, 70 %).

^{1}H NMR (300 MHz, $CDCl_3$) δ/ppm = 4.15 (q, 2 H, H-2, *J* = 6 Hz), 3.14 (t, 2 H, H-5, *J* = 6 Hz), 2.88 (t, 2 H, H-7, *J* = 6 Hz), 2.70 (t, 2 H, H-4, *J* = 6 Hz), 2.61 (t, 2 H, H-8, *J* = 6 Hz), 1.25 (t, 2 H, H-1, *J* = 6 Hz), H-10 not visible. **^{13}C NMR (75 MHz, $CDCl_3$) δ/ppm** = 197.44 (C-6), 177.57 (C-9), 171.76 (C-3), 60.97 (C-2), 38.18 (C-7), 34.50 (C-5), 28.96 (C-8), 24.18 (C-4), 14.30 (C-1). **MS /ASAP) m/z =** 233.0484, calculated $[M-H]^-$: 233.0484. **FT-IR ν/cm^{-1} =** 3043 (b, O-H stretch), 2980 (m, -CH_3, -CH_2 & C-H stretch), 2920 (m, -CH_3, -CH_2 & C-H stretch), 2712 (w, -CH_2 & C-H stretch), 2648 (w, -CH_2 & C-H stretch), 2612 (w, -CH_2 & C-H stretch), 2561 (w, -CH_2 & C-H stretch), 2513 (w, -CH_2 & C-H stretch), 2419 (w, -CH_2 & C-H stretch), 2361 (w, -CH_2 & C-H stretch), 1733 (s, C=O stretch), 1702 (s, C=O stretch), 1673 (s, C=O stretch), 1430 (s, -CH_3 & -CH_2 bend), 1411 (s, -CH_3 & -CH_2 bend), 1372 (s, C=O stretch), 1354 (s, C=O stretch), 1311 (s, C=O stretch), 1245 (s, C-O-C stretch), 1223 (s, C-O-C stretch), 1172 (s, C-O-C stretch), 1084 (s, C-O-C stretch), 1064 (s, C-O-C stretch), 1031 (w, C-O-C stretch), 1014 (w, C-O-C stretch), 994 (s, C-O-C stretch), 907 (m, C-O-C stretch), 873 (m, C-O-C stretch), 792 (m, C-S stretch), 773 (s, C-S stretch). **RAMAN ν/cm^{-1}** = 2952 (s, C-H stretch), 2923 (s, C-H stretch), 1737 (m, C=O stretch), 1676 (m, C=O stretch), 1435 (m, -CH_2 & -CH_3 bend), 1416 (m, -CH_2 & -CH_3 bend), 1279 (m, C-O-C stretch), 1121 (m, C-O-C stretch), 1085 (w, C-O-C stretch), 1070 (w, C-O-C stretch), 1034 (w, C-O-C stretch), 932 (m, C-O-C stretch), 874 (m, C-O-C stretch), 796 (w, C-O-C stretch), 776 (w, C-S stretch), 647 (w, C-S stretch), 586 (w, C-C bend), 530 (w, C-C bend), 497 (w, C-C bend),

455 (w, C-C bend), 385 (w, C-C bend), 329 (w, C-C bend), 212 (m, C-C bend),185 (w, C-C bend).

5.2.1.5 Reaction of P(OEGMEA-co-HEA) with EMP-SA (P(OEGMEA-co-EMP-SA))

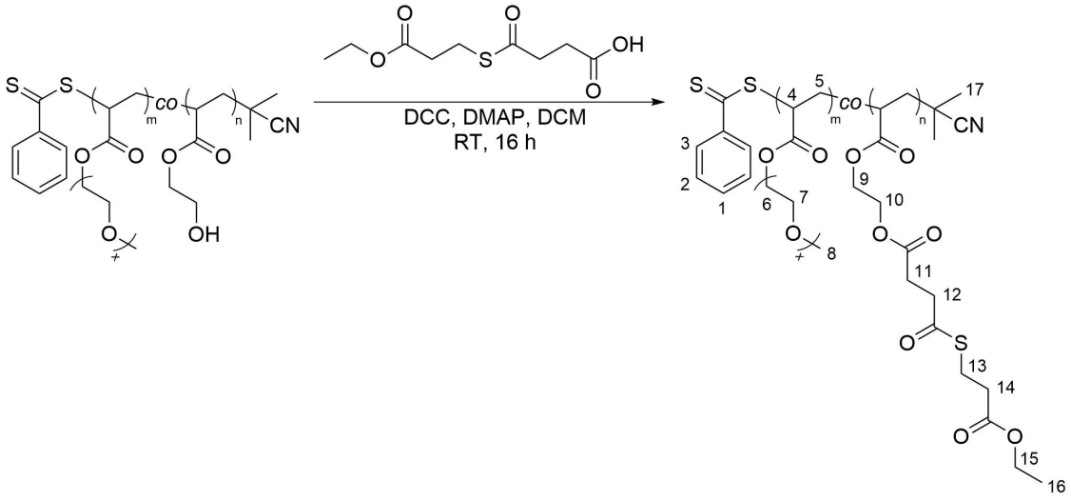

Scheme 5.2.1.5: Synthesis of P(OEGMEA-*co*-EMP-SA).

P(OEGMEA-*co*-HEA) (400 mg, 0.186 mmol OH-groups, 1 eq), EMP-SA (131 mg, 0.559 mmol, 3 eq), DCC (57 mg, 0.276 mmol, 1.5 eq) and DMAP (5 mg, 0.041 mmol, 0.2 eq) were dissolved in DCM (5 mL). The reaction mixture was stirred at RT for 16 h and filtered afterwards. MeOH (20 mL) was added to the residual solution and the reaction mixture was dialysed against MeOH for 3 d by changing solvent twice a day and using dialysis tubes with MWCO = 1 kDa. The solvent was removed *via* rotary evaporator and the polymer was dried at 60 °C under high vacuum for 1 day. A pink viscous liquid (107 mg) was obtained.

^{1}H NMR (300 MHz, $CDCl_3$) δ/ppm = 7.96 (d, 2 H, H-3, *J* = 9 Hz), 7.55 (t, 1 H, H-1, *J* = 6 Hz), 7.39 (t, 2 H, H-2, *J* = 6 Hz), 4.26-4.18 (m, 2(*m*+*n*)H, H-6 (first repeating unit), H-9), 4.15 (q, 2*n*H, H-15, *J* = 6 Hz), 3.65-3.52 (m, 4*mx*H, H-6, H-7; m, 2*n*H, H-10), 3.37 (s, 3*m*H, H-8), 3.12 (t, 2*n*H, H-13, *J* = 6 Hz), 2.89 (t, 2*n*H, H-12, *J* = 6 Hz), 2.68 (bt, 2*n*H, H-14), 2.60 (t, 2*n*H, H-11, *J* = 6 Hz), 2.35-1.54 (m, 3(*m*+*n*)H, H-4, H-5), 1.35/1.30 (2 s, 6 H, H-17), 1.25 (t, 2*n*H, H-16, *J* = 6 Hz). **GPC (DMF, RI):** M_n = 2,193 Da, M_w = 2,682 Da, Đ = 1.22. **FT-IR ν/cm^{-1} =** 3002 (w, -CH_2 & C-H stretch), 2960 (m, -CH_3 stretch), 2904 (m, -CH_2 & C-H stretch), 2870 (m, -CH_3 stretch), 2748 (w, -CH_2 & C-H stretch), 1733 (m, C=O stretch), 1693 (w, C=O stretch), 1451 (m, -CH_2 bend), 1388 (w, -CH_3 bend), 1350 (m, C-O-C stretch), 1258 (m, C-O-C stretch), 1092 (s, C-O-C stretch), 1017 (s, C-O-C stretch), 862 (m, C-O-C stretch), 788 (s, =C-H bend, C-S stretch), 755 (s, =C-H bend, C-S stretch), 701 (m, =C-H

bend, C-S stretch), 665 (m, =C-H bend, C-S stretch). **RAMAN ν/cm^{-1} =** 3057 (=C-H stretch), 2927 (s, C-H stretch), 2880 (s, C-H stretch), 2230 (w, C≡N stretch), 1733 (w, C=O stretch), 1589 (m, C=C stretch), 1458 (m, -CH_2 bend), 1288 (m, C-O-C stretch), 1234 (m, C-O-C stretch), 1184 (w, C-O-C & C=S stretch), 1139 (m, C-O-C stretch), 1048 (m, C-O-C stretch), 996 (m, C-O-C stretch), 849 (m, C-O-C stretch), 647 (w, C-S stretch), 458 (w, C-C bend), 285 (w, C-C bend).

5.2.1.6 RAFT Z-group cleavage

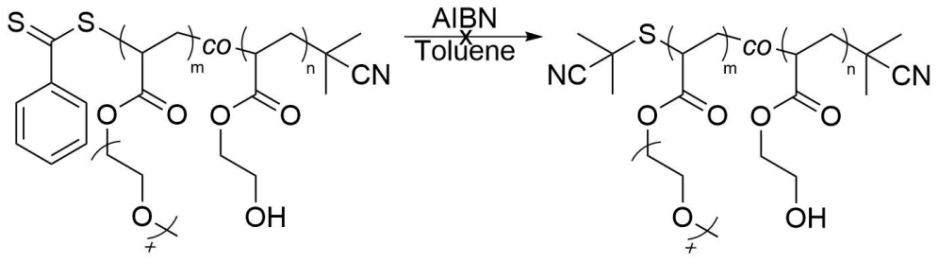

Scheme 5.2.1.6: RAFT Z-group cleavage of P(OEGMEA-*co*-HEA).

P(OEGMEA-*co*-HEA) and AIBN were dissolved in toluene. The solution was degassed by bubbling argon through the solution for 30 min. The reaction mixture was stirred at 85 °C for 2.5 h and the reaction was terminated by placing the vial in an ice-bath. The solvent was removed *via* rotary evaporator and the residue was dissolved in THF (2 mL). The polymer was precipitated in a mixture of *n*-hexane/diethyl ether (40 mL, v/v, 1/1) and dried at 60 °C under high vacuum for 1 day. A pink viscous liquid was obtained. ^{1}H NMR analysis showed that the Z-RAFT group is still present.

Table 5.2.1.6: Reaction conditions for the RAFT Z-group cleavage.

Run	**1**	**2**	**3**
Polymer			
m/mg	660	50	50
n/mmol	0.158	0.0116	0.0116
Eq	1	1	1
AIBN			
m/mg	519	76	38
n/mmol	3.16	0.46	0.232
Eq	20	40	20
V (toluene)/mL	13.2	5	5.8
Temperature/°C	80	80	85
Reaction time/h	2.5	2.5	2.5

5.2.1.7 Reaction of P(OEGMEA-*co*-EMP-SA) with CGGGF

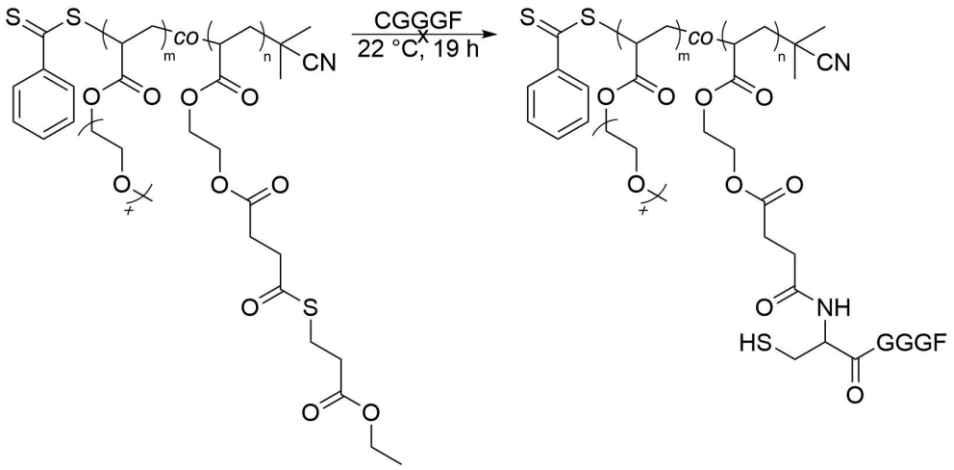

Scheme 5.2.1.7: Reaction of P(OEGMEA-*co*-EMP-SA) with CGGGF.

P(OEGMEA-*co*-EMP-SA) (20 mg, max. $3.249 \cdot 10^{-3}$ mmol thioester-groups, 1 eq) and CGGGF (4.3 mg, $9.748 \cdot 10^{-3}$ mmol thiol-groups, 3 eq) were dissolved (63 µL) and stirred at RT for 19 h. H_2O (2 mL) was added and the reaction mixture was dialysed against H_2O for 3 d by changing solvent twice a day and using dialysis tubes with MWCO = 1 kDa. After freeze drying, the polymer was obtained as a pink viscous liquid.

Table 5.2.1.7: Solvents/yields in reaction with CGGGF.

Run	**1**	**2**
Solvent	PBS	Dry DMF
Yield/mg	24	22

5.2.1.8 Reaction of P(OEGMEA-*co*-TLA) with CGGGF

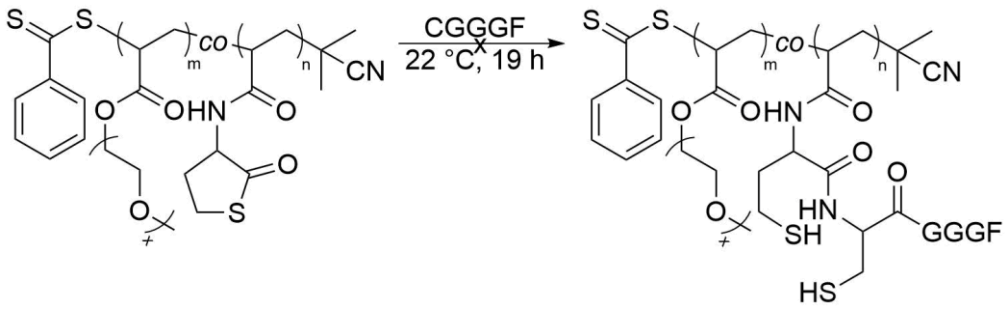

Scheme 5.2.1.8: Reaction of P(OEGMEA-*co*-TLA) with CGGGF.

P(OEGMEA-*co*-TLA) (40 mg, $2.313 \cdot 10^{-2}$ mmol thiolactone-groups, 1 eq) and CGGGF (30.5 mg, $6.939 \cdot 10^{-2}$ mmol thiol-groups, 3 eq) were dissolved (305 µL) and stirred at RT for 19 h. H_2O (2 mL) was added and the reaction mixture was dialysed against H_2O for 3 d by changing solvent twice a day and using dialysis tubes with MWCO = 1 kDa. After freeze drying, the polymer was obtained as a pink viscous liquid.

Table 5.2.1.8: Solvents/yields in reaction with CGGGF.

Run	**1**	**2**
Solvent	PBS	Dry DMF
Yield/mg	24	25

5.2.1.9 Reaction of P(OEGMEA-*co*-VAL) with CGGGF

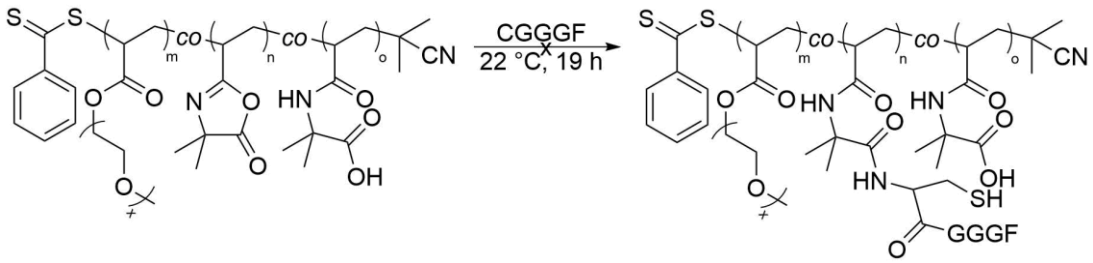

Scheme 5.2.1.9: Reaction of P(OEGMEA-*co*-VAL) with CGGGF.

P(OEGMEA-*co*-VAL) (40 mg, max. $10.632 \cdot 10^{-3}$ mmol azlactone-groups, 1 eq) and CGGGF (14 mg, $3.190 \cdot 10^{-2}$ mmol thiol-groups, 3 eq) were dissolved (140 µL) and stirred at RT for 19 h. H_2O (2 mL) was added and the reaction mixture was dialysed against H_2O for 3 d by changing solvent twice a day and using dialysis tubes with MWCO = 1 kDa. After freeze drying, the polymer was obtained as a pink viscous liquid.

Table 5.2.1.9: Solvents/yields in reaction with CGGGF.

Run	**1**	**2**
Solvent	PBS	Dry DMF
Yield/mg	24	25

5.2.2 Free radical copolymerisation

5.2.2.1 Poly(oligo(ethylene glycol) methyl ether acrylate-*co*-2-hydroxyethyl acrylate) (P(OEGMEA-*co*-HEA))

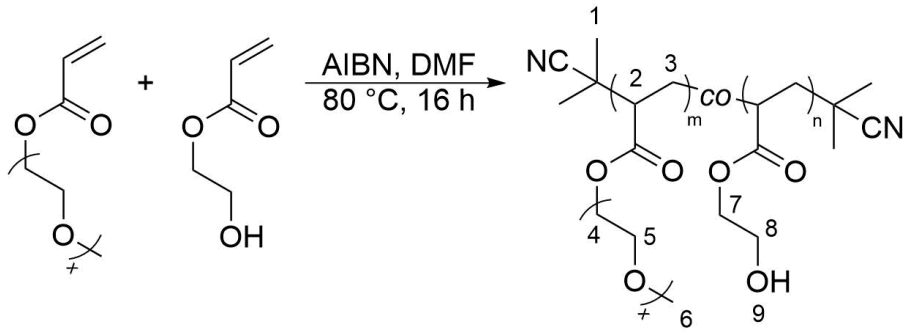

Scheme 5.2.2.1: Synthesis of P(OEGMEA-*co*-HEA).

OEGMEA (1.152 g, 2.40 mmol, 8 eq), HEA (70 mg, 0.60 mmol, 2 eq) and AIBN (24.6 mg, 0.15 mmol, 0.5 eq) were dissolved in DMF (5 mL) and degassed *via* purging with argon for 30 min. The reaction mixture was stirred at 80 °C for 16 h and the polymerisation was terminated by placing the vial in an ice-bath. The solvent was removed *via* rotary evaporator and the residue was dissolved in THF (2 mL). The polymer was precipitated in a mixture of *n*-hexane/diethyl ether (40 mL, v/v, 1/1) and dried at 60 °C under high vacuum for 1 day. A clear viscous liquid was obtained (922 mg).

^{1}H NMR (300 MHz, $CDCl_3$) δ/ppm = 4.19 (bt, 2(*m*+*n*)H, H-4 (first repeating unit), H-7), 3.65-3.53 (m, 4*m*xH, H-4, H-5; m, 2*n*H, H-8), 3.37 (s, 3*m*H, H-6), 2.33-1.64 (m, 3(*m*+*n*)H, H-2, H-3; bs, 1*n*H, H-9), 1.35/1.30 (2 s, 12 H, H-1). **GPC (DMF, RI):** M_n = 4,759 Da, M_w = 11,959 Da, Đ = 2.51. **FT-IR ν/cm^{-1}** = 3511 (b, O-H stretch), 2869 (m, -CH_2 & C-H stretch), 1731 (m, C=O stretch), 1453 (m, -CH_3 & -CH_2 bend), 1388 (m, -CH_3 bend), 1350 (m, C-O-C stretch), 1326 (w, C-O-C stretch), 1284 (m, C-O-C stretch), 1248 (m, C-O-C stretch), 1095 (s, C-O-C stretch), 1038 (m, C-O-C stretch), 947 (m, C-O-C stretch), 850 (m, C-O-C stretch), 759 (w, -CH_2 bend). **RAMAN ν/cm^{-1}** = 2932 (s, C-H stretch), 2873 (s, C-H stretch), 2234 (w, C≡N stretch), 1732 (m, C=O stretch), 1461 (m, -CH_3 & -CH_2 bend), 1295 (m, C-O-C stretch), 1242 (m, C-O-C stretch), 1132 (m, C-O-C stretch), 1043 (m, C-O-C stretch), 848 (m, C-O-C stretch), 818 (m, C-O-C stretch), 683 (w, C-C stretch), 545 (w, C-C stretch), 284 (m, (w, C-C bend).

5.2.2.2 Poly(oligo(ethylene glycol) methyl ether acrylate-*co*-thiolactone acrylamide) (P(OEGMEA-*co*-TLA))

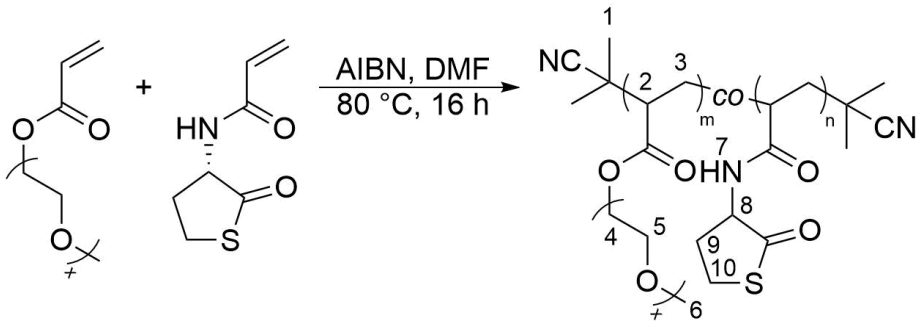

Scheme 5.2.2.2: Synthesis of P(OEGMEA-*co*-TLA).

OEGMEA (1.152 g, 2.40 mmol, 8 eq), TLA (102.7 mg, 0.60 mmol, 2 eq) and AIBN (24.6 mg, 0.15 mmol, 0.5 eq) were dissolved in DMF (5 mL) and degassed *via* purging with argon for 30 min. The reaction mixture was stirred at 80 °C for 16 h and the polymerisation was terminated by placing the vial in an ice-bath. The solvent was removed *via* rotary evaporator and the residue was dissolved in THF (2 mL). The polymer was precipitated in a mixture of *n*-hexane/diethyl ether (40 mL, v/v, 1/1) and dried at 60 °C under high vacuum for 1 day. A clear viscous liquid was obtained (992 mg).

^{1}H NMR (300 MHz, MeCN-d$_3$) δ/ppm = 6.97 (bs, 1*n*H, H-7), 4.56 (bs, 1*n*H, H-8), 4.15 (bt, 2*m*H, H-4 (first repeating unit)), 3.63-3.45 (m, 4*mx*H, H-4, H-5; m, 2*m*H, H-10), 3.30 (s, 3*m*H, H-6), 2.53-1.49 (m, 3(*m*+*n*)H, H-2, H-3; m, 2*m*H, H-9), 1.33/1.29 (2 s, 12 H, H-1). **GPC (DMF, RI):** M_n = 4,729 Da, M_w = 13,083 Da, Đ = 2.77. **FT-IR ν/cm^{-1} =** 3570 (b, N-H stretch), 2867 (m, -CH_2 & C-H stretch)**,** 1731 (m, C=O stretch), 1675 (m, C=O stretch), 1532 (m, N-H bend), 1452 (m, -CH_3 & -CH_2 bend), 1350 (m, C-O-C & C-N stretch), 1325 (w, C-O-C & C-N stretch), 1286 (m, C-O-C & C-N stretch), 1249 (m, C-O-C & C-N stretch), 1096 (s, C-O-C & C-N stretch), 1038 (m, C-O-C & C-N stretch), 996 (w, C-O-C stretch), 946 (m, C-O-C stretch), 849 (m, C-O-C stretch), 742 (w, C-S stretch & -CH_2 bend). **RAMAN ν/cm^{-1} =** 2928 (s, C-H stretch), 2879 (s, C-H stretch), 2237 (w, C≡N stretch), 1730 (w, C=O stretch), 1461 (m, -CH_3 & -CH_2 bend), 1287 (m, C-O-C stretch), 1247 (m, C-O-C stretch), 1137 (m, C-O-C stretch), 1040 (m, C-O-C stretch), 848 (m, C-O-C stretch), 686 (w, C-S stretch), 614 (w, C-C stretch), 486 (w, C-C bend), 431 (w, C-C bend), 279 (w, C-C bend).

5.2.2.3 Poly(oligo(ethylene glycol) methyl ether acrylate-*co*-vinyl azlactone) (P(OEGMEA-*co*-VAL))

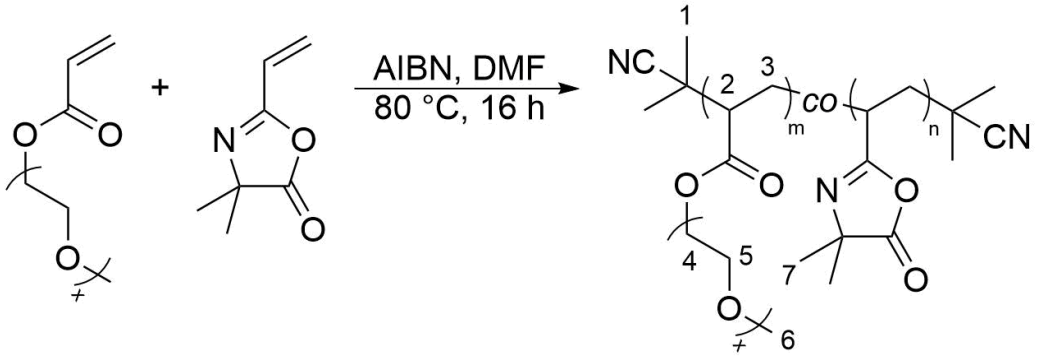

Scheme 5.2.2.3: Synthesis of P(OEGMEA-*co*-VAL).

OEGMEA (1.152 g, 2.40 mmol, 8 eq), VAL (84 mg, 0.60 mmol, 2 eq) and AIBN (24.6 mg, 0.15 mmol, 0.5 eq) were dissolved in DMF (5 mL) and degassed *via* purging with argon for 30 min. The reaction mixture was stirred at 80 °C for 16 h and the polymerisation was terminated by placing the vial in an ice-bath. The solvent was removed *via* rotary evaporator and the residue was dissolved in THF (2 mL). The polymer was precipitated in a mixture of *n*-hexane/diethyl ether (40 mL, v/v, 1/1) and dried at 60 °C under high vacuum for 1 day. A clear viscous liquid was obtained (933 mg).

^{1}H NMR (300 MHz, MeCN-d_3) δ/ppm = 4.15 (bt, 2*m*H, H-4 (first repeating unit)), 3.62-3.45 (m, 4*mx*H, H-4, H-5), 3.30 (s, 3*m*H, H-6), 2.54-1.49 (m, 3(*m*+*n*)H, H-2, H-3), 1.36 (s, 6*n*H, H-7), 1.29 (s, 6 H, H-1). **GPC (DMF, RI):** M_n = 4,396 Da, M_w = 8,907 Da, Đ = 2.03. **FT-IR ν/cm^{-1} =** 2867 (m, -CH_2 & C-H stretch), 1818 (m, C=O stretch), 1732 (m, C=O stretch), 1673 (w, C=N stretch), 1453 (m, -CH_2 bend), 1350 (m, C-O-C & C-N stretch), 1287 (m, C-O-C & C-N stretch), 1249 (m, C-O-C & C-N stretch), 1198 (w, C-O-C & C-N stretch), 1097 (s, C-O-C & C-N stretch), 1039 (m, C-O-C & C-N stretch), 994 (w, C-O-C stretch), 948 (m, C-O-C stretch), 889 (w, C-O-C stretch), 851 (m, C-O-C stretch), 756 (w, -CH_2 bend). **RAMAN ν/cm^{-1} =** 2941 (s, C-H stretch), 2879 (s, C-H stretch), 2233 (w, C≡N stretch), 1826 (w, C=O stretch), 1735 (w, C=O stretch), 1671 (w, C=N stretch), 1462 (m, -CH_3 & -CH_2 bend), 1293 (m, C-O-C stretch), 1243 (m, C-O-C stretch), 1137 (m, C-O-C stretch), 1041 (m, C-O-C stretch), 847 (m, C-O-C stretch), 817 (m, C-O-C stretch), 755 (w, C-C stretch), 619 (w, C-C stretch), 565 (w, C-C stretch), 284 (w, C-C bend).

5.2.2.4 Reaction of P(OEGMEA-co-HEA) with EMP-SA (P(OEGMEA-co-EMP-SA))

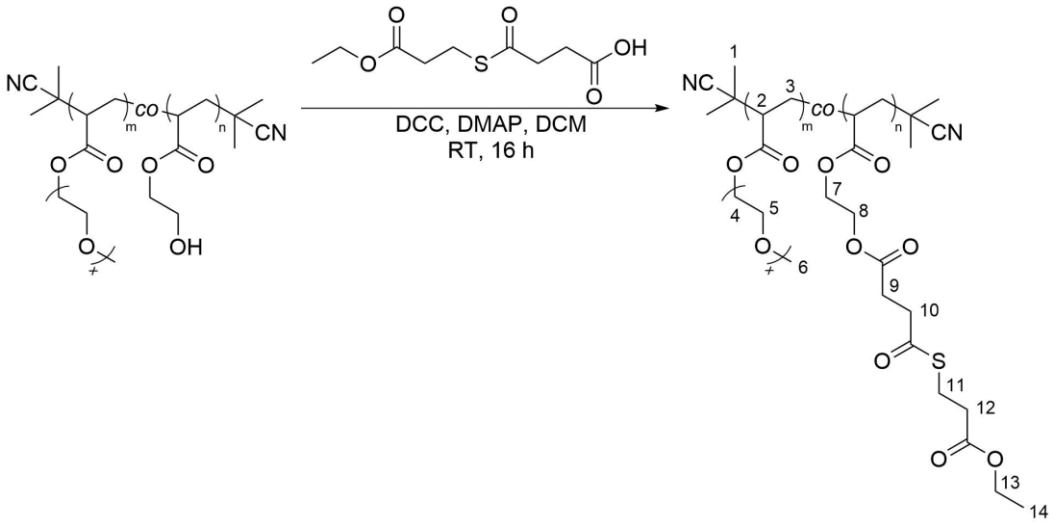

Scheme 5.2.2.4: Synthesis of P(OEGMEA-*co*-EMP-SA).

P(OEGMEA-*co*-HEA) (200 mg, 0.0413 mmol OH-groups, 1 eq), EMP-SA (29 mg, 0.124 mmol, 3 eq), DCC (13 mg, 0.062 mmol, 1.5 eq) and DMAP (1 mg, 0.00826 mmol, 0.2 eq) were dissolved in DCM (2 mL). The reaction mixture was stirred at RT for 16 h and filtered afterwards. MeOH (10 mL) was added to the residual solution and the reaction mixture was dialysed against MeOH for 3 d by changing solvent twice a day and using dialysis tubes with MWCO = 1 kDa. The solvent was removed *via* rotary evaporator and the polymer was dried at 60 °C under high vacuum for 1 day. A clear viscous liquid (126 mg) was obtained.

^{1}H NMR (300 MHz, $CDCl_3$) δ/ppm = 4.25-4.18 (m, 2(*m*+*n*)H, H-4 (first repeating unit), H-7), 4.15 (q, 2*n*H, H-13, *J* = 6 Hz), 3.64-3.52 (m, 4*m*xH, H-4, H-5; m, 2*n*H, H-8), 3.37 (s, 3*m*H, H-6), 3.12 (t, 2*n*H, H-11, *J* = 6 Hz), 2.89 (t, 2*n*H, H-10, *J* = 6 Hz), 2.68 (bt, 2*n*H, H-12), 2.60 (t, 2*n*H, H-9, *J* = 6 Hz), 2.32-1.44 (m, 3(*m*+*n*)H, H-2, H-3), 1.35/1.28 (2 s, 6 H, H-1), 1.25 (t, 2*n*H, H-14, *J* = 6 Hz). **GPC (DMF, RI):** M_n = 3,824 Da, M_w = 8,233 Da, Đ = 2.15. **FT-IR ν/cm^{-1} =** 2932 (m, -CH_2 & C-H stretch), 2869 (m, -CH_3 stretch), 1941 (w, C=O stretch), 1731 (m, C=O stretch), 1452 (m, -CH_2 bend), 1349 (m, C-O-C stretch), 1284 (m, C-O-C stretch), 1248 (m, C-O-C stretch), 1096 (s, C-O-C stretch), 1038 (w, C-O-C stretch), 993 (w, C-O-C stretch), 947 (m, C-O-C stretch), 850 (m, C-O-C stretch). **RAMAN ν/cm^{-1} =** 2933 (s, C-H stretch), 2879 (s, C-H stretch), 2360 (w, C≡N stretch), 1734 (w, C=O stretch), 1467 (m, -CH_3 & -CH_2 bend), 1453 (m, -CH_2 bend), 1287 (m, C-O-C stretch), 1245 (m, C-O-C stretch), 1136

(m, C-O-C stretch), 1041 (m, C-O-C stretch), 848 (m, C-O-C stretch), 546 (w, C-C stretch), 272 (w, C-C bend).

5.2.2.5 Reaction of P(OEGMEA-*co*-TLA) with benzylamine

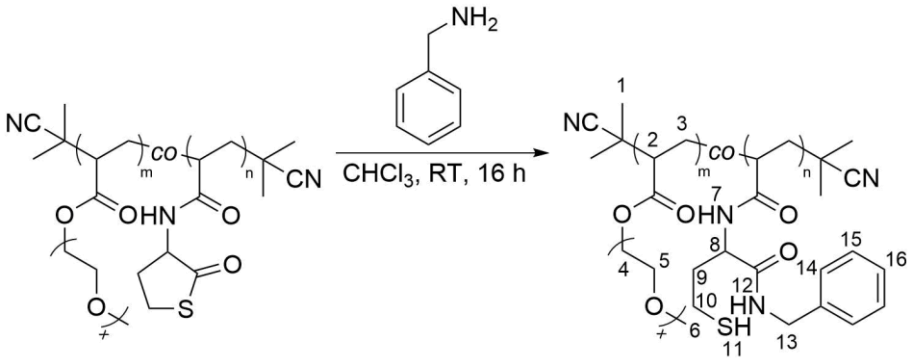

Scheme 5.2.2.5: Reaction of P(OEGMEA-*co*-TLA) with benzylamine.

P(OEGMEA-*co*-TLA) (100 mg, max. 0.0479 mmol TLA units, 1 eq) and benzylamine (25.7 mg, 26.1 µL, 0.2395 mmol, 5 eq) were dissolved in dry chloroform (1 mL) and stirred at RT for 16 h. The solvent was removed *via* rotary evaporator and the residue was dissolved in THF (2 mL). The polymer was precipitated in a mixture of *n*-hexane/diethyl ether (40 mL, v/v, 1/1) and dried at 60 °C under high vacuum for 1 day. A clear viscous liquid was obtained (78 mg).

^{1}H NMR (300 MHz, MeCN-d$_3$) δ/ppm = 7.29 (m, 5*n*H, H-14, H-15, H-16), 6.93 (bs, 2*n*H, H-7, H-12), 4.51 (bs, 1*n*H, H-8), 4.36 (s, 2*n*H, H-13), 4.15 (bt, 2*m*H, H-4 (first repeating unit)), 3.63-3.45 (m, 4*mx*H, H-4, H-5), 3.30 (s, 3*m*H, H-6), 2.54-1.64 (m, 3(*m*+*n*)H, H-2, H-3; m, 2*n*H, H-9, H-10; m, 1*n*H, H-11), 1.29/1.27 (2 s, 12 H, H-1). **GPC (DMF, RI):** M_n = 5,218 Da, M_w = 13,619 Da, Đ = 2.61. **FT-IR ν/cm^{-1} =** 3524 (b, N-H stretch), 2868 (m, -CH_2 & C-H stretch), 1731 (m, C=O stretch), 1671 (m, C=O stretch), 1535 (w, N-H bend), 1452 (m, -CH_3 & -CH_2 bend), 1349 (m, C-O-C & C-N stretch), 1325 (w, C-N stretch), 1283 (m, C-O-C & C-N stretch), 1257 (m, C-O-C & C-N stretch), 1094 (s, C-O-C & C-N stretch), 1032 (m, C-O-C & C-N stretch), 947 (m, C-O-C stretch), 849 (m, C-O-C stretch), 801 (m, =C-H bend, C-S stretch), 755 (w, =C-H bend, C-S stretch), 701 (w, =C-H bend, C-S stretch). **RAMAN ν/cm^{-1} =** 3060 (w, =(C-H) stretch), 2923 (s, C-H stretch), 2881 (s, C-H stretch), 2575 (w, S-H stretch), 2235 (w, C≡N stretch), 1734 (m, C=O stretch), 1608 (w, C=C stretch), 1470 (m, -CH_3 & -CH_2 bend), 1449 (m, -CH_3 & -CH_2 bend), 1285 (m, C-O-C stretch), 1240 (m, C-O-C stretch), 1135 (m, C-O-C stretch), 1029 (m, C-O-C stretch), 1000 (m, C-O-C stretch), 848 (m, C-O-C stretch), 811 (m, C-O-C stretch), 685 (w, C-S stretch), 617 (w, C-S stretch), 487 (w, C-C bend), 432 (w, C-C bend), 275 (w, C-C bend).

5.2.2.6 Reaction of P(OEGMEA-*co*-VAL) with benzylamine

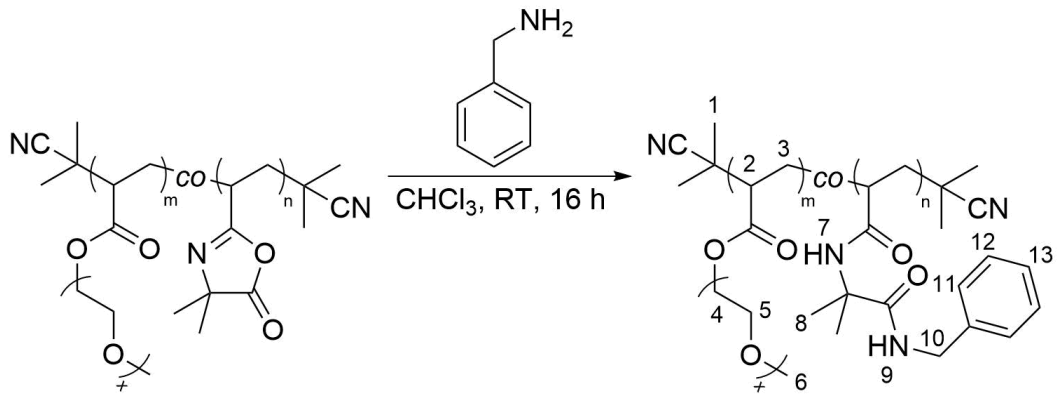

Scheme 5.2.2.6: Reaction of P(OEGMEA-*co*-VAL) with benzylamine.

P(OEGMEA-*co*-VAL) (100 mg, max. 0.0489 mmol VAL units, 1 eq) and benzylamine (26.2 mg, 26.7 µL, 0.2445 mmol, 5 eq) were dissolved in dry chloroform (1 mL) and stirred at RT for 16 h. The solvent was removed *via* rotary evaporator and the residue was dissolved in THF (2 mL). The polymer was precipitated in a mixture of *n*-hexane/diethyl ether (40 mL, v/v, 1/1) and dried at 60 °C under high vacuum for 1 day. A clear viscous liquid was obtained (82 mg).

^{1}H NMR (300 MHz, MeCN-d_3) δ/ppm = 7.28 (m, 5*n*H, H-11, H-12, H-13), 6.90 (bs, 2*n*H, H-7, H-9), 4.35 (s, 2*n*H, H-10), 4.14 (bt, 2*m*H, H-4 (first repeating unit)), 3.62-3.45 (m, 4*mx*H, H-4, H-5), 3.29 (s, 3*m*H, H-6), 2.31-1.62 (m, 3(*m*+*n*)H, H-2, H-3), 1.44 (s, 6*n*H, H-8), 1.29/1.27 (2 s, 12 H, H-1). **GPC (DMF, RI):** M_n = 5,226 Da, M_w = 11,066 Da, Đ = 2.12. **FT-IR ν/cm^{-1} =** 3524 (b, N-H stretch), 2868 (m, -CH_2 & C-H stretch), 1731 (m, C=O stretch), 1651 (m, N-H bend), 1531 (m, N-H bend), 1453 (m, -CH_2 bend), 1384 (w, -CH_3 bend), 1350 (m, C-O-C/C-N stretch), 1325 (w, C-O-C/C-N stretch), 1285 (m, C-O-C/C-N stretch), 1249 (m, C-O-C/C-N stretch), 1096 (s, C-O-C/C-N stretch), 1037 (m, C-O-C/C-N stretch), 998 (w, C-O-C/C-N stretch), 946 (m, C-O-C/C-N stretch), 850 (m, C-O-C/C-N stretch), 751 (w, =C-H bend), 701 (w, =C-H bend). **RAMAN ν/cm^{-1} =** 3060 (w, =(C-H) stretch, 2930 (s, C-H stretch), 2876 (s, C-H stretch), 2233 (w, C≡N stretch), 1730 (w, C=O stretch), 1606 (w, C=C stretch), 1461 (m, -CH_3 & -CH_2 bend), 1288 (m, C-O-C stretch), 1246 (m, C-O-C stretch), 1177 (w, C-O-C stretch), 1137 (m, C-O-C stretch), 1027 (m, C-O-C stretch), 1000 (m, C-O-C stretch), 848 (m, C-O-C stretch), 807 (m, C-O-C stretch), 620 (w, C-C bend), 549 (w, C-C bend), 260 (w, C-C bend).

5.2.2.7 Reaction of P(OEGMEA-*co*-EMP-SA) with CGGGF

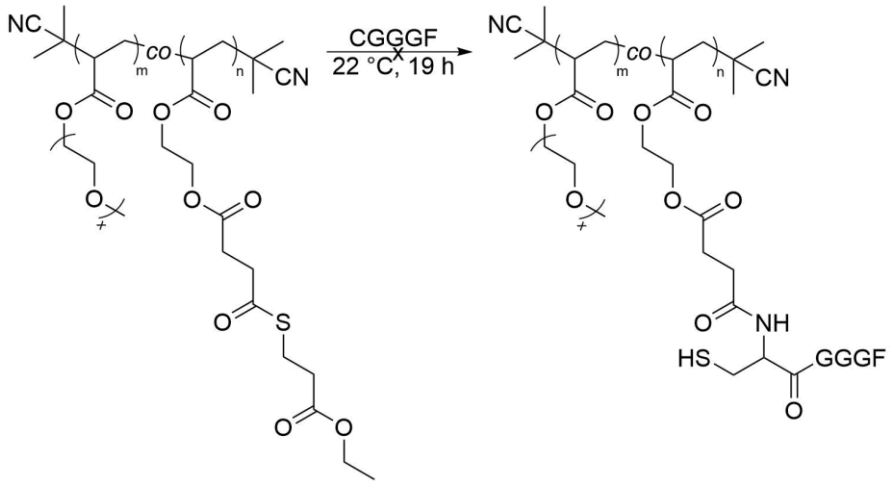

Scheme 5.2.2.7: Reaction of P(OEGMEA-*co*-EMP-SA) with CGGGF.

P(OEGMEA-*co*-EMP-SA) and CGGGF were dissolved and stirred at 22 °C for 19 h. H_2O (2 mL) was added and the reaction mixture was dialysed against H_2O for 3 d by changing solvent twice a day and using dialysis tubes with MWCO = 1 kDa. After freeze drying, the polymer was obtained as a clear viscous liquid.

Table 5.2.2.7: Amounts of used compounds/yields in reaction with CGGGF.

Run	**1**	**2**	**3**	**4**
m (polymer)/mg	40	40	40	50
m (thioester group)/mg	2.60	2.60	2.60	3.25
n (thioester group)/mmol	7.823×10^{-3}	7.823×10^{-3}	7.823×10^{-3}	9.778×10^{-3}
Eq (thioester group)	1	1	1	1
m (CGGGF)/mg	10.3	10.3	10.3	12.9
n (CGGGF)/mg	2.347×10^{-2}	2.347×10^{-2}	2.347×10^{-2}	2.933×10^{-2}
Eq (CGGGF)	3	3	3	3
Solvent	103 µL PBS	103 µL NaAsc PBS	103 µL NaAsc PBS, TCEP·HCl	129 µL dry DMF
Yield/mg	35	36	33	39

5.2.2.8 Reaction of P(OEGMEA-*co*-TLA) with CGGGF

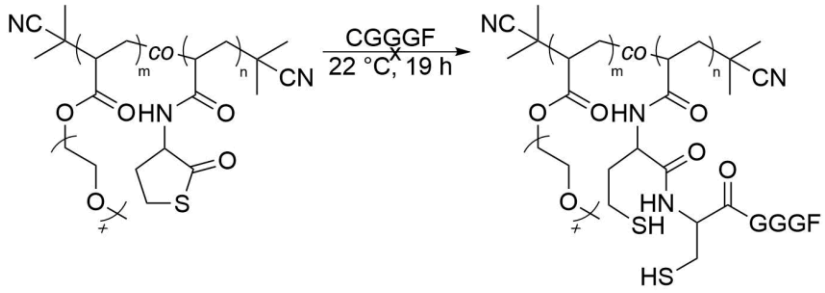

Scheme 5.2.2.8: Reaction of P(OEGMEA-*co*-TLA) with CGGGF.

P(OEGMEA-*co*-TLA) (40 mg, 2.1 mg thioester groups, 1.215 x 10^{-2} mmol thioester groups, 1 eq) and CGGGF (16.0 mg, 3.645 x 10^{-2} mmol, 3 eq) were dissolved and stirred at 22 °C for 19 h. H_2O (2 mL) was added and the reaction mixture was dialysed against H_2O for 3 d by changing solvent twice a day and using dialysis tubes with MWCO = 1 kDa. After freeze drying, the polymer was obtained as a clear viscous liquid.

Table 5.2.2-2: Solvents/yields in reaction with CGGGF.

Run	**1**	**2**	**3**	**4**
Solvent	160 µL PBS	160 µL NaAsc PBS	160 µL NaAsc PBS, TCEP·HCl	160 µL dry DMF
Yield/mg	31	31	33	32

5.2.2.9 Reaction of P(OEGMEA-*co*-VAL) with CGGGF

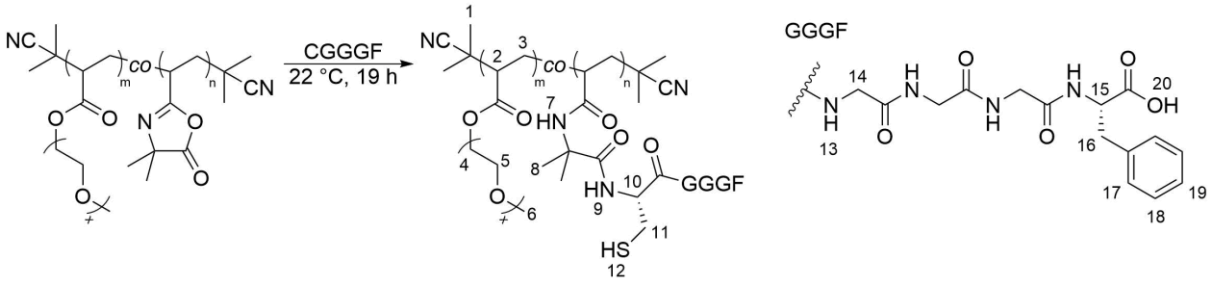

Scheme 5.2.2.9: Reaction of P(OEGMEA-*co*-VAL) with CGGGF.

P(OEGMEA-*co*-VAL) (40 mg, 3.2 mg azlactone groups, 2.328 x 10^{-2} mmol azlactone groups, 1 eq) and CGGGF (30.7 mg, 6.984 x 10^{-2} mmol, 3 eq) were dissolved and stirred at 22 °C for 19 h. H_2O (2 mL) was added and the reaction mixture was dialysed against H_2O for 3 d by changing solvent twice a day and using dialysis tubes with MWCO = 1 kDa. After freeze drying, the polymer was obtained as a clear viscous liquid.

Table 5.2.2.9: Solvents/yields in reaction with CGGGF.

Run	**1**	**2**	**3**	**4**
Solvent	307 µL PBS	307 µL NaAsc PBS	307 µL NaAsc PBS, TCEP·HCl	307 µL dry DMF
Yield/mg	33	35	11	37
DS/%	0	15	15	19

^{1}H NMR (300 MHz, MeCN-d_3) δ/ppm = 7.27 (m, 5*n*H, H-17 – H-19), 7.00 (bs, 6*n*H, H-7, H-9, H-13), 4.57 (bs, 1*n*H, H-15), 4.15 (bt, 2*m*H, H-4 (first repeating unit); m, 2*n*H, H-14), 3.63-3.45 (m, 4*mx*H, H-4, H-5; m, 2*n*H, H-16), 3.30 (s, 3*m*H, H-6), 3.32-1.63 (m, 3(*m*+*n*)H, H-2, H-3; m, 4*n*H, H-10 – H-12), 1.43 (s, 6*n*H, H-8), 1.34/1.29 (2 s, 12 H, H-1), H-20 not visible. **GPC (DMF, RI):** M_n = 5,771 Da, M_w = 14,383 Da, Đ = 2.49. **FT-IR ν/cm^{-1} =** 3511 (b, N-H stretch), 3336 (b, N-H stretch), 2868 (m, -CH_2 & C-H stretch), 1731 (m, C=O stretch), 1671 (m, C=C stretch), 1531 (m, N-H bend), 1453 (m, -CH_2 bend), 1385 (w, CH_3 bend), 1350 (m, C-O-C & C-N stretch), 1325 (w, C-N & C-N stretch), 1282 (m, C-O-C & C-N stretch), 1249 (m, C-O-C & C-N stretch), 1096 (s, C-O-C & C-N stretch), 1038 (m, C-O-C & C-N stretch), 995 (w, C-O-C stretch), 946 (m, C-O-C stretch), 850 (m, C-O-C stretch), 702 (w, =C-H & C-S stretch). **RAMAN ν/cm^{-1} =** 2936 (s, C-H stretch), 2879 (s, C-H stretch), 2649 (w, S-H stretch), 1737 (w, C=O stretch), 1459 (m, -CH_3 & -CH_2 bend), 1293 (m, C-O-C stretch), 1247 (m, C-O-C stretch), 1136 (m, C-O-C stretch), 1037 (m, C-O-C stretch), 1005 (w, C-O-C stretch), 851 (m, C-O-C stretch), 807 (m, C-O-C & C-S stretch), 548 (w, C-C stretch), 276 (w, C-C bend).

5.2.2.10 Stability tests of P(OEGMEA-*co*-EMP-SA), P(OEGMEA-*co*-TLA) and P(OEGMEA-*co*-VAL)

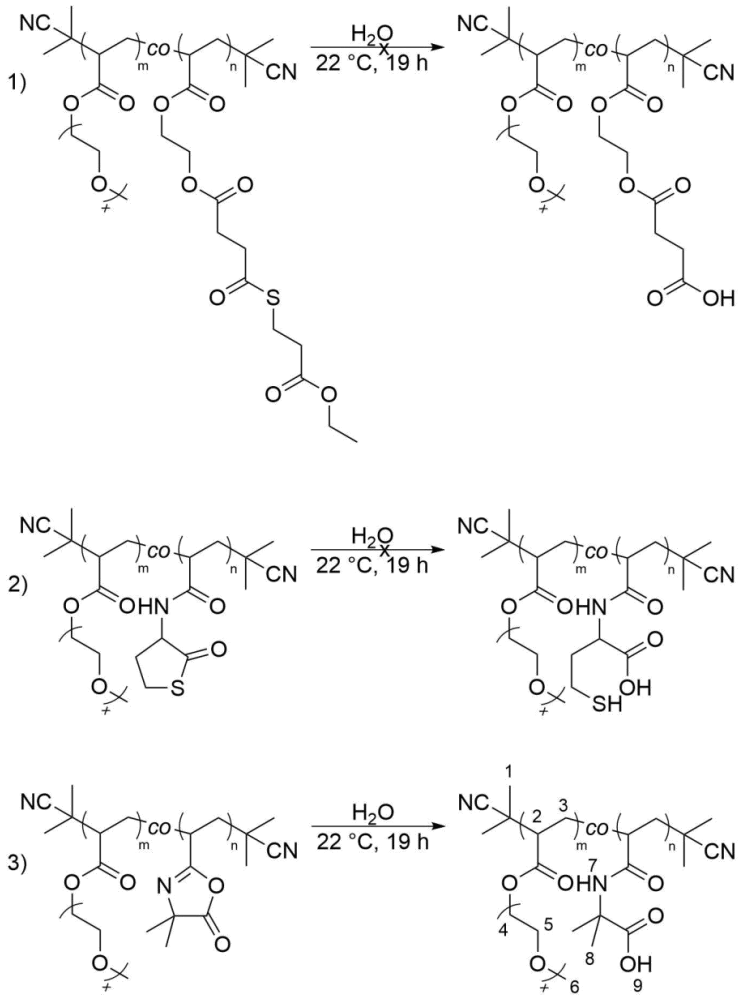

Scheme 5.2.2.10: Stability tests of P(OEGMEA-*co*-EMP-SA), P(OEGMEA-*co*-TLA) and P(OEGMEA-*co*-VAL).

The polymers were dissolved in PBS and stirred at 22 °C for 19 h. H_2O (2 mL) was added and the reaction mixture was dialysed against H_2O for 3 d by changing solvent twice a day and using dialysis tubes with MWCO = 1 kDa. After freeze drying, the polymers were obtained as clear viscous liquids.

Table 5.2.2.10: Amounts of compounds/yields in reaction with H_2O.

Run	P(OEGMEA-*co*-EMP-SA)	P(OEGMEA-*co*-TLA)	P(OEGMEA-*co*-VAL)
m/mg	26.2	40	40
V (PBS)/µL	67.5	160	307
Yield/mg	23	31	33

Hydrolysed P(OEGMEA-*co*-VAL): ^{1}H NMR (300 MHz, MeCN-d$_3$) δ/ppm = 9.06 (s, 1*n*H, H-9), 7.54 (s, 1*n*H, H-7), 4.15 (bt, 2*m*H, H-4 (first repeating unit)), 3.63-3.45 (m, 4*mx*H, H-4, H-5), 3.30 (s, 3*m*H, H-6), 2.54-1.57 (m, 3(*m*+*n*)H, H-2, H-3), 1.43 (s, 6*n*H, H-8), 1.33/1.30 (2 s, 12 H, H-1). **GPC (DMF, RI):** M_n = 4,500 Da, M_w = 6,993 Da, Đ = 1.55. **FT-IR ν/cm^{-1} =** 3518 (b, N-H stretch), 2868 (m, -CH_2 & C-H stretch), 1731 (m, C=O stretch), 1657 (m, N-H bend), 1531 (w, N-H bend), 1453 (m, -CH_2 bend), 1389 (w, C=O stretch), 1350 (m, C-O-C & C-N stretch), 1325 (w, C-O-C & C-N stretch), 1286 (m, C-O-C & C-N stretch), 1249 (m, C-O-C & C-N stretch), 1096 (s, C-O-C & C-N stretch), 1039 (m, C-O-C & C-N stretch), 996 (w, C-O-C stretch), 946 (m, C-O-C stretch), 850 (m, C-O-C stretch). **RAMAN ν/cm^{-1} =** 2930 (s, C-H stretch), 2883 (s, C-H stretch), 2236 (w, C≡N stretch), 1737 (w, C=O stretch), 1669 (w, C=O stretch), 1474 (m, -CH_3 & -CH_2 bend), 1459 (m, -CH_3 & -CH_2 bend), 1289 (m, C-O-C stretch), 1254 (m, C-O-C stretch), 1139 (m, C-O-C stretch), 1043 (m, C-O-C stretch), 853 (m, C-O-C stretch), 813 (m, C-O-C stretch), 567 (w, C-C stretch), 435 (w, C-C bend), 271 (w, C-C bend).

5.3 Low molecular weight polyglycidols

5.3.1 Ethoxyethyl glycidyl ether (EEGE)

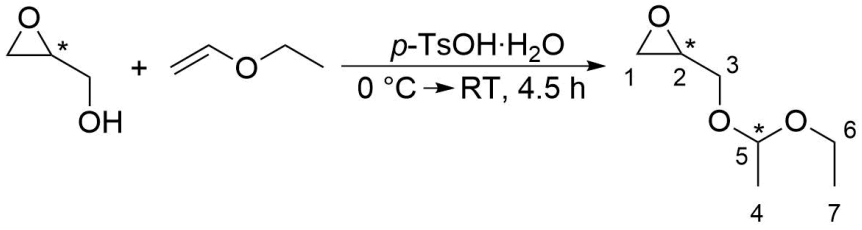

Scheme 5.3.1: Synthesis of EEGE.

Glycidol (100 g, 90.1 mL, 1.350 mol, 1 eq) and ethyl vinyl ether (399.1 g, 532.1 mL, 5.535 mol, 4.1 eq) were mixed in a flask in an ice-bath. During stirring, *p*-toluenesulfonic acid (2.568 g, 13.5 mol, 0.01 eq) was added slowly for 1.5 h so that the temperature stayed below 20 °C. The reaction mixture was stirred for further 3 h and the solution was allowed to warm up to RT. The solution was washed with saturated $NaHCO_3$ solution (3 x 70 mL). The residual ethyl vinyl ether was removed under reduced pressure (50 °C, 900 → 150 mbar). Afterwards, CaH_2 (2 spatula tips) was added and the reaction mixture was stirred at RT overnight. The solution became turbid and changed from colourless to yellow. The monomer was purified *via* distillation (60 °C bath temperature, 2.8 – 4.0 x 10^{-2} mbar) and was obtained as a colourless liquid (109.1 g, 0.767 mol, 57 %) which was stored in the fridge of the glovebox until usage.

^{1}H NMR (300 MHz, $CDCl_3$) δ/ppm = 4.64 (q, 1 H, H-5, *J* = 6 Hz), 3.72-3.27 (m, 2 H, 3-H, H-6), 3.05-2.99 (m, 1 H, H-2)$^{\#}$, 2.69-2.66 (m, 1 H, H-1)$^{\#}$, 2.53-2.47 (m, 1 H, H-1‘)$^{\#}$, 1.22-1.18 (2 d, 3 H, H-4, *J* = 6 Hz)$^{\#}$, 1.08 (t, 3 H, H-7, *J* = 9 Hz). **^{13}C NMR (75 MHz, $CDCl_3$) δ/ppm =** 99.55/99.53 (C-5)$^{\#}$, 65.68/65.02 (C-3)$^{\#}$, 60.78 (C-6), 50.73/50.62 (C-2)$^{\#}$, 44.35/44.30 (C-1)$^{\#}$, 19.61/19.49 (C-4)$^{\#}$, 15.11 (C-7). $^{\#}$Splitting due to enantiomeric mixture. **MS (ASAP) m/z =** 145.0855, calculated [M-H]$^-$: 145.0855. **FT-IR ν/cm^{-1} =** 3053 (w, C-H stretch), 2980 (m, -CH_3 stretch), 2932 (m, -CH_2 stretch), 2898 (m, C-H stretch), 2878 (m, -CH_3 stretch), 2841 (w, -CH_2 stretch), 1483 (w, -CH_2 & -CH_3 bend), 1445 (m, -CH_2 & -CH_3 bend), 1384 (m, -CH_3 bend), 1338 (m, C-O-C stretch), 1254 (m, C-O-C stretch), 1130 (s, C-O-C stretch), 1085 (s, C-O-C stretch), 1052 (s, C-O-C stretch), 1003 (m, C-O-C stretch), 946 (m, C-O-C stretch), 930 (m, C-O-C stretch), 915 (m, C-O-C stretch), 855 (m, C-O-C stretch), 797 (w, -CH_2 bend), 762 (m, -CH_2 bend). **RAMAN ν/cm^{-1} =** n.d.

5.3.2 Poly(ethoxyethyl glycidyl ether-*co*-allyl glycidyl ether) (P(EEGE-*co*-AGE))

Scheme 5.3.2: Synthesis of P(EEGE-*co*-AGE).

EEGE, AGE and KO^{t}Bu were mixed in a flask in the glovebox. A yellow solution was obtained and stirred at 60 °C for 24 h. The solution turned brown and the polymerisation was terminated by adding a few drops of EtOH with subsequent stirring at RT for 10 min. A crude ^{1}H NMR was measured in $CDCl_3$ to determine the monomer conversion. THF and EtOH were removed under reduced pressure. For analysis, 200 mg of the product was dried at 60 °C under high vacuum for 1 day and was obtained as a brown viscous liquid.

Table 5.3.2-1: Compounds/yields in the synthesis of P(EEGE-*co*-AGE).

Run	**1**	**2**	**3**	**4**
EEGE:AGE/%	95:5	90:10	85:15	80:20
[EEGE]:[AGE]:[KO^{t}Bu]	57:3:1	54:6:1	51:9:1	48:12:1
EEGE				
m/g	14.273	13.522	12.771	12.020
V/mL	14.273	13.522	12.771	12.020
n/mmol	97.641	92.502	87.363	82.224
Eq	57	54	51	48
AGE				
m/g	0.587	1.173	1.760	2.346
V/mL	0.606	1.211	1.816	2.421
n/mmol	5.139	10.278	15.417	20.556
Eq	3	6	9	12
KO^{t}Bu				
m/g	0.296	0.296	0.296	0.296
V/mL	1.713	1.713	1.713	1.713
n/mmol	1.713	1.713	1.713	1.713
Eq	1	1	1	1
Conversion/%	100	100	100	100
Yield/g	15.2	15.0	14.8	14.0

^{1}H NMR (300 MHz, $CDCl_3$) δ/ppm = 5.94-5.81 (m, 1*n*H, H-10), 5.25 (d, 1*n*H, H-12, *J* = 18 Hz), 5.15 (d, 1*n*H, H-11, *J* = 9 Hz), 4.69 (q, 1*m*H, H-6, *J* = 6 Hz; bs, 1 H, H-13), 3.98 (d, 2*n*H, H-9, *J* = 6 Hz), 3.69-3.40 (m, 5(*m*+*n*)H, H-2 – H4; m, 2*m*H, H-7), 1.28 (d, 3*m*H, H-5, *J* = 6 Hz), 1.18 (t, 3*m*H, H-8, *J* = 9 Hz; s, 9 H, H-1).

GPC (DMF, RI):

Table 5.3.2-2: GPC data of series of P(EEGE-*co*-AGE).

Run	**1**	**2**	**3**	**4**
M_n/Da	2,061	2,142	2,020	2,173
M_w/Da	2,305	2,399	2,318	2,484
Đ	1.12	1.12	1.15	1.14

FT-IR ν/cm^{-1} = 2977 (m, -CH_3 & C-H stretch), 2930 (m, -CH_2 & C-H stretch), 2874 (m, -CH_3 & C-H stretch), 1456 (m, -CH_2 & -CH_3 bend), 1446 (m, -CH_2 & -CH_3 bend), 1379 (m, -CH_3 bend), 1340 (m, C-O-C stretch), 1300 (w, C-O-C stretch), 1272 (w, C-O-C stretch), 1129 (s, C-O-C stretch), 1082 (s, C-O-C stretch), 1054 (s, C-O-C stretch), 999 (m, C-O-C stretch), 945 (m, C-O-C stretch), 929 (m, C-O-C stretch), 874 (m, C-O-C stretch), 816 (w, C-O-C stretch). **RAMAN ν/cm^{-1} =** 2980 (m, C-H stretch), 2936 (s, C-H stretch), 2874 (s, C-H stretch), 2801 (w, C-H stretch), 1646 (w, C=C stretch), 1455 (m, -CH_2 bend), 1401 (w, -CH_2 & -CH_3 bend), 1349 (w, C-C stretch), 1276 (m, C-O-C stretch), 1138 (m, C-O-C stretch), 1096 (m, C-O-C stretch), 1027 (w, C-O-C stretch), 1005 (w, C-O-C stretch), 918 (m, C-O-C stretch), 876 (m, C-O-C stretch), 832 (m, C-O-C stretch), 811 (m, C-O-C stretch), 753 (w, C-O-C stretch), 670 (w, C-C stretch), 527 (m, C-C stretch), 354 (w, C-C bend), 271 (w, C-C bend).

5.3.3 Poly(glycidol-*co*-allyl glycidyl ether) (P(G-*co*-AGE))

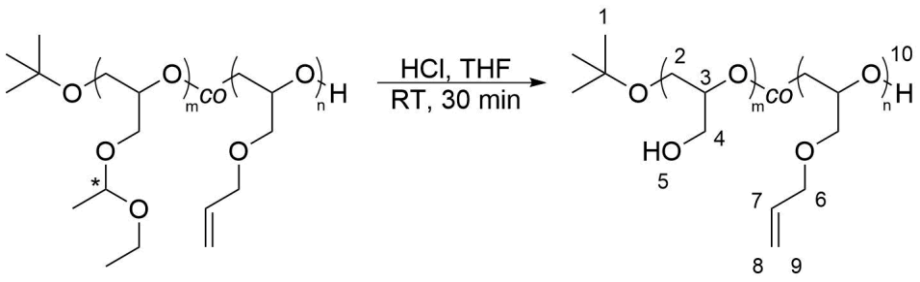

Scheme 5.3.3: Synthesis of P(G-*co*-AGE).

P(EEGE-*co*-AGE) was dissolved in THF and conc. HCl was added dropwise while stirring. The yellow solution became colourless and was stirred at RT for 30 min. A yellow oil

precipitated and the solvent was removed *via* decantation. The polymer was dissolved in H_2O and dialysed against H_2O for 3 d by changing solvent twice a day, using dialysis tubes with MWCO = 1 kDa. After freeze drying, the polymer was obtained as a clear sticky solid.

Table 5.3.3-1: Compounds/yields in the synthesis of P(G-*co*-AGE).

Run	**1**	**2**	**3**	**4**
EEGE:AGE/%	95:5	90:10	85:15	80:20
RU (EEGE:AGE)	57:3	54:6	51:9	48:12
m (P(EEGE-*co*-AGE))/g	15.2	15.0	14.8	14.0
V (HCl)/mL	16.8	16.0	15.1	12.0
V (THF)/mL	500	500	500	650
V (H_2O)/mL	150	150	150	200
Yield/g	3.406	4.546	4.392	3.271

^{1}H NMR (300 MHz, DMSO-d_6) δ/ppm = 5.94-5.81 (m, 1*n*H, H-7), 5.25 (d, 1*n*H, H-9, *J* = 18 Hz), 5.14 (d, 1*n*H, H-8, *J* = 9 Hz), 4.50 (bs, 1*m*H, H-5; bs, 1 H, H-10), 3.95 (d, 2*n*H, H-6, *J* = 6 Hz), 3.54-3.37 (m, 5(*m*+*n*)H, H-2 – H4), 1.12 (s, 9 H, 1-H).

GPC (DMF, RI):

Table 5.3.3-2: GPC data of series of P(G-*co*-AGE).

Run	**1**	**2**	**3**	**4**
M_n/Da	4,299	4,245	4,073	4,774
M_w/Da	5,380	4,641	4,452	5,443
Đ	1.25	1.09	1.09	1.14

FT-IR ν/cm^{-1} = 3363 (b, O-H stretch), 2923 (m, -CH_2 & C-H stretch), 2875 (m, C-H stretch), 1461 (m, -CH_2 bend), 1409 (m, -CH_2 bend), 1348 (m, C-O-C stretch), 1305 (m, C-O-C stretch), 1258 (m, C-O-C stretch), 1235 (m, C-O-C stretch), 1225 (m, C-O-C stretch), 1040 (s, C-O-C stretch), 919 (m, C-O-C stretch), 853 (m, C-O-C stretch). **RAMAN ν/cm^{-1} =** 2933 (s, C-H stretch), 2879 (s, C-H stretch), 1643 (m, C=C stretch), 1463 (m, -CH_2 bend), 1413 (w, -CH_2 & -CH_3 bend), 1349 (m, C-C stretch), 1287 (m, C-O-C stretch), 1257 (m, C-O-C stretch), 1124 (m, C-O-C stretch), 1067 (m, C-O-C stretch), 971 (w, C-O-C stretch), 907 (m, C-O-C stretch), 850 (m, C-O-C stretch), 751 (w, C-C stretch), 679 (w, C-C stretch), 473 (w, C-C bend).

5.3.4 Thiol modification of P(G-*co*-AGE) (P(G-*co*-SH))

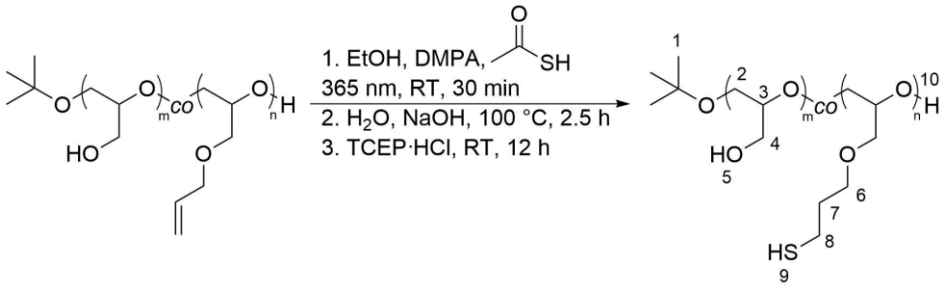

Scheme 5.3.4: Synthesis of P(G-*co*-SH).

P(G-*co*-AGE) (G:AGE = 54:6, 500 mg, 72.5 mg AGE, 0.636 mmol allyl groups, 1 eq), DMPA (81.5 mg, 0.318 mmol, 1 eq) and thioacetic acid (145 mg, 135.5 µL, 1.905 mmol, 3 eq) were dissolved in EtOH (50 mL). The solution was degassed by purging argon through the solution for 30 min and afterwards stirred under UV-light at 365 nm at RT for 30 min. The solution turned yellow and the solvent was removed under reduced pressure. The polymer was dissolved in EtOH (3 mL) and precipitated in cold diethyl ether (40 mL). After centrifugation and decantation, the polymer was dissolved in H_2O (25 mL) and NaOH (1.27 g, 31.75 mmol, 50 eq) was added. The solution was stirred at 100 °C for 2.5 h. After cooling to RT, the mixture was neutralised to pH = 7. TCEP·HCl (200 mg, 0.699 mmol, 1.1 eq) was added and the solution was stirred at RT for 12 h. The solution was dialysed against degassed H_2O for 3 d by changing solvent twice a day and using dialysis tubes with MWCO = 1 kDa. After freeze drying, the polymer was obtained as a yellow sticky solid (560 mg).

^{1}H NMR (300 MHz, DMSO-d_6) δ/ppm = 4.50 (bs, 1*m*H, H-5; bs, 1 H, H-10), 3.53-3.37 (m, 5(*m*+*n*)H, H-2 – H4; 2*n*H, H-6), 2.53 (q, 2*n*H, H-8, *J* = 6 Hz, overlap with solvent signal), 2.22 (t, 1*n*H, H-9, *J* = 6 Hz), 1.76 (quint, 2*n*H, H-7, *J* = 6 Hz), 1.12 (s, 9 H, H-1). **GPC (DMF, RI):** M_n = 3,418 Da, M_w = 4,504 Da, Đ = 1.32. **FT-IR ν/cm^{-1} =** 3372 (b, O-H stretch), 2921 (m, -CH_2 & C-H stretch), 2873 (m, C-H stretch), 2557 (w, S-H stretch), 1460 (m, -CH_2 & -CH_3 bend), 1406 (m, -CH_2 & -CH_3 bend), 1348 (m, C-O-C stretch), 1303 (m, C-O-C stretch), 1257 (m, C-O-C stretch), 1226 (m, C-O-C stretch), 1039 (s, C-O-C stretch), 914 (m, C-O-C stretch), 855 (m, C-O-C & C-S stretch). **RAMAN ν/cm^{-1} =** 2926 (s, C-H stretch), 2881 (s, C-H stretch), 2567 (m, S-H stretch), 1459 (m, -CH_2 bend), 1346 (m, C-C stretch), 1257 (m, C-O-C stretch), 1069 (m, C-O-C stretch), 973 (w, C-O-C stretch), 902 (m, C-O-C stretch), 850 (m, C-O-C stretch), 751 (w, C-S stretch), 655 (m, C-C stretch), 493 (w, C-C bend).

5.4 Electrolyte functionalised polyglycidols

5.4.1 1-Methyl-3-(3-propanethiol)-imidazolium chloride

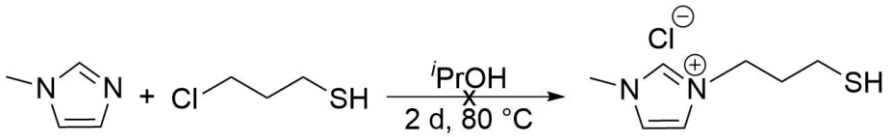

Scheme 5.4.1: Synthesis of 1-methyl-3-(3-propanethiol)-imidazolium chloride.

1-Methylimidazole (1 g, 966 µL, 12.18 mmol, 1 eq) and 3-chloro-1-propanethiol (1.347 g, 1.186 mL, 12.18 mmol, 1 eq) were dissolved in isopropanol (15 mL) under inert atmosphere. The mixture was stirred for 2 d at 80 °C. Afterwards, the solvent was removed under reduced pressure and the residue was washed with EtOAc (2 x 20 mL). After decantation, the residue was dissolved in chloroform and dried under high vacuum. The yellow oil (380 mg) was analysed *via* ^{1}H NMR in $CDCl_3$ and found to be impure with 1-methylimidazole and the oxidised disulfide form.

5.4.2 Chloride modification of P(G-*co*-AGE) (P(G-*co*-Cl))

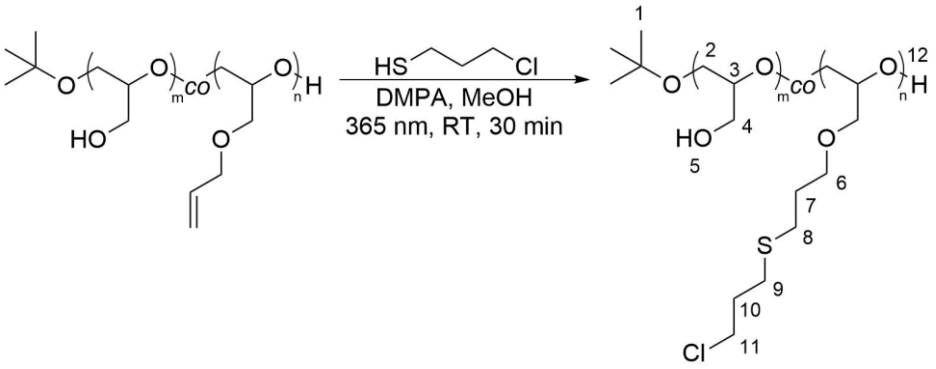

Scheme 5.4.2: Synthesis of P(G-*co*-Cl).

P(G-*co*-AGE), 3-chloro-1-propanethiol and DMPA were dissolved in MeOH. The solution was degassed with argon for 30 min and stirred at RT for 30 min under UV-light. Afterwards, the solution was dialysed against MeOH for 3 d by changing solvent once a day and using dialysis tubes with MWCO = 1 kDa. MeOH was removed *via* rotary evaporator and the polymer was dried at 60 °C for 1 day. The polymer was obtained as a yellow viscous liquid.

Table 5.4.2-1: Compounds/yields in the synthesis of P(G-*co*-Cl).

Run	**1**	**2**	**3**	**4**
EEGE:AGE/%	95:5	90:10	85:15	80:20
RU (G:AGE)	57:3	54:6	51:9	48:12
P(G-*co*-AGE)				
m/g	1.678	2.246	2.171	1.600
m (AGE)/mg	125.9	328.2	464.6	445
n (AGE)/mmol	1.103	2.875	4.070	3.899
Eq	1	1	1	1
Thiol-compound				
m/mg	366	994	1350.5	1.294
V/mL	0.322	0.875	1.189	1.139
n/mmol	3.309	8.625	12.21	11.697
Eq	3	3	3	3
DMPA				
m/mg	141	368	522	500
n/mmol	0.5515	1.4375	2.035	1.950
Eq	0.5	0.5	0.5	0.5
V (MeOH)/mL	55	75	70	50
Yield/g	1.173	1.951	1.864	1.212

^{1}H NMR (300 MHz, DMSO-d_6) δ/ppm = 4.50 (bs, 1*m*H, H-5; bs, 1 H, H-12), 3.70 (t, 2*n*H, H-11, *J* = 6 Hz), 3.72-3.33 (m, 5(*m*+*n*)H, H-2 – H4; 2*n*H, H-6), 2.58 (2t, 4*n*H, H-8, H-9, *J* = 6 Hz, overlap with solvent signal)**,** 1.95 (quint, 2*n*H, H-10, *J* = 6 Hz)**,** 1.74 (quint, 2*n*H, H-7, *J* = 6 Hz)**,** 1.12 (s, 9 H, H-1).

GPC (DMF, RI):

Table 5.4.2-2: GPC data of series of P(G-*co*-Cl).

Run	1	2	3	4
M_n/Da	4,543	4,622	4,525	5,633
M_w/Da	5,930	5,447	5,748	9,048
Đ	1.31	1.18	1.27	1.61

FT-IR ν/cm^{-1} = 3359 (b, O-H stretch), 2931 (m, -CH_2 & C-H stretch), 2874 (m, C-H stretch), 1458 (m, -CH_2 bend), 1417 (m, -CH_2 bend), 1347 (m, C-O-C stretch), 1307 (m, C-O-C stretch), 1265 (m, C-O-C stretch), 1223 (m, C-O-C stretch), 1041 (s, C-O-C stretch), 913 (m, C-O-C stretch), 855 (m, C-O-C & C-S stretch). **RAMAN ν/cm^{-1} =** 2922 (s, C-H stretch), 2883 (s, C-H stretch), 1459 (m, -CH_2 bend), 1421 (m, -CH_2 bend), 1348 (m, C-C stretch), 1301 (m, C-C stretch), 1261 (m, C-O-C stretch), 1126 (m, C-O-C stretch), 1064 (m, C-O-C stretch), 748 (w, C-S stretch), 651 (m, C-C & C-Cl stretch), 474 (w, C-C bend), 226 (w, C-C bend).

5.4.3 Imidazolium modification of P(G-*co*-Cl) P(G-*co*-Im)

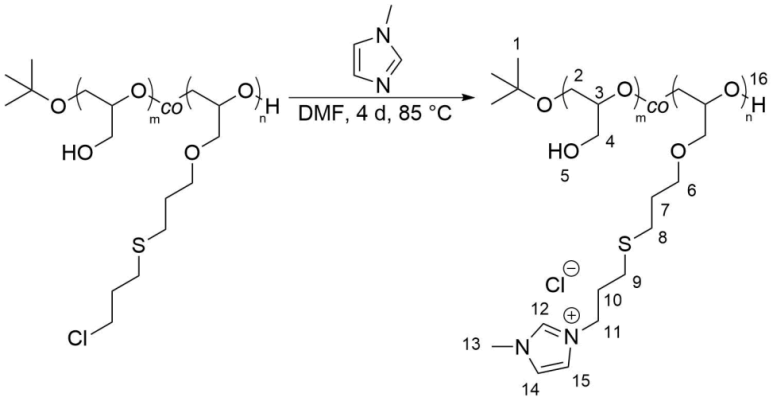

Scheme 5.4.3: Synthesis of P(G-*co*-Im).

The chloride functionalised polyglycidol and 1-methylimidazole were dissolved in DMF. The solution was heated at 85 °C for 4 d. H_2O (30 mL) was added afterwards. The solution was dialysed against H_2O for 3 d by changing solvent twice a day and using dialysis tubes with MWCO = 1 kDa. After freeze drying, the polymer was obtained as a yellow sticky solid.

Table 5.4.3-1: Compounds/yields in the synthesis of P(G-*co*-Im).

Run	**1**	**2**	**3**	**4**
G:Cl/%	95:5	90:10	85:15	80:20
RU (G:Cl)	57:3	54:6	51:9	48:12
P(G-*co*-Cl)				
m/g	1.123	1.899	1.814	0.894
m (Cl-monomer)/mg	155.0	478.5	633.1	386.2
n (Cl-monomer)/mmol	0.690	2.129	2.817	1.718
Eq	1	1	1	1
1-Methylimidazole				
m/g	1.133	3.496	4.626	2.821
V/mL	1.095	3.378	4.470	2.726
n/mmol	13.8	42.58	56.34	34.36
Eq	20	20	20	20
V (DMF)/mL	22.46	37.98	36.28	17.88
Yield/mg	272	271	273	273

^{1}H NMR (300 MHz, DMSO-d_6) δ/ppm = 9.14 (bs, 1*n*H, H-12)**,** 7.79-7.71 (m, 2*n*H, H-14, H-15)**,** 4.55 (bs, 1*m*H, H-5; bs, 1 H, H-16)**,** 4.31-4.24 (m, 2*n*H, H-11)**,** 3.85 (s, 3*n*H, H-13)**,** 3.54-3.37 (m, 5(*m*+*n*)H, H-2 – H4; 2*n*H, H-6), 2.77-2.68 (m, 4*n*H, H-8, H-9)**,** 2.05 (quint, 2*n*H, H-10, *J* = 6 Hz), 1.75 (quint, 2*n*H, H-7, *J* = 6 Hz), 1.12 (s, 9 H, H-1).

GPC (DMF, RI):

Table 5.4.3-2: GPC data of series of P(G-*co*-Im).

Run	**1**	**2**	**3**	**4**
M_n/Da	4,560	3,955	3,308	1,824
M_w/Da	5,953	5,138	3,931	2,362
Đ	1.31	1.30	1.19	1.30

FT-IR ν/cm^{-1} = 3356 (b, O-H stretch), 3112 (w, =C-H stretch), 2931 (m, -CH_2 & C-H stretch), 2872 (m, C-H stretch), 1597 (m, aromatic ring vibration), 1575 (m, C=C stretch), 1460 (m, -CH_2 & -CH_3 bend & C=C stretch), 1393 (w, -CH_3 bend), 1347 (m, C-O-C & C-N stretch), 1300 (m, C-O-C & C-N stretch), 1263 (m, C-O-C & C-N stretch), 1223 (m, C-O-C & C-N stretch), 1041 (s, C-O-C & C-N stretch), 913 (m, C-O-C stretch), 851 (m, C-O-C & C-S stretch). **RAMAN ν/cm^{-1} = n.d.**

5.4.4 Bis(diethylphosphonamide)disulfide

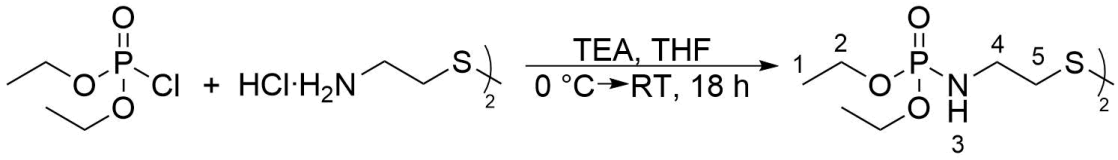

Scheme 5.4.4: Synthesis of bis(diethylphosphonamide)disulfide.

A solution of diethyl chlorophosphate (4.74 g, 3.97 mL, 27.468 mmol, 2.1 eq) in THF (30 mL) was added dropwise to a cooled suspension of cystamine dihydrochloride (2.947 g, 13.08 mmol, 1.0 eq) and TEA (5.823 g, 8.0 mL, 57.552 mmol, 4.4 eq) in THF (60 mL) under inert atmosphere. The mixture was allowed to cool to RT the resumed stirring for 18 h. After filtration, the solvent was removed under reduced pressure. The product was purified *via* column chromatography (SiO_2, EtOAc:MeOH = 4:1 (v/v), R_f = 0.50), dried under high vacuum and obtained as a yellow solid (3.951 g, 9.309 mmol, 71 %).

^{1}H NMR (300 MHz, DMSO-d_6) δ/ppm = 5.05 (m, 1 H, H-3), 3.90 (m, 4 H, H-2), 3.03 (m, 2 H, H-4), 2.74 (t, 2 H, H-5, *J* = 6 Hz), 1.21 (t, 6 H, H-1, *J* = 6 Hz). **^{13}C NMR (75 MHz, DMSO-d_6) δ/ppm =** 61.30/61.23 (C-2)$^{\#}$, 39.51 (C4, C-5, overlap with solvent peak), 16.13/16.04 (C-1)$^{\#}$, $^{\#}$Splitting due to partial hydrolysis. **^{31}P{^{1}H} NMR (162 MHz, DMSO-d_6) δ/ppm =** 9.31, 0.07$^{\#}$, #Hydrolysed form (1.4 %). **MS (ASAP) m/z =** 425.1081, calculated $[M+H]^+$: 425.1099. **FT-IR ν/cm^{-1} =** 3180 (b, N-H stretch), 2979 (m, -CH_3, -CH_2 & C-H stretch), 2905 (m, C-H stretch), 1463 (m, -CH_2 bend), 1396 (m, -CH_3 bend), 1367 (w, -CH_3 bend), 1353 (w, C-N & C-O-P stretch), 1293 (m, C-N & C-O-P stretch), 1226 (s, P=O stretch), 1179 (m, C-N & C-O-P stretch), 1164 (m, C-N & C-O-P stretch), 1117 (m, C-N & C-O-P stretch), 1029 (s, C-N & C-O-P stretch), 961 (s, P-O stretch), 905 (m, C-O-P stretch), 883 (m, C-O-P stretch), 802 (m, C-S stretch), 768 (m, -CH_2 bend). **RAMAN ν/cm^{-1} = n.d.**

5.4.5 Diethylphosphonamide modification of P(G-*co*-AGE) (P(G-*co*-POEt))

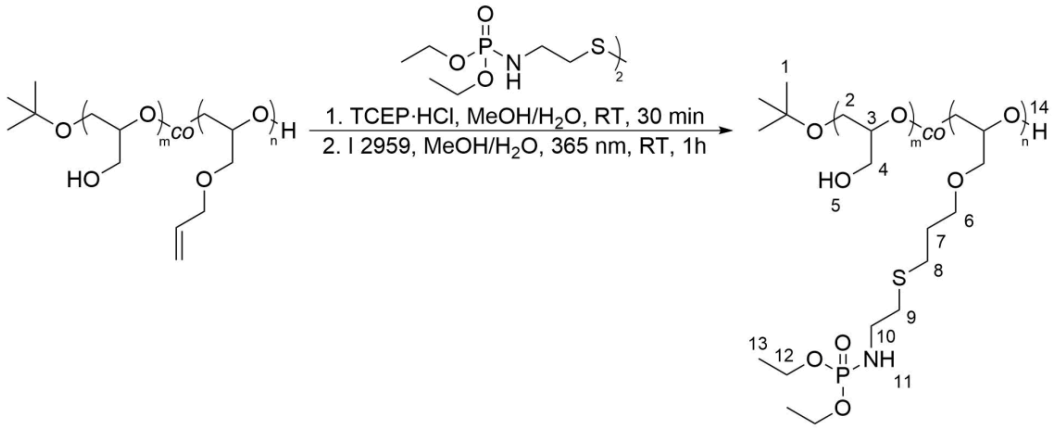

Scheme 5.4.5: Synthesis of P(G-*co*-POEt).

The protected phosphonamide linker was dissolved in MeOH and tris(2-carboxyethyl)phosphine hydrochloride was dissolved in H_2O. Both solutions were mixed and stirred at RT for 30 min. Afterwards, a solution of P(G-*co*-AGE) in H_2O/MeOH (v/v = 1:1) and I 2959 were added. The mixture was degassed with argon for 30 min and stirred at RT for 1 h under UV-light. The solution was dialysed against H_2O for 3 d by changing solvent twice a day and using dialysis tubes with MWCO = 1 kDa. After freeze drying, the polymer was obtained as a yellow viscous liquid.

Table 5.4.5-1: Compounds/yields in the synthesis of P(G-*co*-POEt).

Run	**1**	**2**	**3**	**4**
EEGE:AGE/%	95:5	90:10	85:15	80:20
RU (G:AGE)	57:3	54:6	51:9	48:12
P(G-*co*-AGE)				
m/g	1.678	2.248	2.171	1.666
m (AGE)/mg	125.9	328.2	464.6	463.2
n (AGE)/mmol	1.103	2.875	4.070	4.058
Eq	1	1	1	1
Disulfide-compound				
m/g	0.702	1.830	2.591	2.584
n/mmol	1.655	4.313	6.105	6.087
Eq	1.5	1.5	1.5	1.5
TCEP·HCl				
m/g	0.474	1.236	1.750	1.745
n/mmol	1.655	4.313	6.105	6.087
Eq	1.5	1.5	1.5	1.5

I 2959				
m/mg	124	322	456	455
n/mmol	0.552	1.438	2.035	2.029
Eq	0.5	0.5	0.5	0.5
V (MeOH)/mL	85	115	110	85
V (H_2O)/mL	85	110	110	85
Yield/g	0.645	1.232	1.209	1.291

^{1}H NMR (300 MHz, DMSO-d_6) δ/ppm = 4.99-4.91 (m, 1*n*H, H-11), 4.50 (bs, 1*m*H, H-5; bs, 1 H, H-14), 3.95-3.85 (m, 2*n*H, H-12), 3.53-3.37 (m, 5(*m*+*n*)H, H-2 – H4; 2*n*H, H-6), 2.96-2.85 (m, 2*n*H, H-10), 2.53 (2t, 4*n*H, H-8, H-9, *J* = 6 Hz, overlap with solvent signal), 1.73 (quint, 2*n*H, H-7, *J* = 6 Hz), 1.21 (t, 2*n*H, H-13, *J* = 6 Hz), 1.12 (s, 9 H, H-1). **^{31}P{^{1}H} NMR (162 MHz, DMSO-d_6) δ/ppm =** 9.43.

GPC (DMF, RI):

Table 5.4.5-2: GPC data of series of P(G-*co*-POEt).

Run	**1**	**2**	**3**	**4**
M_n/Da	4,355	4,283	3,960	5,026
M_w/Da	5,080	4,989	4,590	6,091
Đ	1.17	1.17	1.16	1.21

FT-IR ν/cm^{-1} = 3352 m (b, O-H & N-H stretch), 2933 (m, -CH_3, -CH_2 & C-H stretch), 2875 (m, C-H stretch), 1457 (m, -CH_2 bend), 1414 (w, -CH_2 & -CH_3 bend), 1394 (m, -CH_3 bend), 1349 (m, C-O-C & C-N stretch), 1301 (m, C-O-C & C-N stretch), 1215 (m, C-O-C & C-O-P & C-N & P=O stretch), 1039 (s, C-O-C & C-O-P & C-N stretch), 973 (m, C-O-C & C-O-P & P-O stretch), 917 (w, C-O-C & C-O-P stretch), 797 (w, C-O-C stretch). **RAMAN ν/cm^{-1}** = 2933 (s, C-H stretch), 2884 (s, C-H stretch), 1462 (m, -CH_2 & -CH_3 bend), 1421 (m, -CH_2 & -CH_3 bend), 1352 (m, C-C stretch), 1300 (m, C-C stretch), 1261 (m, C-O-C stretch), 1081 (m, C-O-C stretch), 979 (w, C-O-C stretch), 905 (m C-O-C stretch), 859 (m, C-O-C stretch), 755 (m, C-S stretch), 684 (w, C-C stretch). 656 (w, C-C stretch), 497 (w, C-C bend), 337 (w, C-C bend), 229 (w, C-C bend).

5.4.6 Phosphonamide modification of P(G-*co*-POEt) (P(G-*co*-POH))

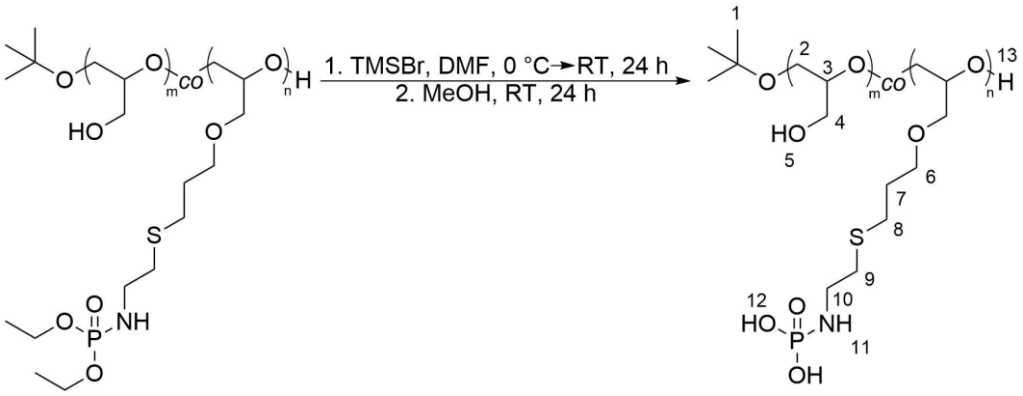

Scheme 5.4.6: Synthesis of P(G-*co*-POH).

The protected phosphonamide functionalised polyglycidol was dissolved in dry DMF. The solution was cooled to 0 °C and bromotrimethylsilane was added. The solution was stirred from 0 °C to RT for 24 h. The solvent was removed *via* rotary evaporator and the polymer was dissolved in MeOH. The mixture was stirred at RT for 24 h. The solvent was removed *via* rotary evaporator and the polymer was dissolved in H_2O. The solution was dialysed against H_2O for 3 d by changing solvent twice a day and using dialysis tubes with MWCO = 1 kDa. After freeze drying, the polymer was obtained as an orange sticky solid.

Table 5.4.6-1: Compounds/yields in the synthesis of P(G-*co*-POH).

Run	**1**	**2**	**3**	**4**
G:POEt/%	95:5	90:10	85:15	80:20
RU (G:POEt)	57:3	54:6	51:9	48:12
P(G-*co*-POEt)				
m/mg	595	1182	1159	400
m (POEt-monomer)/mg	112.5	338.9	507.6	210
n (POEt-monomer)/mmol	0.344	1.035	1.551	0.642
Eq	1	1	1	1
TMSBr				
m/g	1.580	3.169	4.749	1.966
V/mL	1.362	2.732	4.094	1.694
n/mmol	10.32	20.7	31.02	12.84
Eq	20	20	20	20
V (DMF)/mL	30	40	40	20
V (MeOH)/mL	60	80	80	40
Yield/mg	262	456	483	156

^{1}H NMR (300 MHz, DMSO-d_6) δ/ppm = 4.52 (bs, 1*m*H, H-5; 1*n*H, H-11; 2*n*H, H-12; 1 H, H-13), 3.54-3.37 (m, 5(*m*+*n*)H, H-2 – H4; 2*n*H, H-6), 2.96 (m, 2*n*H, H-10), 2.69 (t, 2*n*H, H-9, *J* = 6 Hz), 2.57 (t, 2*n*H, H-8, *J* = 6 Hz), 1.75 (quint, 2*n*H, H-7, *J* = 6 Hz), 1.12 (s, 9 H, H-1). **^{31}P{^{1}H} NMR (162 MHz, DMSO-d_6) δ/ppm =** -0.10.

GPC (DMF, RI for 1-3; H_2O, RI for 4):

Table 5.4.6-2: GPC data of series of P(G-*co*-POH).

Run	**1**	**2**	**3**	**4**
M_n/Da	4,282	3,582	2,850	2,440
M_w/Da	4,850	4,194	3,708	2,883
Đ	1.13	1.17	1.30	1.18

FT-IR ν/cm^{-1} = 3347 (b, O-H & N-H stretch), 2923 (m, -CH_3, -CH_2 & C-H stretch), 2874 (m, C-H stretch), 1461 (m, -CH_2 bend), 1412 (m, -CH_2 bend), 1347 (m, C-O-C & C-N stretch), 1305 (m, C-O-C & C-N stretch), 1259 (m, C-O-C & C-N stretch), 1222 (m, C-O-C & C-N & P=O stretch), 1039 (s, C-O-C & C-N stretch), 981 (w, C-O-C & P-O stretch), 913 (m, C-O-C stretch), 852 (m, C-O-C stretch). **RAMAN ν/cm^{-1} =** n.d.

5.4.7 Gel tests

Polymers carrying phosphonamide groups (solution 1) and polymers carrying imidazolium groups (solution 2) were dissolved. Both solutions were stirred at RT for 18 h, then combined to give equimolar ratio of functional groups with a total amount of 20 mg of polymer and stirred again at RT for 18 h. Note: V (solution 1) = V (solution 2) = 0.5·V_{total} (solvent).

Table 5.4.7: Compounds for gel tests.

RU (G:Im)	**m/mg**	**RU (G:POH)**	**m/mg**
57:1.2	10.4	57:3	9.6
54:4.0	10.6	54:6	9.4
51:8.3	12.0	51:9	8.0
48:11.6	14.3	48:12	5.7
w/w (polymer) / %	10	20	30
V_{total} (solvent) / µL	180	80	46.7

Solvent for 10 wt-%: H_2O and buffer solutions with pH = 4.0, 7.0, 7.4 and 10.0. Solvent for 20 and 30 wt-%: H_2O.

5.5 π–π Functionalised polyglycidols

5.5.1 Bis(1-pyrenebutyric)cystamide

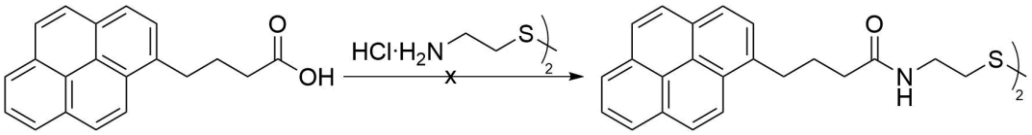

Scheme 5.5.1: Synthesis of bis(1-pyrenebutyric)cystamide.

1: 1-Pyrenebutyric acid (250 mg, 0.867 mmol, 2.2 eq) was dissolved in DMF (2 mL). CDI (154.5 mg, 0.953 mg, 2.42 mmol) was added and the solution was stirred at RT for 90 min. CA·2 HCl (44.8 mg, 0.394 mmol, 1.0 eq) and TEA (87.7 mg, 120 µL, 0.867 mmol, 2.2 eq) were added and the solution was stirred at 60 °C for 18 h. After cooling to RT, the solvent was removed under reduced pressure. The residue was dissolved in $CHCl_3$ (10 mL), washed with sat. NaCl solution (3 x 10 mL) and dried over $MgSO_4$. After filtration, the solvent was removed under reduced pressure. The product was purified *via* column chromatography (SiO_2, DCM:MeOH = 98:2 (v/v), R_f = 0.2). A yellow solid was obtained (78 mg).

2: 1-Pyrenebutyric acid (290 mg, 1.0 mmol, 1.0 eq) was suspended in dry DCM (2 mL). Oxalyl chloride in DCM (254 mg, 1 mL, 2.0 mmol, 2.0 eq) was added and the suspension was stirred at RT for 2 h. The solvent and remaining oxalyl chloride were removed under reduced pressure and the residue was dissolved in DCM (5 mL). CA·2 HCl (90 mg, 0.4 mmol, 0.4 eq) and TEA (304 mg, 0.42 mL, 3.0 mmol, 3.0 eq) were added and the solution was stirred at RT for 24 h. The solvent was removed under reduced pressure. The product could not be found after column chromatography with EtOAc.

3: DCC (220 mg, 1.066 mmol, 2.4 eq) and DMAP (22 mg, 0.178 mmol, 0.4 eq) were dissolved in THF (5 mL). CA·2 HCl (100 mg, 0.444 mmol, 1.0 eq) was added to give a white suspension. A solution of 1-pyrenebutyric acid (282 mg, 0.977 mmol, 2.2 eq) in THF (5 mL) was added dropwise to the suspension and was stirred at RT for 18 h. After filtration, the solvent was removed under reduced pressure. The product could not be isolated after column chromatography (SiO_2, DCM:MeOH = 98:2 (v/v), R_f = 0.2).

5.5.2 Carboxylic acid modification of P(G-*co*-AGE) (P(G-*co*-COOH))

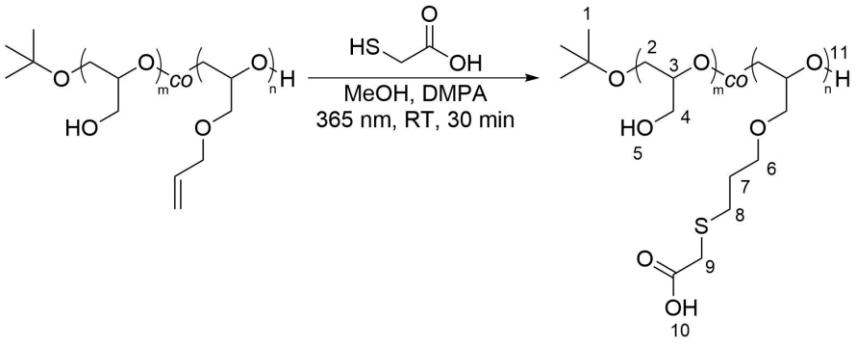

Scheme 5.5.2: Synthesis of P(G-*co*-COOH).

P(EEGE-*co*-AGE), thioglycolic acid and DMPA were dissolved in MeOH. The reaction mixture was degassed by purging argon through the solution for 30 min. The solution was stirred under UV-light at 365 nm at RT for 30 min. The solution turned yellow and the solvent was removed under reduced pressure. The residue was dissolved in H_2O and dialysed against H_2O for 3 d by changing solvent twice a day and using dialysis tubes with MWCO = 1 kDa. After freeze drying, the polymer was obtained as a yellow sticky solid.

Table 5.5.2-1: Compounds/yields in the synthesis of P(G-*co*-COOH).

Run	**1**	**2**
G:AGE/%	95:5	90:10
RU (G:AGE)	57:3	54:6
P(G-*co*-AGE)		
m/g	1.174	1.000
m (AGE)/mg	88.1	145.0
n (AGE)/mmol	0.771	1.270
Eq	1	1
Thiol-compound		
m/mg	213	351
V/µL	161.4	265.9
n/mmol	2.313	3.810
Eq	3	3
DMPA		
m/mg	99	162.8
n/mmol	0.386	0.635
Eq	0.5	0.5
V (MeOH)/mL	35	30
V (H_2O)/mL	50	100
Yield/mg	734	1005

^{1}H NMR (300 MHz, DMSO-d_6) δ/ppm = 4.51 (bs, 1*m*H, H-5; bs, 1 H, H-11), 3.54-3.37 (m, 5(*m*+*n*)H, H-2 – H4; 2*n*H, H-6), 3.21 (s, 2*n*H, H-9), 2.61 (t, 2*n*H, H-8, *J* = 6 Hz), 1.75 (quint, 2*n*H, H-7, *J* = 6 Hz), 1.12 (s, 9 H, H-1), H-10 not visible.

GPC (DMF, RI):

Table 5.5.2-2: GPC data of series of P(G-*co*-COOH).

Run	**1**	**2**
M_n/Da	2,926	2,103
M_w/Da	3,629	2,795
Đ	1.24	1.33

FT-IR ν/cm^{-1} = 3364 (b, O-H stretch), 2922 (m, -CH_2 & C-H stretch), 2874 (m, C-H stretch), 2652 (w, O-H stretch), 1717 (m, C=O stretch), 1587 (w, C=O stretch), 1460 (m, -CH_2 bend), 1405 (m, -CH_2 bend), 1348 (m, C-O-C stretch), 1296 (m, C-O-C stretch), 1223 (m, C-O-C stretch), 1039 (s, C-O-C stretch), 912 (m, C-O-C stretch), 857 (m, C-O-C & C-S stretch). **RAMAN ν/cm^{-1} =** 3046 (w, O-H stretch), 2931 (s, C-H stretch), 2883 (s, C-H stretch), 1712 (w, C=O stretch), 1596 (w, C=O stretch), 1462 (m, -CH_2 bend), 1347 (m, C-C stretch), 1305 (m, C-C stretch)**,** 1259 (m, C-O-C stretch), 1184 (w, C-O-C stretch), 1119 (m, C-O-C stretch), 1069 (m, C-O-C stretch), 997 (w, C-O-C stretch), 977 (w, C-O-C stretch), 901 (m, C-O-C stretch), 855 (m, C-O-C stretch), 767 (w, C-C stretch), 752 (w, C-C stretch), 675 (w, C-S stretch), 581 (w, C-C stretch), 465 (w, C-C bend), 426 (w, C-C bend), 214 (w, C-C bend).

5.5.3 Pyrene modification of P(G-*co*-COOH) (P(G-*co*-Pyr))

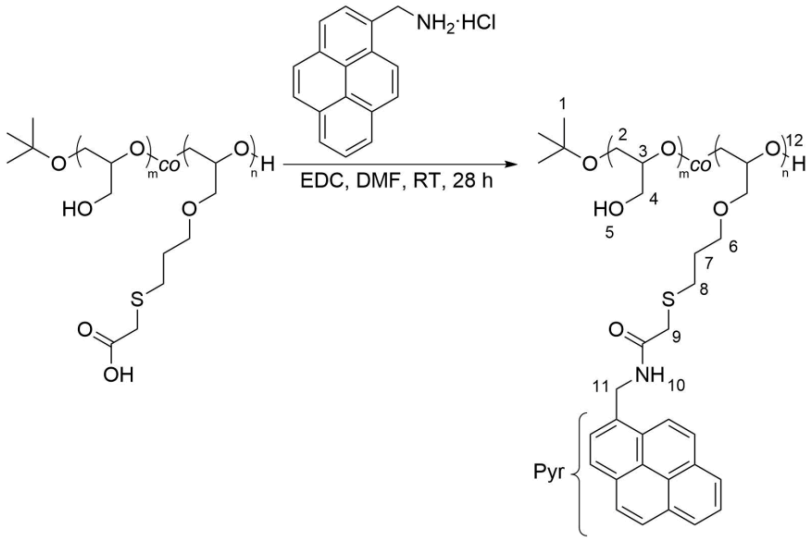

Scheme 5.5.3: Synthesis of P(G-*co*-Pyr).

P(G-*co*-COOH), 1-pyrenemethylamine hydrochloride and EDC were dissolved in DMF. The solution was stirred at RT for 28 h. The yellow solution was dialysed against H_2O for 3 d by changing solvent twice a day and using dialysis tubes with MWCO = 1 kDa. After freeze drying, the polymer was obtained as a yellow sticky solid.

Table 5.5.3-1: Compounds/yields in the synthesis of P(G-*co*-Pyr).

Run	**1**	**2**
G:COOH/%	95:5	90:10
RU (G:COOH)	57:3	54:6
P(G-*co*-COOH)		
m/mg	713	217
m (COOH-monomer)/mg	91.3	51.2
n/mmol	0.443	0.248
Eq	1	1
EDC		
m/mg	255	143
n/mmol	1.329	0.744
Eq	3	3
1-pyrenemethylamine hydrochloride		
m/mg	356	199
n/mmol	1.329	0.744
Eq	3	3
V (DMF)/mL	35.65	10.85
Yield/mg	322	163

^{1}H NMR (300 MHz, DMSO-d_6) δ/ppm = 8.66 (bt, 1*n*H, H-10), 8.35-8.05 (m, 9*n*H, H-Pyr), 5.02 (bt, 2*n*H, H-11), 4.50 (bs, 1*m*H, H-5; bs, 1 H, H-12), 3.53-3.33 (m, 5(*m*+*n*)H, H-2 – H4; 2*n*H, H-6), 3.19 (s, 2*n*H, H-9), 2.59 (bt, 2*n*H, H-8), 1.71 (bquint, 2*n*H, H-7), 1.12 (bs, 9 H, H-1).

GPC (DMF, RI):

Table 5.5.3-2: GPC data of series of P(G-*co*-Pyr).

Run	**1**	**2**
M_n/Da	5,692	5,830
M_w/Da	8,551	10,922
Đ	1.50	1.87

FT-IR ν/cm^{-1} = 3359 (b, O-H & N-H stretch), 3048 (w, =C-H stretch), 2934 (m, -CH_2 & C-H stretch), 2873 (m, C-H stretch), 1726 (m, C=O stretch), 1649 (m, C=O & C=C stretch), 1536 (m, N-H bend, aromatic ring), 1457 (m, -CH_2 bend), 1415 (m, -CH_2 bend), 1348 (m, C-O-C & C-N stretch), 1299 (m, C-O-C & C-N stretch), 1264 (w, C-O-C & C-N stretch), 1219 (w, C-O-C & C-N stretch), 1041 (s, C-O-C & C-N stretch), 912 (m, C-O-C & C-N stretch), 847 (m, C-O-C, C-S & C-N stretch, =C-H bend), 757 (w, =C-H bend). **RAMAN ν/cm^{-1} =** n.d.

5.5.4 *n*-Propyl naphthalene monoimide (*n*Pr-NMI)

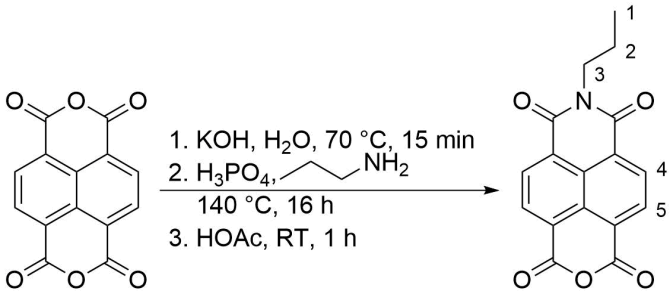

Scheme 5.5.4: Synthesis of *n*Pr-NMI.

1,4,5,8-Naphthalenetetracarboxylic dianhydride (1.000 g, 3.729 mmol, 1 eq) was suspended in H_2O (175 mL) and ultra-sonicated for 10 min. 1 M KOH solution (20 mL) was added to the grey suspension which was stirred at 70 °C for 15 min. The solution turned black. A few drops of 1 M H_3PO_4 (pH = 6), then *n*-propylamine (0.220 g, 306 µL, 3.729 mmol, 1 eq) (pH = 10), then again a few drops of 1 M H_3PO_4 was added dropwise to the solution to keep the pH value at 6 in the end. The solution was stirred at 140 °C for 16 h. After cooling to RT, the solution was filtered. Conc. HOAc (2.5 mL) was added dropwise to the filtrate and kept stirring for 30 min. A grey precipitate that formed was filtered and washed with H_2O (10 mL). After drying at 40 °C under high vacuum, the product was obtained as a grey solid (660 mg, 2.134 mmol, 57 %).

^{1}H NMR (300 MHz, DMSO-d_6) δ/ppm = 8.52 (d, 2 H, H-5, *J* = 9 Hz), 8.10 (d, 2 H, H-4, *J* = 9 Hz), 4.01 (t, 2 H, H-3, *J* = 6 Hz), 1.67 (sext, 2 H, H-2, *J* = 6 Hz), 0.93 (t, 3 H, H-1, *J* = 6 Hz). **^{13}C NMR (75 MHz, DMSO-d_6) δ/ppm =** 169.29 (anhydride carbonyl), 163.04 (imide carbonyl), 130.13/128.52/128.35/125.52/123.67 (naphthalene ring), 39.52 (C-3, overlap with solvent-signal), 20.81 (C-2), 11.38 (C-1). **MS (ASAP) m/z =** 310.0695, calculated $[M+H]^+$: 310.0715. **FT-IR ν/cm^{-1} =** 2964 (m, -CH_3 stretch), 2935 (m, -CH_2 & C-H stretch), 2876 (m, -CH_3 stretch), 2603 (m, C-H stretch), 2532 (m, C-H stretch), 1700 (s, C=O stretch), 1655 (s, C=C stretch), 1561 (m, aromatic ring), 1441 (m, -CH_2 & -CH_3 bend), 1374 (m, -CH_3 bend), 1346 (m, C-O-C & C-N stretch), 1323 (m, C-O-C & C-N stretch), 1289 (m,

C-O-C & C-N stretch), 1269 (s, C-O-C & C-N stretch), 1196 (s, C-O-C & C-N stretch), 1158 (w, C-O-C & C-N stretch), 1132 (w, C-O-C & C-N stretch), 1079 (m, C-O-C & C-N stretch), 946 (m, C-O-C & C-N stretch), 877 (m, C-O-C & C-N stretch), 822 (w, =C-H bend), 803 (m, =C-H bend), 763 (s, =C-H bend), 690 (w, =C-H bend), 680 (w, =C-H bend). **RAMAN ν/cm^{-1}** = n.d.

5.5.5 Bis(*n*-propyl naphthalene)cystdiimide (*n*Pr-CA-NDI)

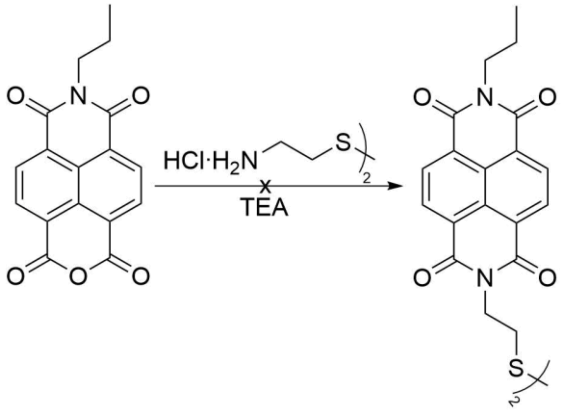

Scheme 5.5.5: Synthesis of *n*Pr-CA-NDI.

*n*Pr-NMI, CA·2 HCl and TEA were suspended in DMF or DMSO and stirred under high temperatures, cooled afterwards to RT and was tried to be purified in different ways but no pure product could be isolated:

1: 0.1 M HCl (30 mL) was added and the product was extracted with EtOAc (3 x 50 mL). The organic phase was washed with sat. NaCl solution (3 x 150 mL) and dried over $MgSO_4$, filtered and solvent was removed under reduced pressure. An orange solid was obtained.

2: The solvent was removed under reduced pressure and a black solid remained which was suspended in DCM (20 mL). After filtration, the solvent was reduced under reduced pressure and the solid was purified *via* column chromatography (SiO_2, DCM:MeOH = 97:3 → 90:10 (v/v), R_f = 0.08). A black solid was obtained.

3: The reaction mixture was added dropwise into H_2O (30 mL) during stirring and a brown solid precipitated. After filtration, the solid was washed with H_2O (3 x 30 mL). A brown solid was obtained.

4: Extraction in diethyl ether failed. After removing diethyl ether under reduced pressure, the reaction mixture was added dropwise into H_2O (50 mL) during stirring and a black solid precipitated. After filtration, the precipitate was dissolved in DCM (30 mL), washed with H_2O

(2 x 30 mL), sat. NaCl solution (1 x 30 mL) and dried over $MgSO_4$. A brown solid was obtained.

Table 5.5.5: Compounds/yields in the synthesis of *n*Pr-CA-NDI.

Run	**1**	**2**	**3**	**4**
***n*Pr-NMI**				
m/mg	100	200	100	150
n/mmol	0.324	0.647	0.324	0.485
Eq	2.5	2.5	2.5	2.5
CA·2 HCl				
m/mg	29	58	29	43.7
n/mmol	0.130	0.259	0.130	0.194
Eq	1.0	1.0	1.0	1.0
TEA				
m/mg	26	65	26	49.1
V/µL	35.6	89.0	35.6	67.3
n/mmol	0.260	0.647	0.260	0.485
Eq	2.0	2.5	2.0	2.5
Solvent	5 mL DMF	5 mL DMF	2.5 mL DMSO	10 mL DMSO
Reaction Temperature/°C	120	120	140	140
Reaction time/h	19	20	48	48
Yield/mg	13	25	9	14

5.5.6 *n*-Propyl allyl naphthalene diimide (*n*Pr-Allyl-NDI)

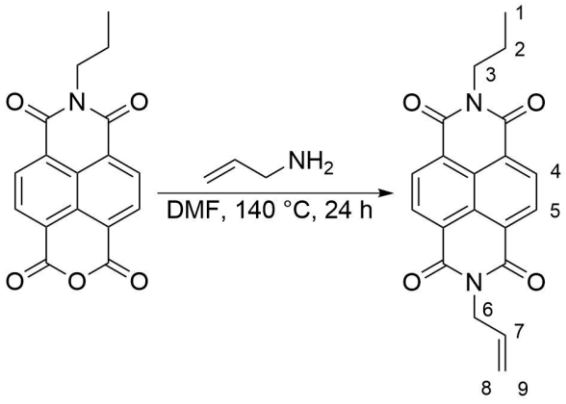

Scheme 5.5.6: Synthesis of *n*Pr-Allyl-NDI.

nPr-NDI (528 mg, 1.705 mmol, 1 eq) was suspended in DMF (7.92 mL) and ultra-sonicated at RT for 5 min. Allylamine (195 mg, 257 µL, 3.410 mmol, 2 eq) was added to the grey

suspension and the solution turned black. The solution was stirred at 140 °C for 24 h. After cooling to RT, the solution was filtered. The solvent was removed under reduced pressure and the residue was dissolved in DCM (100 mL), washed with sat. NaCl solution (4 x 100 mL) and dried over $MgSO_4$. After removing the solvent, the product was dried at 60 °C for 1 day and was obtained as a black solid (253 mg, 0.726 mmol, 43 %).

^{1}H NMR (300 MHz, $CDCl_3$) δ/ppm = 8.76 (s, 4 H, H-4, H-5), 5.99 (m, 1 H, H-7), 5.36 (d, 1 H, H-8, *J* = 18 Hz), 5.25 (d, 1 H, H-9, *J* = 12 Hz), 4.82 (d, 2 H, H-6, *J* = 6 Hz), 4.17 (t, 2 H, H-3, *J* = 9 Hz), 1.77 (sext, 2 H, H-2, *J* = 6 Hz), 1.03 (t, 3 H, H-1, *J* = 6 Hz). **^{13}C NMR (75 MHz, $CDCl_3$) δ/ppm =**162.93/162.69 (imide carbonyl), 131.19/131.07/126.89 (naphthalene ring), 126.61 (C-7), 118.60 (C-8/9), 42.98 (C-3), 42.57 (C-6), 21.50 (C-2), 11.60 (C-1). **MS (ASAP) m/z =** 349.1168, calculated $[M+H]^+$: 349.1188. **FT-IR ν/cm^{-1} =** 3089 (w, =C-H stretch), 2963 (w, -CH_3 & C-H stretch), 2875 (w, -CH_3, -CH_2 & C-H stretch), 1702 (s, C=O stretch), 1658 (s, C=O stretch), 1579 (m, aromatic ring), 1514 (w, aromatic ring), 1451 (m, -CH_2 & -CH_3 bend), 1375 (m, -CH_3 bend), 1330 (s, C-N stretch), 1259 (w, C-N stretch), 1242 (s, C-N stretch), 1217 (w, C-N stretch), 1177 (w, C-N stretch), 1152 (w, C-N stretch), 1092 (w, C-N stretch), 1074 (m, C-N stretch), 1019 (m, C-N stretch), 989 (w, C-N stretch), 930 (m, C-N stretch), 881 (m, =C-H bend), 793 (s, =C-H bend), 766 (s, =C-H bend), 749 (m, =C-H bend), 717 (w, =C-H bend), 680 (w, =C-H bend). **RAMAN ν/cm^{-1} =** n.d.

5.5.7 Reaction of P(G-*co*-SH) with *n*Pr-Allyl-NDI (P(G-*co*-*n*Pr-NDI))

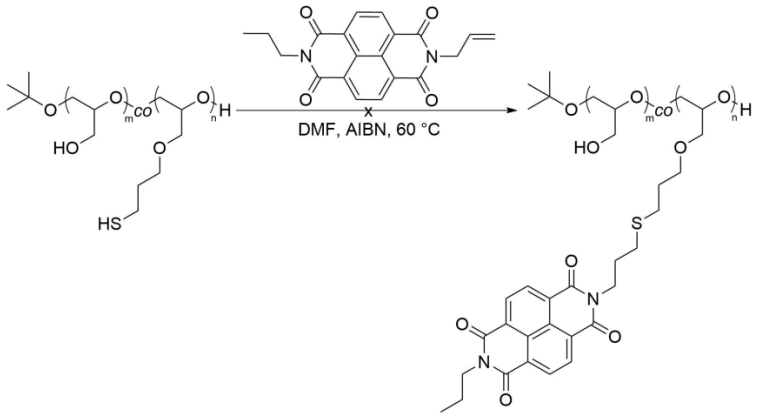

Scheme 5.5.7: Synthesis of P(G-*co*-*n*Pr-NDI).

P(G-*co*-SH) (G:SH = 54:6), *n*Pr-NMI and AIBN were dissolved in DMF or DMSO. The solution was degassed by bubbling argon through the solution for 30 min. The reaction mixture was stirred at 100 °C and terminated by placing in an ice-bath. Afterwards, the solution was dialysed against DMF for 2 d and then H_2O for 2 d by changing solvent twice a

day and using dialysis tubes with MWCO = 1 kDa. After freeze drying, a black material was obtained. ^{1}H NMR analysis shows a maximum degree of substitution of 5 %.

Table 5.5.7: Compounds/yields in the synthesis of P(G-*co*-*n*Pr-NDI).

Run	**1**	**2**	**3**	**4**
P(G-*co*-SH)				
m/mg	70	50	28	50
m (SH-monomer)/mg	12.7	9.1	5.1	9.1
n (SH-monomer)/mmol	0.086	0.061	0.034	0.061
Eq (SH-monomer)	1	1	1	1
***n*Pr-NMI**				
m/mg	90	42.5	46.0	21.3
n/mmol	0.258	0.122	0.132	0.061
Eq	3	2	3.9	1
AIBN				
m/mg	7	5.1	2.8	5.1
n/mmol	0.043	0.031	0.017	0.031
Eq	0.5	0.5	0.5	0.5
Solvent	3.5 mL DMF	2.5 mL DMF	3 mL DMSO	2.5 mL DMF
Reaction time/h	4	24	24	24
Yield/mg	60	35	21	48
DS/%	3	0	5	5

5.5.8 Reaction of P(G-*co*-AGE) with cysteamine hydrochloride (P(G-*co*-NH_2))

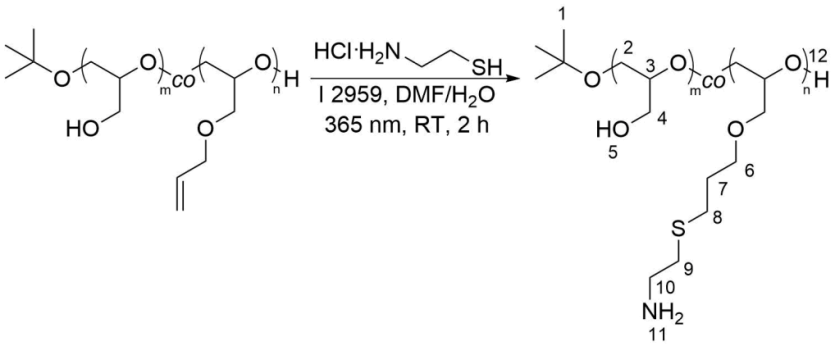

Scheme 5.5.8: Synthesis of P(G-*co*-NH_2).

P(G-*co*-AGE) (G:AGE = 54:6, 1 g, 145 mg AGE, 1.270 mmol allyl groups, 1 eq) was dissolved in DMF (25 mL, solution 1) and cysteamine hydrochloride (432.8 mg, 3.810 mmol,

3 eq) was dissolved in H_2O (25 mL, solution 2). Both solutions were combined, I 2959 (142.6 mg, 0.636 mmol, 0.5 eq) was added and the mixture was degassed by bubbling argon through the solution for 30 min. The reaction mixture was stirred under UV-light at 365 nm at RT for 2 h. The solvent was removed under reduced pressure and the residual solution was dialysed against H_2O for 3 d by changing solvent twice a day and using dialysis tubes with MWCO = 1 kDa. After freeze drying, the polymer was obtained as a yellow sticky solid (186 mg).

^{1}H NMR (300 MHz, DMSO-d_6) δ/ppm = 4.52 (bs, 1*m*H, H-5; bs, 1 H, H-12), 3.53-3.37 (m, 5(*m*+*n*)H, H-2 – H4; 2*n*H, H-6), 2.94 (t, 2*n*H, H-10, *J* = 6 Hz), 2.70 (t, 2*n*H, H-9, *J* = 6 Hz), 2.57 (t, 2*n*H, H-8, *J* = 6 Hz), 1.75 (quint, 2*n*H, H-7, *J* = 6 Hz), 1.12 (s, 9 H, H-1), H-11 not visible. **GPC (DMF, RI):** M_n = 3,829 Da, M_w = 5,140 Da, Đ = 1.34. **FT-IR ν/cm^{-1} =** 3349 (b, O-H & N-H stretch), 2931 (m, -CH_2 & C-H stretch), 2874 (m, C-H stretch), 1633 (m, N-H bend), 1460 (m, -CH_2 bend), 1411 (m, -CH_2 bend), 1347 (m, C-O-C & C-N stretch), 1305 (m, C-O-C & C-N stretch), 1259 (m, C-O-C & C-N stretch), 1225 (m, C-O-C & C-N stretch), 1039 (s, C-O-C & C-N stretch), 913 (m, C-O-C stretch), 855 (m, C-O-C & C-S stretch). **RAMAN ν/cm^{-1} =** 3150 (w, O-H stretch), 2927 (s, C-H stretch), 2881 (s, C-H stretch), 1461 (m, -CH_2 bend), 1344 (m, C-C stretch), 1307 (m, C-C stretch), 1258 (m, C-O-C stretch), 1124 (m, C-O-C stretch), 1064 (m, C-O-C stretch), 973 (w, C-O-C stretch), 903 (m, C-O-C stretch), 849 (m, C-O-C stretch), 752 (w, C-C stretch), 654 (m, C-S stretch), 493 (w, C-C bend), 393 (w, C-C bend), 243 (w, C-C bend).

5.5.9 Reaction of P(G-*co*-NH_2) with *n*Pr-NMI (P(G-*co*-*n*Pr-NDI))

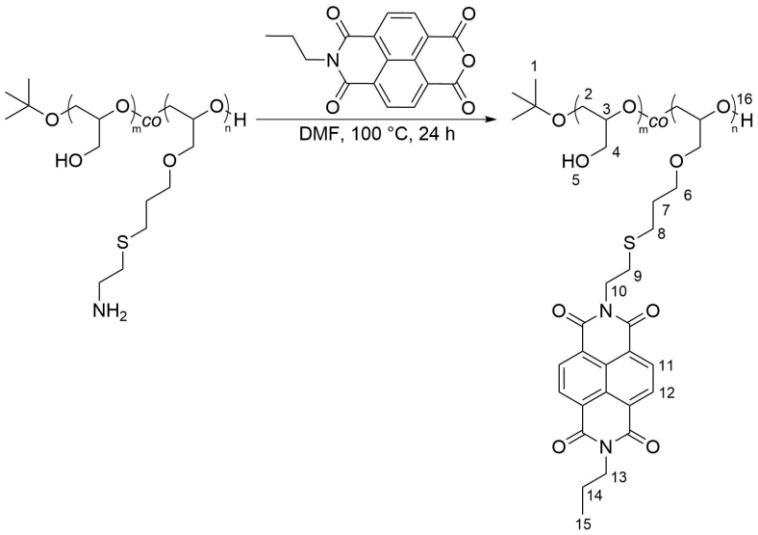

Scheme 5.5.9: Synthesis of P(G-*co*-*n*Pr-NDI).

P(G-*co*-NH_2) (G:NH_2 = 54:6, 40 mg, 8.92 mg amine-monomer, 0.0466 mmol amine groups, 1 eq) and *n*Pr-NMI (43.2 mg, 0.1398 mmol, 3 eq) were dissolved in DMF (2 mL). The solution was stirred at 100 °C for 24 h. After cooling to RT, the solution was dialysed against DMF for 2 d, then DMSO for 2 d and then H_2O for 2 d by changing solvent twice a day and using dialysis tubes with MWCO = 1 kDa. After freeze drying, the polymer was obtained as a grey solid (13 mg).

^{1}H NMR (300 MHz, DMSO-d_6) δ/ppm = 8.69-8.12 (m, 4*n*H, H-11, H-12), 4.49 (bs, 1*m*H, H-5; bs, 1 H, H-16), 4.18 (bt, 2*n*H, H-10), 4.01 (bt, 2*n*H, H-13), 3.53-3.33 (m, 5(*m*+*n*)H, H-2 – H4; 2*n*H, H-6), 2.79 (bt, 2*n*H, H-9), 2.67 (t, 2*n*H, H-8, *J* = 6 Hz), 1.82 (bquint, 2*n*H, H-7)**,** 1.67 (bsext, 2*n*H, H-14), 1.12 (bs, 9 H, H-1), 0.95 (t, 3*n*H, H-15, J = 6 Hz). **GPC (DMF, RI):** M_n = 5,228 Da, M_w = 6,677 Da, Đ = 1.28. **FT-IR ν/cm^{-1} =** 3360 (b, O-H stretch), 2932 (m, -CH_2 & C-H stretch), 2874 (m, C-H stretch), 1705 (m, C=O stretch), 1663 (s, C=O stretch), 1580 (m, aromatic ring), 1453 (m, -CH_2 bend), 1374 (m, C-O-C & C-N stretch), 1336 (m, C-O-C & C-N stretch), 1243 (m, C-O-C & C-N stretch), 1064 (s, C-O-C & C-N stretch), 1040 (s, C-O-C & C-N stretch), 914 (m, C-O-C & C-N stretch), 882 (m, =C-H & C-S stretch), 857 (m, =C-H stretch), 765 (m, =C-H stretch). **RAMAN ν/cm^{-1} =** n.d.

5.5.10 Gel tests

Polymers carrying pyrene groups (RU (G:Pyr) = 57:3, 6.14 mg) were dissolved in H_2O (45 µL, solution 1, pH = 7.0) and polymers carrying naphthalene diimide groups (RU (G:NDI) = 54:6, 3.86 mg) were dissolved in H_2O (45 µL, solution 2, pH = 7.0). Both solutions were stirred at RT for 18 h, combined to give equimolar ratio of functional groups with a total amount of 10 mg of polymer (w/w (polymer) = 10 %) and stirred again at RT for 18 h.

5.6 High molecular weight polyglycidols

5.6.1 Poly(ethoxyethyl glycidyl ether) (PEEGE)

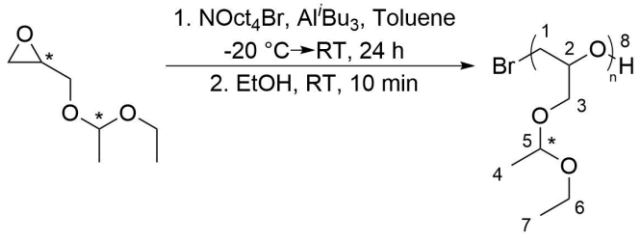

Scheme 5.6.1: Synthesis of PEEGE.

The initiator tetraoctylammonium bromide was weighted into a Schlenk flask and a stir bar was added. The flask was heated at 110 °C for 1 h under high vacuum. After cooling to RT, the dry solvent toluene and the monomer EEGE were added under argon flow. The flask was then cooled at -20 °C for 5 min and the catalyst solution triisobutylaluminium in toluene was added under argon flow. The flask was subsequently closed with a glass stopper. The solution was stirred from -20 °C to RT for 24 h following by termination with a few drops of ethanol. A crude sample was taken for ^{1}H NMR measurement in $CDCl_3$ to determine the monomer conversion. The reaction mixture was dialysed against acetone for 3 d by changing solvent once a day and using dialysis tubes with MWCO = 1 kDa. Acetone was removed *via* rotary evaporator and the polymer was dried at 60 °C for 1 day. The polymer was obtained as a clear viscous liquid.

Table 5.6.1-1: Compounds/yields in the synthesis of PEEGE.

Run	**1**	**2**	**3**	**4**	**5**
$M_{n,theo}$/kDa	10	20	30	70	100
[EEGE]:[Al^{i}Bu$_3$]: [NOct$_4$Br]	68:4:1	136:2:1	205:4:1	478:2:1	684:5:1
[EEGE]/M	0.5	0.5	1	2	2
EEGE					
m/mg	250	500	600	1300	2000
V/µL	250	500	600	1300	2000
n/mmol	1.71	3.420	4.105	8.893	13.682
Eq	68	136	205	478	684
NOct$_4$Br					
m/mg	13.75	13.75	10.95	10.17	10.94
n/mmol	0.025	0.025	0.02	0.0186	0.02
Eq	1	1	1	1	1
Al^{i}Bu$_3$					
m/mg	19.95	9.98	15.88	7.379	19.835
V/µL	94.1	47	74.9	34.8	93.6
n/mmol	0.1	0.05	0.08	0.0372	0.1
Eq	4	2	4	2	5
V(Toluene)/mL	3.076	6.294	3.430	3.112	4.747
Conversion/%	100	100	100	88	100
Yield/mg	239	472	558	989	1573

^{1}H NMR (300 MHz, acetone-d_6) δ/ppm = 4.73 (q, 1*n*H, H-5, *J* = 6 Hz; bs, 1 H), 3.69-3.43 (m, 7*n*H, H-1 – H3, H-6; bs, 1 H, H-8), 1.26 (d, 3*n*H, H-4, *J* = 6 Hz), 1.17 (t, 3*n*H, H-7, *J* = 9 Hz).

GPC (DMF, RI):

Table 5.6.1-2: GPC data of series of PEEGE.

	1	**2**	**3**	**4**	**5**
M_n/Da	4,750	8,841	11,776	11,104	19,008
M_w/Da	5,788	9,853	15,255	27,075	40,774
Đ	1.22	1.11	1.30	2.44	2.15

FT-IR ν/cm^{-1} = 2976 (m, -CH_3 & C-H stretch), 2931 (m, -CH_2 & C-H stretch), 2875 (m, -CH_3 & C-H stretch), 1446 (m, -CH_2 & -CH_3 bend), 1379 (m, -CH_3 bend), 1340 (m, C-O-C stretch), 1300 (m, C-O-C stretch), 1260 (m, C-O-C stretch), 1129 (s, C-O-C stretch), 1082 (s, C-O-C stretch), 1054 (s, C-O-C stretch), 1001 (m, C-O-C stretch), 946 (m, C-O-C stretch), 930 (m, C-O-C stretch), 874 (m, C-O-C stretch), 801 (m, C-O-C stretch). **RAMAN ν/cm^{-1} =** 2984 (s, C-H stretch), 2940 (s, C-H stretch), 2878 (s, C-H stretch), 2803 (m, C-H stretch), 1460 (m, -CH_2 & -CH_3 bend), 1350 (m, C-C stretch), 1275 (m, C-O-C stretch), 1226 (w, C-O-C stretch), 1139 (m, C-O-C stretch), 1096 (m, C-O-C stretch), 1068 (m, C-O-C stretch), 1035 (w, C-O-C stretch), 1008 (w, C-O-C stretch), 927 (m, C-O-C stretch), 882 (m, C-O-C stretch), 834 (m, C-O-C stretch), 816 (m, C-O-C stretch), 681 (w, C-Br stretch), 532 (m, C-C bend), 363 (w, C-C bend).

5.6.2 Polyglycidol (PG)

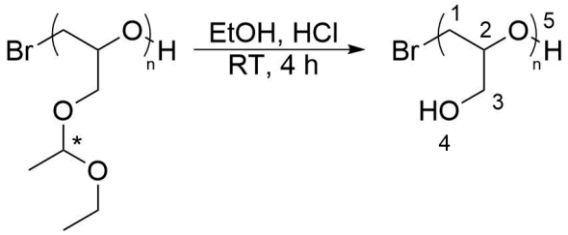

Scheme 5.6.2: Synthesis of PG.

PEEGE was suspended in EtOH and conc. HCl. The mixture was stirred at RT for 4 h. A white precipitate formed. The solvent was removed under reduced pressure and H_2O was added to the remaining polymer. The solution was dialysed against H_2O for 3 d by changing solvent twice a day and using dialysis tubes with MWCO = 1 kDa. After freeze drying, the polymer was obtained as a clear sticky solid.

Table 5.6.2-1: Compounds/yields in the synthesis of PEEGE.

Run	1	2	3	4	5
RU (EEGE)	68	136	205	478	684
m (PEEGE)/mg	150	150	250	150	150
V (HCl)/mL	0.8	0.8	1.36	0.8	0.8
V (EtOH)/mL	10	10	16.7	10	10
Yield/mg	60	74	125	65	62

^{1}H NMR (300 MHz, DMSO-d$_6$) δ/ppm = 4.51 (t, 1*n*H, H-4, *J* = 6 Hz; bs, 1 H, H-5), 3.54-3.37 (m, 5*n*H, H-1 – H3).

GPC (DMF, RI):

Table 5.6.2-2: GPC data of series of PG.

Run	1	2	3	4	5
M_n/Da	9,867	14,434	18,959	18,700	28,681
M_w/Da	11,161	16,345	23,179	34,664	49,860
Đ	1.13	1.13	1.22	1.85	1.74

FT-IR ν/cm^{-1} = 3372 (b, O-H stretch), 2921 (m, -CH_2 & C-H stretch), 2874 (m, C-H stretch), 1460 (m, -CH_2 bend), 1408 (m, -CH_2 bend), 1348 (m, C-O-C stretch), 1304 (m, C-O-C stretch), 1259 (m, C-O-C stretch), 1222 (m, C-O-C stretch), 1040 (s, C-O-C stretch), 919 (m, C-O-C stretch), 853 (m, C-O-C stretch). **RAMAN ν/cm^{-1}** = 2941 (s, C-H stretch), 2887 (s, C-H stretch), 1468 (m, -CH_2 bend), 1411 (w, -CH_2 & -CH_3 bend), 1355 (m, C-C stretch), 1306 (m, C-C stretch), 1262 (m, C-O-C stretch), 1126 (m, C-O-C stretch), 1070 (m, C-O-C stretch), 983 (w, C-O-C stretch), 911 (m, C-O-C stretch), 855 (m, C-O-C stretch), 689 (w, C-Br stretch), 494 (w, C-C bend), 402 (w, C-C bend), 253 (w, C-C bend).

5.6.3 Poly(allyl glycidyl ether) (PAGE)

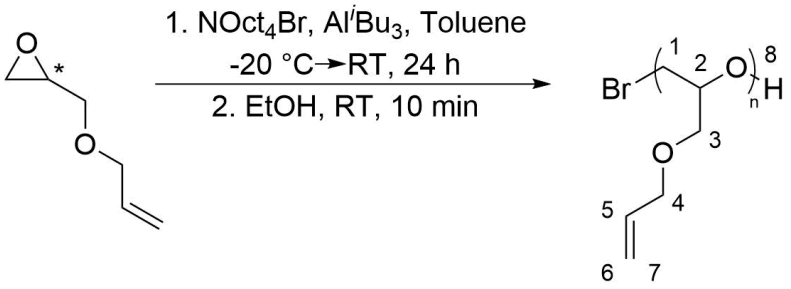

Scheme 5.6.3: Synthesis of PAGE.

The initiator tetraoctylammonium bromide was weighted into a Schlenk flask and a stir bar was added. The flask was heated at 110 °C for 1 h under high vacuum. After cooling to RT, the dry solvent toluene and the monomer AGE were added under argon flow. The flask was then cooled at -20 °C for 5 min and the catalyst solution triisobutylaluminium in toluene was added under argon flow. The flask was subsequently closed with a glass stopper. The solution was stirred from -20 °C to RT for 24 h followed by termination with a few drops of ethanol. A crude sample was taken for ^{1}H NMR measurement in $CDCl_3$ to determine the monomer conversion. The reaction mixture was dialysed against acetone for 3 d by changing solvent once a day and using dialysis tubes with MWCO = 1 kDa. Acetone was removed *via* rotary evaporator and the polymer was dried at 60 °C for 1 day. The polymer was obtained as a clear viscous liquid.

Table 5.6.3-1: Compounds/yields in the synthesis of PAGE.

Run	**1**	**2**	**3**	**4**	**5**
$M_{n,theo}$/kDa	10	20	30	70	100
[AGE]:[Al^{i}Bu$_3$]: [NOct$_4$Br]	68:4:1	136:2:1	205:4:1	478:2:1	684:5:1
[AGE]/M	0.5	0.5	1	2	2
AGE					
m/mg	195.2	388.1	468.5	1015.0	1561.7
V/µL	201.4	400.5	483.5	1047.5	1611.7
n/mmol	1.71	3.40	4.105	8.893	13.682
Eq	68	136	205	478	684
NOct$_4$Br					
m/mg	13.75	13.75	10.95	10.17	10.94
n/mmol	0.025	0.025	0.02	0.0186	0.02
Eq	1	1	1	1	1
Al^{i}Bu$_3$					
m/mg	19.95	9.98	15.88	7.379	19.835
V/µL	94.1	47.0	74.9	34.8	93.6
n/mmol	0.1	0.05	0.08	0.0372	0.1
Eq	4	2	4	2	5
V(Toluene)/mL	3.076	6.294	3.430	3.112	4.747
Conversion/%	100	100	100	100	94
Yield/mg	204	424	480	732	931

^{1}H NMR (300 MHz, acetone-d_6) δ/ppm = 5.99-5.86 (m, 1*n*H, H-5), 5.29 (d, 1*n*H, H-7, *J* = 18 Hz), 5.14 (d, 1*n*H, H-6, *J* = 12 Hz), 4.01 (d, 2*n*H, H-4, *J* = 6 Hz), 3.69-3.47 (m, 5*n*H, H-1 – H3; bs, 1 H, H-8).

GPC (DMF, RI):

Table 5.6.3-2: GPC data of series of PG.

Run	1	2	3	4	5
M_n/Da	6,293	11,076	18,091	27,144	14,257
M_w/Da	8,715	14,432	30,719	49,141	50,055
Đ	1.39	1.30	1.70	1.81	3.41

FT-IR ν/cm^{-1} = 2979 (w, -CH_2 & C-H stretch), 2928 (m, -CH_2 & C-H stretch), 2900 (m, -CH_2 & C-H stretch), 2865 (m, -CH_2 & C-H stretch), 1460 (m, -CH_2 bend), 1422 (m, -CH_2 bend), 1350 (m, -CH_2 bend), 1302 (w, C-O-C stretch), 1264 (m, C-O-C stretch), 1085 (s, C-O-C stretch), 995 (m, C-O-C stretch), 920 (m, C-O-C stretch). **RAMAN ν/cm^{-1}** = 3084 (m, =(C-H) stretch), 3013 (s, =(C-H) stretch), 2872 (s, C-H stretch), 1645 (s, C=C stretch), 1469 (m, -CH_2 bend), 1422 (m, -CH_2 bend), 1349 (m, C-C stretch), 1289 (s, C-O-C stretch), 1247 (m, C-O-C stretch), 1148 (m, C-O-C stretch), 1104 (m, C-O-C stretch), 1001 (w, C-O-C stretch), 970 (w, C-O-C stretch), 916 (m, C-O-C stretch), 868 (m, C-O-C stretch), 564 (w, C-Br stretch).

5.6.4 Poly(ethoxyethyl glycidyl ether-*co*-allyl glycidyl ether) (P(EEGE-*co*-AGE))

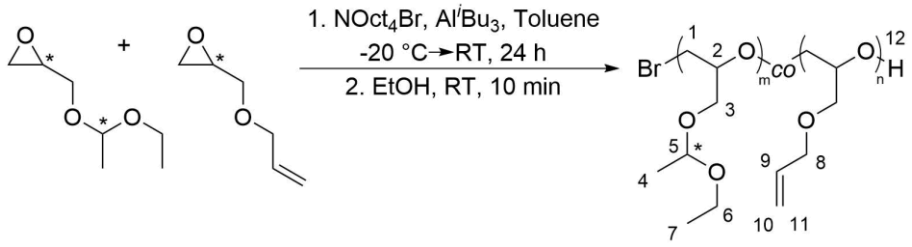

Scheme 5.6.4: Synthesis of P(EEGE-*co*-AGE).

The initiator tetraoctylammonium bromide was weighted into a Schlenk flask and a stir bar was added. The flask was heated at 110 °C for 1 h under high vacuum. After cooling to RT, the dry solvent toluene and the monomers EEGE and AGE ([EEGE]:[AGE] = 10:1 or 9:1) were added under argon flow. The flask was then cooled at -20 °C for 5 min and the catalyst solution triisobutylaluminium in toluene was added under argon flow. The flask was

subsequently closed with a glass stopper. The solution was stirred from -20 °C to RT for 24 h followed by termination with a few drops of ethanol. A crude sample was taken for ^{1}H NMR measurement in $CDCl_3$ to determine the monomer conversion. The reaction mixture was dialysed against acetone for 3 d by changing solvent once a day and using dialysis tubes with MWCO = 1 kDa. Acetone was removed *via* rotary evaporator and the polymer was dried at 60 °C for 1 day. The polymer was obtained as a clear viscous liquid.

Table 5.6.4-1: Compounds/yields in the synthesis of P(EEGE-*co*-AGE).

Run	**1**	**2**	**3**	**4**	**5**
$M_{n,theo}$/kDa	10	20	30	70	100
[EEGE]:[AGE]: [Al^{i}Bu$_3$]:[NOct$_4$Br]	60:6:4:1	126:14:2:1	189:21:4:1	440:44:2:1	640:64:5:1
$[Monomers]_{total}$/M	0.5	0.5	1	2	2
EEGE					
m/mg	219.3	460.5	552.6	1196.3	1871.1
V/µL	219.3	460.5	552.6	1196.3	1871.1
n/mmol	1.50	3.15	3.78	8.184	12.80
Eq	60	126	189	440	640
AGE					
m/mg	17.12	39.9	47.9	93.4	146.1
V/µL	17.17	41.2	49.4	96.4	150.8
n/mmol	0.15	0.35	0.42	0.8184	1.28
Eq	6	14	21	44	64
NOct$_4$Br					
m/mg	13.75	13.75	10.95	10.17	10.94
n/mmol	0.025	0.025	0.02	0.0186	0.02
Eq	1	1	1	1	1
Al^{i}Bu$_3$					
m/mg	19.95	9.98	15.88	7.379	19.835
V/µL	94.1	47.0	74.9	34.8	93.6
n/mmol	0.1	0.05	0.08	0.0372	0.1
Eq	4	2	4	2	5
V(Toluene)/mL	3.076	6.294	3.430	3.112	4.747
Conversion/%	100	100	100	98	100
Yield/mg	277	452	569	1.066	1.307

^{1}H NMR (300 MHz, acetone-d$_6$) δ/ppm = 6.00-5.87 (m, 1*n*H, H-9), 5.30 (d, 1*n*H, H-11, *J* = 18 Hz), 5.15 (d, 1*n*H, H-10, *J* = 9 Hz), 4.73 (q, 1*m*H, H-5, *J* = 6 Hz), 4.02 (d, 2*n*H, H-8,

J = 6 Hz), 3.69-3.43 (m, 5(*m*+*n*)H, H-1 – H-3; m, 2*m*H, H-6; bs, 1 H, H-12), 1.26 (d, 3*m*H, H-4, *J* = 6 Hz), 1.17 (t, 3*m*H, H-7, *J* = 9 Hz).

GPC (DMF, RI):

Table 5.6.4-2: GPC data of series of P(EEGE-*co*-AGE).

Run	**1**	**2**	**3**	**4**	**5**
M_n/Da	4,628	9,669	13,997	15,088	21,829
M_w/Da	5,596	11,270	18,595	31,303	49,432
Đ	1.21	1.17	1.33	2.08	2.26

FT-IR ν/cm^{-1} = 2978 (m, -CH_3 & C-H stretch), 2932 (m, -CH_2 & C-H stretch), 2875 (m, -CH_3 & C-H stretch), 1455 (m, -CH_2 & -CH_3 bend), 1380 (m, -CH_3 bend), 1340 (m, C-O-C stretch), 1300 (m, C-O-C stretch), 1262 (m, C-O-C stretch), 1129 (s, C-O-C stretch), 1082 (s, C-O-C stretch), 1054 (s, C-O-C stretch), 999 (m, C-O-C stretch), 945 (m, C-O-C stretch), 929 (m, C-O-C stretch), 874 (m, C-O-C stretch), 814 (w, C-O-C stretch). **RAMAN ν/cm^{-1}** = 2981 (s, C-H stretch), 2933 (s, C-H stretch), 2873 (s, C-H stretch), 2770 (m, C-H stretch), 1644 (m, C=C stretch), 1453 (m, -CH_2 & -CH_3 bend), 1350 (w, C-C stretch), 1270 (m, C-O-C stretch), 1133 (m, C-O-C stretch), 1092 (m, C-O-C stretch), 1059 (m, C-O-C stretch), 998 (w, C-O-C stretch), 920 (m, C-O-C stretch), 873 (m, C-O-C stretch), 830 (m, C-O-C stretch), 807 (m, C-O-C stretch), 665 (w, C-Br stretch), 522 (m, C-C bend), 354 (m, C-C bend).

5.6.5 Poly(glycidol-*co*-allyl glycidyl ether) (P(G-*co*-AGE))

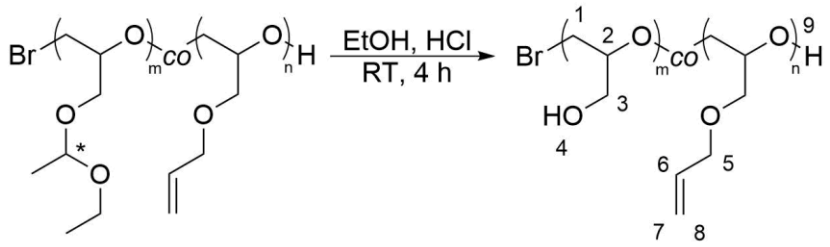

Scheme 5.6.5: Synthesis of P(G-*co*-AGE).

P(EEGE-*co*-AGE) was suspended in EtOH and conc. HCl. The mixture was stirred at RT for 4 h. A white precipitate formed. The solvent was removed under reduced pressure and H_2O was added to the remaining polymer. The solution was dialysed against H_2O for 3 d by changing solvent twice a day and using dialysis tubes with MWCO = 1 kDa. After freeze drying, the polymer was obtained as a clear sticky solid.

Table 5.6.5-1: Compounds/yields in the synthesis of P(G-*co*-AGE).

Run	**1**	**2**	**3**	**4**	**5**
RU (EEGE:AGE)	60:6	126:14	189:21	440:44	640:64
m (PEEGE)/mg	150	150	150	150	150
V (HCl)/mL	0.8	0.8	0.8	0.8	0.8
V (EtOH)/mL	10	10	10	10	10
Yield/mg	57	75	74	74	84

^{1}H NMR (300 MHz, DMSO-d_6) δ/ppm = 5.94-5.81 (m, 1*n*H, H-6), 5.25 (d, 1*n*H, H-8, *J* = 18 Hz), 5.14 (d, 1*n*H, H-7, *J* = 9 Hz), 4.50 (bt, 1*m*H, H-4; bs, 1 H, H-9), 3.95 (d, 2*n*H, H-5, *J* = 6 Hz), 3.54-3.37 (m, 5(*m*+*n*)H, H-1 – H3).

GPC (DMF, RI):

Table 5.6.5-2: GPC data of series of P(G-*co*-AGE).

Run	**1**	**2**	**3**	**4**	**5**
M_n/Da	9,441	16,823	21,654	22,218	31,926
M_w/Da	10,597	25,636	45,055	72,736	79,256
Đ	1.12	1.52	2.08	3.27	2.48

FT-IR ν/cm^{-1} = 3356 (b, O-H stretch), 2923 (m, -CH_2 & C-H stretch), 2875 (m, C-H stretch), 1461 (m, -CH_2 bend), 1409 (m, -CH_2 bend), 1347 (m, C-O-C stretch), 1305 (w, C-O-C stretch), 1257 (w, C-O-C stretch), 1222 (m, C-O-C stretch), 1039 (s, C-O-C stretch), 982 (w, C-O-C stretch), 914 (m, C-O-C stretch), 851 (m, C-O-C stretch). **RAMAN ν/cm^{-1} =** 3014 (m, =(C-H) stretch), 2932 (s, C-H stretch), 2881 (s, C-H stretch), 1644 (m, C=C stretch), 1460 (m, -CH_2 bend), 1413 (m, -CH_2 bend), 1349 (m, C-C stretch), 1286 (m, C-O-C stretch), 1259 (m, C-O-C stretch), 1119 (m, C-O-C stretch), 1069 (m, C-O-C stretch), 979 (w, C-O-C stretch), 907 (m, C-O-C stretch), 854 (m, C-O-C stretch), 674 (w, C-Br stretch), 465 (w, C-C bend), 241 (w, C-C bend).

5.7 Electrolyte functionalised high molecular weight polyglycidols

5.7.1 Poly(ethoxyethyl glycidyl ether-*co*-allyl glycidyl ether) (P(EEGE-*co*-AGE))

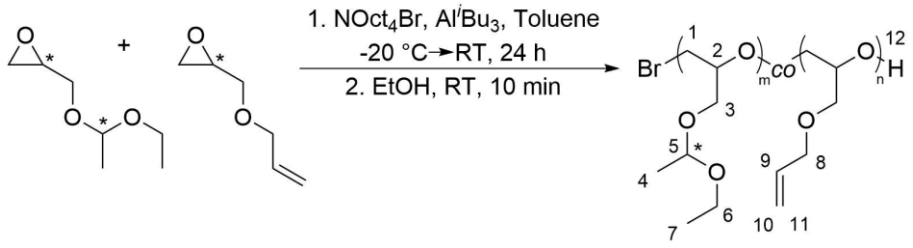

Scheme 5.7.1: Synthesis of P(EEGE-*co*-AGE).

The initiator tetraoctylammonium bromide (109.5 mg, 0.2 mmol, 1 eq) was weighted into a Schlenk flask and a stir bar was added. The flask was heated at 110 °C for 1 h under vacuum. After cooling to RT, the dry solvent toluene (34.3 mL) and the monomers EEGE (5.526 mL, 37.8 mmol, 189 eq) and AGE (0.495 µL, 4.2 mmol, 21 eq) were added under argon flow. The flask was then cooled at -20 °C for 5 min and the catalyst solution triisobutylaluminium in toluene (0.749 µL, 0.8 mmol, 4 eq) was added under argon flow by subsequent closing the flask with a glass stopper. The solution was stirred from -20 °C to RT for 24 h following by termination with a few drops of ethanol. A crude sample was taken for ^{1}H NMR measurement in $CDCl_3$ to determine the monomer conversion (100 %). The reaction mixture was dialysed against acetone for 3 d by changing solvent once a day and using dialysis tubes with MWCO = 1 kDa. Acetone was removed *via* rotary evaporator and the polymer was dried at 60 °C for 1 day. The polymer was obtained as a clear viscous liquid (3.52 g).

^{1}H NMR (300 MHz, acetone-d_6) δ/ppm = 6.00 – 5.87 (m, 1*n*H, H-9), 5.30 (d, 1*n*H, H-11, *J* = 18 Hz), 5.15 (d, 1*n*H, H-10, *J* = 9 Hz), 4.72 (q, 1*m*H, H-5, *J* = 6 Hz), 4.02 (d, 2*n*H, H-8, *J* = 6 Hz), 3.67 – 3.43 (m, 5(*m*+*n*)H, H-1 – H3; 2*m*H, H-6; 1 H, H-12), 1.26 (d, 3*m*H, H-4, *J* = 6 Hz), 1.17 (t, 3*m*H, H-7, *J* = 9 Hz). **GPC (DMF, RI):** M_n = 8.3 kDa, M_w = 10.1 kDa, Đ = 1.22. **FT-IR ν/cm^{-1} =** 2977 (m, -CH_3 & C-H stretch), 2926 (m, -CH_2 & C-H stretch), 2874 (m, -CH_3 & C-H stretch), 1456 (m, -CH_2 & -CH_3 bend), 1446 (m, -CH_2 & -CH_3 bend), 1379 (m, -CH_3 bend), 1300 (w, C-O-C stretch), 1271 (w, C-O-C stretch), 1227 (w, C-O-C stretch), 1129 (s, C-O-C stretch), 1082 (s, C-O-C stretch), 1054 (s, C-O-C stretch), 999 (m, C-O-C stretch), 929 (m, C-O-C stretch), 874 (m, C-O-C stretch). **RAMAN ν/cm^{-1} =** 2981 (s, C-H stretch), 2932 (s, C-H stretch), 2874 (s, C-H stretch), 1642 (w, C=C stretch), 1451 (m, -CH_2 & -CH_3 bend), 1351 (m, C-C stretch), 1270 (m, C-O-C stretch), 1137 (m, C-O-C stretch),

1093 (m, C-O-C stretch), 998 (w, C-O-C stretch), 919 (m, C-O-C stretch), 874 (m, C-O-C stretch), 828 (m, C-O-C stretch), 807 (m, C-O-C stretch), 660 (w, C-Br stretch), 524 (m, C-C bend), 355 (w, C-C bend).

5.7.2 Poly(glycidol-*co*-allyl glycidyl ether) (P(G-*co*-AGE))

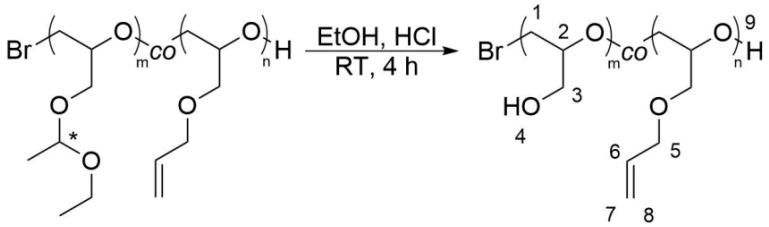

Scheme 5.7.2: Synthesis of P(G-*co*-AGE).

A suspension of the P(EEGE-*co*-AGE) (3.42 g) and ethanol (200 mL) was stirred while adding dropwise concentrated hydrochloric acid (16 mL). A clear solution was formed which was allowed to stir at RT for 4 h. Ethanol was removed *via* rotary evaporator and the polymer was dissolved in H_2O which was dialysed against H_2O for 3 d by changing solvent twice a day and using dialysis tubes with MWCO = 1 kDa. After freeze drying, the polymer was obtained as a clear sticky solid (1.70 mg).

^{1}H NMR (300 MHz, DMSO-d_6) δ/ppm = 5.94 – 5.81 (m, 1*n*H, H-6), 5.25 (d, 1*n*H, H-8, *J* = 18 Hz), 5.14 (d, 1*n*H, H-7, *J* = 12 Hz), 4.50 (bs, 1*m*H, H-4; 1 H, H-9), 3.95 (d, 2*n*H, H-5, *J* = 6 Hz), 3.58 – 3.37 (m, 5(*m*+*n*)H, H-1 – H3). **GPC (DMF, RI):** M_n = 15.6 kDa, M_w = 19.2 kDa, Đ = 1.24. **FT-IR ν/cm^{-1} =** 3371 (b, O-H stretch), 2921 (m, -CH_2 & C-H stretch), 2874 (m, C-H stretch), 1461 (m, -CH_2 bend), 1408 (m, -CH_2 bend), 1348 (m, C-O-C stretch), 1304 (w, C-O-C stretch), 1260 (w, C-O-C stretch), 1222 (w, C-O-C stretch), 1039 (s, C-O-C stretch), 918 (m, C-O-C stretch), 851 (m, C-O-C stretch). **RAMAN ν/cm^{-1} =** 3010 (s, =(C-H) stretch), 2934 (s, C-H stretch), 2884 (s, C-H stretch), 1646 (m, C=C stretch), 1463 (m, -CH_2 bend), 1416 (m, -CH_2 & -CH_3 bend), 1353 (m, C-C stretch), 1289 (m, C-O-C stretch), 1263 (m, C-O-C stretch), 1130 (m, C-O-C stretch), 1072 (m, C-O-C stretch), 982 (w, C-O-C stretch), 909 (m, C-O-C stretch), 857 (m, C-O-C stretch), 687 (w, C-Br stretch), 474 (w, C-C bend), 220 (w, C-C bend).

5.7.3 Chloride modification of P(G-*co*-AGE) (P(G-*co*-Cl))

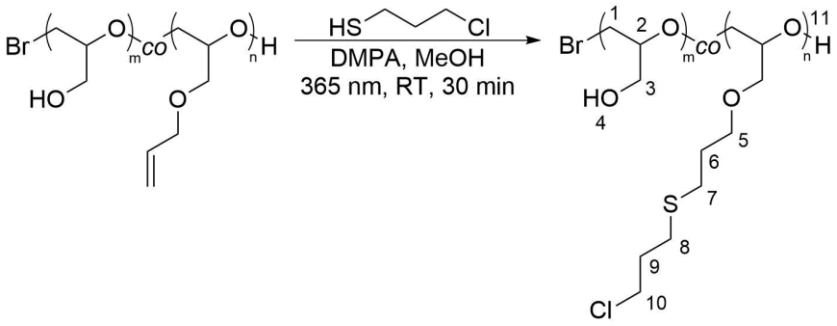

Scheme 5.7.3: Synthesis of P(G-*co*-Cl).

P(G-*co*-AGE) (674 mg, 0.862 mmol allyl groups, 1 eq), 3-chloro-1-propanethiol (251.8 µL, 2.586 mmol, 3 eq) and DMPA (110.5 mg, 0.431 mmol, 0.5 eq) were dissolved in MeOH (25 mL). The solution was degassed with argon for 30 min and stirred at RT for 30 min under UV-light. Afterwards, the solution was dialysed against MeOH for 3 d by changing solvent once a day and using dialysis tubes with MWCO = 1 kDa. MeOH was removed *via* rotary evaporator and the polymer was dried at 60 °C for 1 day. The polymer was obtained as a yellow viscous liquid (648 mg).

^{1}H NMR (300 MHz, DMSO-d_6) δ/ppm = 4.50 (bs, 1*m*H, H-4; 1 H, H-11), 3.70 (t, 2*n*H, H-10, *J* = 6 Hz), 3.53 – 3.37 (m, 5(*m*+*n*)H, H-1 – H3; 2*n*H, H-5), 2.60 (t, 2*n*H, H-7, *J* = 6 Hz), 2.54 (t, 2*n*H, H-8, *J* = 6 Hz), 1.95 (quint, 2*n*H, H-9, *J* = 6 Hz), 1.74 (quint, 2*n*H, H-6, *J* = 6 Hz). **GPC (DMF, RI):** M_n = 19.8 kDa, M_w = 29.7 kDa, Đ = 1.50. **FT-IR ν/cm^{-1} =** 3362 (b, O-H stretch), 2919 (m, -CH_2 & C-H stretch), 2873 (m, C-H stretch), 1459 (m, -CH_2 bend), 1413 (m, -CH_2 bend), 1348 (m, C-O-C stretch), 1305 (m, C-O-C stretch), 1266 (m, C-O-C stretch), 1221 (m, C-O-C stretch), 1064 (s, C-O-C stretch), 1027 (s, C-O-C stretch), 913 (m, C-O-C stretch), 856 (m, C-O-C & C-S stretch). **RAMAN ν/cm^{-1} =** 2935 (s, C-H stretch), 2886 (s, C-H stretch), 1466 (m, -CH_2 bend), 1354 (m, C-C stretch), 1307 (m, C-C stretch), 1264 (m, C-O-C stretch), 1130 (m, C-O-C stretch), 1072 (m, C-O-C stretch), 1035 (m, C-O-C stretch), 983 (w, C-O-C stretch), 908 (m, C-O-C stretch), 863 (m, C-O-C stretch), 659 (m, C-Br & C-Cl stretch), 247 (w, C-C bend).

5.7.4 Imidazolium modification of P(G-*co*-Cl) (P(G-*co*-Im))

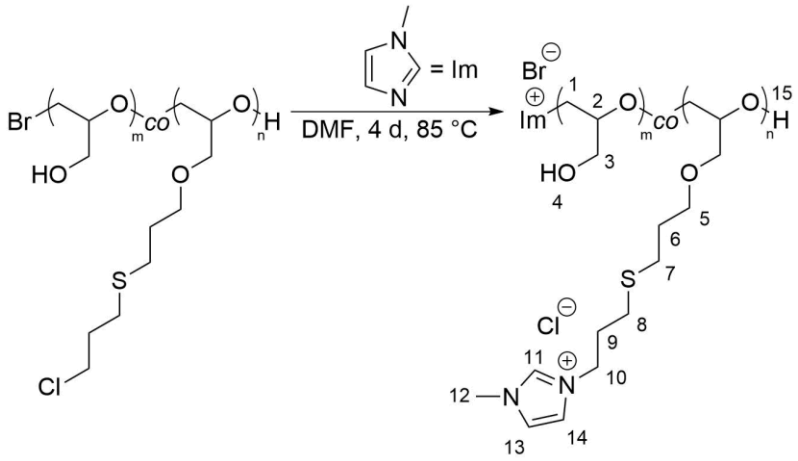

Scheme 5.7.4: Synthesis of P(G-*co*-Im).

The chloride functionalised polyglycidol (632 mg, 0.709 mmol chloride groups, 1 eq) and 1-methylimidazole (1.125 mL, 14.18 mmol, 20 eq) were dissolved in DMF (21 mL). The solution was heated at 85 °C for 4 d. 30 mL H_2O was added afterwards. The solution was dialysed against H_2O for 3 d by changing solvent twice a day and using dialysis tubes with MWCO = 1 kDa. After freeze drying, the polymer was obtained as a yellow sticky solid (308 mg). ^{1}H NMR shows a conversion of 85 %.

^{1}H NMR (300 MHz, DMSO-d_6) δ/ppm = 9.17 (bs, 1*n*H, H-11), 7.77 (s, 1*n*H, H-14), 7.70 (s, 1*n*H, H-13), 4.58 (bs, 1*m*H, H-4; 1 H, H-15), 4.24 (t, 2*n*H, H-10, *J* = 6 Hz), 3.85 (s, 3*n*H, H-12), 3.54 – 3.37 (m, 5(*m*+*n*)H, H-1 – H3; 2*n*H, H-5), 2.50 (overlap with solvent signal: t, 2*n*H, H-7, *J* = 6 Hz; t, 2*n*H, H-8, *J* = 6 Hz), 2.06 (quint, 2*n*H, H-9, *J* = 6 Hz), 1.73 (quint, 2*n*H, H-6, *J* = 6 Hz). **GPC (DMF, RI):** M_n = 7.0 kDa, M_w = 9.4 kDa, Đ = 1.35. **FT-IR ν/cm^{-1} =** 3355 (b, O-H stretch), 3112 (m, =C-H stretch), 2920 (m, -CH_2 & C-H stretch), 2871 (m, C-H stretch), 1649 (m, C=N & C=C stretch), 1601 (w, aromatic ring vibration), 1573 (w, C=C stretch), 1459 (m, -CH_2 & -CH_3 bend & C=C stretch), 1390 (w, -CH_3 bend), 1346 (m, C-O-C & C-N stretch), 1288 (m, C-O-C & C-N stretch), 1222 (w, C-O-C & C-N stretch), 1041 (s, C-O-C & C-N stretch), 912 (m, C-O-C stretch), 851 (m, C-O-C & C-S stretch), 750 (w, CH_2 bend). **RAMAN ν/cm^{-1} =** n.d.

5.7.5 Diethylphosphonamide modification of P(G-*co*-AGE) (P(G-*co*-POEt))

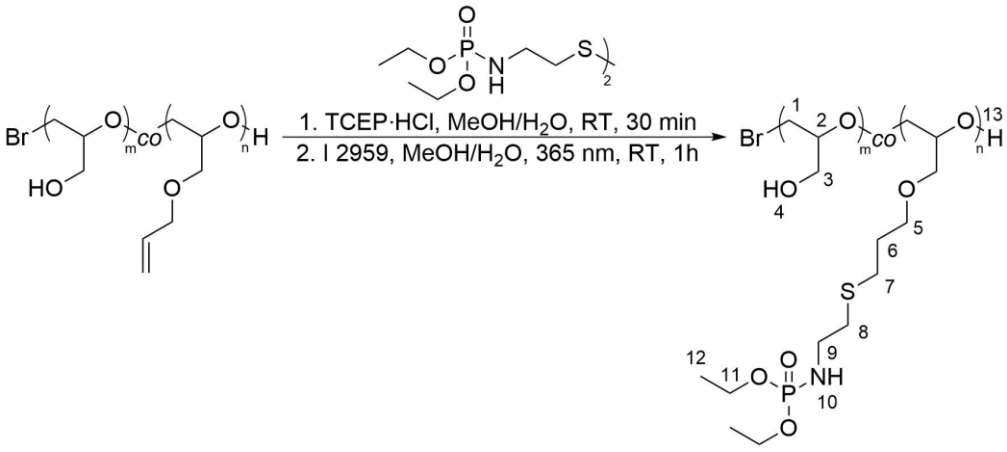

Scheme 5.7.5: Synthesis of P(G-*co*-POEt).

The protected phosphonamide linker (548.4 mg, 1.292 mmol, 1.5 eq) was dissolved in MeOH (15 mL) and tris(2-carboxyethyl)phosphine hydrochloride was dissolved in H_2O (15 mL). Both solutions were mixed and stirred at RT for 30 min. Afterwards, a solution of P(G-*co*-AGE) (673 mg, 0.861 mmol allyl groups, 1 eq) in H_2O/MeOH (40 mL, v/v = 1:1) and I 2959 (96.6 mg, 0.431 mmol, 0.5 eq) were added. The mixture was degassed with argon for 30 min and stirred at RT for 1 h under UV-light. The solution was dialysed against H_2O for 3 d by changing solvent twice a day and using dialysis tubes with MWCO = 1 kDa. After freeze drying, the polymer was obtained as a yellow viscous liquid (628 mg).

^{1}H NMR (300 MHz, DMSO-d_6) δ/ppm = 4.95 (m, 1*n*H, H-10), 4.49 (bs, 1*m*H, H-4; 1 H, H-13), 3.90 (m, 2*n*H, H-11), 3.54 – 3.40 (m, 5(*m*+*n*)H, H-1 – H-3; 2*n*H, H-5), 2.90 (m, 2*n*H, H-9), 2.50 (overlap with solvent signal: t, 2*n*H, H-7, *J* = 6 Hz; t, 2*n*H, H-8, *J* = 6 Hz), 1.73 (quint, 2*n*H, H-6, *J* = 6 Hz), 1.21 (t, 3*n*H, H-12, *J* = 6 Hz). **^{31}P{^{1}H} NMR (400 MHz, DMSO-d_6) δ/ppm** = 9.43**. GPC (DMF, RI):** M_n = 17.8 kDa, M_w = 25.4 kDa, Đ = 1.42. **FT-IR ν/cm^{-1} =** 3354 (b, O-H & N-H stretch), 2920 (m, -CH_2 & C-H stretch), 2873 (m, C-H stretch), 1584 (w, N-H bend), 1457 (m, -CH_2 bend), 1411 (w, -CH_2 & -CH_3 bend), 1394 (w, -CH_3 bend), 1349 (m, C-O-C & C-N stretch), 1299 (m, C-O-C & C-N stretch), 1221 (m, C-O-C & C-O-P & C-N & P=O stretch), 1026 (s, C-O-C & C-O-P & C-N stretch), 970 (m, C-O-C & C-O-P & P-O stretch), 916 (w, C-O-C & C-O-P stretch), 863 (w, C-O-C stretch), 800 (w, C-O-C stretch). **RAMAN ν/cm^{-1} =** 2931 (s, C-H stretch), 2882 (s, C-H stretch), 1462 (m, -CH_2 & -CH_3 bend), 1355 (m, C-C stretch), 1302 (m, C-C stretch), 1261 (m, C-O-C stretch), 1098 (m, C-O-C stretch), 1074 (m, C-O-C stretch), 980 (w, C-O-C stretch), 905 (m C-O-C stretch), 858

(m, C-O-C stretch), 751 (m, C-S stretch), 662 (m, C-Br stretch), 496 (w, C-C bend), 332 (w, C-C bend), 231 (w, C-C bend).

5.7.6 Phosphonamide modification of P(G-*co*-POEt) (P(G-*co*-POH))

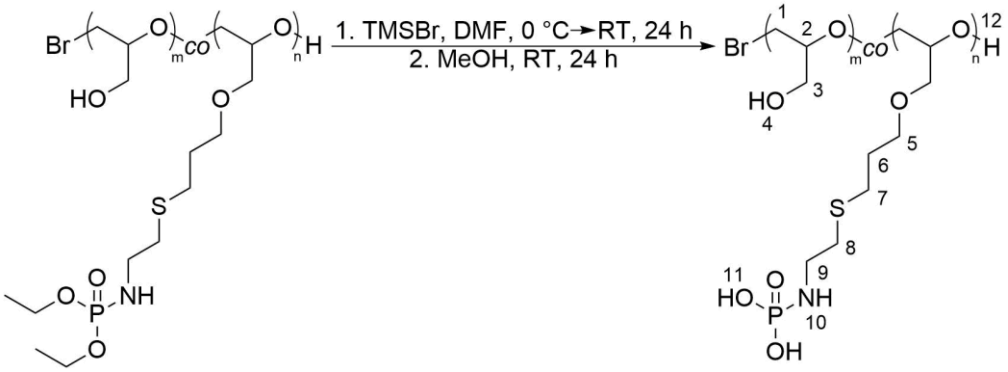

Scheme 5.7.3: Synthesis of P(G-*co*-POH).

The protected phosphonamide functionalised polyglycidol (628 mg, 0.629 mmol protected phosphonamide groups, 1 eq) was dissolved in dry DMF (30 mL). The solution was cooled to 0 °C and TMSBr (1.66 mL, 20 eq) was added. The solution was stirred from 0 °C to RT for 24 h. The solvent was removed *via* rotary evaporator and the polymer was dissolved in MeOH (60 mL). The mixture was stirred at RT for 24 h. The solvent was removed *via* rotary evaporator and the polymer was dissolved in H_2O. The solution was dialysed against H_2O for 3 d by changing solvent twice a day and using dialysis tubes with MWCO = 1 kDa. After freeze drying, the polymer was obtained as an orange sticky solid (453 mg).

^{1}H NMR (300 MHz, DMSO-d_6) δ/ppm = 4.52 (bs, 1*m*H, H-4; 1*n*H, H-10; 2*n*H, H-11; 1 H, H-12), 3.54 – 3.40 (m, 5(*m*+*n*)H, H-1 – H-3; 2*n*H, H-5), 2.94 (m, 2*n*H, H-9), 2.69 (t, 2*n*H, H-8, *J* = 6 Hz), 2.57 (t, 2*n*H, H-7, *J* = 6 Hz), 1.75 (quint, 2*n*H, H-6, *J* = 6 Hz). **^{31}P{^{1}H} NMR (400 MHz, DMSO-d_6) δ/ppm =** 0.26. **GPC (DMF, RI):** M_n = 9.4 kDa, M_w = 14.4 kDa, Đ = 1.53. **FT-IR ν/cm^{-1} =** 3344 (b, O-H & N-H stretch), 2921 (m, -CH_2 & C-H stretch), 2873 (m, C-H stretch), 1510 (w, N-H bend), 1460 (m, -CH_2 bend), 1411 (w, -CH_2 bend), 1347 (m, C-O-C & C-N stretch), 1304 (w, C-O-C & C-N stretch), 1261 (w, C-O-C & C-N stretch), 1223 (w, C-O-C & C-N & P=O stretch), 1039 (s, C-O-C & C-N stretch), 978 (m, C-O-C & P-O stretch), 912 (m, C-O-C stretch), 853 (m, C-O-C stretch). **RAMAN ν/cm^{-1} =** n.d.

5.7.7 Gel tests

5.7.7.1 P(G-*co*-Im) with P(G-*co*-POH)

Polymers carrying phosphonamide groups (9.0 mg) were dissolved (90 μL, solution 1) and polymers carrying imidazolium groups (11.0 mg) were dissolved (90 μL, solution 2). Both solutions were stirred at RT for 18 h, combined to give equimolar ratio of functional groups with a total amount of 20 mg of polymer (10 wt-%) and stirred again at RT for 18 h. Solvent was varied: H_2O and buffer solutions with pH = 4.0, 7.0, 7.4 and 10.0.

5.7.7.2 P(G-*co*-POH) with $CaCl_2$

P(G-co-POH) (15 mg) was dissolved in H_2O (pH = 7.0) and stirred at RT for 18 h. $CaCl_2$ solution (15 μL) was added and the solution was stirred again at RT for 18 h.

Table 5.7.7.2: Solutions for gel tests.

w/w (polymer)/%	**V ($CaCl_2$ solution)/mL**	**w/v ($CaCl_2$ solution)/%**
15	15	2, 4, 6, 8, 10
20	45	2, 10
30	20	2, 10

5.7.7.3 High molecular weight P(G-*co*-POH) with low molecular weight P(G-*co*-Im)

Polymers carrying phosphonamide groups (RU (G:POH) = 189:21, 12.0 mg) were dissolved (solution 1) and polymers carrying imidazolium groups (RU (G:Im) = 48:11.6, 8.0 mg) were dissolved (solution 2). Both solutions were stirred at RT for 18 h, combined to give equimolar ratio of functional groups with a total amount of 20 mg of polymer and stirred again at RT for 18 h. Note: V (solution 1) = V (solution 2) = $0.5 \cdot V_{total}$ (solvent).

Table 5.7.7.3: Solutions for gel tests.

w/w (polymer)/%	10	15	20	30
V_{total} (H_2O)/μL	180	113.3	80	46.7

6 References

[1] H. Namazi, Polymers in our daily life, BioImpacts: BI 7(2) (2017) 73-74.
[2] J. Chen, Q. Peng, X. Peng, L. Han, X. Wang, J. Wang, H. Zeng, Recent Advances in Mechano-Responsive Hydrogels for Biomedical Applications, ACS Applied Polymer Materials 2(3) (2020) 1092-1107.
[3] L.S. Nair, C.T. Laurencin, Polymers as biomaterials for tissue engineering and controlled drug delivery, Tissue engineering I, Springer2005, pp. 47-90.
[4] M.J. Majcher, T. Hoare, Applications of Hydrogels, in: M.A. Jafar Mazumder, H. Sheardown, A. Al-Ahmed (Eds.), Functional Biopolymers, Springer International Publishing, Cham, 2019, pp. 453-490.
[5] R. P Garay, J. P Labaune, Immunogenicity of polyethylene glycol (PEG), The Open Conference Proceedings Journal, 2011, pp. 104-107.
[6] J. Herzberger, K. Niederer, H. Pohlit, J. Seiwert, M. Worm, F.R. Wurm, H. Frey, Polymerization of ethylene oxide, propylene oxide, and other alkylene oxides: synthesis, novel polymer architectures, and bioconjugation, Chemical Reviews 116(4) (2016) 2170-2243.
[7] J.F. Lutz, Polymerization of oligo (ethylene glycol)(meth) acrylates: Toward new generations of smart biocompatible materials, Journal of Polymer Science Part A: Polymer Chemistry 46(11) (2008) 3459-3470.
[8] W.R. Algar, A Brief Introduction to Traditional Bioconjugate Chemistry, Chemoselective and Bioorthogonal Ligation Reactions: Concepts and Applications (2017) 3-36.
[9] P.E. Dawson, T.W. Muir, I. Clark-Lewis, S. Kent, Synthesis of proteins by native chemical ligation, Science 266(5186) (1994) 776-779.
[10] Z. Fan, Y. Zhang, J. Ji, X. Li, Hybrid polypeptide hydrogels produced via native chemical ligation, RSC Advances 5(22) (2015) 16740-16747.
[11] S.K. Schmitt, A.W. Xie, R.M. Ghassemi, D.J. Trebatoski, W.L. Murphy, P. Gopalan, Polyethylene glycol coatings on plastic substrates for chemically defined stem cell culture, Advanced healthcare materials 4(10) (2015) 1555-1564.
[12] G. Chen, W. Tang, X. Wang, X. Zhao, C. Chen, Z. Zhu, Applications of Hydrogels with Special Physical Properties in Biomedicine, Polymers 11(9) (2019) 1420 1-17.
[13] A. Thomas, S.S. Müller, H. Frey, Beyond poly(ethylene glycol): linear polyglycerol as a multifunctional polyether for biomedical and pharmaceutical applications, Biomacromolecules 15(6) (2014) 1935-1954.
[14] J. Malda, J. Visser, F.P. Melchels, T. Jüngst, W.E. Hennink, W.J. Dhert, J. Groll, D.W. Hutmacher, 25th anniversary article: engineering hydrogels for biofabrication, Advanced materials 25(36) (2013) 5011-5028.
[15] G. Radenković, D. Petković, Metallic Biomaterials, in: F. Zivic, S. Affatato, M. Trajanovic, M. Schnabelrauch, N. Grujovic, K.L. Choy (Eds.), Biomaterials in Clinical Practice : Advances in Clinical Research and Medical Devices, Springer International Publishing, Cham, 2018, pp. 183-224.
[16] M.S. Shoichet, Polymer scaffolds for biomaterials applications, Macromolecules 43(2) (2010) 581-591.
[17] A. Jenkins, P. Kratochvíl, R. Stepto, U. Suter, Glossary of basic terms in polymer science (IUPAC Recommendations 1996), Pure and applied chemistry 68(12) (1996) 2287-2311.
[18] P.S. Kowalski, C. Bhattacharya, S. Afewerki, R. Langer, Smart biomaterials: recent advances and future directions, ACS Biomaterials Science & Engineering 4(11) (2018) 3809-3817.

[19] A.J. Teo, A. Mishra, I. Park, Y.-J. Kim, W.-T. Park, Y.-J. Yoon, Polymeric biomaterials for medical implants and devices, ACS Biomaterials Science & Engineering 2(4) (2016) 454-472.
[20] M. Mir, M.N. Ali, A. Barakullah, A. Gulzar, M. Arshad, S. Fatima, M. Asad, Synthetic polymeric biomaterials for wound healing: a review, Progress in biomaterials 7(1) (2018) 1-21.
[21] D. Shan, E. Gerhard, C. Zhang, J.W. Tierney, D. Xie, Z. Liu, J. Yang, Polymeric biomaterials for biophotonic applications, Bioactive materials 3(4) (2018) 434-445.
[22] M. Szwarc, M. Levy, R. Milkovich, Polymerization initiated by electron transfer to monomer. A new method of formation of block polymers, Journal of the American Chemical Society 78(11) (1956) 2656-2657.
[23] O.W. Webster, Living polymerization methods, Science 251(4996) (1991) 887-893.
[24] J. Chiefari, Y. Chong, F. Ercole, J. Krstina, J. Jeffery, T.P. Le, R.T. Mayadunne, G.F. Meijs, C.L. Moad, G. Moad, Living free-radical polymerization by reversible addition− fragmentation chain transfer: the RAFT process, Macromolecules 31(16) (1998) 5559-5562.
[25] S. Perrier, P. Takolpuckdee, Macromolecular design via reversible addition–fragmentation chain transfer (RAFT)/xanthates (MADIX) polymerization, Journal of Polymer Science Part A: Polymer Chemistry 43(22) (2005) 5347-5393.
[26] K.J. Abd Karim, S. Binauld, W. Scarano, M.H. Stenzel, Macromolecular platinum-drugs based on statistical and block copolymer structures and their DNA binding ability, Polymer Chemistry 4(22) (2013) 5542-5554.
[27] H. Lai, M. Lu, H. Lu, M.H. Stenzel, P. Xiao, pH-Triggered release of gemcitabine from polymer coated nanodiamonds fabricated by RAFT polymerization and copper free click chemistry, Polymer Chemistry 7(40) (2016) 6220-6230.
[28] H.T. Duong, C.P. Marquis, M. Whittaker, T.P. Davis, C. Boyer, Acid degradable and biocompatible polymeric nanoparticles for the potential codelivery of therapeutic agents, Macromolecules 44(20) (2011) 8008-8019.
[29] H. Keul, M. Möller, Synthesis and degradation of biomedical materials based on linear and star shaped polyglycidols, Journal of Polymer Science Part A: Polymer Chemistry 47(13) (2009) 3209-3231.
[30] S.R. Sandler, F.R. Berg, Room temperature polymerization of glycidol, Journal of Polymer Science Part A-1: Polymer Chemistry 4(5) (1966) 1253-1259.
[31] E. Vandenberg, Polymerization of glycidol and its derivatives: A new rearrangement polymerization, Journal of Polymer Science: Polymer Chemistry Edition 23(4) (1985) 915-949.
[32] M. Imran ul-haq, B.F. Lai, R. Chapanian, J.N. Kizhakkedathu, Influence of architecture of high molecular weight linear and branched polyglycerols on their biocompatibility and biodistribution, Biomaterials 33(35) (2012) 9135-9147.
[33] M. Gosecki, M. Gadzinowski, M. Gosecka, T. Basinska, S. Slomkowski, Polyglycidol, its derivatives, and polyglycidol-containing copolymers—Synthesis and medical applications, Polymers 8(6) (2016) 227 1-25.
[34] M. Erberich, H. Keul, M. Möller, Polyglycidols with two orthogonal protective groups: preparation, selective deprotection, and functionalization, Macromolecules 40(9) (2007) 3070-3079.
[35] S. Halacheva, S. Rangelov, C. Tsvetanov, Poly(glycidol)-based analogues to pluronic block copolymers. Synthesis and aqueous solution properties, Macromolecules 39(20) (2006) 6845-6852.
[36] M. Hans, P. Gasteier, H. Keul, M. Moeller, Ring-opening polymerization of ε-caprolactone by means of mono-and multifunctional initiators: Comparison of chemical and enzymatic catalysis, Macromolecules 39(9) (2006) 3184-3193.

[37] D. Steinhilber, S. Seiffert, J.A. Heyman, F. Paulus, D.A. Weitz, R. Haag, Hyperbranched polyglycerols on the nanometer and micrometer scale, Biomaterials 32(5) (2011) 1311-1316.
[38] D. Wilms, S.-E. Stiriba, H. Frey, Hyperbranched polyglycerols: from the controlled synthesis of biocompatible polyether polyols to multipurpose applications, Accounts of chemical research 43(1) (2010) 129-141.
[39] M. Kuhlmann, J. Groll, Dispersity control of linear poly(glycidyl ether) s by slow monomer addition, RSC Advances 5(82) (2015) 67323-67326.
[40] S. Carlotti, C. Billouard, E. Gautriaud, P. Desbois, A. Deffieux, Activation mechanisms of trialkylaluminum in alkali metal alkoxides or tetraalkylammonium salts/propylene oxide controlled anionic polymerization, Macromolecular Symposia, Wiley Online Library, 2005, pp. 61-68.
[41] M. Gervais, A.-L. Brocas, G. Cendejas, A. Deffieux, S. Carlotti, Synthesis of linear high molar mass glycidol-based polymers by monomer-activated anionic polymerization, Macromolecules 43(4) (2010) 1778-1784.
[42] M. Gervais, A. Labbé, S. Carlotti, A. Deffieux, Direct synthesis of α-azido, ω-hydroxypolyethers by monomer-activated anionic polymerization, Macromolecules 42(7) (2009) 2395-2400.
[43] A.L. Brocas, G. Cendejas, S. Caillol, A. Deffieux, S. Carlotti, Controlled synthesis of polyepichlorohydrin with pendant cyclic carbonate functions for isocyanate-free polyurethane networks, Journal of Polymer Science Part A: Polymer Chemistry 49(12) (2011) 2677-2684.
[44] S. Liu, F. Zhang, Y. Zhang, J. Xu, Synthesis of Novel Glycidol Copolymers with Pendant Alkene and Hydroxyl Groups, Chinese Journal of Chemistry 31(10) (2013) 1315-1320.
[45] S. Heinen, S. Rackow, A. Schäfer, M. Weinhart, A Perfect Match: Fast and Truly Random Copolymerization of Glycidyl Ether Monomers to Thermoresponsive Copolymers, Macromolecules 50(1) (2016) 44-53.
[46] S. Heinen, M. Weinhart, Poly(glycidyl ether)-based monolayers on gold surfaces: control of grafting density and chain conformation by grafting procedure, surface anchor, and molecular weight, Langmuir 33(9) (2017) 2076-2086.
[47] D.D. Stöbener, M. Uckert, J.L. Cuellar-Camacho, A. Hoppensack, M. Weinhart, Ultrathin Poly(glycidyl ether) Coatings on Polystyrene for Temperature-Triggered Human Dermal Fibroblast Sheet Fabrication, ACS Biomaterials Science & Engineering 3(9) (2017) 2155-2165.
[48] A.B. Lowe, Thiol-ene "click" reactions and recent applications in polymer and materials synthesis, Polymer Chemistry 1(1) (2010) 17-36.
[49] A.K. Sinha, D. Equbal, Thiol− Ene Reaction: Synthetic Aspects and Mechanistic Studies of an Anti-Markovnikov-Selective Hydrothiolation of Olefins, Asian Journal of Organic Chemistry 8(1) (2019) 32-47.
[50] C.E. Hoyle, C.N. Bowman, Thiol–ene click chemistry, Angewandte Chemie International Edition 49(9) (2010) 1540-1573.
[51] A.B. Lowe, Thiol–ene "click" reactions and recent applications in polymer and materials synthesis: a first update, Polymer Chemistry 5(17) (2014) 4820-4870.
[52] M. Kuhlmann, O. Reimann, C.P. Hackenberger, J. Groll, Cysteine-Functional Polymers via Thiol-ene Conjugation, Macromolecular Rapid Communications 36(5) (2015) 472-476.
[53] S. Stichler, T. Jungst, M. Schamel, I. Zilkowski, M. Kuhlmann, T. Böck, T. Blunk, J. Teßmar, J. Groll, Thiol-ene Clickable Poly(glycidol) Hydrogels for Biofabrication, Annals of Biomedical Engineering 45(1) (2017) 273-285.
[54] S. Feineis, J. Lutz, L. Heffele, E. Endl, K. Albrecht, J. Groll, Thioether–Polyglycidol as Multivalent and Multifunctional Coating System for Gold Nanoparticles, Advanced Materials 30(8) (2018) 1704972 1-6.

[55] I. Zilkowski, F. Ziouti, A. Schulze, S. Hauck, S. Schmidt, L. Mainz, M. Sauer, K. Albrecht, F. Jundt, J. Groll, Nanogels enable efficient miRNA delivery and target gene downregulation in transfection-resistant multiple myeloma cells, Biomacromolecules 20(2) (2018) 916-926.
[56] I. Zilkowski, I. Theodorou, K. Albrecht, F. Ducongé, J. Groll, Subtle changes in network composition impact the biodistribution and tumor accumulation of nanogels, Chemical Communications 54(83) (2018) 11777-11780.
[57] J. Kalia, R.T. Raines, Advances in bioconjugation, Current organic chemistry 14(2) (2010) 138-147.
[58] M.H. Stenzel, Bioconjugation using thiols: old chemistry rediscovered to connect polymers with nature's building blocks, 2 (1) (2013) 14-18.
[59] J.M. Ravasco, H. Faustino, A. Trindade, P.M. Gois, Bioconjugation with maleimides: A useful tool for chemical biology, Chemistry–A European Journal 25(1) (2019) 43-59.
[60] O. Boutureira, G.a.J. Bernardes, Advances in chemical protein modification, Chemical reviews 115(5) (2015) 2174-2195.
[61] O. Koniev, A. Wagner, Developments and recent advancements in the field of endogenous amino acid selective bond forming reactions for bioconjugation, Chemical Society Reviews 44(15) (2015) 5495-5551.
[62] S.B. Gunnoo, A. Madder, Bioconjugation–using selective chemistry to enhance the properties of proteins and peptides as therapeutics and carriers, Organic & biomolecular chemistry 14(34) (2016) 8002-8013.
[63] Z. Liu, X. Chen, Simple bioconjugate chemistry serves great clinical advances: albumin as a versatile platform for diagnosis and precision therapy, Chemical Society Reviews 45(5) (2016) 1432-1456.
[64] X. Hu, X. Zhao, B. He, Z. Zhao, Z. Zheng, P. Zhang, X. Shi, R.T. Kwok, J.W. Lam, A. Qin, A simple approach to bioconjugation at diverse levels: metal-free click reactions of activated alkynes with native groups of biotargets without prefunctionalization, Research (2018) Article ID 3152870 1-12.
[65] C. Zhang, E.V. Vinogradova, A.M. Spokoyny, S.L. Buchwald, B.L. Pentelute, Arylation chemistry for bioconjugation, Angewandte Chemie International Edition 58(15) (2019) 4810-4839.
[66] L. Berrade, J.A. Camarero, Expressed protein ligation: a resourceful tool to study protein structure and function, Cellular and molecular life sciences 66(24) (2009) 3909-3922.
[67] P.E. Dawson, S.B. Kent, Synthesis of native proteins by chemical ligation, Annual review of biochemistry 69(1) (2000) 923-960.
[68] P. Thapa, R.-Y. Zhang, V. Menon, J.-P. Bingham, Native chemical ligation: a boon to peptide chemistry, Molecules 19(9) (2014) 14461-14483.
[69] T.M. Hackeng, J.H. Griffin, P.E. Dawson, Protein synthesis by native chemical ligation: expanded scope by using straightforward methodology, Proceedings of the National Academy of Sciences 96(18) (1999) 10068-10073.
[70] E.C. Johnson, S.B. Kent, Insights into the mechanism and catalysis of the native chemical ligation reaction, Journal of the American Chemical Society 128(20) (2006) 6640-6646.
[71] W. Hou, L. Liu, X. Zhang, C. Liu, A new method of N to C sequential ligation using thioacid capture ligation and native chemical ligation, Royal Society Open Science 5(6) (2018) 172455 1-10.
[72] A.C. Conibear, E.E. Watson, R.J. Payne, C.F. Becker, Native chemical ligation in protein synthesis and semi-synthesis, Chemical Society Reviews 47(24) (2018) 9046-9068.
[73] D.T. Flood, J.C. Hintzen, M.J. Bird, P.A. Cistrone, J.S. Chen, P.E. Dawson, Leveraging the Knorr pyrazole synthesis for the facile generation of thioester surrogates for use in native chemical ligation, Angewandte Chemie 130(36) (2018) 11808-11813.

[74] H. Rohde, J. Schmalisch, Z. Harpaz, F. Diezmann, O. Seitz, Ascorbate as an alternative to thiol additives in native chemical ligation, ChemBioChem 12(9) (2011) 1396-1400.
[75] M. Schmitz, M. Kuhlmann, O. Reimann, C.P. Hackenberger, J. Groll, Side-chain cysteine-functionalized poly(2-oxazoline) s for multiple peptide conjugation by native chemical ligation, Biomacromolecules 16(4) (2015) 1088-1094.
[76] B.-H. Hu, J. Su, P.B. Messersmith, Hydrogels cross-linked by native chemical ligation, Biomacromolecules 10(8) (2009) 2194-2200.
[77] K.W. Boere, B.G. Soliman, D.T. Rijkers, W.E. Hennink, T. Vermonden, Thermoresponsive injectable hydrogels cross-linked by native chemical ligation, Macromolecules 47(7) (2014) 2430-2438.
[78] S. Reinicke, P. Espeel, M.M. Stamenović, F.E. Du Prez, One-pot double modification of p (NIPAAm): a tool for designing tailor-made multiresponsive polymers, ACS Macro Letters 2(6) (2013) 539-543.
[79] P. Espeel, F.E. Du Prez, One-pot multi-step reactions based on thiolactone chemistry: A powerful synthetic tool in polymer science, European Polymer Journal 62 (2015) 247-272.
[80] Z. Fan, P. Cheng, M. Liu, D. Li, G. Liu, Y. Zhao, Z. Ding, F. Chen, B. Wang, X. Tan, Poly(glutamic acid) hydrogels crosslinked via native chemical ligation, New Journal of Chemistry 41(16) (2017) 8656-8662.
[81] S.K. Schmitt, D.J. Trebatoski, J.D. Krutty, A.W. Xie, B. Rollins, W.L. Murphy, P. Gopalan, Peptide conjugation to a polymer coating via native chemical ligation of azlactones for cell culture, Biomacromolecules 17(3) (2016) 1040-1047.
[82] J. Liebscher, J. Teßmar, J. Groll, In Situ Polymer Analogue Generation of Azlactone Functions at Poly(oxazoline)s for Peptide Conjugation, Macromolecular Chemistry and Physics 221(1) (2020) 1900500 1-7.
[83] V. Agouridas, O.a. El Mahdi, V. Diemer, M. Cargoët, J.-C.M. Monbaliu, O. Melnyk, Native chemical ligation and extended methods: mechanisms, catalysis, scope, and limitations, Chemical reviews 119(12) (2019) 7328-7443.
[84] P.A. Cistrone, M.J. Bird, D.T. Flood, A.P. Silvestri, J.C. Hintzen, D.A. Thompson, P.E. Dawson, Native Chemical Ligation of Peptides and Proteins, Current protocols in chemical biology 11(1) (2019) e61 1-25.
[85] M. Bahram, N. Mohseni, M. Moghtader, An introduction to hydrogels and some recent applications, Emerging concepts in analysis and applications of hydrogels, IntechOpen2016, pp. 9-38.
[86] N. Das, Preparation methods and properties of hydrogel: a review, Int J Pharm Pharm Sci 5(3) (2013) 112-117.
[87] S. Mishra, P. Rani, G. Sen, K.P. Dey, Preparation, properties and application of hydrogels: a review, Hydrogels, Springer2018, pp. 145-173.
[88] M. Mahinroosta, Z.J. Farsangi, A. Allahverdi, Z. Shakoori, Hydrogels as intelligent materials: A brief review of synthesis, properties and applications, Materials today chemistry 8 (2018) 42-55.
[89] O. Erol, A. Pantula, W. Liu, D.H. Gracias, Transformer Hydrogels: A Review, Advanced Materials Technologies 4(4) (2019) 1900043 1-27.
[90] Y.S. Zhang, A. Khademhosseini, Advances in engineering hydrogels, Science 356(6337) (2017) eaaf3627 1-10.
[91] N. Chirani, L. Gritsch, F.L. Motta, S. Fare, History and applications of hydrogels, Journal of biomedical sciences 4(2) (2015) 1-23.
[92] T. Jungst, W. Smolan, K. Schacht, T. Scheibel, J. Groll, Strategies and molecular design criteria for 3D printable hydrogels, Chemical reviews 116(3) (2016) 1496-1539.
[93] W.E. Hennink, C.F. van Nostrum, Novel crosslinking methods to design hydrogels, Advanced drug delivery reviews 64 (2012) 223-236.

[94] W. Hu, Z. Wang, Y. Xiao, S. Zhang, J. Wang, Advances in crosslinking strategies of biomedical hydrogels, Biomaterials science 7(3) (2019) 843-855.
[95] K. Petrak, Polyelectrolyte complexes in biomedical applications, Journal of bioactive and compatible polymers 1(2) (1986) 202-219.
[96] T. Zhu, Y. Sha, J. Yan, P. Pageni, M.A. Rahman, Y. Yan, C. Tang, Metallo-polyelectrolytes as a class of ionic macromolecules for functional materials, Nature communications 9(1) (2018) 1-15.
[97] D.A. Mortimer, Synthetic polyelectrolytes—a review, Polymer International 25(1) (1991) 29-41.
[98] V.S. Meka, M.K. Sing, M.R. Pichika, S.R. Nali, V.R. Kolapalli, P. Kesharwani, A comprehensive review on polyelectrolyte complexes, Drug discovery today 22(11) (2017) 1697-1706.
[99] P.K. Singh, V.K. Singh, M. Singh, Zwitterionic polyelectrolytes: a review, e-Polymers 7(1) (2007) 030 1-34.
[100] P.A. Woodfield, Y. Zhu, Y. Pei, P.J. Roth, Hydrophobically modified sulfobetaine copolymers with tunable aqueous UCST through postpolymerization modification of poly(pentafluorophenyl acrylate), Macromolecules 47(2) (2014) 750-762.
[101] N. Pekel, O. Güven, Synthesis and characterization of poly(N-vinyl imidazole) hydrogels crosslinked by gamma irradiation, Polymer international 51(12) (2002) 1404-1410.
[102] M.J. Molina, M.R. Gómez-Antón, I.F. Piérola, Factors driving the protonation of poly(N-vinylimidazole) hydrogels, Journal of Polymer Science Part B: Polymer Physics 42(12) (2004) 2294-2307.
[103] W. Nan, W. Wang, H. Gao, W. Liu, Fabrication of a shape memory hydrogel based on imidazole–zinc ion coordination for potential cell-encapsulating tubular scaffold application, Soft Matter 9(1) (2013) 132-137.
[104] E.B. Anderson, T.E. Long, Imidazole-and imidazolium-containing polymers for biology and material science applications, Polymer 51(12) (2010) 2447-2454.
[105] S. Hayano, K. Ota, Syntheses, characterizations and functions of cationic polyethers with imidazolium-based ionic liquid moieties, Polymer Chemistry 9(8) (2018) 948-960.
[106] R.A. Gemeinhart, C.M. Bare, R.T. Haasch, E.J. Gemeinhart, Osteoblast-like cell attachment to and calcification of novel phosphonate-containing polymeric substrates, Journal of Biomedical Materials Research Part A: An Official Journal of The Society for Biomaterials, The Japanese Society for Biomaterials, and The Australian Society for Biomaterials and the Korean Society for Biomaterials 78(3) (2006) 433-440.
[107] C.M. Sevrain, M. Berchel, H. Couthon, P.-A. Jaffrès, Phosphonic acid: preparation and applications, Beilstein journal of organic chemistry 13(1) (2017) 2186-2213.
[108] B. Canniccioni, S. Monge, G. David, J.-J. Robin, RAFT polymerization of dimethyl (methacryloyloxy) methyl phosphonate and its phosphonic acid derivative: a new opportunity for phosphorus-based materials, Polymer chemistry 4(13) (2013) 3676-3685.
[109] D. Hoang Phuc, N. Thi Hiep, N.P. Do Chau, N. Thi Thu Hoai, H. Chan Khon, V. Van Toi, N. Dai Hai, B. Chi Bao, Fabrication of hyaluronan-poly(vinylphosphonic acid)-chitosan hydrogel for wound healing application, International Journal of Polymer Science Article ID 6723716 (2016) 1-9.
[110] J. Tan, R.A. Gemeinhart, M. Ma, W.M. Saltzman, Improved cell adhesion and proliferation on synthetic phosphonic acid-containing hydrogels, Biomaterials 26(17) (2005) 3663-3671.
[111] S.Y. Kim, S.C. Lee, Thermo-responsive injectable hydrogel system based on poly(N-isopropylacrylamide-co-vinylphosphonic acid). I. Biomineralization and protein delivery, Journal of applied polymer science 113(6) (2009) 3460-3469.

[112] T. Huang, H. Liu, P. Liu, P. Liu, L. Li, J. Shen, Zwitterionic copolymers bearing phosphonate or phosphonic motifs as novel metal-anchorable anti-fouling coatings, Journal of Materials Chemistry B 5(27) (2017) 5380-5389.
[113] H. Srour, O. Ratel, M. Leocmach, E.A. Adams, S. Denis-Quanquin, V. Appukuttan, N. Taberlet, S. Manneville, J.C. Majesté, C. Carrot, Mediating Gel Formation from Structurally Controlled Poly(Electrolytes) Through Multiple "Head-to-Body" Electrostatic Interactions, Macromolecular Rapid Communications 36(1) (2015) 55-59.
[114] J. Köhler, H. Keul, M. Möller, Post-polymerization functionalization of linear polyglycidol with diethyl vinylphosphonate, Chemical Communications 47(28) (2011) 8148-8150.
[115] R. Zhou, Modeling of Nanotoxicity, Springer2015, pp. 169-189.
[116] K. Molčanov, B. Kojić-Prodić, Towards understanding π-stacking interactions between non-aromatic rings, International Union of Crystallography 6(2) (2019) 156-166.
[117] C.R. Martinez, B.L. Iverson, Rethinking the term "pi-stacking", Chemical Science 3(7) (2012) 2191-2201.
[118] L.J. Riwar, N. Trapp, B. Kuhn, F. Diederich, Substituent Effects in Parallel-Displaced π–π Stacking Interactions: Distance Matters, Angewandte Chemie International Edition 56(37) (2017) 11252-11257.
[119] M. Tang, S. Zhu, Z. Liu, C. Jiang, Y. Wu, H. Li, B. Wang, E. Wang, J. Ma, C. Wang, Tailoring π-conjugated systems: from π-π stacking to high-rate-performance organic cathodes, Chem 4(11) (2018) 2600-2614.
[120] G.B. McGaughey, M. Gagné, A.K. Rappé, π-Stacking interactions alive and well in proteins, Journal of Biological Chemistry 273(25) (1998) 15458-15463.
[121] S.R. Nelli, R.D. Chakravarthy, Y.-M. Xing, J.-P. Weng, H.-C. Lin, Self-assembly of single amino acid/pyrene conjugates with unique structure–morphology relationship, Soft Matter 13(45) (2017) 8402-8407.
[122] H. Shao, J.R. Parquette, A π-conjugated hydrogel based on an Fmoc-dipeptide naphthalene diimide semiconductor, Chemical Communications 46(24) (2010) 4285-4287.
[123] N.S. Kumar, M.D. Gujrati, J.N. Wilson, Evidence of preferential π-stacking: a study of intermolecular and intramolecular charge transfer complexes, Chemical Communications 46(30) (2010) 5464-5466.
[124] S. Mukherjee, T. Kar, P. Kumar Das, Pyrene-Based Fluorescent Supramolecular Hydrogel: Scaffold for Energy Transfer, Chemistry–An Asian Journal 9(10) (2014) 2798-2805.
[125] T. Kar, N. Patra, Pyrene-based fluorescent supramolecular hydrogel: scaffold for nanoparticle synthesis, Journal of Physical Organic Chemistry 33(2) (2020) e4026 1-9.
[126] D.P. Hickey, K. Lim, R. Cai, A.R. Patterson, M. Yuan, S. Sahin, S. Abdellaoui, S.D. Minteer, Pyrene hydrogel for promoting direct bioelectrochemistry: ATP-independent electroenzymatic reduction of N2, Chemical science 9(23) (2018) 5172-5177.
[127] X. Yang, S. Kootala, J. Hilborn, D.A. Ossipov, Preparation of hyaluronic acid nanoparticles via hydrophobic association assisted chemical cross-linking—an orthogonal modular approach, Soft Matter 7(16) (2011) 7517-7525.
[128] B. Chen, K.L. Liu, Z. Zhang, X. Ni, S.H. Goh, J. Li, Supramolecular hydrogels formed by pyrene-terminated poly(ethylene glycol) star polymers through inclusion complexation of pyrene dimers with γ-cyclodextrin, Chemical Communications 48(45) (2012) 5638-5640.
[129] L.-H. Hsu, S.-M. Hsu, F.-Y. Wu, Y.-H. Liu, S.R. Nelli, M.-Y. Yeh, H.-C. Lin, Nanofibrous hydrogels self-assembled from naphthalene diimide (NDI)/amino acid conjugates, RSC Advances 5(26) (2015) 20410-20413.
[130] N. Singha, P. Gupta, B. Pramanik, S. Ahmed, A. Dasgupta, A. Ukil, D. Das, Hydrogelation of a Naphthalene Diimide Appended Peptide Amphiphile and Its Application in Cell Imaging and Intracellular pH Sensing, Biomacromolecules 18(11) (2017) 3630-3641.

[131] P. Rajdev, S. Chakraborty, M. Schmutz, P. Mesini, S. Ghosh, Supramolecularly Engineered π-Amphiphile, Langmuir 33(19) (2017) 4789-4795.
[132] S.R. Nelli, R.D. Chakravarthy, M. Mohiuddin, H.-C. Lin, The role of amino acids on supramolecular co-assembly of naphthalenediimide–pyrene based hydrogelators, RSC Advances 8(27) (2018) 14753-14759.
[133] S. Burattini, H.M. Colquhoun, J.D. Fox, D. Friedmann, B.W. Greenland, P.J. Harris, W. Hayes, M.E. Mackay, S.J. Rowan, A self-repairing, supramolecular polymer system: healability as a consequence of donor–acceptor π–π stacking interactions, Chemical communications (44) (2009) 6717-6719.
[134] L.R. Hart, J.L. Harries, B.W. Greenland, H.M. Colquhoun, W. Hayes, Supramolecular approach to new inkjet printing inks, ACS Applied Materials & Interfaces 7(16) (2015) 8906-8914.
[135] S. Binauld, W. Scarano, M.H. Stenzel, pH-Triggered release of platinum drugs conjugated to micelles via an acid-cleavable linker, Macromolecules 45(17) (2012) 6989-6999.
[136] M.M. Shoaib, V. Huynh, Y. Shad, R. Ahmed, A.H. Jesmer, G. Melacini, R.G. Wylie, Controlled degradation of low-fouling poly(oligo (ethylene glycol) methyl ether methacrylate) hydrogels, RSC Advances 9(33) (2019) 18978-18988.
[137] I. Urosev, E. Bakaic, R.J. Alsop, M.C. Rheinstädter, T. Hoare, Tuning the properties of injectable poly(oligoethylene glycol methacrylate) hydrogels by controlling precursor polymer molecular weight, Journal of Materials Chemistry B 4(40) (2016) 6541-6551.
[138] V.T. Huynh, S. Pearson, J.-M. Noy, A. Abboud, R.H. Utama, H. Lu, M.H. Stenzel, Nanodiamonds with Surface Grafted Polymer Chains as Vehicles for Cell Imaging and Cisplatin Delivery: Enhancement of Cell Toxicity by POEGMEMA Coating, ACS Macro Letters 2(3) (2013) 246-250.
[139] S. Perrier, P. Takolpuckdee, C.A. Mars, Reversible Addition−Fragmentation Chain Transfer Polymerization: End Group Modification for Functionalized Polymers and Chain Transfer Agent Recovery, Macromolecules 38(6) (2005) 2033-2036.
[140] J.T. Barry, D.J. Berg, D.R. Tyler, Radical Cage Effects: Comparison of Solvent Bulk Viscosity and Microviscosity in Predicting the Recombination Efficiencies of Radical Cage Pairs, Journal of the American Chemical Society 138(30) (2016) 9389-9392.
[141] C.P. Jesson, C.M. Pearce, H. Simon, A. Werner, V.J. Cunningham, J.R. Lovett, M.J. Smallridge, N.J. Warren, S.P. Armes, H_2O_2 Enables Convenient Removal of RAFT End-Groups from Block Copolymer Nano-Objects Prepared via Polymerization-Induced Self-Assembly in Water, Macromolecules 50(1) (2017) 182-191.
[142] D.J. Keddie, G. Moad, E. Rizzardo, S.H. Thang, RAFT agent design and synthesis, Macromolecules 45(13) (2012) 5321-5342.
[143] S. Perrier, 50th Anniversary Perspective: RAFT Polymerization - A User Guide, Macromolecules 50(19) (2017) 7433-7447.
[144] P.J. Flory, Molecular Size Distribution in Linear Condensation Polymers, Journal of the American Chemical Society 58(10) (1936) 1877-1885.
[145] Y. Zhu, J.-M. Noy, A.B. Lowe, P.J. Roth, The synthesis and aqueous solution properties of sulfobutylbetaine (co)polymers: comparison of synthetic routes and tuneable upper critical solution temperatures, Polymer Chemistry 6(31) (2015) 5705-5718.
[146] A.O. Fitton, J. Hill, D.E. Jane, R. Millar, Synthesis of simple oxetanes carrying reactive 2-substituents, Synthesis 1987(12) (1987) 1140-1142.
[147] M.J. Covitch, K.J. Trickett, How polymers behave as viscosity index improvers in lubricating oils, Advances in Chemical Engineering and Science 5(02) (2015) 134.
[148] T. Zhang, Z. Liao, L.M. Sandonas, A. Dianat, X. Liu, P. Xiao, I. Amin, R. Gutierrez, T. Chen, E. Zschech, Polymerization driven monomer passage through monolayer chemical vapour deposition graphene, Nature communications 9(1) (2018) 1-9.

[149] B.M. Blunden, D.S. Thomas, M.H. Stenzel, Macromolecular ruthenium complexes as anti-cancer agents, Polymer Chemistry 3(10) (2012) 2964-2975.
[150] P.J. Roth, J.Y. Quek, Y. Zhu, B.M. Blunden, A.B. Lowe, Mechano-responsive polymer solutions based on CO_2 supersaturation: shaking-induced phase transitions and self-assembly or dissociation of polymeric nanoparticles, Chemical Communications 50(67) (2014) 9561-9564.
[151] C. Baleizão, B. Gigante, H. Garcia, A. Corma, Vanadyl salen complexes covalently anchored to an imidazolium ion as catalysts for the cyanosilylation of aldehydes in ionic liquids, Tetrahedron letters 44(36) (2003) 6813-6816.
[152] K.J. van Bommel, A. Friggeri, D. Mateman, F.A. Geurts, K.G. van Leerdam, W. Verboom, F.C. van Veggel, D.N. Reinhoudt, Self-Assembled Monolayers on Gold for the Fabrication of Radioactive Stents, Advanced functional materials 11(2) (2001) 140-146.
[153] P. Bilalis, D. Katsigiannopoulos, A. Avgeropoulos, G. Sakellariou, Non-covalent functionalization of carbon nanotubes with polymers, Rsc Advances 4(6) (2014) 2911-2934.
[154] X. Liu, A. Basu, Core functionalization of hollow polymer nanocapsules, Journal of the American Chemical Society 131(16) (2009) 5718-5719.
[155] F. Wurm, A.M. Hofmann, A. Thomas, C. Dingels, H. Frey, α,ω_n-Heterotelechelic Hyperbranched Polyethers Solubilize Carbon Nanotubes, Macromolecular Chemistry and Physics 211(8) (2010) 932-939.
[156] J. Horak, N.M. Maier, W. Lindner, Investigations on the chromatographic behavior of hybrid reversed-phase materials containing electron donor–acceptor systems: II. Contribution of π–π aromatic interactions, Journal of Chromatography A 1045(1-2) (2004) 43-58.
[157] S.K.M. Nalluri, C. Berdugo, N. Javid, P.W.J.M. Frederix, R.V. Ulijn, Biocatalytic Self-Assembly of Supramolecular Charge-Transfer Nanostructures Based on n-Type Semiconductor-Appended Peptides, Angewandte Chemie 126(23) (2014) 5992-5997.
[158] S. Bhattacharya, R. Shunmugam, Unraveling the Effect of PEG Chain Length on the Physical Properties and Toxicant Removal Capacities of Cross-Linked Network Synthesized by Thiol–Norbornene Photoclick Chemistry, ACS Omega 5(6) (2020) 2800-2810.
[159] B. Tieke, Makromolekulare Chemie: Eine Einführung, WILEY-VCH Verlag GmbH & Co. KGaA2005, pp. 75-76.
[160] C. Bakewell, A.J. White, M.R. Crimmin, Reversible alkene binding and allylic C–H activation with an aluminium (I) complex, Chemical science 10(8) (2019) 2452-2458.
[161] C. Osterwinter, C. Schubert, C. Tonhauser, D. Wilms, H. Frey, C. Friedrich, Rheological consequences of hydrogen bonding: Linear viscoelastic response of linear polyglycerol and its permethylated analogues as a general model for hydroxyl-functional polymers, Macromolecules 48(1) (2015) 119-130.